

**Synthetic Alkyl Glycolipids as Therapeutic Agents: Their
Synthesis as Potential *i*NKT Cell Stimulators and their Anti-
Microbial Properties**

A thesis submitted to the National University of Ireland in fulfilment of
the requirements for the degree of

Doctor of Philosophy

by

Róisín M. O'Flaherty, B.Sc.



NUI MAYNOOTH

Ollscoil na hÉireann Má Nuad

Department of Chemistry,
National University of Ireland Maynooth,
Maynooth, Co.Kildare, Ireland.

October 2012

Research Supervisor: Dr. Trinidad Velasco-Torrijos

Head of Department: Dr. John Stephens

Table of Contents

Acknowledgements.....	i
Declaration.....	iii
Abstract.....	iv
Abbreviations.....	v
Chapter 1: Perspective	
1.1. Glycolipids in nature: structure, occurrence and functions.....	2
1.1.1. Alkyl glycolipids.....	2
1.1.2. Resin glycolipids.....	3
1.1.3. Glycoglycerolipids.....	4
1.1.4. Lipopolysaccharides.....	5
1.1.5. Glycosphingolipids.....	6
1.1.6. Gangliosides.....	6
1.2. Synthetic glycolipids and therapeutic applications.....	6
1.2.1. Alkyl glycolipids.....	7
1.2.2. Macrocyclic glycolipids.....	8
1.2.3. Glycoglycerolipids.....	8
1.2.4. Glycosphingolipids.....	8
1.3. Research aims.....	9
Chapter 2: Alkyl Glycolipids as Anti-Microbial Agents and Organogelators	
2.1. Alkyl <i>O</i> -glycolipids and biological importance.....	12
2.2. Anti-adhesion approach for anti-microbial studies.....	14
2.3. <i>N</i> -glycosides and biological importance.....	16
2.4. Organogelators.....	18
2.5. Research objective.....	21
2.6. Synthesis of simple <i>O</i> -linked glycolipids 2.18 and 2.19.....	22
2.7. Synthesis of 1,4-disubstituted 1,2,3-triazole containing β - <i>N</i> -glycolipid 2.20.....	25
2.8. Synthesis of L-aspartic acid based β - <i>N</i> -glycolipids 2.21-2.23.....	26
2.8.1. Initial attempts to the synthesis of β - <i>N</i> -glycolipid 2.23.....	27
2.8.2. Alternative method to form β - <i>N</i> -glycolipids 2.21- 2.23.....	32
2.8.3. Synthesis of <i>N</i> -glycolipid 2.21.....	35
2.8.4. Synthesis of <i>N</i> -glycolipid 2.22.....	38
2.8.5. Synthesis of <i>N</i> -glycolipid 2.23.....	40

2.9. Gelation and self-assembly properties of glycolipid 2.18, <i>N</i> -glycolipid 2.37, lipid 2.66, and L-aspartic acid <i>N</i> -glycolipids 2.58, 2.21 and 2.62.....	42
2.9.1. SEM imaging of <i>N</i> -glycolipid 2.62 and lipid 2.66.....	50
2.10. <i>O</i> -Glycolipid 2.19 and <i>N</i> -glycolipid 2.22 as anti-adhesion agents.....	53
2.11. Summary	56
Chapter 3: Synthesis of GI-X based glycolipid for biochemical evaluation	
3.1. Introduction	59
3.2. Current tuberculosis treatment.....	59
3.3. Mycobacterial cell wall associated glycolipids.....	61
3.4. PIMs, LM and LAM	62
3.5. Introduction to GI-X, GI-A, GI-LM.....	63
3.5.1. Biological function of GI-X, GI-A, GI-LM	66
3.6. Research objective	66
3.7. Design of GI-X analogue 3.1	67
3.7.1. Synthesis of α -mannosyl donor 3.2	70
3.7.2. Intramolecular Aglycon Delivery.....	71
3.7.3. Synthesis of Glycosyl Donor 3.3 for Intramolecular Aglycon Delivery.....	74
3.7.4. Initial Attempts at Intramolecular Aglycon Delivery Glycosylation	77
3.7.5. Investigations into Alternative Aglycons for their use in Intramolecular Aglycon Delivery	81
3.8. Summary	87
Chapter 4: Synthesis of L-serinyl based glycolipid analogues of the immunostimulant KRN7000	
4.1. Introduction	89
4.1.1. Immunological functions of iNKT cells.....	89
4.1.2. KRN7000.....	90
4.2. KRN7000 Analogues	92
4.2.1. Sugar modifications on <i>O</i> -glycoside analogues of KRN7000	93
4.2.2. Modifications on the ceramide backbone of the <i>O</i> -glycoside analogues of KRN7000.....	95
4.2.3. Modifications and/or functionalization of the lipid chains.....	97
4.2.4. Miscellaneous analogues of KRN7000	99
4.2.5. β -glycoside analogues.....	100
4.2.6. L-Serine glycosides as KRN7000 analogues.....	101
4.2.7. Perspective.....	102

4.3. Research objective	102
4.4. Stereoselective synthesis of β -galactoside building blocks for KRN7000 analogues ...	104
4.4.1. Design considerations for stereoselective β -galactosyl building block formation	104
4.4.2. Use of galactosyl acetate donors for β -galactosyl building block formation.....	105
4.4.3. A Koenigs-Knorr glycosylation for formation of a β -galactosyl building block ..	110
4.4.4. Schmidt's trichloroacetimidate glycosylation for the formation of β -galactosyl building block	112
4.4.5. Use of silylated glycosyl acceptors for the formation of β -galactosyl building block	120
4.4.6. Investigation of nucleophilicity of L-serine acceptor for β -galactosyl building block formation	122
4.4.7. L-Serine azido acceptor 4.43 for β -galactosyl building block formation	125
4.5. Mitsunobu conditions in formation of α/β -galactosyl building block	126
4.6. Design considerations for the synthesis of α/β -galactoside building blocks for KRN7000 analogues	129
4.6.1. Armed thioglycosides for α/β -galactosyl building block formation.....	130
4.6.2. Revised syntheses of L-serine azido acceptors	131
4.6.3. Glycosylation of armed thioglycosides with various acceptors for α/β -galactosyl building block formation.....	134
4.7. Stereoselective synthesis of α -galactoside building blocks for KRN7000 analogues ...	137
4.7.1. Effects of temperature and solvent on α -stereoselectivity of glycosylation reactions.....	138
4.7.2. Effects of remote protecting group participation using Li's method on α -stereoselectivity of glycosylation reactions	140
4.7.3. Effects of halide-ion catalysis on α -stereoselectivity of glycosylation using glycosyl iodides	143
4.7.4. Synthesis of glycolipids 4.14 and 4.16 using lipidic L-serine acceptors	146
4.8. Concluding remarks	152
Chapter 5: Synthesis of L-serinyl based macrocyclic analogues of KRN7000	
5.1. Introduction	155
5.1.1. Carbohydrate macrocycles	155
5.1.2. Carbohydrate macrocycles formed by CuAAC reactions	156
5.1.3. Cu catalysed azide-alkyne cycloaddition (CuAAC)	158
5.1.4. Mechanistic considerations of Cu(I) catalysed azide-alkyne cycloaddition.....	159
5.2. Research objective	160

5.3. Design strategy for the formation of macrocycles 5.14 and 5.15	162
5.3.1. Synthesis of thiogalactosyl donor 5.16	163
5.3.2. Synthesis of bifunctional galactosyl building block 5.17.....	166
5.3.3. Design Considerations of macrocycles 5.14 and 5.15.....	169
5.3.4. Synthesis of products possibly containing macrocycles 5.24 and 5.25	172
5.3.5. Elucidation of proposed macrocyclic mixture containing macrocycles 5.24, 5.25 and 5.26	181
5.3.6. Global debenylation of proposed macrocycles 5.24, 5.25 and 5.26.....	184
5.4. Conclusion and perspective	187
Chapter 6: Conclusions and future work	
6.1. Conclusions	190
6.2. Future work.....	191
Chapter 7: Experimental details	
7.1. General Procedures and Instrumentation	195
7.2. Experimental procedures.....	196
7.2.1. Experimental procedures for Chapter 2	196
7.2.2. Experimental procedures for Chapter 3	221
7.2.3. Experimental procedures for Chapter 4	234
7.2.4. Experimental procedures for Chapter 5	264
Bibliography	271
Author Publications.....	282

To my mother Mary and my late father Beartla

Acknowledgements

Firstly to my supervisor Dr. Trinidad Velasco-Torrijos, thank you for all the help and support throughout my Ph.D. I really appreciate all the work you have done. To my former Head of Department, Prof. John Lowry, thank you for the chats and encouragement throughout my years in Maynooth. To the current Head of Department, Dr. John Stephens thank you for your support. To all the lecturing and technical staff at NUIM I give a warm thank you. A special mention to Prof. Carmel Breslin for her help and encouragement with the Endeavour Award, to Noel who revived my computer several times and to Ria and Barbara who would bend over backwards. Thanks also to Dr. Frances Heaney, Dr. Denise Rooney, Dr. John McGinly. Thanks to Dr. Fintan Kelleher for the use of the hydrogenator, and to Dr. John O' Brien for NMR experiments.

To all the post graduate students, you have made my stay at NUIM both an amusing and entertaining place (and of course educational). To my undergraduate/postgraduate gang, it was nice to go the whole way through my education with you, despite all your little habits: Conor (sleepwalking and speaking with your mouth full), Joey (sleeping and eating), Lynn (cleaning everything in sight) and John M (moaning and multiplying everything by ten). I wouldn't have had it any other way! To Lorna (for her dreadful eating habits) and Rob (for his terrible sweat pants) it's been great craic in the lab. To a whole clatter of people it wouldn't have been the same without you: Ursula, Colin (even though you have ruined my image with those impersonations), Dec, John W, Dennis, Gillian, Claire, Richard, Finno, Ross, Ruth and Fi. A special thanks to FOXY (for endless chats and craic). Carol, thanks for helping me when I first came to the department even when I did break a column or two. Dec, on a similar vein, thanks for being my personal NMR assistant. That's chicks man!! Valeria, thanks for the chats at ciggie time. Trish, thanks for the bruises at hockey and John K, thanks for the chess lessons, I'm a pro now! Thanks to the Velasco gang: Lorna, Gama and Andrew. Thanks also to all the post grads I didn't

mention, everyone in the synthesis lab, the write-up room, the electrochemists and the in-betweeners.

To the gang at Melbourne, I thoroughly enjoyed my tenure with you. To my supervisor Assoc. Prof. Spencer Williams, Ben, Rowan, Zal, Chrissie, the Ilaria's and all the troops, I hope our paths will meet again. To all the girls (Sue, Aine, Jean, Aoife, Gill, Lisa and Sarah) and my music friends (Sean, Gearoid, Barry F, Tommy, Siobhan, Conor and Dara). I'm sorry I haven't spent as much time as I would have liked to spend with you this last year but needs must! Next year you will be sick of looking at me (and we'll kick ass at the ceili band competitions!). A special thanks to Elaine, for meeting me throughout the year for the chats. It was really appreciated.

Most importantly, a huge thank you goes out to my family. To Mam, thank you for feeding me, cleaning up after me, giving out to me and always looking out for me. To Dad, who gave me my love of music, I hope you are proud of your daughter and are smiling down at me. To Matt, my big bro, we didn't get a long enough time together (but the times we had were great). To Carmel, Colm, Aine, Fionnuala and Eoin thank you for listening to my moans and for giving me money when I was broke (so broke I was smoking rollies). Una, thank you for all the clothes I ruined in the lab. A special mention to my nieces and nephews: Niall, Aaron, Sarah, Ciara (my favourite godchild but also my only one), Cathal and Aisling also. To Barry, thank you so much for not complaining this last year and for distracting me with non-chemistry related topics. Don't worry it'll be worth it. Someday we will be filthy rich and that snooker table and yacht you are always harping on about will be ours!

Declaration

I hereby certify that this thesis has not been submitted before, in whole or in part, to this or any other university for any degree and is, except where otherwise stated, the original work of the author.

Signed: _____

Date: _____

Abstract

The focus of the novel research reported in this thesis is the synthesis of glycolipids for anti-microbial studies and to act as *i*NKT cell stimulatory ligands. Simple glycolipids, L-aspartic acid based glycolipids, glycolycerolipids and L-serine based glycolipids were explored.

Simple galactosyl glycolipids containing *O*- and *N*-glycosidic linkages and L-aspartic acid based glycolipids were constructed as in Chapter 2 with a view to test their anti-microbial properties against cystic fibrosis pathogens (*Burkholderia cepacia complex*). Preliminary testing of these glycolipids revealed promising anti-microbial activities. Glycolipids were also tested for their organogelator properties, whereby two of the compounds exhibited supramolecular assembly to form gels.

GI-X is a naturally occurring glycolipid found in the cell walls of certain *Mycobacteriaceae* species and has been reported to be involved in important biochemical processes. Intramolecular aglycon delivery, an elegant synthetic strategy for the construction of difficult 1,2-*cis* glycosidic linkages, was used in the formation of a GI-X analogue described in Chapter 3.

A series of L-serine based analogues of KRN7000, a potent *i*NKT cell ligand, were investigated in Chapter 4 to probe their potential application as immunomodulators. Focus was applied to the synthesis of a suitable building block which could provide access to a range of different analogues, possessing α - and β -glycosidic linkages. A short chain α -analogue of KRN7000 was successfully synthesised. A benzyl ether protected analogue of KRN7000, containing a 1,4-disubstituted 1,2,3-triazole moiety was also synthesised by a copper catalysed azide alkyne cycloaddition.

Preliminary investigations into a new class of rigid macrocyclic L-serinyl analogues of KRN7000 was explored in Chapter 5 using a copper catalysed azide alkyne cycloaddition as the key synthetic step. The synthesis of a monomeric macrocycle and a dimeric macrocycle was explored, both compounds protected as benzyl ethers to ultimately function as a new class of rigid *i*NKT cell stimulatory ligands.

Abbreviations

Ac = Acetyl

AgOTf = Silver trifluoromethanesulfonate

Atm = Atmospheric pressure

Bcc = Burkholderia cepacia complex

BnBr = Benzyl bromide

Boc = *t*-Butyloxycarbonyl

BrBnBr = Bromobenzyl bromide

BzCl = Benzoyl chloride

Cat. = Catalytic

CD = Cyclodextrins

CD1 = Cluster of differentiation 1

CF = Cystic fibrosis

CGC = Critical gelation concentration

COMO = (1-Cyano-2-ethoxy-2-oxoethylideneaminoxy)-dimethylamino-morpholino-carbenium hexafluorophosphate

COSY = Correlation spectroscopy

CuAAC = Copper(I)-catalyzed azide-alkyne cycloaddition

*d*₄-MeOD = Deuterated methanol

*d*₆-DMSO = Deuterated dimethylsulfoxide

*d*₆-Pyr = Deuterated pyridine

DBU = 1,8-Diazabicyclo[5.4.0]undec-7-ene

DC = Dendritic cell

DCE = Dichloroethane

DDQ = 2,3-Dichloro-5,6-dicyano-1,4-benzoquinone

DEPT = Distortionless enhancement by polarization transfer

DIAD = Diisopropyl azodicarboxylate

DIPEA = *N,N*-Diisopropylethylamine

DMAP = Dimethylaminopyridine

DMF = Dimethylformamide

DMSO = Dimethylsulfoxide

DTBMP = Di-*t*-butyl-4-methylpyridine

EMB = Ethambutol

Et = Ethyl

Fmoc = 9-Fluorenylmethyloxycarbonyl

FT-IR = Fourier transfer infrared spectrometry

α -GalCer = α -Galactosylceramide

HIV = Human immunodeficiency virus

HOBt = Hydroxybenzotriazole

HPLC = High performance liquid chromatography

HR-MS = High resolution mass spectroscopy

HSQC = Heteronuclear single quantum coherence

IAD = Intramolecular aglycon delivery

IFN- γ = Interferon- γ

IL-2 = Interleukin-2

INH = Isoniazid

*i*NKT = invariant Natural killer T

IR = Infrared spectroscopy

LAM = Lipoaribinomannan

LM = Lipomannan

LMWG = Low molecular weight organogelator

LPS = Lipopolysaccharide
MDR-TB = Multi-drug resistant tuberculosis
MeCN = Acetonitrile
Me = methyl
MIC = Minimum inhibitory concentration
MS = Molecular sieves
N₃ = Azide
NaOMe = Sodium methoxide
NBS = *N*-Bromosuccinimide
NIS = *N*-Iodosuccinimide
NMR = Nuclear magnetic resonance
PBB = *p*-Bromobenzyl
PBPh = *p*-Bromobenzylidene group
Pd(C) = Palladium on activated charcoal
PetEt = Petroleum ether
PIM = Phosphatidyl-*myo*-inositol mannoside
PMB = *p*-Methoxybenzyl
Pyr = Pyridine
PZA = Pyrazinamide
RCM = Ring closing metathesis
RIF = Rifampicin
Rt = Room temperature
SEM = Scanning electron microscopy
SM = Streptomycin
TB = Tuberculosis
TBAB = Tetrabutylammonium bromide

TBAI = Tetrabutylammonium iodide

TBDMS = *t*-Butyldimethylsilyl

TBDPS = *t*-Butyldiphenylsilyl

TBTU = *O*-Benzotriazol-1-yl-1,13,3-tetramethyluronium tetrafluoroborate

t-Bu = *t*-Butyl

TCR = T cell receptor

TDR-TB = Totally drug resistant tuberculosis

TEMPO = (2,2,6,6-Tetramethylpiperidin-1-yl)oxidanyl

TES= Triethylsilyl

Tf = Trifluoromethanesulfonate

TFA = Trifluoroacetic acid

T_{gs} = Gel to sol temperature

T_H1 = T helper 1

T_H2 = T helper 2

THF = Tetrahydrofuran

TIC = Total ion chromatogram

TLC = Thin layer chromatography

TLR4 = Toll like receptor 4

TMS = Trimethylsilyl

TNF- α = Tumor necrosis factor-alpha

TOCSY = Total correlation spectroscopy

TOF = Time of flight

Ts = Toluenesulfonyl

UV-Vis = Ultraviolet-visible spectroscopy

XDR-TB = Extensively drug-resistant tuberculosis

Chapter 1: Perspective

1.1. Glycolipids in nature: structure, occurrence and functions

Glycolipids contain one or more saccharide units bound to a hydrophobic lipid chain by a glycosidic bond. These hydrophobic chains can be attached either directly to the saccharide or via a linker. As a result of the amphiphilic nature of glycolipids, they commonly act as recognition molecules for both hydrophilic and lipophilic molecules within the biological system. In the context of medicine, this dual nature is often exploited, as is the case in the biological system. As a result the synthesis of glycolipids is also of great interests, both to chemists and biochemists alike.

Found in bacteria, plants and animals, glycolipids play key roles in pathogenesis of bacteria,^[1] photosynthesis,^[2] cellular recognition^[3] and immunogenic processes to name but a few.^[4] Their structures are varied and the carbohydrate component ranges from simple monosaccharides to complex oligosaccharides. Glycolipids found in bacteria and plants consist of simple alkyl glycolipids, glyco glycerolipids, lipopolysaccharides, resin glycolipids and glycosphingolipids. Glycolipids found in animals include glycosphingolipids and gangliosides. Figure 1.1 illustrates the principal structures of glycolipids commonly found in Nature. Some examples of these glycolipids and their biological functions are highlighted in Table 1.1.

1.1.1. Alkyl glycolipids

An abundance of simple alkyl glycolipids, comprising of fatty alcohols linked to a carbohydrate moiety by a glycosidic linkage, have been found in Nature, from animals, plants and microorganisms.^[5] One such example is the heterocyst glycolipid (Entry 1 in Table 1.1), who's structure consists of a glucose residue bound to a long chain diol through a glycosidic linkage. This glycolipid was isolated from the cyanobacterium *Anabaena* CCY9922 and was found to protect it against oxygen intake by creating a hydrophobic barrier.^[6] Sophorolipids and rhamnolipids (described in Chapter 2) are also nice examples of alkyl glycolipids and they display interesting properties such as surfactant and anti-microbial properties.^[5, 7]

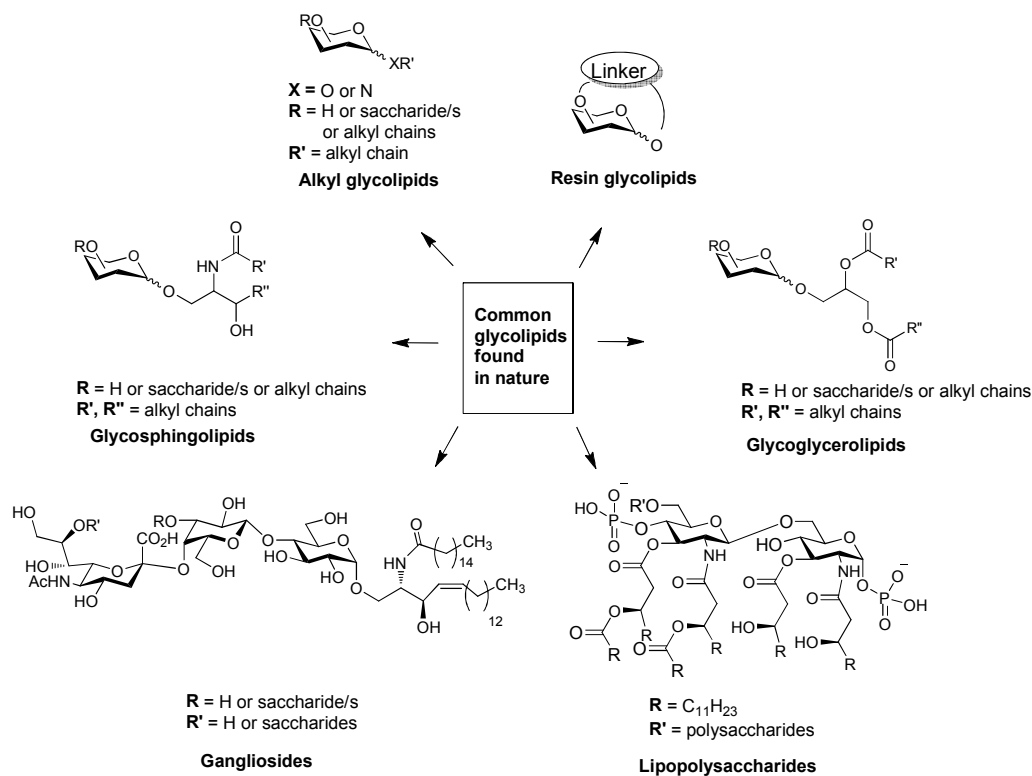
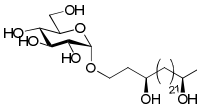
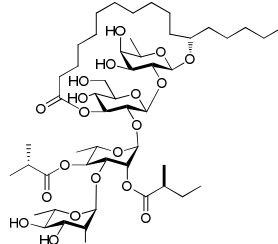
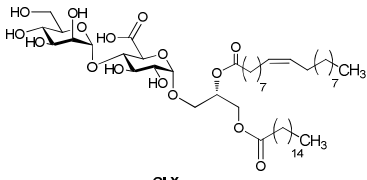
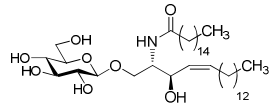
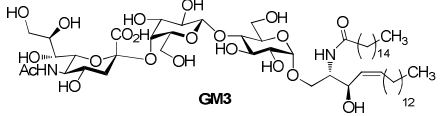


Figure 1.1 Principal structures of glycolipids found in bacteria, plants and animals.

1.1.2. Resin glycolipids

Resin glycolipids are glycolipids of plant origin, which are mainly isolated from *Convolvulaceae* (Morning Glory family) and *Scrophulariaceae* plants. Most resin glycolipids have macrocyclic structures in the form of a lactone, thus serve as interesting targets for total synthesis.^[8] Tricolorin A (Entry 2 in Table 1.1), a member of the resin glycoside family was first isolated in 1993 by Pereda-Miranda from the plant *Ipomoea tricolor Cav.*,^[9] a plant traditionally employed in Mexican horticulture as a weed controller. Tricolorin A was found to be the active ingredient in the inhibition of weed growth.^[9] The macrocycle was also found to have cytotoxic activity against human breast cancer cells.^[9] Other examples of resin glycolipids with biological relevance include woodrosin I, tricolorin G and calonyctin A.^[10]

Table 1.1 Examples of glycolipids found in nature and their biological function.

Entry	Classification (Occurrence in Nature)	Example	Biological Function	Ref
1	Alkyl glycolipid (Bacteria, Plants)	 heterocyst glycolipid	cyanobacterial cell wall protection against O ₂ uptake	[6]
2	Resin glycolipids (Plants)	 Tricolorin A	phytostimulant	[9]
3	Glycoglycerolipids (Bacteria, Plants)	 GI-X	involved in GI-LM biosynthesis in <i>C. glutamicum</i>	[12]
4	Glycosingolipids (Bacteria, Plants, Animals)	 Glucosylceramide (C_{16:0}/C_{18:1})	to maintain the water permeability barrier for skin	[18]
5	Gangliosides (Vertebrates)	 GM3	involved in neuronal cell death	[22]

1.1.3. Glycoglycerolipids

Glycoglycerolipids are lipids derived from a glycerol, in which one of the hydroxyl groups of the glycerol has been functionalised with a mono- or oligosaccharide. They are the most abundant class of glycolipids found in plants and bacteria. Monogalactosyldiacylglycerol, a member of the glycoglycerolipids is the most abundant glycolipid found in Nature.^[11] GI-X (Entry 3 in Table 1.1) is a glycoglycerolipid found in the bacterial cell walls of *C. glutamicum* and is involved in

GI-LM biosynthesis; it is implicated in the pathogenicity of the bacteria (discussed in Chapter 3, Section 3.5).^[12] Not only are glycolipids involved in important cellular functions such as structural support and membrane anchors, they have been shown to exhibit anti-tumour^[13] and autoimmune properties.^[14] Glycophospholipids are glycolipids that contain phosphate groups and a sugar moiety, but the majority of this class of compounds also contain a glycerol backbone and can be classified as glycolipids. This group of compounds are mainly found in the *Corynebacterineae* family, which includes *M. tuberculosis*, one of the most serious infectious diseases in the world.

1.1.4. Lipopolysaccharides

Lipopolysaccharides (LPS) are complex macromolecules found in Gram-negative bacteria that typically consist of a hydrophobic domain known as lipid A (endotoxin) linked to inner core oligosaccharides. These, in turn, are linked to outer core oligosaccharides which are bound to a distal polysaccharide as shown in Figure 1.2.^[15] They play key roles in the pathogenicity of Gram-negative infection and septic shock, and are also implicated in immunomodulation.^[16]

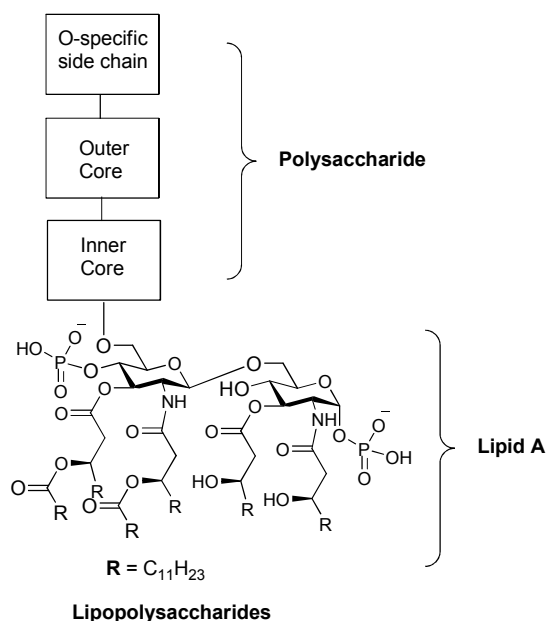


Figure 1.2 Principal structural regions of LPS glycolipids. The structure of Lipid A is given for an *Escherichia coli* strain F515.^[17]

1.1.5. Glycosphingolipids

Glycosphingolipids refer to lipids derived from a ceramide, in which the head group is either a mono- or oligosaccharide. Glucosylceramide (Entry 4 in Table 1.1) is an important glycosphingolipid that has been found in numerous animal tissues, such as in spleen and central nervous system as well as in individual cells such as erythrocytes.^[18] Glucosylceramide has also been found to be a major component of skin lipids, and it is believed to maintain a water permeability barrier for the skin.^[19] Furthermore glucosylceramides are also of importance in the biosynthesis of lactosyl ceramides and gangliosides.^[20] Another important glycosphingolipid termed α -GalCer (its synthetic analogue is known as KRN7000), was isolated from a marine sponge, *Agelas Mauritanus*.^[21] α -GalCer was found to be the first highly toxic iNKT cell stimulatory ligand (discussed in Chapter 4, Section 4.1.2) and has shown several promising therapeutic applications.^[22]

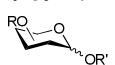
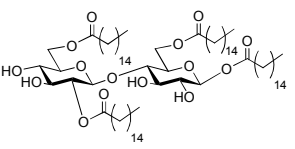

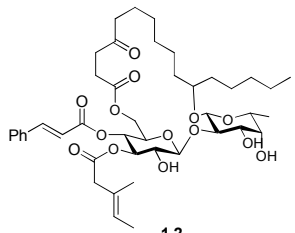
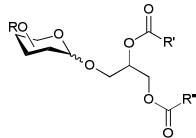
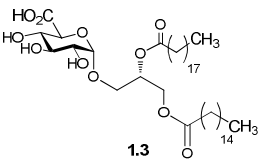
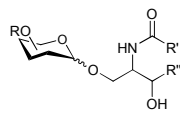
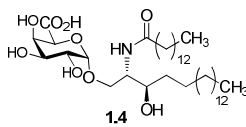
1.1.6. Gangliosides

Gangliosides are oligoglycosylceramides derived from lactosylceramide which contain sialic acid residues and are only found in vertebrates. In the naming of gangliosides, the Svennerholm designation is most frequently employed. For example, in the case of GM3 (Entry 5 in Table 1.1) the G refers to ganglioside, the M refers to monosialo- and the 3 refers to the number of neutral sugar chains in the ganglioside. Structural functions of gangliosides are varied and include roles in cell proliferation, differentiation, development, regeneration and death.^[17]

1.2. Synthetic glycolipids and therapeutic applications

Huge interest lies in the synthesis of glycolipids sharing the principal structures of natural glycolipids for therapeutic applications.^[23] Some examples of synthetic glycolipids reported in the literature and their biological applications are highlighted in Table 1.2.

Table 1.2. Examples of synthetic glycolipids and their therapeutic applications.

Entry	Classification (Principal Structure)	Example	Biological Application	Ref
1	<p>Alkyl glycolipids</p>  <p>R = H or saccharide or alkyl chains R' = alkyl chain</p>	 <p>1.1</p>	anti-tumour properties	[24b]
2	<p>Macrocyclic glycolipids</p>  <p>Linker</p>	 <p>1.2</p>	anti-tumour properties	[27]
3	<p>Glycoglycerolipids</p>  <p>R = H or saccharide/s or alkyl chains R', R'' = alkyl chains</p>	 <p>1.3</p>	stimulated a novel subtype of NKT cell in a CD1d dependent manner	[14]
4	<p>Glycosphingolipids</p>  <p>R = H or saccharide/s or alkyl chains R', R'' = alkyl chains</p>	 <p>1.4</p>	<i>i</i> NKT cell stimulatory ligand	[30]

1.2.1. Alkyl glycolipids

Despite their biological potential, relatively few studies have been carried out relating to the therapeutic applications of synthetic alkyl *O*-glycolipids. Nonetheless, synthetic alkyl glycolipids have been reported possessing anti-tumour^[24] and anti-microbial^[25] properties (discussed in detail in Chapter 2). They also have potential uses in autoimmune diseases.^[26] For example, *in vivo* studies on mice were performed using the maltose tetrapalmitate glycolipid **1.1** (Entry 1 in Table 1.2) and this compound exhibited strong immunogenic properties against cancer cell lines.^[24b] There is plenty of scope for further study of this simple class of glycolipids.

1.2.2. Macrocyclic glycolipids

Relatively few studies have been conducted on synthetic macrocyclic glycolipids owing to the structural complexities of the compounds, with the syntheses of resin glycolipids and their analogues taking up the majority of the scientific interest to date (discussed in detail in Chapter 5).^[8, 10, 27] The synthesis and biological evaluation was carried out on the Ipomoeassin family (Ipomoeassin A-F) by Nagano and co-workers, including a non-natural Ipomoeassin analogue **1.2** (Entry 2 in Table 1.2).^[27] This group reported anti-tumour properties against mice cell lines for the Ipomoeassin analogue, however weaker cytotoxicities were reported compared to the parent compound Ipomoeassin F.

1.2.3. Glycoglycerolipids

Scientific interest in the synthesis of glycoglycerolipids mainly concern phospholipids containing a glycerol backbone. Particular interest is held in the synthesis of glycoglycerolipids PIMs, LM and LAM and related glycolipids, which are found in the bacterial cell walls of *M. tuberculosis* (discussed in detail in Chapter 3).^[28] Related to these types of compounds are glucuronic based glycoglycerolipids which were also found in species of the *Corynebacterinaea* family.^[12] The synthesis of a glucuronic glycoglycerolipid GI-A **1.3** was executed by Uldrich *et al.* (Entry 3 in Table 1.2).^[14] This compound was found to stimulate a novel subtype of NKT cell, thus implicating the glycolipid as a therapeutic agent for cancer treatment. Synthetic glycoglycerolipids have also been used as tools in unravelling biological processes. For example, synthetic glycoglycerolipids were used in binding studies to eukaryotic cells, which provided strong evidence that glycoglycerolipids found in *A. laidlawii* participate in bacterial binding to eukaryotic cells.^[29]

1.2.4. Glycosphingolipids

Perhaps the most interesting class of synthetic glycolipids found in the literature relates to the glycosphingolipids, with the emergence of a synthetic glycosphingolipid known as KRN7000 displaying a range of therapeutic applications, from anti-viral to autoimmune properties (discussed in Chapter 4).^[22] Numerous synthetic analogues of this glycosphingolipid have been prepared and one such

glycolipid **1.4** is highlighted (Entry 4 in Table 1.2). Kinjo and colleagues synthesised a carboxylic glycosphingolipid amongst a range of other glycolipids and observed that the compound displayed improved *i*NKT cell stimulatory properties compared to the parent compound.^[30]

1.3. Research aims

Glycolipids play an important role in a variety of different biological processes, as outlined above. The study of glycolipids has aided in the understanding of how natural glycolipids interact biologically, and has also carved the path for numerous applications of glycolipids as biomedical and medicinal agents.^[23] As carbohydrate chemists, we are interested in the synthesis of a range of structurally diverse glycolipids with a view to assess their bioactivities, as anti-microbial agents or as *i*NKT cell stimulatory ligands.

In particular, we were interested in the synthesis of glycolipid mimetics incorporating amino acids (aspartic acid and serine) as linker moieties (Chapters 2 and 4). The role of the amino acid allows the introduction of two alkyl chains, for increased hydrophobic character. The aspartic acid glycolipids (Chapter 2) were designed to perform anti-microbial studies, along with a range of simple glycolipids. These anti-microbial studies will be performed in the laboratory of Dr. Siobhan McClean (Institute of Technology Tallaght) using the anti-adhesion methodology (described in Section 2.2). The serine glycolipids were designed to act as *i*NKT cell stimulatory ligands (described in Section 4.1.2). The biological evaluation will be performed by Dr. Derek Doherty (St. James Hospital, Dublin) on human *i*NKT cells.

Appropriate functionalization of the serine glycolipid mimetics allowed us to explore the synthesis of highly constrained macrocyclic derivatives (Chapter 5). We were interested to see whether the strained molecules would alter biological binding in the context of *i*NKT cells (Section 4.1.2). We were also interested in synthesising a glycoacylglycerolipid, a GI-X analogue (Section 3.5) for biochemical studies (Chapter 3). These biochemical studies may ultimately aid in the understanding of the role of GI-X and related glycolipids in bacterial cell walls.

Chapter 1: Perspective

Inherently to their amphiphilic nature, glycolipids can also exhibit interesting physiochemical properties, prompting them to act as surfactants and organogelators.^[5, 7, 31] By serendipity, we noted aspartic acid derivatives displayed organogelator properties. We completed preliminary investigations on the properties of some synthetic glycolipids as a result (Chapter 2).

**Chapter 2: Alkyl Glycolipids as Anti-Microbial Agents and
Organogelators**

2.1. Alkyl O-glycolipids and biological importance

Owing to their amphiphilic nature, glycolipids are surfactants. Surfactants are chemical compounds that display surface activity properties. They are adsorbed between different phases (e.g. air-liquid or liquid-liquid) and lower the interfacial tension between these phases, i.e. they can facilitate the formation of emulsions. Surfactants are thus largely utilised as detergents, wetting agents, emulsifiers, solubilisers, dispersing agents and foaming agents.^[7a] Biosurfactants are surfactants produced by microorganisms. These compounds offer several advantages over other surfactants commonly in use today which include high purity, biodegradability and the fact that they are obtained from renewable sources. This greater environmental compatibility, amongst other factors, leads to a significant commercial interest.^[32] Examples of biosurfactants include glycolipids, lipopeptides, phospholipids and fatty acids. Of special interest to the biomedical industry are the glycolipid biosurfactants, which include sophorolipids and rhamnolipids (Figure 2.1).^[5, 7]

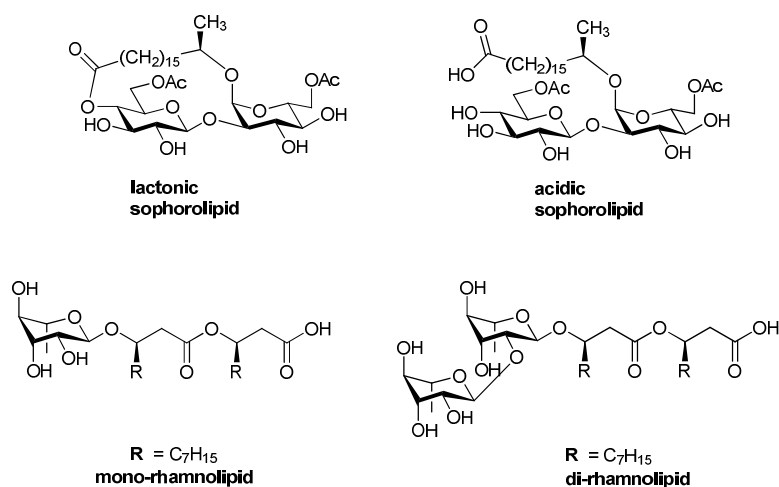


Figure 2.1 Examples of lactonic and acidic sophorolipids and mono- and di-rhamnolipids extracted from microorganisms.^[7a]

Sophorolipids are lipids obtained from the yeast *Candida* species, which were originally extracted from *C. bomicola*.^[33] They contain a sophorose disaccharide moiety (β -D-Glcpⁱ-(1 \rightarrow 2)-D-Glcp) linked via an α -glycosidic linkage to a fatty acid or a lactone ring to the C-4 position of the β -D-Glcp moiety. Rhamnolipids are lipids

ⁱD-Glcp refers to D-glucofuranose.

obtained from the Gram-negative *Pseudomonas* family which contain rhamnose units (a 6-deoxy sugar) linked to fatty acids, originally produced from the cultivation of *P. aeruginosa*.^[34] Not only do their surfactant properties lend to their use in cosmetics, but they also exhibit anti-microbial and anti-fungal activities.^[7a, 35]

Examples of anti-microbial studies carried out on synthetic alkyl *O*-glycolipids are limited. Matsumura and colleagues reported a range of simple alkyl glycolipids (Figure 2.2) that exhibited anti-microbial activity against Gram-positive bacterial strains (*Staphylococcus aureus* and *Bacillus subtilis*, *Sarcinalutea*), Gram-negative bacterial strains (*Pseudomonas aeruginosa*) and fungal strains (*Saccharomyces cerevisiae*, *Trichophytoninter digitale*).^[25] A summary of their findings appear in Table 2.1, where anti-microbial activities are represented in terms of minimum inhibitory concentrations (MICs). It was generally recognised that glycolipids **2.1-2.7** showed a broad spectrum of anti-microbial activity. In the glycolipids tested, dodecyl- α -D-mannopyransoide **2.3** was found to be the most effective anti-microbial candidate, with an MIC value of 5 $\mu\text{g}/\text{mL}$ for *S. lutea* (shown in red). Generally, it was observed that anti-microbial properties were influenced by the glycopyranosyl residue, the length of the lipid chain and the stereochemistry of the anomeric substituent. No glycolipids with longer alkyl substituents than C_{12} were tested in the current study.

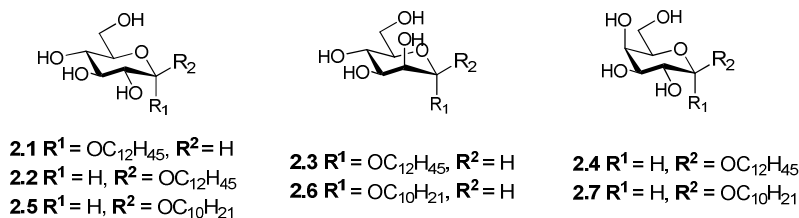


Figure 2.2 Structures of alkyl glycolipids used in anti-microbial evaluation.

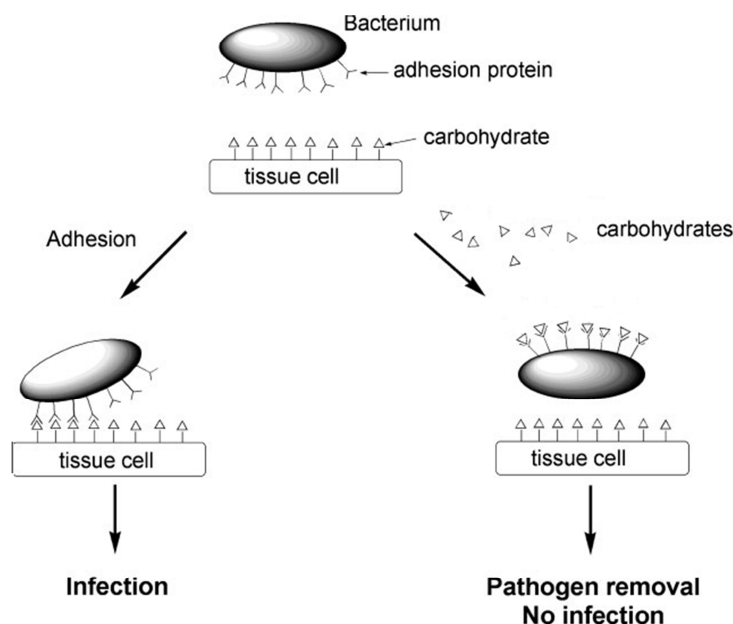
Table 2.1 Anti-microbial activity of alkyl glycolipids **2.1-2.7**.*

Entry	Bacteria/Fungi	MIC ($\mu\text{g/mL}$)						
		$\text{C}_{12}\alpha\text{Glc}$	$\text{C}_{12}\beta\text{Glc}$	$\text{C}_{12}\alpha\text{Man}$	$\text{C}_{12}\beta\text{Gal}$	$\text{C}_{10}\beta\text{Glc}$	$\text{C}_{10}\alpha\text{Man}$	$\text{C}_{10}\beta\text{Gal}$
		2.1	2.2	2.3	2.4	2.5	2.6	2.7
1	<i>S. aureus</i>	10	25	25	200	100	50	100
2	<i>B. subtilis</i>	25	50	25	200	100	50	100
3	<i>S. lutea</i>	10	50	5	200	50	25	50
4	<i>P. aeruginosa</i>	200	>400	>400	>400	200	200	400
5	<i>S. cerevisiae</i>	400	25	10	200	100	50	100
6	<i>T. interdigitale</i>	200	25	10	200	200	50	100

* Control always produced growth of the microorganism.

2.2. Anti-adhesion approach for anti-microbial studies

Anti-adhesion therapies are a novel approach in the treatment of bacterial infections. They represent a suitable alternative to the use of traditional antibiotics, as bacterial antibiotic resistance is becoming a major problem.^[36] This approach mimics nature. For example, human breast milk contains many oligosaccharides acting as anti-adhesives which protect infants against infection.^[37] A schematic representation of the anti-adhesion approach is illustrated in Scheme 2.1.^[38] The bacteria preferentially adhere to free carbohydrates, instead of adhering to the carbohydrate epitopes present at the cell surface (the lung epithelial cell, in this case). This renders the bacteria effectively unable to infect the cell, and is eventually excreted/secreted from the body.



Scheme 2.1 Bacterial adhesion to cells can result in infection (left). Free carbohydrates binding to the pathogen (right) prevent bacterial adhesion to cells and, as a result, prevents infection.^{[38]ii}

Cystic fibrosis (CF) is a genetically inherited disease caused by mutations in the cystic fibrosis transmembrane regulator (CFTR), which affects the transport of ions through the chloride channel. The main cause of death in people suffering with CF is chronic respiratory infections which result in lung damage and weakening of the lung function. *Burkholderia cepacia complex* (Bcc) is a group of opportunistic CF pathogens that invade lung epithelial cells.^[39] Studies from several countries indicate that two species of Bcc, *Burkholderia cenocepacia* and *Burkholderia multivorans*, account for most Bcc infection in CF patients.^[40] The mechanisms by which Bcc strains invade lung epithelial cells are not well understood. Krivan, and subsequently Sylvester, found Bcc isolates bound to galactose containing glycolipid receptors on the surface of lung epithelia.^[41] Developing their predecessors findings, McClean and co-workers provided the first evidence that galactose based glycolipids were involved in the invasion of Bcc isolates into lung epithelial cells.^[39a]

ⁱⁱ Illustration from Pieter and co-workers was edited.

The same research team reported that glycoconjugates containing terminal galactose moieties showed promising preliminary results in the inhibition of attachment of *B. multivorans* to human lung cells.^[42] The design of galactose containing glycolipids which can reduce bacterial adhesion to the lung epithelial cells of CF patients, and thus prevent infection, is therefore an attractive potential treatment.

2.3. *N*-glycosides and biological importance

N-glycosides contain an *N*-linked glycosidic bond, and are an important class of compounds because they are naturally present in many glycoproteins, proteoglycans, peptidoglycans and, to a lesser degree, glycolipids.^[43] As a result, numerous studies have been dedicated to analyse the biological effects of naturally occurring *N*-glycosides, their analogues and related compounds.^[43-44] *N*-linked glycolipids can be included in a special class of compounds, termed glycomimetics. Glycomimetics are small organic molecules designed to mimic the function of a naturally occurring carbohydrate, with improved pharmacological properties. Strong interest lies in the rational design of glycomimetic drugs as alternatives to complex and naturally occurring oligosaccharides.^[45] Glycomimetic drugs currently approved on the market are used for the treatment of diabetes (Voglibose)ⁱⁱⁱ,^[46] anti-viral agents (Zanamivir)^[47] and anticoagulants (Fondaparinux).^[48] The structures of these compounds are shown in Figure 2.3. Voglibose serves as an example of an *N*-glycoside glycomimetic drug.

ⁱⁱⁱ Brackets contain trade names of currently approved glycomimetic drugs.

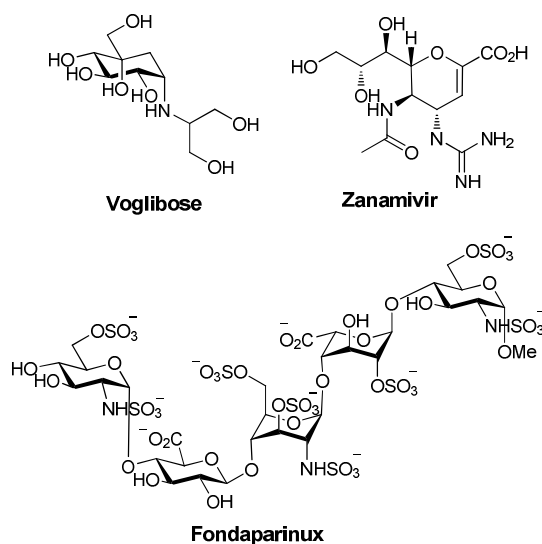


Figure 2.3 Glycomimetic drugs currently on the market: Voglibose, Zanamivir, Fondaparinux, all acting as enzyme inhibitors.^[46-48]

Recent progress regarding the use of *N*-linked glycosides and other glycomimetics in microbial anti-adhesion have been reviewed by Imberty and co-workers, and many of the processes discussed involve glycoconjugate-lectin interactions.^[49] Marotte and colleagues described the synthesis of a ligand for PA-IIL, a calcium-dependent lectin from *P. aeruginosa*. This bacteria is also an opportunistic pathogen which causes respiratory-track infections and may cause death in CF patients.^[50] As in the case for Bcc isolates described earlier, this lectin displays specificity for both D-galactose and L-fucose containing compounds.^[51] It was later found that this lectin also showed a high affinity for Lewis a (Figure 2.4), with a high K_d value of 210 nM.^[52] Marotte and co-workers synthesised the structurally simpler glycomimetics **2.8** and **2.9** (Figure 2.4), with an aim to obtain higher affinities than that observed for the trisaccharide Lewis a. However, they obtained lower binding to the lectin compared to Lewis a (K_d of 310 and 290 nM, respectively). Undeterred, Marotte and colleagues developed a second generation glycomimetic **2.10** (Figure 2.4), and successfully observed a higher affinity compared to Lewis a (K_d of 90 nM).^[53] To the best of our knowledge, no *N*-linked glycolipids have been studied for their anti-microbial properties with Bcc isolates.

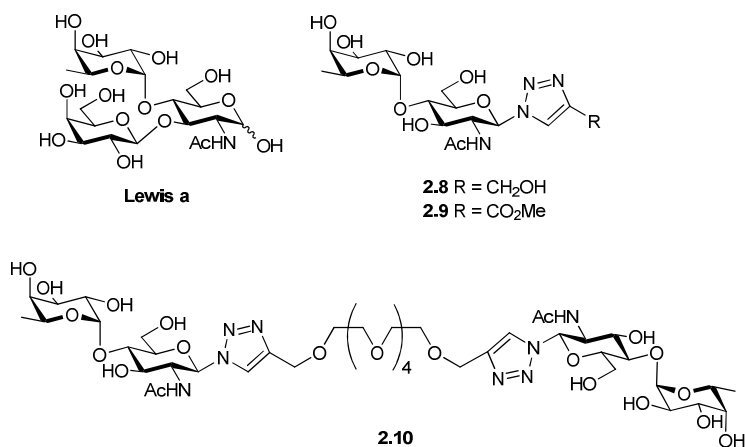


Figure 2.4 Structure of ligands for PA-IIL: structure of the natural epitope Lewis a, and structures of first generation glycomimetics **2.8** and **2.9** and second generation glycomimetic **2.10**.^[52-53]

2.4. Organogelators

A gel may be defined as a semi-solid formulation having an external solvent phase, which can be organic (in organogels) or aqueous (in hydrogel), and is immobilized within the available spaces of a three-dimensional network structure.^[54] This network is generated by a gelator species. Gels can be classified into two types: polymer gels (in which the gelator network is linked by covalent bonds) or supramolecular gels (in which the gelator network is held together by non-covalent interactions).^[55] The polymer gel network is completely covalent in nature, and as a direct result the formation of such gels is an irreversible process. Examples of polymer gels include silica and cross-linked polymers. Supramolecular gels display characteristic reversible transformations from the gel phase to the solution phase (generally denoted as gel→sol transitions) at mild temperatures, as a consequence of the weaker nature of these non-covalent interaction. Proteins, peptides and saccharides can act as gelators in certain solvents to generate supramolecular gels.^[54]

Low molecular weight organogelators (LMWGs) are low molecular weight compounds that can immobilise organic solvents through the formation of

supramolecular networks (Figure 2.5).^[56] Interactions such as hydrogen-bonding,^[57] electrostatic interactions,^[58] π - π stacking^[58] and London dispersion forces^[59] play fundamental roles in the self-assembly of LMWGs.

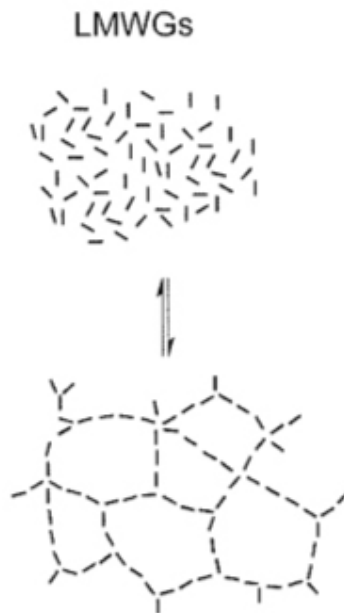


Figure 2.5 Schematic representation of LMWG formation by supramolecular networks.^[60]

To date, only a limited number of LMWGs have been documented in the literature, and most have been found by serendipity rather than by design. Anthracene derivatives **2.11** and **2.13**,^[61] fatty acids such as **2.12**,^[62] amino acids including **2.14**,^[63] the glycolipid **2.15**,^[31] triazole containing peptidomimetic **2.16**^[64] and L-aspartic acid based derivative **2.17**^[65] are some representative examples of LMWGs (Figure 2.6).

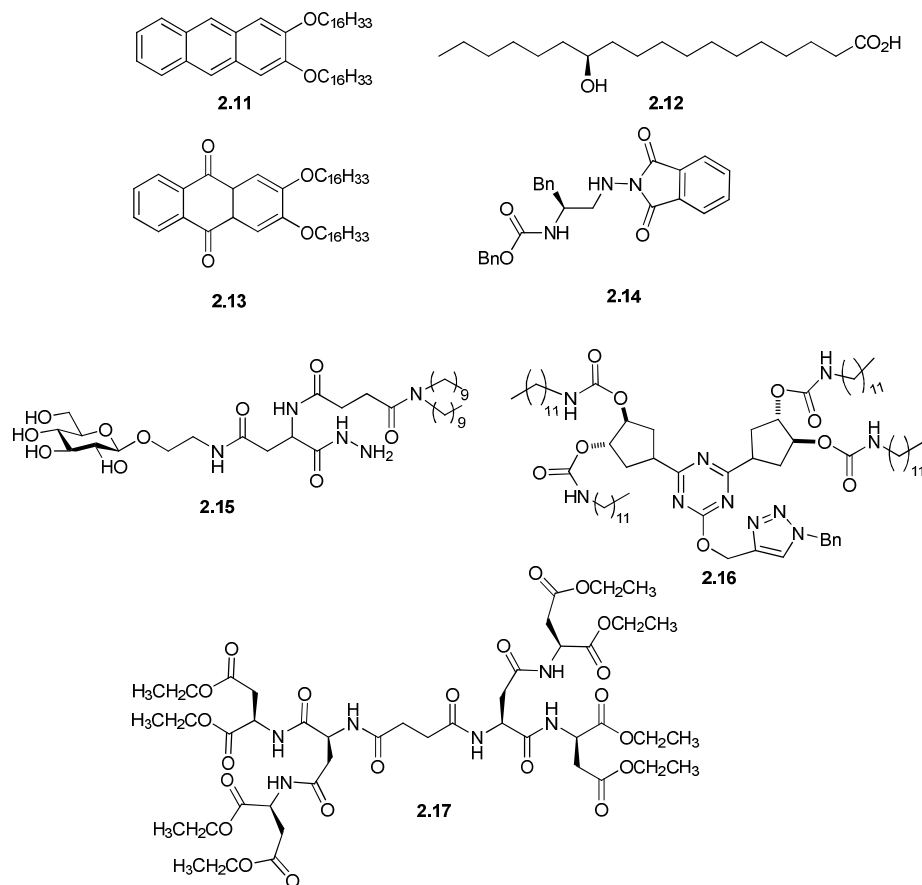


Figure 2.6 Chemical structures of some LMWGs.^[31, 61-65]

Intense interest lies in the development of LMWGs due to their potential applications as organic soft materials. One exciting area involves their use as templates for the preparation of nanosized structures.^[66] The process involves i) formation of the organogel in a polymerisable solvent; ii) polymerisation of the matrix; iii) solvent extraction of organic gelling agent. This is termed the “gel-template leaching process” and allows the formation of porous membranes with channels of micrometer and sometimes nanometer dimensions. Another application of LMWGs is in the development of new drug-delivery systems, by taking advantage of the thermoreversibility of this class of materials.^[67] One such example reported the use of L-alanine based organogels encapsulating a bioactive agent (leuprolidine) in a solvent mixture of safflower oil and *N*-methyl pyrrolidone, and this formulation was injected subcutaneously into rats. A slow release period of 14-25 days was observed for the system, with biodegradation of the L-alanine based gelling agent, indicating its biocompatibility.^[68]

2.5. Research objective

This chapter describes the synthesis of the simple *O*-glycolipids **2.18** and **2.19**, a simple *N*-linked glycolipid **2.20** and L-aspartic acid based *N*-linked glycolipids **2.21-2.23** (Figure 2.7). These glycoconjugates were intended for evaluation of their anti-microbial activities. Importantly, all of the designed glycolipids contain a terminal galactose head group. As discussed earlier in section 2.2, McClean *et al.* reported that galactose based glycolipids on lung epithelial cells from CF patients mediated bacterial adhesion of Bcc isolates.^[39a] With a view to explore their potential usage in biomedical applications, we investigated the possibility that synthetic galactosyl glycolipids may preferentially bind to Bcc instead of the galactosides on the surface of the epithelial lung cells and therefore, prevent infection by an anti-adhesion approach.

We aimed to synthesise galactose based *O*-glycolipids **2.18** and **2.19** using Koenig-Knorr methodologies to compare the different alkyl length on the anti-microbial results. As discussed earlier, promising anti-microbial results were reported by Marotte *et al.* of a triazole containing glycolipid **2.10** carried out on the bacterium *P. aeruginosa*.^[53] We aimed to synthesise the novel 1,4-disubstituted-1,2,3- triazole containing *N*-glycolipid **2.20** using a CuAAC reaction. Ultimately we aimed to probe the effect that the introduction of aromaticity in the glycolipid structure would have on their anti-microbial activity.

We were also interested in the synthesis of a range of novel L-aspartic acid based *N*-glycolipid mimetics **2.21-2.23**. The presence of the L-aspartic acid linker would provide a suitable scaffold for introducing functionalities into the molecule as necessary, whereby two different alkyl chains could be introduced to the glycolipids. Various different length chains could also be investigated and the anti-microbial studies performed to investigate the effect of the hydrophobic chains.

Preliminary anti-microbial studies were carried out on compounds **2.19** and **2.22**, as representative examples of these synthetic *O*- and *N*-glycolipid mimetics, for their potential application in an anti-adhesion approach for Bcc infection. By chance, we observed organogelator properties for one aspartic acid derivative. Therefore we

investigated the ability of some of these amphiphilic glycolipids to act as LMWGs in a range of organic solvents of different polarities, in order to explore the potential biomedical applications of this type of glycoconjugates.

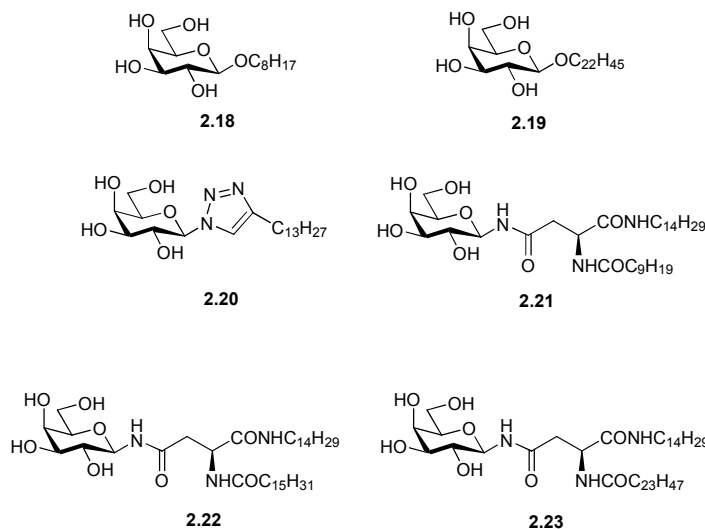
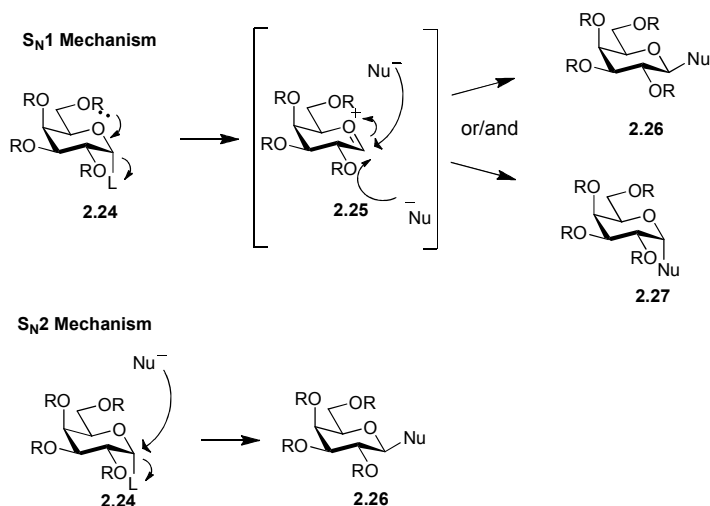


Figure 2.7 Structure of simple *O*-glycolipids **2.18**, **2.19**, *N*-glycolipid **2.20** and L-aspartic acid based *N*-glycolipids **2.21-2.23**.

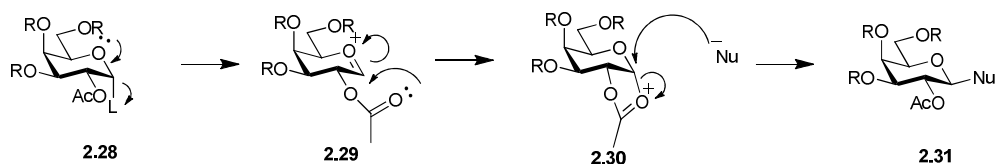
2.6. Synthesis of simple *O*-linked glycolipids **2.18** and **2.19**

In carbohydrate chemistry, one of the main challenges is to control the stereochemical outcome of the nucleophilic substitution at the anomeric centre during the formation of an *O*-glycosidic bond.^[69] Both $\text{S}_{\text{N}}1$ and $\text{S}_{\text{N}}2$ type reactions can occur at the anomeric centre. $\text{S}_{\text{N}}1$ reactions give a mixture of anomers as shown in Scheme 2.2. The configuration of the product at the anomeric carbon depends on which face the nucleophilic attack to the oxycarbenium ion **2.25** takes place, allowing the possible formation of both products **2.26** and **2.27**. The occurrence of an $\text{S}_{\text{N}}1$ reaction can depend on various parameters, including solvent choice, reaction time and the type of protecting groups used. $\text{S}_{\text{N}}2$ reactions result in an inversion of stereochemistry at the anomeric position with respect to the configuration of the leaving group. An example of an $\text{S}_{\text{N}}2$ reaction is shown in Scheme 2.2.



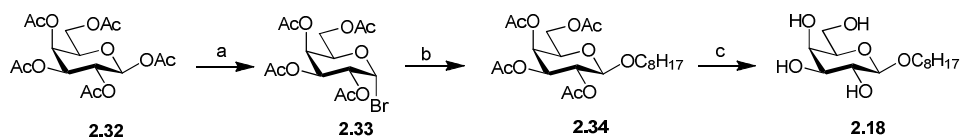
Scheme 2.2 S_N1 mechanism allows the formation of 1,2-*trans* product **2.26** or 1,2-*cis* product **2.27** while S_N2 mechanism involves an inversion of the configuration of the anomeric carbon with respect to that of the leaving group, to form the 1,2-*trans* product **2.26**. R groups refer to any protecting groups; L refers to leaving group.

One strategy for controlling the stereochemical outcome of the glycosylation reaction makes use of a phenomenon called neighbouring group participation. An ester protecting group, such as an acetyl protecting group at the C-2 position, facilitates neighbouring group participation to give the 1,2-*trans* product **2.31**, as shown in Scheme 2.3. The leaving group (L) is displaced at the anomeric centre of glycosyl donor **2.28** to form the oxycarbenium ion **2.29**. Participation by the carbonyl oxygen stabilises the oxycarbenium ion **2.29** to form the corresponding cyclic oxonium ion **2.30**. S_N2 type attack of a nucleophile occurs with an inversion of configuration to give a 1,2-*trans* product. For example, a β-galactoside **2.31** was selectively formed in Scheme 2.3. If an ester is not present at the C-2 position of the sugar, neighbouring group participation cannot occur and the reaction can proceed via either an S_N1 or S_N2 mechanism which can result in a mixture of anomers (Scheme 2.2). Thus, in the majority of cases, the synthesis of 1,2-*trans* glycosides (by using of an ester protecting group at the C-2 position) involves simpler purification and a more efficient procedure than those used for the corresponding 1,2-*cis* glycosides.



Scheme 2.3 Formation of a 1,2-*trans* product **2.31** resulting from neighbouring group participation of the C-2 protecting group.

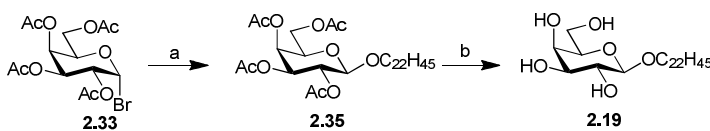
The synthesis of the short chain glycolipid **2.18** was first explored using the classic Koenigs Knorr methodology as shown in Scheme 2.4. A Koenigs Knorr glycosylation involves the reaction of a glycosyl halide, as a glycosyl donor, with a variety of glycosyl acceptors, using halophilic activators (such as AgCO_3 or AgOTf) to activate the anomeric halide leaving group. Many successful glycosylations have been reported in the literature using this methodology, due to the straightforward synthesis of the glycosyl donors and to the high yields of the glycosylation reactions.^[70] The synthesis of the galactosyl halide **2.33** was performed following a literature procedure, where *per*-acetylated galactose **2.32** was treated with 33% HBr/AcOH to give the desired galactosyl bromide **2.33** in a 96% yield (Scheme 2.4).^[71] The reaction of the galactosyl bromide **2.33** with octanol in the presence of Ag_2CO_3 and I_2 for 22 h yielded the acetyl protected β -glycolipid **2.34** in a 17% yield. Global deacetylation of the protected glycolipid **2.34** was performed using Zemplén conditions (NaOMe in MeOH) to yield the desired glycolipid **2.18** in a 90% yield. The spectroscopic data of glycolipid **2.18** was in agreement with the literature.^[72]



Scheme 2.4 Reagents and conditions. a) 33% HBr/AcOH , CH_2Cl_2 , rt, N_2 , 2 h, 96%; b) Ag_2CO_3 , I_2 , octanol, 4 Å MS, N_2 , 22 h, 17%; c) NaOMe , MeOH , 0 °C, 2 h, 90%.

We envisaged the synthesis of the C_{22} alkyl chain glycolipid **2.19** (Scheme 2.5) to be more difficult than that of the C_8 alkyl chain glycolipid **2.18** because of the increased length of the hydrocarbon chain, as it is documented that the lipid chain length is known to affect glycolipid and fatty alcohol solubility.^[73] Initial investigations led us

to react the galactosyl halide **2.33** with docosanol under the same reaction conditions described earlier using Ag_2CO_3 , I_2 , and docosanol in CH_2Cl_2 . However, none of the desired glycolipid **2.35** was detected by TLC or ^1H NMR analysis after 22 h of reaction time.



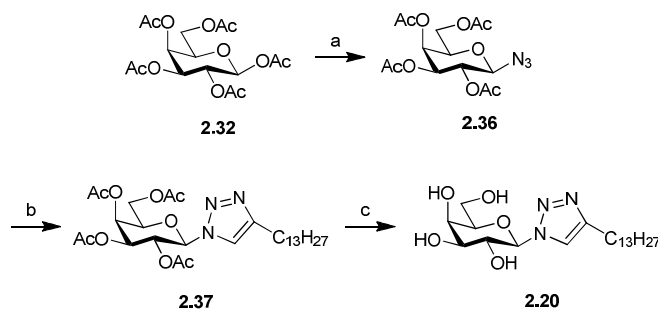
Scheme 2.5 Reagents and conditions. a) Ag_2CO_3 , I_2 , docosanol, CH_2Cl_2 , 4Å MS, N_2 , 22 h, 11%; b) NEt_3 , THF/MeOH/ H_2O , rt, 48 h, 50%.

Optimisation of the reaction involved grinding of the docosanol with a mortar and pestle to increase the surface area of the fatty alcohol particles and improve its solubility. A reverse addition approach was used for the glycosylation reaction, whereby the glycosyl bromide **2.33** was added to a suspension of ground docosanol containing Ag_2CO_3 and I_2 in CH_2Cl_2 to afford the desired glycolipid **2.35** in an 11% yield (Scheme 2.5). Global deprotection of the acetyl protecting groups on glycolipid **2.35** involved the use of mild basic hydrolysis using catalytic NEt_3 in a tricomponent solvent system of THF/ H_2O /MeOH. The deprotected glycolipid **2.19** was precipitated in 50% yield after 48 h of reaction time, with the filtrate consisting of unreacted starting material **2.35**. Attempts to hydrolyse the filtrate using the same conditions over a longer period of time (96 h) resulted in degradation of the precursor glycolipid **2.35**.

2.7. Synthesis of 1,4-disubstituted 1,2,3-triazole containing β -*N*-glycolipid **2.20**

As part of our continuing studies on a chemical approach to carbohydrate-based antibacterial agents, we were interested in synthesising the 1,4-disubstituted 1,2,3-triazole containing β -*N*-glycolipid **2.20**. We intended to compare its ability to inhibit bacterial adhesion to that of the simple *O*-glycolipids **2.18** and **2.19** (described in Section 2.6). The synthesis of the *N*-glycolipid **2.20** began with the reaction of the *per*-acetylated galactosyl donor **2.32** with TMSN_3 , promoted by the Lewis acid SnCl_4 at rt to yield 80% of the β -galactosylazide **2.36** (Scheme 2.6).^[74] A subsequent

CuAAC reaction (discussed in detail in Chapter 5) with pentadecyne using a promoter system of $\text{CuSO}_4 \cdot 5\text{H}_2\text{O}$ and sodium ascorbate afforded the novel 1,4-disubstituted 1,2,3-triazole *N*-glycolipid **2.37** in a regiospecific manner and in a yield of 89%. Global deacetylation was achieved using Zemplén conditions (NaOMe, MeOH) at a low temperature to afford the *N*-glycolipid **2.20** in an 88% yield. Structural characterisation was carried out using specific optical rotations and ^1H NMR, ^{13}C NMR, IR and HR-mass spectrometry on the novel *N*-glycolipid **2.20**.



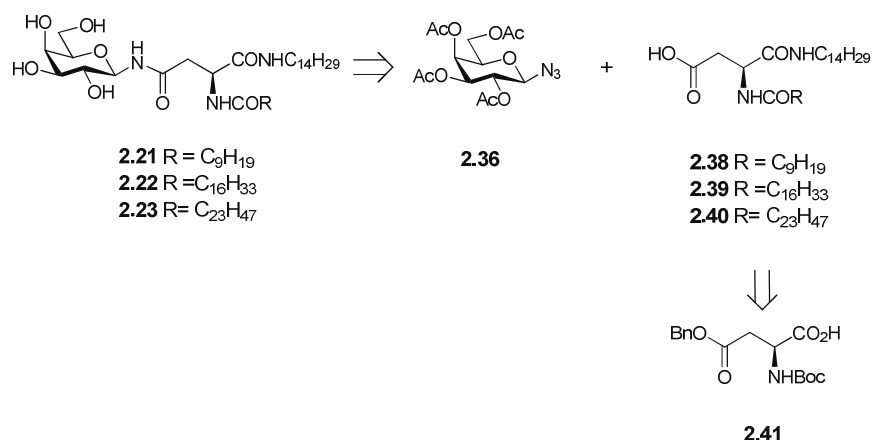
Scheme 2.6 Reagents and conditions. a) SnCl_4 , TMSN_3 , CH_2Cl_2 , N_2 , 18 h, 80%; b) pentadecyne, $\text{CuSO}_4 \cdot 5\text{H}_2\text{O}$, Na ascorbate, THF/MeOH/ H_2O , 48 h, 89%; c) NaOMe, MeOH, 0 °C, 1 h, 88%.

2.8. Synthesis of L-aspartic acid based β -*N*-glycolipids **2.21-2.23**

The structure of the L-aspartic acid based *N*-glycolipids **2.21-2.23** were designed to introduce a spacer group that would allow the functionalization of the glycolipids with two hydrocarbon chains. The naturally occurring amino acid L-aspartic acid features an acid group on its side chain, which would allow for the connection with the galactosyl moiety through the formation of an amide bond. The carboxylic acid and amino groups at the α -carbon of the L-aspartic acid would also allow for the introduction of hydrocarbon chains through the formation of amide bonds. We were interested in incorporating alkyl chains of different lengths (C_{10} , C_{16} and C_{24}) onto the L-aspartic acid derivatives to compare their effect on the anti-microbial properties of each of the *N*-glycolipids **2.21-2.23** respectively.

The retrosynthetic approach for the synthesis of the *N*-glycolipids is shown in Scheme 2.7, whereby the easily accessible β -galactosyl azide **2.36** and the commercially available protected L-aspartic acid derivative **2.41** serve as suitable

building blocks. The glycosyl azide **2.36** serves as a precursor to a glycosyl amine. The glycosyl amine can be reacted with aspartic acid derivatives **2.38-2.40** using a peptide coupling reaction, followed by global deprotection to yield the *N*-glycolipids **2.21-2.23**. The aspartic acid derivatives **2.38-2.40** can be obtained by reaction of aspartic acid derivative **2.41** with tetradecylamine, followed by *N*-Boc deprotection and a subsequent peptide coupling reaction with fatty acids of various different lengths.

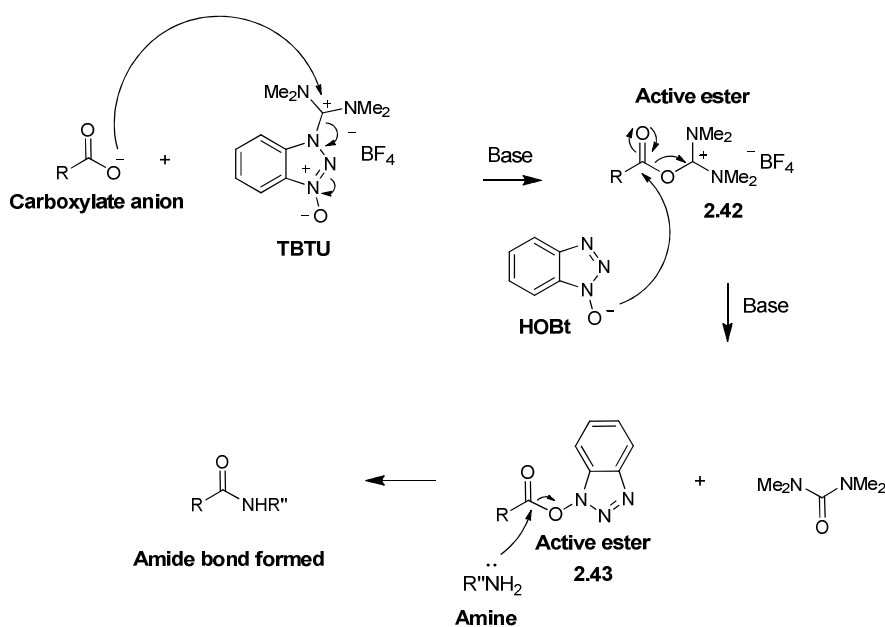


Scheme 2.7 Retrosynthesis of L-aspartic acid glycolipids **2.21**, **2.22** and **2.23** from the building blocks galactosyl azide **2.36** and L-aspartic acid derivative **2.41**.

2.8.1. Initial attempts to synthesise the β -*N*-glycolipid **2.23**

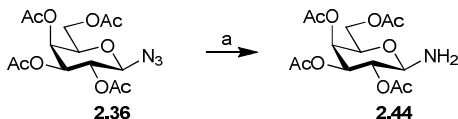
A plethora of methods for the formation of the amide bonds have been reported in the literature, with the different types of coupling reagents and conditions evolving every day.^[75] Various different coupling reagents have been developed, such as azides, active esters, acyl halides, anhydrides, carbodiimides, pyrocarbonates, isoxazolium, phosphonium and phosphonic salts, immonium salts and aminium salts to name but a few.^[75] In the realm of this work, only the use of aminium salts will be described. TBTU and HBTU are two popular aminium coupling reagents. TBTU (*O*-benzotriazol-1-yl)-1,13,3-tetramethyluronium tetrafluoroborate), as the name suggests was first believed to have a uronium structure, but crystal and solution studies revealed that it has an aminium structure.^[76] When used in conjunction with HOBt, minimal racemisation occurs during amide bond formation,

as HOBt acts as a racemisation suppressant.^[77] HOBt was first introduced in 1970 by König and Geiger^[78] with carbodiimide coupling reagents, and has been used as an additive with various different methodologies ever since. However, present day use of HOBt has diminished due to the explosive nature of the anhydrous form which has hindered transport due to safety concerns. Oxyma (ethyl(hydroxyimino)cianoacetate),^[79] or COMU (1-cyano-2-ethoxy-2-oxoethylideneaminoxy)-dimethylamino-morpholino-carbenium hexafluorophosphate) serve as safer alternatives.^[80] A reaction mechanism for the coupling of a carboxylic acid and an amine with TBTU and HOBt is proposed in Scheme 2.8. The mechanism proceeds with attack of the carboxylate anion (generated under basic conditions) to the TBTU aminium carbocation to form an active ester species **2.42**. Subsequent attack of HOBt to the electrophilic carbon of the active ester **2.42** in basic conditions yields a second active ester intermediate **2.43**, which is then attacked by the amine to lead to the formation of a new amide bond.



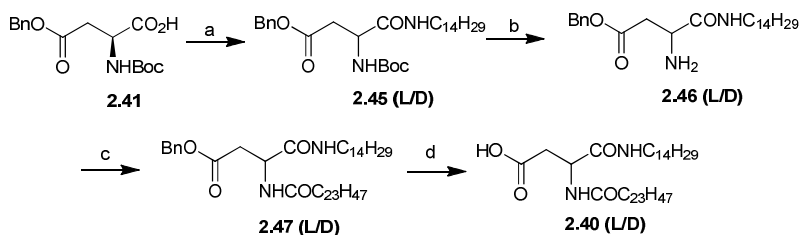
Scheme 2.8 Reaction mechanism of TBTU and HOBt coupling reagents to form a new amide bond.

First, the synthesis of the β -galactosyl amine **2.44** was performed by reduction of the galactosylazide **2.36** (described in Scheme 2.6) by hydrogenolysis to yield 96% of the β -galactosyl amine **2.44** (Scheme 2.9).^[74]



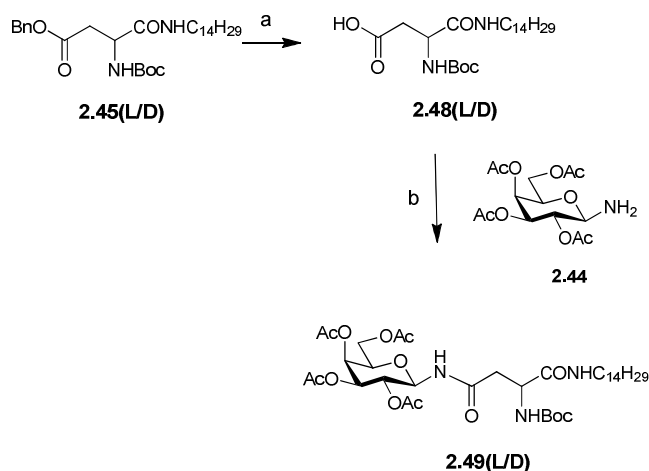
Scheme 2.9 Reagents and conditions. a) H₂, Pd (C), EtOAc, 1 atm, rt, 18 h, 96%.

The synthesis of the L-aspartic acid derivative **2.48** (Scheme 2.10) commenced with the coupling of the commercially available *N*-Boc-L-aspartic acid-4-benzyl ester **2.41** with tetradecylamine using TBTU/ HOBt with NEt₃ to yield 87% of the building block **2.45 (L/D)**. *N*-Boc deprotection of the amino derivative **2.45(L/D)** using TFA in CH₂Cl₂ afforded 77% of the desired free amine **2.46(L/D)**. This material was subsequently coupled to tetracosanoic acid using TBTU/HOBt coupling conditions with NEt₃ to yield 89% of the benzyl ester building block **2.47(L/D)**. Deprotection of the benzyl ester of L-aspartic acid derivative **2.47(L/D)** to yield the free carboxylic acid **2.40(L/D)**, suitable for coupling to the galactosyl amine **2.44**, proved to be a difficult task. Attempts at deprotection of the benzyl ester using Lewis acid catalysed deprotection (SnCl₄ in CH₂Cl₂),^[81] basic hydrolysis (2 N NaOH solution in CH₂Cl₂) or harshly acidic conditions (10 equivalents of BF₃·OEt₂ in CH₂Cl₂) failed. Reduction of the benzyl ester could only be achieved by bubbling of the H₂ gas (instead of a balloon as previously attempted) at 50 °C in EtOAc at 1 atm, to yield the carboxylic acid aspartic acid derivative **2.40(L/D)** in a 72% yield.



Scheme 2.10 Reagents and conditions. a) TBTU, HOBt, NEt₃, tetradecylamine, DMF, 4Å MS, rt, 3 h, 87%; b) TFA, CH₂Cl₂, 0 °C, 3 h, 77%; c) tetracosanoic acid, TBTU, HOBt, NEt₃, DMF, 4Å MS, rt, 18 h, 89%; d) H₂, Pd (C), EtOAc, 50 °C, 2 h, 72%.

Structural elucidation was carried out on the building block **2.45(L/D)** using ^1H NMR and HR-MS spectrometry, and the ^1H NMR values seemed to correlate to the values described in the literature for the desired product **2.45(L)**.^[82] However, we observed a specific optical rotation value of 0 for the tetradecylamine aspartic acid derivative **2.45(L/D)**, which indicated that racemisation had occurred during the reaction. Although the combination of TBTU and HOBT in peptide coupling reactions is common place,^[75] the activation of the α -carboxylic acid in the building block **2.41** under these conditions is likely to increase the acidity of the α -proton, and it may be abstracted in the presence of a base such as NEt_3 . To the best of our knowledge, the racemisation of this common building block for peptide synthesis under the reaction conditions described above had not been explicitly described in the literature prior to our report.^[83] In order to confirm that racemisation had occurred in this step using ^1H NMR evidence, the benzyl ester in the racemised aspartic acid derivative **2.45(L/D)** was deprotected with H_2 , Pd (C) in EtOAc to yield 97% of the carboxylic acid **2.48(L/D)**. This was then coupled with the galactosylamine **2.44** using TBTU and HOBT to yield 59% of the *N*-Boc protected *N*-glycolipid **2.49(L/D)** as a racemic mixture (Scheme 2.11).



Scheme 2.11 Reagents and conditions. a) H_2 , Pd (C), EtOAc, rt, 18 h, 97%, b) TBTU, HOBT, DMF, 4 Å MS, rt, 18 h, 59%.

The racemisation now only became evident by ^1H NMR spectrometry with the introduction of the chiral sugar moiety. The ^1H NMR spectrum in Figure 2.8 shows

N-glycolipid **2.49(L/D)** as a mixture of diastereoisomers, which confirms that racemisation has occurred. Duplication of the amide protons of the NHBoc protecting groups (5.7 and 6.2 ppm) was the clearest indication of this. Also, the signals corresponding to the β -protons (2.5 and 2.8 ppm) looked more complicated than expected for a single diastereoisomer of compound **2.49(L/D)**. A mixture of diastereoisomers was much more clearly observed during the synthesis of a more flexible aspartic acid derivative **2.51(L/D)** (Scheme 2.12), which was being undertaken in the Velasco-Torrijos laboratory,^[83] which was obtained from the racemised **2.41(L/D)**, thereby supporting the findings reported herein.

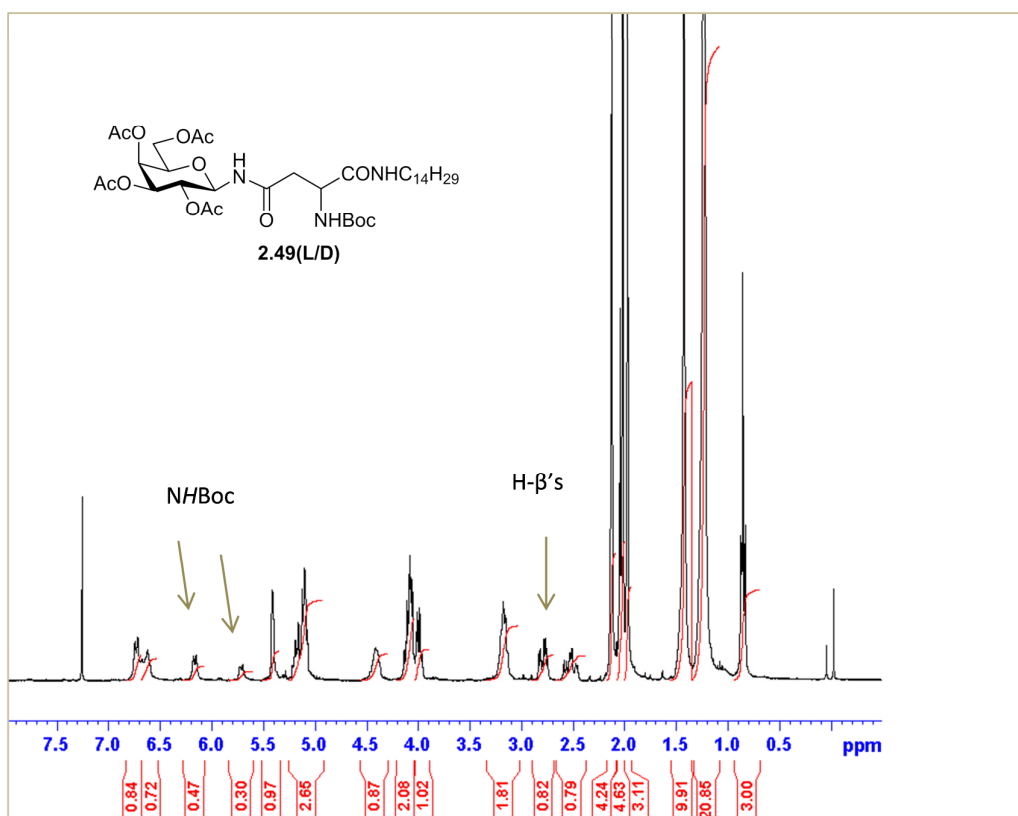
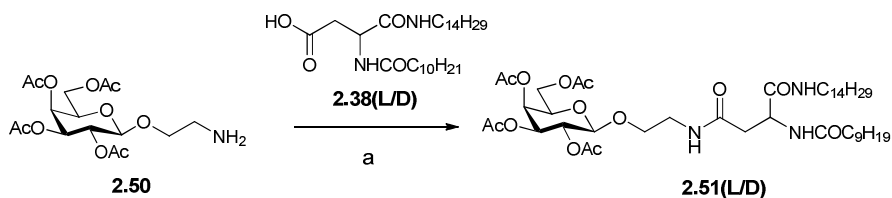
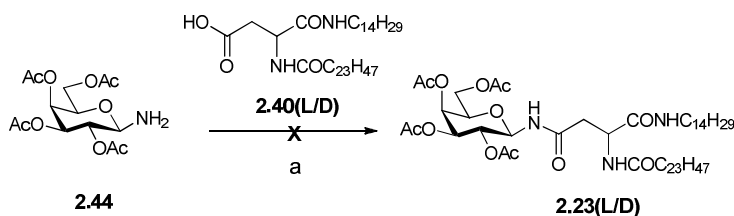


Figure 2.8 ¹H NMR spectrum of racemised *N*-glycolipid **2.49(L/D)** showing duplication of certain signals.



Scheme 2.12 Reagents and conditions. a) TBTU, HOBT, NEt₃, DMF, 4 Å MS, N₂, rt, 18 h.^[83]

Song and colleagues recently found that an anomeric mixture of a series of *O*-galactolipid derivatives were revealed to be more toxic against several cancer cell lines than their single component with the pure α - or β -configuration.^[84] Therefore, despite the problematic racemisation, the synthesis of the aspartic acid building block **2.23(L/D)** (Scheme 2.13) was still desirable to compare the anti-microbial properties of the resulting mixture of diastereoisomers **2.23(L/D)** to a single L-diastereoisomer **2.23**. The coupling of this derivative **2.40(L/D)** with the galactosyl amine **2.44** using the TBTU/HOBT methodology using NEt₃ in DMF was next performed (Scheme 2.13). However, none of the desired product **2.23(L/D)** was formed, possibly due to the presence of the two long hydrocarbon chains in **2.40(L/D)**. The ¹H NMR spectrum showed a complicated and unidentifiable mixture of products. This approach was abandoned for this reason.

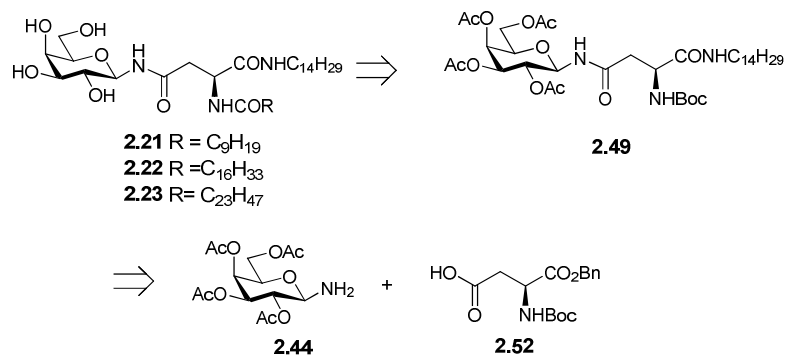


Scheme 2.13 Reagents and conditions a) TBTU, HOBT, NEt₃, DMF, 4 Å MS, N₂, 18 h.

2.8.2. Alternative method to form β -N-glycolipid 2.21- 2.23

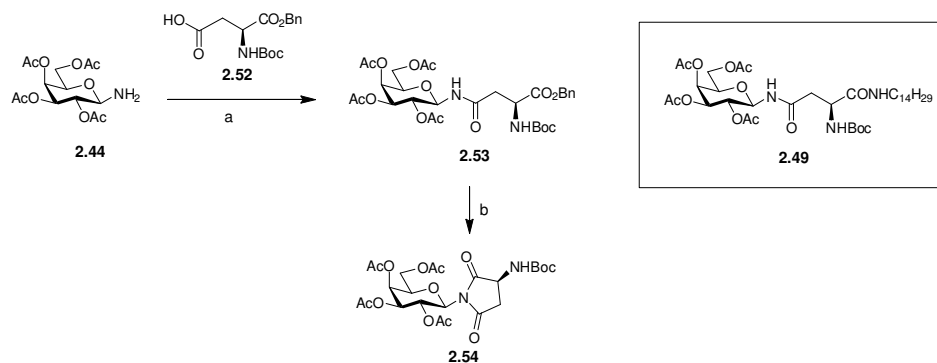
With these observations in mind, we carefully constructed an alternative synthetic approach in the quest to synthesise the various L-aspartic acid derivatives **2.21-2.23**. A retrosynthetic pathway was proposed as in Scheme 2.14. We chose to introduce the galactosyl moiety early on in the methodology to ensure a means of

observation (by NMR spectroscopy) whether racemisation had occurred. We also chose to perform the activation of the C- α in the absence of base to maintain the L-configuration at the α -position of the L-aspartic acid derivatives **2.21-2.23**.



Scheme 2.14 Alternative retrosynthesis of β -*N*-glycolipid **2.21**, **2.22** and **2.23** using galactosylamine **2.44** and L-aspartic acid derivative **2.52**.

The synthesis of the building block **2.53** described previously by Harrison and colleagues, was performed by reaction of the galactosyl amine **2.44** and the commercially available *N*-Boc-L-aspartic acid-1-benzyl ester **2.52** using TBTU/HOBT coupling conditions with DIPEA in DMF to yield 71% of the β -*N*-glycoside **2.53** (Scheme 2.15).^[85] Deprotection of the benzyl ester was performed by reaction with H₂, Pd (C) in EtOAc at rt for 18 h to yield 81% of the crude carboxylic acid, which was reacted with tetradecylamine using TBTU/HOBT in DMF in the absence of base (to avoid racemisation). However, none of the desired β -*N*-glycolipid building block **2.49** was obtained. Instead a novel cyclic by-product **2.54** (Figure 2.9) was obtained as a major product in the reaction (48%). The ¹H NMR spectrum (Figure 2.9) of the product **2.54** with characteristic signals are highlighted including the H-2 proton with an unusually high chemical shift (6.1 ppm), the anomeric proton (5.5 ppm), the α -proton (4.2 ppm) and the β -protons (2.7 ppm – 3.2 ppm). The H-2 proton was found to resonate in a chemical environment typical for a succinimide product containing a carbamate group.^[86] ¹³C NMR analysis, IR analysis and HR-MS confirmed its formation also.



Scheme 2.15 Reagents and conditions. a) TBTU, HOBT, DIPEA, DMF, 4 Å MS, N₂, rt, 18 h, 71%; b) i) H₂, Pd (C), EtOAc, rt, 18 h, 81%; ii) Tetradecylamine, HOBT, TBTU, DMF, rt, 4 h, 48%. Desired glycoside **2.49** in step b was not isolated.

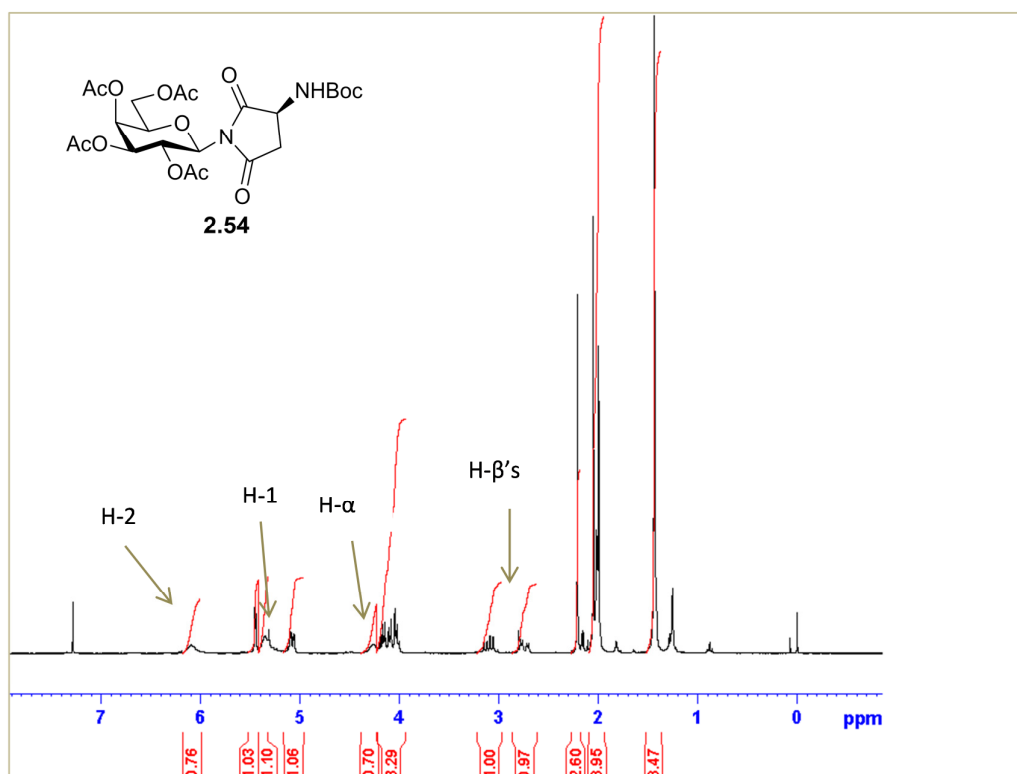


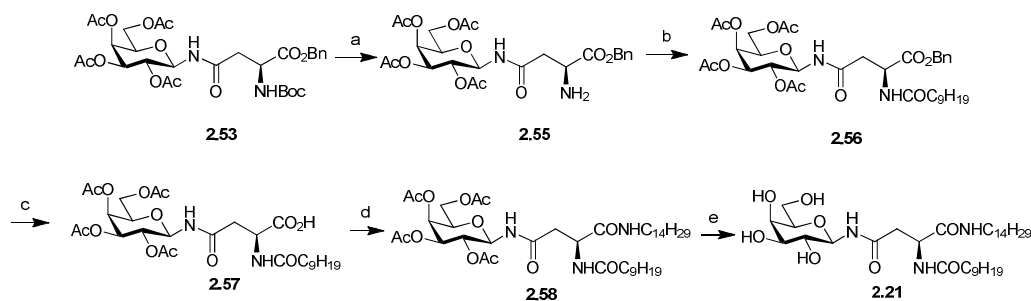
Figure 2.9 ¹H NMR spectrum of undesired succinimide product **2.54** with characteristic signals highlighted.

It is well documented that L-aspartic acid derivatives are susceptible to cyclic imide formation through dehydration reactions so this cyclisation comes as no major surprise.^[87] We hypothesise the formation of a thermodynamically favourable 5-

membered ring could occur from the attack onto the activated carboxylic ester by the nucleophilic anomeric amide nitrogen atom, driven by the formation of the TBTU based leaving group. In order to combat this undesired cyclisation reaction, we changed the synthetic approach whereby we planned to functionalise the amino moiety with alkyl chains prior to functionalization of the carboxylic ester of building block **2.52** in the hope that it would discourage/minimise the cyclisation.

2.8.3. Synthesis of *N*-glycolipid **2.21**

The revised synthesis of the novel L-aspartic acid derivative **2.21** proceeded smoothly, as shown in Scheme 2.16. The synthesis began with the removal of the *N*-Boc amine protecting group of the L-aspartic acid building block **2.53** under acidic conditions (TFA in CH₂Cl₂) to afford 74% of the free amine building block **2.55**. A peptide coupling reaction of the free amine **2.55** (synthesised as described in section 2.8.1) with pre-activated decanoic acid with TBTU/HOBt, coupling conditions and DIPEA, gave the novel benzyl ester protected building block **2.56** in a yield of 54%. Reduction of the benzyl ester to give the free carboxylic acid by hydrogenolysis catalysed by Pd (C) afforded a yield of 61% of **2.57**, which was used without further purification. A coupling reaction of acid **2.57** was performed using the TBTU/HOBt methodology in the absence of external base with tetradecylamine to give a 55% yield of the protected *N*-glycolipid **2.58**. Finally, mildly basic cleavage of the acetyl protecting groups was performed with catalytic NEt₃ in a homogenous solvent system (CH₂Cl₂/MeOH/H₂O, 1:2:1) at 40 °C to yield the glycolipid **2.21** in a 22% yield after 18 h. In order to push the reaction to completion, the remaining unreacted starting material was treated under the same conditions (NEt₃ in CH₂Cl₂/MeOH/H₂O). However, the reaction resulted in complete degradation of the starting material, with evident cleavage at the amide bonds as observed by ¹H NMR spectroscopy. No further optimisations were performed to achieve higher yields of the *N*-glycolipid **2.21**.



Scheme 2.16 Reagents and conditions. a) TFA, CH_2Cl_2 , 0°C to rt, 6 h, 74%; b) i) Decanoic acid, TBTU, HOBT, DIPEA, DMF, 4 \AA MS, N_2 , rt, 20 min ii) **2.55**, 18 h, 54%; c) H_2 , Pd (C), EtOAc, rt, 3 h, 61%; d) i) TBTU, HOBT, DMF, 4 \AA MS, N_2 , rt, 30 min ii) Tetradecylamine, 3 h, 55%; e) NEt_3 , $\text{CH}_2\text{Cl}_2/\text{MeOH}/\text{H}_2\text{O}$ 1:2:1, 40°C , 18 h, 22%.

Structural elucidation of the acetyl protected glycolipid **2.58** was carried out with ^1H NMR and ^{13}C NMR spectrometry. Assignment of the signals was confirmed by 2D NMR (COSY, HSQC) experiments. The ^1H NMR spectrum of glycolipid **2.58** (Figure 2.10) clearly indicates only a single diastereoisomer **2.58** is present, corresponding to an L-configuration of the chiral center in the L-aspartic acid backbone. The characteristic signals belonging to the amide protons (NH(H- α), NH(C-1) and NHCH_2 at 7.6, 6.9 and 6.8 ppm respectively) are highlighted. Also highlighted are the signals corresponding to the H- α (4.8 ppm) and the methyl protons of the acetyl protecting groups (2-2.4 ppm). A signal present at 7.1 ppm (1: 0.1 desired N-glycolipid **2.58**: cyclised product **2.59**) was indicative of the amide proton of a succinimide side-product **2.59** (Figure 2.11) which must have formed from intramolecular attack during the activation of the carboxylic acid **2.57**, as discussed earlier. HR-MS confirmed its presence in the reaction mixture.

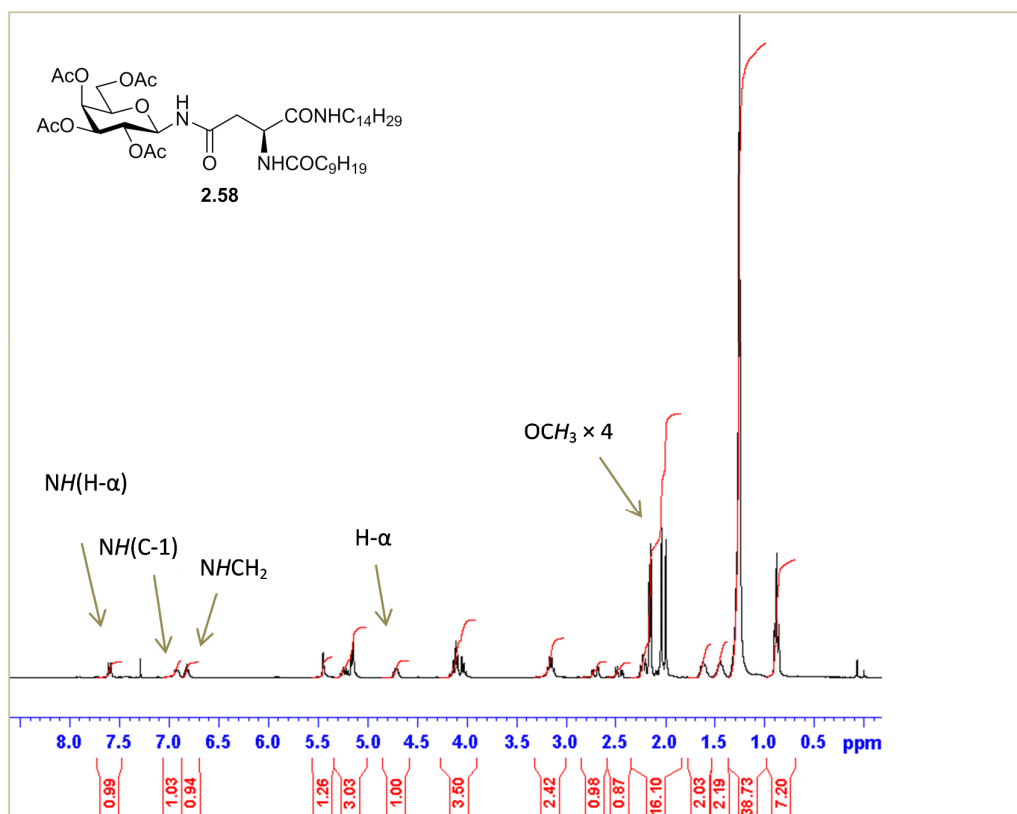


Figure 2.10 ^1H NMR spectrum of acetyl protected *N*-glycolipid **2.58**. Characteristic signals are highlighted.

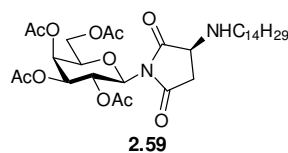


Figure 2.11 Structure of the undesired succinimide side-product **2.59**.

Structural elucidation was difficult to perform on the *N*-glycolipid **2.21** as the solubility of the final deprotected compound was poor in many organic solvents. After solubility tests in various different solvents, the *N*-glycolipid **2.21** was found to be partially soluble in Pyr. ^1H NMR and ^{13}C NMR analysis was performed in d_6 -Pyr. Structural elucidation was confirmed by HR-MS and IR spectrometry. The ^1H NMR spectrum of the *N*-glycolipid **2.21** is shown in Figure 2.12. The characteristic signals are highlighted in the figure, including the proton signals of the amide protons (at 10.1, 9.0, 8.5 ppm respectively), the anomeric proton (at 5.9 ppm) and the α -proton

(at 5.7 ppm). Fortunately, no signals corresponding to the deprotected cyclic product were observed, and this was confirmed by HR-MS.

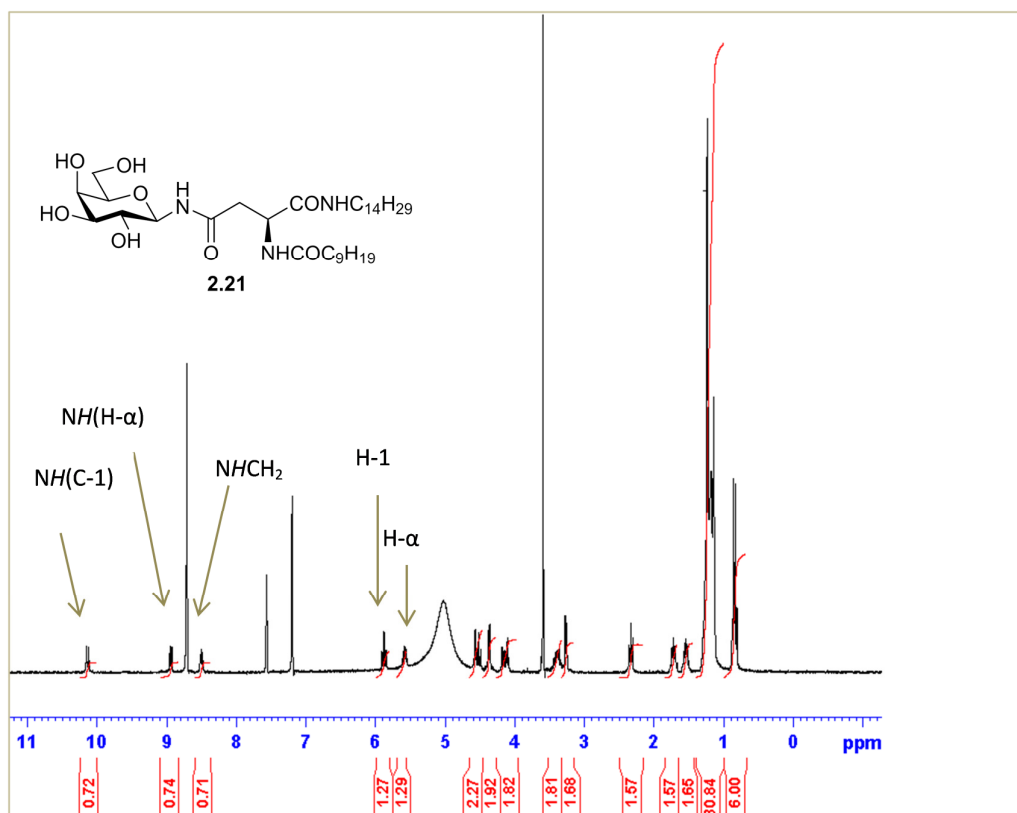
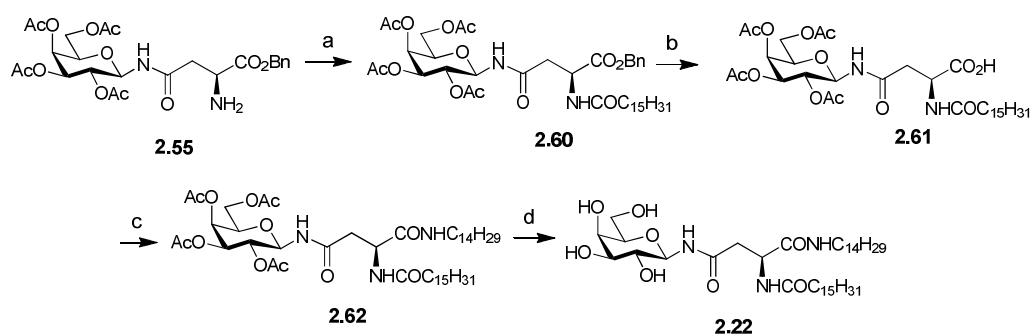


Figure 2.12 ^1H NMR of *N*-glycolipid **2.21** in $\text{d}_6\text{-Pyr}$. Characteristic signals are highlighted.

2.8.4. Synthesis of *N*-glycolipid **2.22**

The construction of the hexadecanoyl derivative of L-aspartic acid **2.22** generally proceeded in a smooth fashion, with increased yields compared to the shorter chain *N*-glycolipid **2.21**. The synthesis began with the reaction of the free amine **2.55** (described in Section 2.8.3) with hexadecanoyl chloride to obtain a 42% yield of the building block **2.60** (Scheme 2.17). Hydrogenolysis of the benzyl ester with H_2 and Pd (C) allowed access to the carboxylic acid **2.61** in 86% yield, which was reacted with tetradecylamine with TBTU/ HOBT to afford the protected *N*-glycolipid **2.62** in 98% yield. As discussed earlier in Section 2.8.3, a small signal at 7 ppm (1:0.2 ratio desired *N*-glycolipid **2.62**: cyclic product), corresponding to a cyclic

succinimide side-product, was present in negligible amounts in the ^1H NMR spectrum of the reaction mixture.



Scheme 2.17 Reagents and conditions. a) Hexadecanoyl chloride, NEt₃, CH₂Cl₂, 4Å MS, N₂, rt, 18 h, 42%; b) H₂, Pd (C), EtOAc, rt, 18 h, 86%; c) i) TBTU, HOBT, DMF, 4Å MS, N₂, rt, 30 min ii) tetradecylamine, 18 h, 98%; d) NEt₃, CH₂Cl₂/MeOH/H₂O 1:2:1, 40 °C, 18 h, 50%.

Deprotection of the acetylated *N*-glycolipid **2.62** using NEt₃ in CH₂Cl₂/MeOH/H₂O afforded the novel β -*N*-glycolipid **2.22** as a white precipitate in a yield of 50%. Structural elucidation of the novel *N*-glycolipid **2.22** was carried out using ^1H NMR and ^{13}C NMR spectrometry. The assignment of the signals was confirmed by 2D NMR (COSY, HSQC) experiments. The solubility of the deprotected *N*-glycolipid **2.22** was limited in many organic solvents. ^1H NMR and ^{13}C NMR analysis was carried out in *d*₆-Pyr. The ^1H NMR spectrum of β -*N*-glycolipid **2.22** is displayed in Figure 2.13. Possibly due to the limited solubility of the hexadecanoyl derivative *N*-glycolipid **2.22** in *d*₆-Pyr, the signals in the ^1H NMR spectrum are very broad. Characteristic signals are evident in the spectrum, albeit the multiplicities of the signals were impossible to ascertain. No signals for the corresponding cyclisation side product were evident in the ^1H NMR spectrum, and again this was confirmed by HR-MS spectrometry.

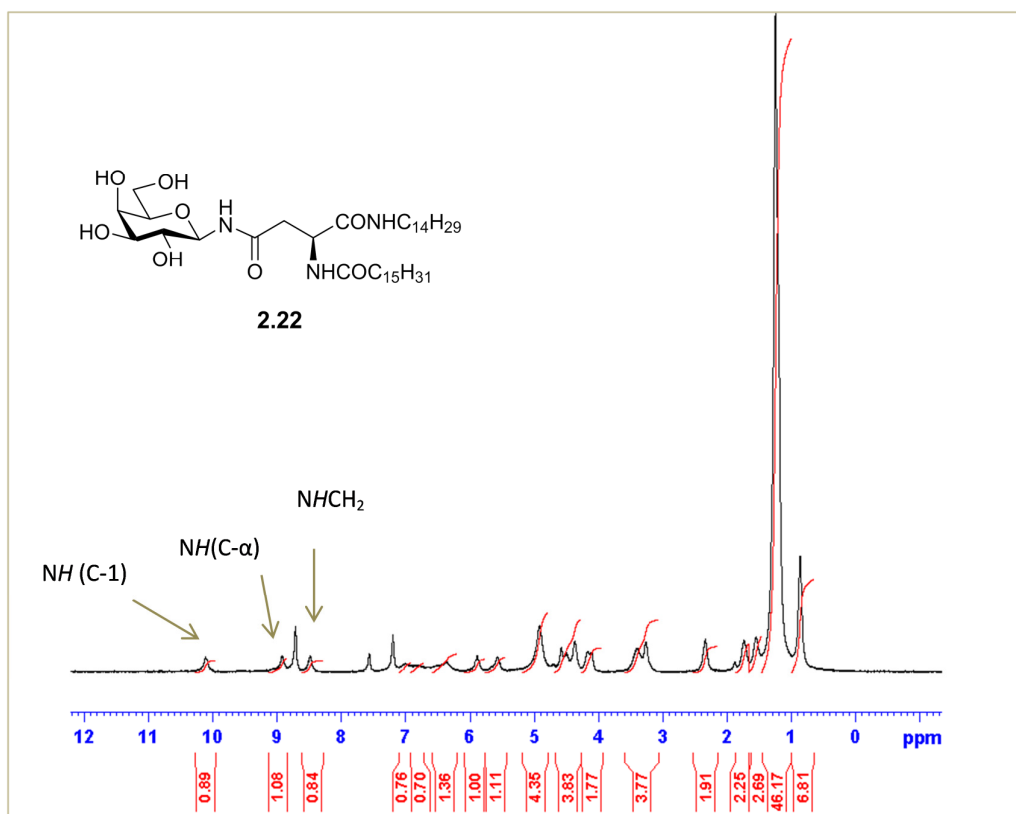
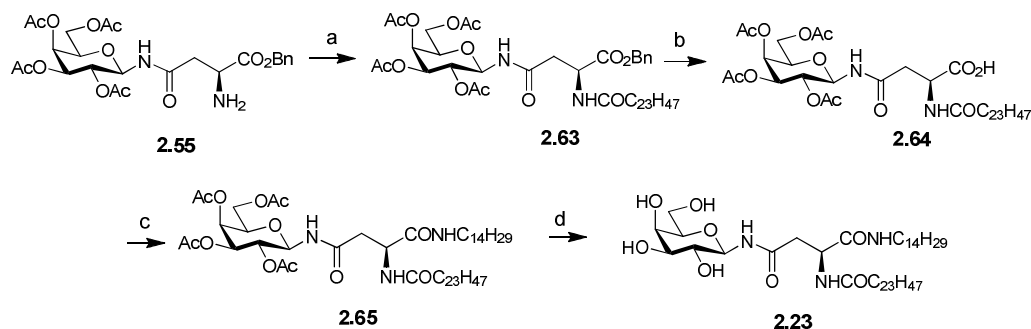


Figure 2.13 ¹H NMR spectrum of *N*-glycolipid **2.22** in *d*₆-Pyr. Characteristic signals are highlighted.

2.8.5. Synthesis of *N*-glycolipid **2.23**

The novel tetracosanoyl derivative of L-aspartic acid **2.23**, featured a long hydrocarbon (C₂₄) acyl chain and was synthesised using very similar conditions to those used for the short acyl chain (C₁₀) *N*-glycolipid **2.21** and medium chain (C₁₆) derivative **2.22** (Scheme 2.18). Coupling of the free amine building block **2.55** with tetracosanoic acid using the TBTU/HOBt methodology afforded a yield of 42% of the desired compound **2.63** upon heating to 50 °C. The moderate yield was due to the poor solubility of the tetracosanoic acid in DMF. Deprotection of the benzyl ester of intermediate **2.63** afforded the carboxylic acid **2.64** in 55% yield, which was subsequently reacted with TBTU/ HOBt followed by tetradecylamine, to yield 45% of the acetylated *N*-glycolipid **2.65**. As discussed previously (Sections 2.8.3 and 2.8.4), a signal at 7 ppm (1: 0.4 desired *N*-glycolipid **2.65**: cyclised product) was observed in the ¹H NMR of *N*-glycolipid **2.65**, indicating the formation of an

undesired intramolecular cyclisation product during the reaction of glycolipid **2.64**, albeit in a small amount. Deprotection by mild basic conditions using NEt_3 in a homogenous solvent system ($\text{CH}_2\text{Cl}_2/\text{MeOH}/\text{H}_2\text{O}$, 1:2:1) was employed as in the previous cases (Sections 2.8.3 and 2.8.4) to afford the desired *N*-glycolipid **2.23** in 79% yield.



Scheme 2.18 Reagents and conditions. a) Tetracosanoic acid, TBTU, HOBT, DIPEA, DMF, 4Å MS, N_2 , 50°C, 18 h, 42%; b) H_2 , Pd (C), EtOAc, rt, 18 h, 55%; c) i) TBTU, HOBT, DMF, 4Å MS, N_2 , rt, 20 min ii) Tetradecylamine, 18 h, 45%; d) NEt_3 , $\text{CH}_2\text{Cl}_2/\text{MeOH}/\text{H}_2\text{O}$ 1:2:1, 40 °C, 18 h, 79%.

Poor yields are prevalent in the synthesis of *N*-glycolipid **2.23** due to the poor solubility of the long C_{24} chain, with the notable exception of the deprotection step with the highest yield compared to the deacetylation of the L-aspartic acid derivatives **2.21** or **2.22**. Again, this is attributed to the limited solubility of the *N*-glycolipid **2.23**; however, for this last step, this is advantageous. Structural elucidation of the final deprotected *N*-glycolipid **2.23** was extremely difficult for the same reasons. The precipitate **2.23** was partially soluble in d_6 -Pyr, which allowed ^1H NMR analysis to be carried out to confirm its structure. Figure 2.14 shows the ^1H NMR of *N*-glycolipid **2.23**. Characteristic signals include the amide proton at the anomeric centre (at 10.1 ppm), the amide proton of the α -carbon (at 9.0 ppm) and the amide proton linked to the tetradecyl alkyl chain (8.6 ppm). The signals in the ^1H NMR were assigned with the aid of a 2D COSY experiment. The solubility of *N*-glycolipid **2.23** in d_6 -Pyr was so limited that it was not possible to carry out ^{13}C NMR spectrometry analysis or optical rotations. However, similarities in the ^1H NMR spectrum to the shorter chain analogues **2.21** and **2.22** gave us sufficient evidence

that the desired compound was present, and this was further confirmed by HR-MS data.

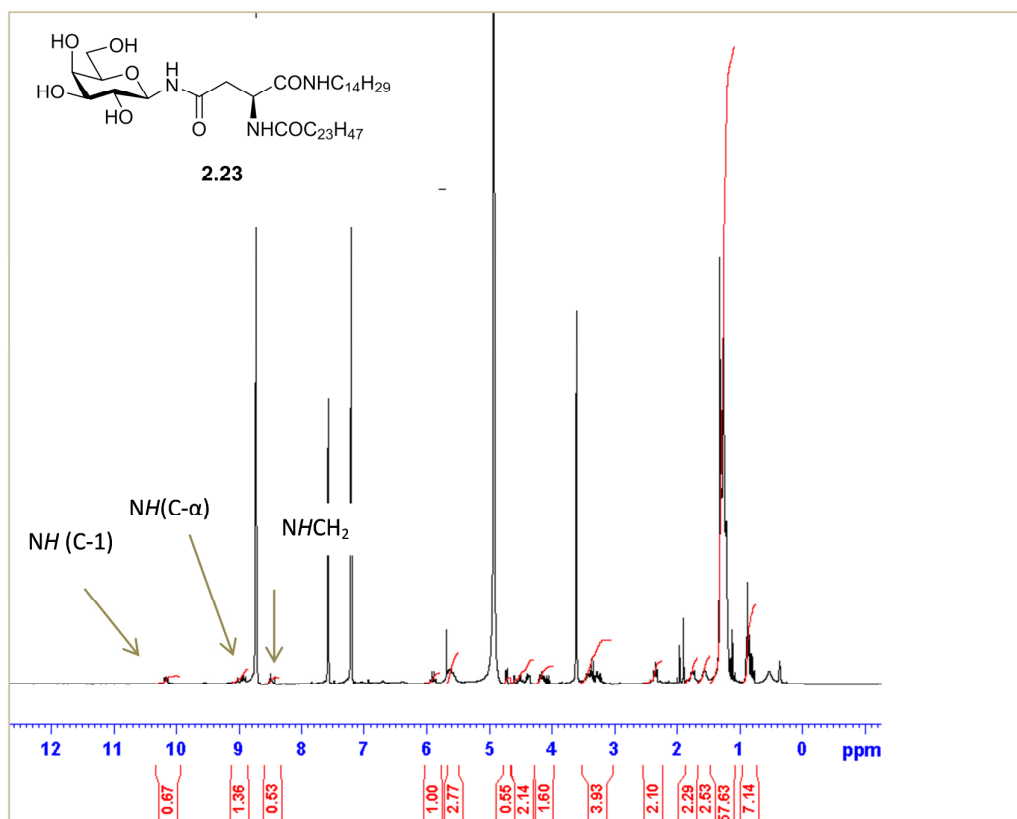


Figure 2.14 ^1H NMR spectrum of *N*-glycolipid **2.23** in d_6 -Pyr. Characteristic signals are highlighted.

2.9. Gelation and self-assembly properties of glycolipid **2.18**, *N*-glycolipid **2.37**, lipid **2.66**, and L-aspartic acid *N*-glycolipids **2.58**, **2.21** and **2.62**

The ability of a molecule to induce gelation in a certain solvent has wide applications in chemistry. These include their use as organic soft materials, drug delivery systems and water purification systems, to name but a few examples.^[66-67]

During the course of our research, we observed by chance that the L-aspartic acid derivative **2.62** formed a gel in certain organic solvents, and we recognised the potential applications of the *N*-glycolipid **2.62** to act as a LMWG. With this observation in mind, we decided to test the gelation abilities of a range of lipidic species such as compounds **2.18**, **2.37**, **2.66**, **2.58**, **2.21**, **2.62** (Figure 2.15). This

group of diverse compounds were selected in order to investigate the structural features that may influence the ability to induce solvent gelation. All are amphiphilic in nature and they all feature the presence of one or two saturated hydrocarbon chains, in which the length ranges from C₈ (in compound **2.18**) to C₁₅ (in compound **2.62**). Other structural characteristics that may influence their behaviour as LMWG are the presence of aromatic groups, amide bonds or glycosidic moieties. For these reasons, an example of a simple glycolipid **2.18** (described in Section 2.6), an aromatic containing *N*-glycolipid **2.37** (described in Section 2.7), a lipid derivative from *N*-Fmoc protected L-serine amino acid **2.66**, with no carbohydrate head group (described in Chapter 4) and L-aspartic acid derivatives **2.58**, **2.21** and **2.62** (described in Sections 2.8.3, 2.8.4, and 2.8.5) with increased hydrophobic characters were investigated.

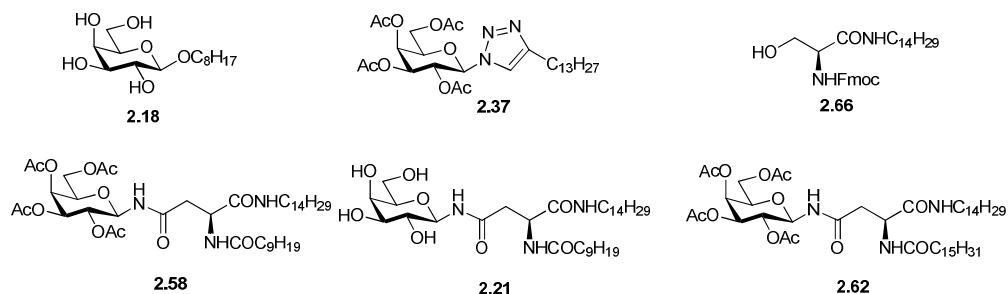
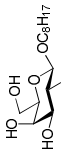
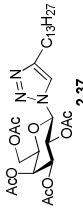
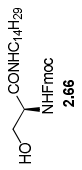
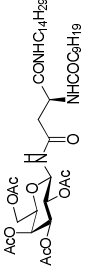
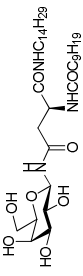
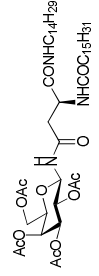


Figure 2.15 Structures of compounds **2.18**, **2.37**, **2.66**, **2.58**, **2.21** and **2.62** tested for gelling abilities in organic solvents.

Gelation tests were performed using an “inverted test-tube method” as described by Tanake *et al.*^[88] The glycolipids were placed in glass vials and the chosen solvent was added to give a concentration of 20 mg mL⁻¹. The mixtures were heated in the chosen solvent, allowed to cool to rt and their ability to form a gel was analysed after 2 h. The gelation results are presented in Table 2.2.

Table 2.2 Gelation studies of lipid species **2.18**, **2.37**, **2.66**, **2.58**, **2.21**, **2.62** in various solvents in order of increasing polarity.

	Hexane	Toluene	Diethyl ether	Dichloromethane	Iso-propanol	Chloroform	Ethyl acetate	Methanol	Ethanol	Acetonitrile	Water
 2.18	I	I	I	I	I	I	I	I	I	I	I
 2.37	I	S	S	S	pS	S	S	S	I	S	I
 2.66	A	G	I	S	S	S	S	A	S	pS	I
 2.58	I	S	pS	S	pS	S	S	S	S	pS	I
 2.21	I	pS	I	I	pS	pS	I	I	I	pS	I
 2.62	S	S	S	S	S	S	S	G	G	A	S

S = soluble, pS = partially soluble, I = insoluble, G = gel, A = aggregates.

No gelation was observed for the octyl-*O*-galactoside **2.18** or for the aromatic containing *N*-glycolipid **2.37** in any of the solvents quoted in Table 2.2. Both of these glycolipids have only one hydrocarbon chain, and neither of them features amide groups in their structure. The short chain C₁₀ L-aspartic acid derivatives **2.58** and **2.21**, which have two hydrocarbon chains and peptide bonds in their structure, did not form a gel in any solvent either. However, gelation in MeOH and EtOH was observed for the C₁₅ acetyl protected L-aspartic acid derivative **2.62**. The minor difference between L-aspartic acid derivatives **2.62** and **2.58**, varying by the length of one of the hydrocarbon chains, suggests the importance of Van der Waal interactions in a compound's ability to act as a LMWG. In this case, the increased hydrocarbon content in **2.62** compared to **2.58** favours intermolecular assembly to form an organogelator. The lipidic amino acid derivative **2.66** also favourably formed a gel in toluene.

For the L-aspartic acid derivative **2.62**, the self-association behaviour was observed in some polar solvents: aggregates were formed in MeCN, but gelation only occurred in MeOH and EtOH. We were particularly excited about its gelation in EtOH, as EtOH is a biocompatible solvent and this result may open up the possibility for the use of this LMWG in drug-delivery systems. Images of the gels and aggregates formed through the self-assembly of L-aspartic acid derivative *N*-glycolipid **2.62** in different solvents are illustrated in Figure 2.16. From these images, one can see aggregation occurring in MeCN and gelation in both MeOH and EtOH to give transparent gels. The formation of the LMWGs in MeOH and EtOH was found to be thermo-reversible, i.e. the gels turned into solutions upon heating and slowly reverted back into gels after cooling. The *gel* to *sol* transition temperatures (T_{gs}) were found to be 35 °C and 34 °C at 20 mg/mL concentrations, in EtOH and MeOH respectively.

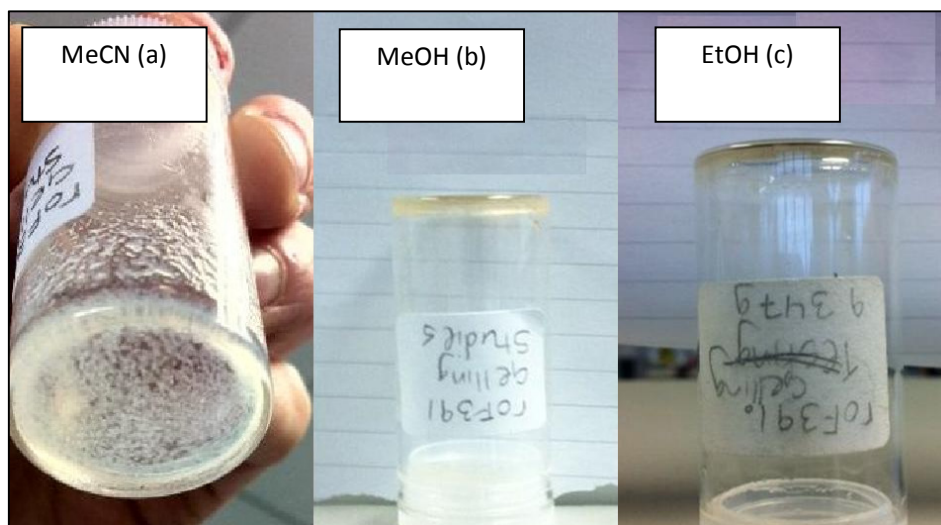


Figure 2.16 Images of the gels and aggregates formed through the self-assembly of L-aspartic acid derivative *N*-glycolipid **2.62** in a) MeCN (aggregates) b) MeOH (gel) and c) EtOH (gel).

The critical gelation concentration (CGC) is defined as the threshold at which infinite percolation is achieved within a network system, although microgel network structures can still be observed below the CGC.^[89] In simple terms it defines the point at which gelation can still occur for an organogelator in an excess of solvent. For the L-aspartic acid glycolipid derivative **2.62**, the CGC in MeOH was quantified as the concentration at which the failure of the whole solvent to flow utilising the “inverted test tube method”, described above, was observed. The CGC value was found to be 20 mg mL⁻¹. For the L-aspartic acid glycolipid derivative **2.62**, the CGC in EtOH was found to give the same value of 20 mg mL⁻¹.

The self-assembly behaviour of the L-aspartic acid glycolipid derivative **2.62** in MeOH was investigated using FT-IR spectrometry. With this technique, we intended to probe the possibility that the formation of an intermolecular hydrogen-bonding network was implicated in the gelation process. In FT-IR spectrometry, differences in frequencies between solution and gel states can be attributed to differences in hydrogen-bonding patterns.^[31b] The process involved the dissolution of the solid sample of glycolipid **2.62** in MeOH, followed by heating of the solution to 40 °C. FT-IR analysis was then performed in real time as the MeOH gel was being formed

(with deduction of the MeOH background). The FT-IR spectra are shown in Figure 2.17.

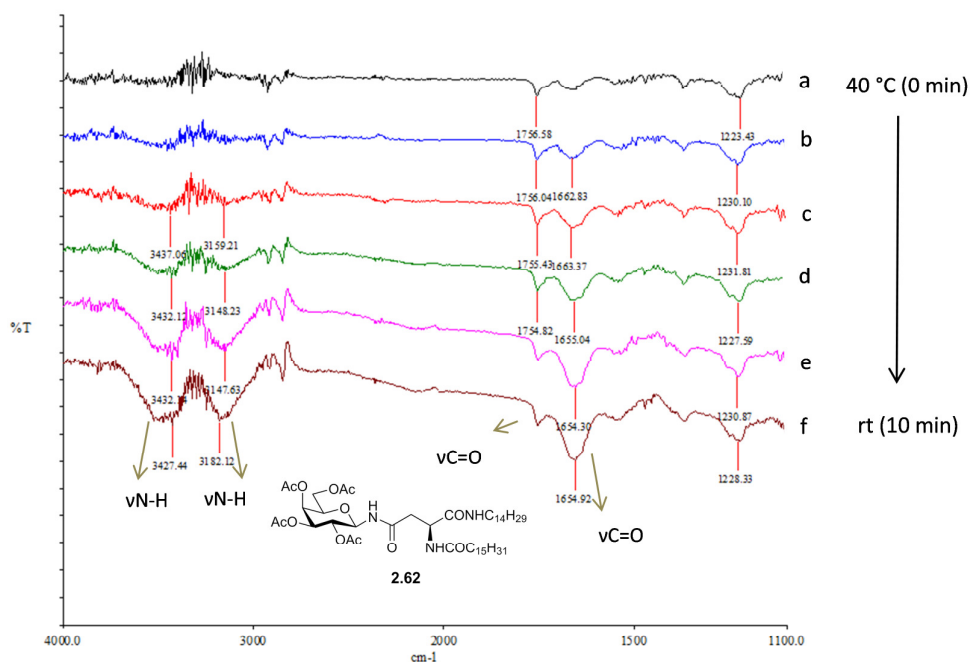


Figure 2.17 FT-IR spectra of LMWG **2.62** formation from solution to gel in MeOH. IR spectrum for LMWG **2.62** in solution phase is highlighted as spectrum a, while IR spectrum for LMWG **2.62** in gel phase is highlighted as spectrum f. The FT-IR measurements were performed over a period of 10 min, from 40 °C to rt.

The wavenumber values of the functional groups of the glycolipid **2.62** in the gel phase (spectrum f) were compared to those of the glycolipid **2.62** in solution phase (spectrum a). Minor differences in the wavenumbers and in the intensity of the bands were observed. In the initial spectrum recorded (spectrum a), very weak bands are observed. A difference was observed for the final spectrum (spectrum f) with three significant peaks. The emergence of two broad N-H amide bands at 3427 and 3182 cm^{-1} are indicative that the amide bonds may play a role in intermolecular hydrogen-bonding of the organogelator **2.62**. Similarly, the carbonyl amide band at 1660 cm^{-1} in the solution phase (spectrum a) has increased in intensity and has slightly shifted to a lower frequency at 1654 cm^{-1} in the gel phase (spectrum f). This frequency shift indicates that hydrogen-bonding may play a role in the formation of the gel of **2.62** in MeOH.^[90] It is more likely, due to the relatively

small shifts in frequency, that van der Waal interactions play a more dominant role in the formation of the network to support assembly of gel **2.62** in MeOH. A combination of these interactions is proposed.

For the L-serine derivative **2.66**, aggregates were formed in MeOH and hexane and gelation occurred only in toluene. Images of the self-assembled structures are shown in Figure 2.18. From these images, one can see aggregation occurring in MeOH, a polar protic solvent. More obvious to the naked eye is the aggregation in hexane and the gelling in toluene to give a clear gel; both solvents are non-polar. The formation of the gels in toluene induced by the self-assembly of the LMWG was found to be thermo-reversible with a *gel* to *sol* transition temperature (T_{gs}) of 38 °C. A CGC value of 10 mg mL⁻¹ in toluene (measured as described earlier), was obtained for lipid **2.66**.

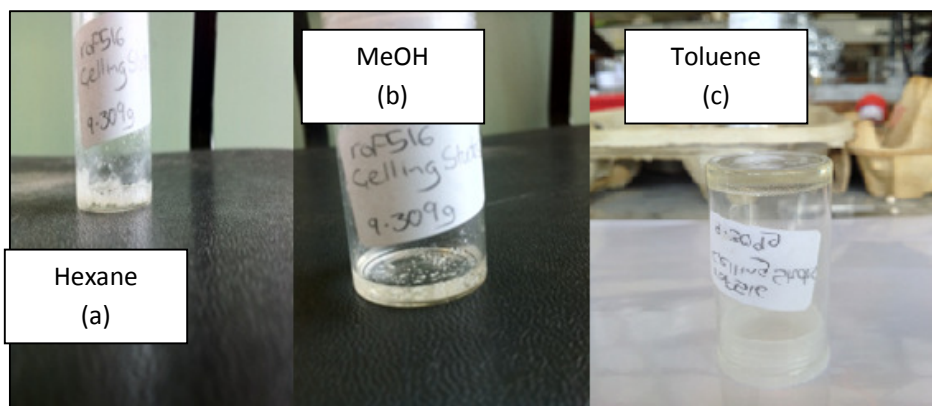


Figure 2.18 Images of the aggregates and gels formed through self-assembly of *N*-Fmoc-L-serine tetradecyl **2.66** in a) hexane (aggregates), b) MeOH (aggregates) and c) toluene (gel).

The self-assembly behaviour of the LMWG **2.66** in toluene was investigated using FT-IR spectrometry, as performed for the L-aspartic acid derivative **2.62**. The solid sample **2.66** was dissolved in toluene, heated and FT-IR analysis was performed in real time as the organogel was being formed (with deduction of the toluene background). The FT-IR spectra are shown in Figure 2.19. The wavenumbers of the bands corresponding to the different functional groups of lipid **2.66** in the gel state

(spectrum f) were compared to those in solution state (spectrum a). Key differences in both the wavenumbers and the intensity of the bands were observed. In the initial spectrum recorded (spectrum a), a broad band at 3474 cm^{-1} is representative of either the O-H stretching band or the N-H stretching band of lipid **2.66**. In the final spectrum recorded once the gel had formed (spectrum f), the band has shifted dramatically to a lower frequency to give a more intense band at 3392 cm^{-1} . Similarly, the two bands in the initial spectrum (spectrum a) corresponding to the carbonyl amide (1681 cm^{-1}) and the carbonyl carbamate (1727 cm^{-1}), both shifted to lower frequencies to give more intense bands at 1662 and 1714 cm^{-1} respectively in the final spectrum (spectrum f). The amide II band at 1541 cm^{-1} in the initial spectrum has also been affected from the gelation and shifted to a lower frequency to 1534 cm^{-1} . These changes indicate that hydrogen-bonding plays a role in the self-assembly of L-serinyl compound **2.66** in toluene and that it occurs via the amide and carbamate functional groups and possibly through the free hydroxyl groups also.^[31b] To investigate the potential role of the hydroxyl group of lipid **2.66** to act as a hydrogen-bond donor, we evaluated the gelation ability of its glycosylated product **2.67** (Figure 2.20). Details for the synthesis of glycolipid **2.67** will be discussed in Chapter 4. The “inverted test tube method” was performed as described above in toluene. No gel was formed in this case, indicating that the primary hydroxyl group may play an important role as hydrogen-bond donor in the self-assembly of L-serine derivative **2.66**. It is likely also that π - π stacking interactions between the aromatic *N*-Fmoc carbamate groups in derivative **2.66** and toluene contribute to stabilise the supramolecular network that leads to the formation of the gel.

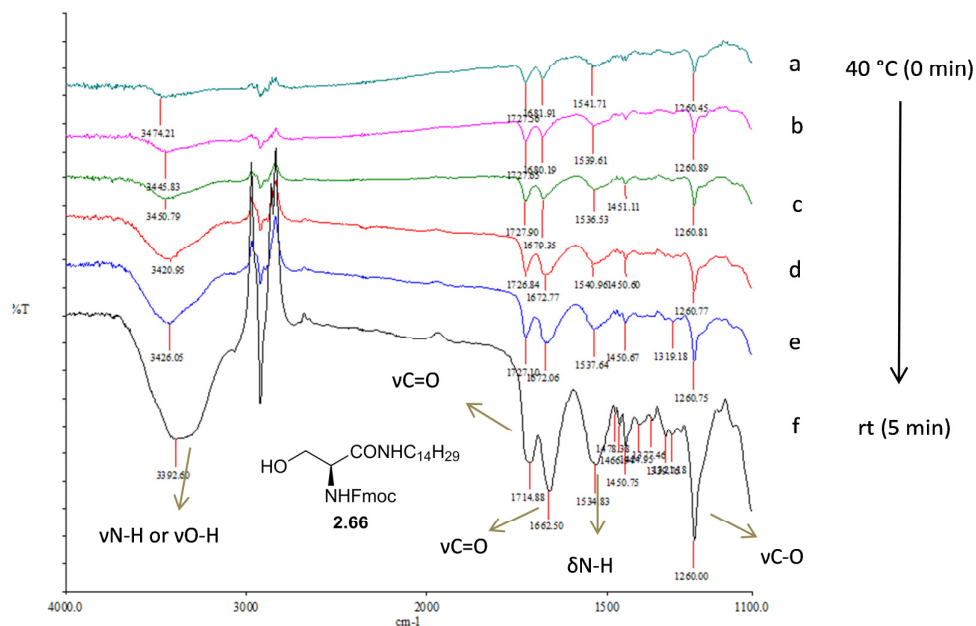


Figure 2.19 FT-IR spectra of LMWG **2.66** formation from solution to gel in toluene. IR spectrum for LMWG **2.66** in solution phase is highlighted as spectrum a, while IR spectrum for LMWG **2.66** in gel phase is highlighted as spectrum f. The FT-IR measurements were performed over a period of 5 min, from 40 °C to rt.

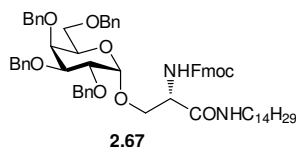


Figure 2.20. Structure of glycolipid **2.67** tested for organogelator properties in toluene.

2.9.1. SEM imaging of N-glycolipid **2.62** and lipid **2.66**

Scanning Electron Microscopy (SEM) is a technique commonly employed to give information about a sample's morphology. To gain a microscopic insight into the self-assembled structures **2.62** and **2.66** as LMWGs, the morphologies of galactosyl L-aspartic acid derivative **2.62** and L-serine derivative **2.66** were observed by SEM in the solid state (prior to gelation), as cryogels (obtained by the freeze-drying of the gels) and as xerogels (obtained by a drop casting method). The cryogels were obtained by prior formation of the toluene gel, as explained above, and the solvent

was removed by freeze-drying the sample.^[91] The drop-cast technique involved heating of the LMWG in question in the gelling solvent, pipetting the solution onto a silicon wafer, and allowing the sample to evaporate at rt and atmospheric pressure.^[92] The SEM micrographs were recorded at 8 kV. This low voltage ensured that the sample morphology remained intact during SEM imaging; however a trade-off with the resolution of the SEM micrographs was incurred as a result.

The SEM micrographs of a solid sample of L-aspartic acid derivative **2.62**, obtained from rotary evaporation and the EtOH xerogel of **2.62** (prepared by the drop-cast method) appear in Figure 2.21. The surface of the solid sample of compound **2.62** (Figure 2.21a) shows a rounded amorphous structure. The SEM micrograph for the drop-cast EtOH xerogel illustrated a different type of packing altogether (Figure 2.21b,c). The removal of the solvent in the gel revealed the network of thick bundles of the glycolipid **2.62** forming part of a “porous” structure. The cavities in which the solvent was entrapped in the gel can be clearly observed. The type of morphology shown in these images is consistent with those of xerogels obtained by similar methodologies described in the literature.^[93]

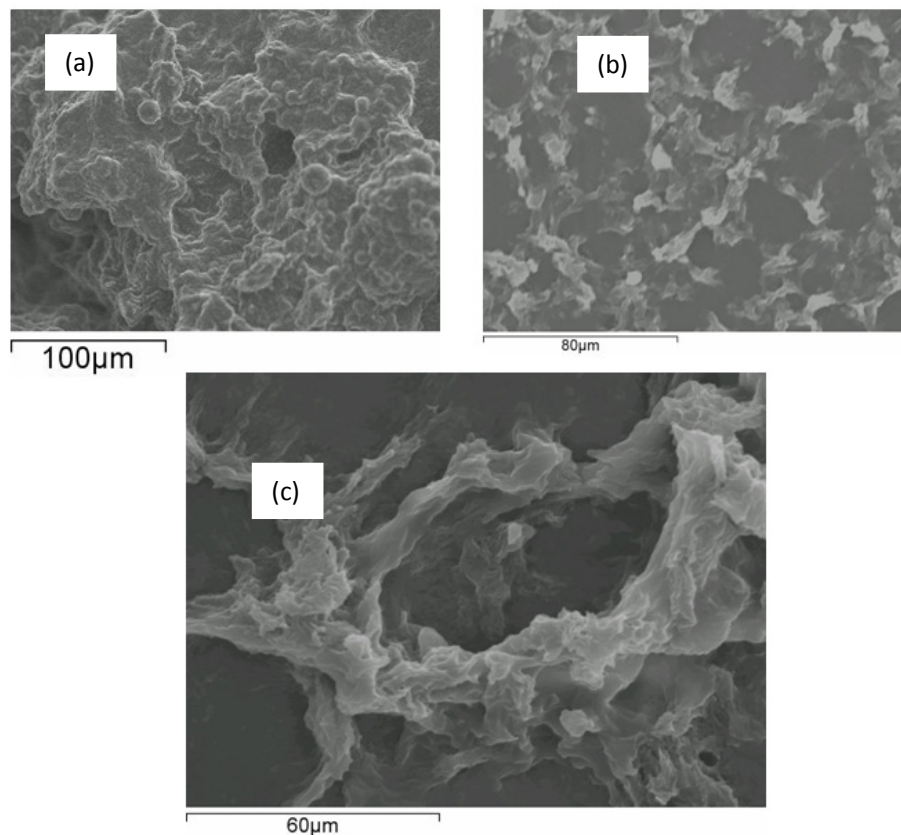


Figure 2.21 SEM micrographs of a) solid sample of L-aspartic acid derivative **2.62**; b) the EtOH xerogel of **2.62** from drop-cast method; c) magnification of the EtOH xerogel of **2.62** from drop-cast method.

The SEM micrographs of a solid sample of L-serinyl derivative **2.66**, the toluene cryogel and the toluene xerogel obtained by the drop-cast method (both prepared by forming a solution of **2.66** in toluene) appear in Figure 2.22. Quite a different surface morphology was observed for the solid sample of the lipid species **2.66**, as compared to that of the solid sample of glycolipid **2.62**, in that in this case none of the rounded structures described above were observed (Figure 2.21a). The SEM image for the toluene cryogel from **2.66** showed a dense and fragmented structure, which was most likely obtained from the collapse of the gel microstructure during the freeze-drying process (Figure 2.21b). A clear difference is illustrated in the SEM image of the drop-cast xerogel (Figure 2.21c,d) from toluene, compared to those of the EtOH xerogels from glycolipid **2.62** described earlier. The self-assembly of LMWG **2.66** in toluene results in a very compact three-dimensional network

containing long thin fibrils that are woven tightly together in an ordered fashion (Figure 2.21c). These fibrils can further aggregate, forming highly entangled and thicker fibrous bundles and/or ribbons (Figure 2.21d). SEM micrographs of organogelators are commonly encountered as three dimensional fibrous networks, and our observations are in line with those reported.^[93]

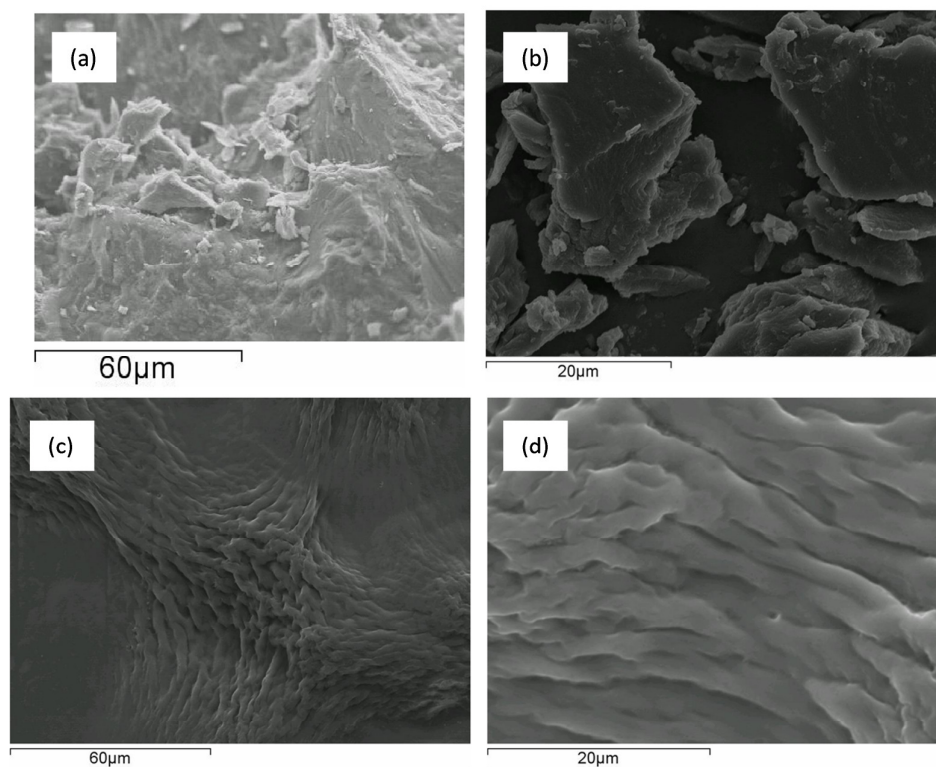


Figure 2.22 SEM micrographs of a) solid L-serinyl derivative **2.66**; b) toluene cryogel of **2.66** c) toluene xerogel of **2.66** from drop-cast method; d) magnification of the toluene xerogel of **2.66** from drop-cast method .

2.10. *O*-Glycolipid **2.19** and *N*-glycolipid **2.22** as anti-adhesion agents

This section presents preliminary studies conducted by Dr. Ciara Wright (for the evaluation of glycolipid **2.19**) and Ms. Lorna Abbey (for the evaluation of glycolipid **2.22**), in the laboratory of Dr. Siobhan McClean at the Institute of Technology Tallaght, Dublin. These studies aimed to investigate the potential for two representative glycolipids, such as *O*-glycolipid **2.19** and *N*-glycolipid **2.22**, to inhibit the adhesion of strains of the pathogen Bcc to lung epithelial cells.

The anti-adhesion approach for *O*-glycolipid **2.19** was performed using a real-time PCR method, which was developed by Wright and colleagues to determine the attachment of *B. multivorans* (LMG13010) to lung epithelial cells and its subsequent inhibition with the synthetic glycolipid **2.19**.^[42, 94] One major problem encountered during the biological evaluation was the solubility of the long chain glycolipid **2.19**, whereby it could not be fully solubilised in aqueous mixtures of DMF or DMSO. As a result, suspensions of glycolipid **2.19** were tested. The assays were performed on two separate batches of glycolipid **2.19** and repeated four times. Good reproducibility was reported, and two concentrations of the glycolipid (47 μ M and 90 μ M) were tested. The results are presented in Figure 2.23. Attachment of the pathogen to epithelial cells in the absence of synthetic glycolipid **2.19** or monosaccharide was used as a control. Docosanol (the C₂₂ alcohol) was not soluble in the above solvent mixtures and thus was not tested for its anti-microbial properties. From the data, we can conclude that glycolipid **2.19** does inhibit *B. multivorans* binding to lung epithelial cells. For example, at a concentration of 47 μ M, bacterial adhesion has reduced to 70% (compared to 100% for control). At a higher concentration of 90 μ M, bacterial binding has reduced to 50%, a significant improvement (compared to 100% for control). This pronounced inhibition of the attachment was not observed in the presence of the monosaccharide alone (D-galactose).

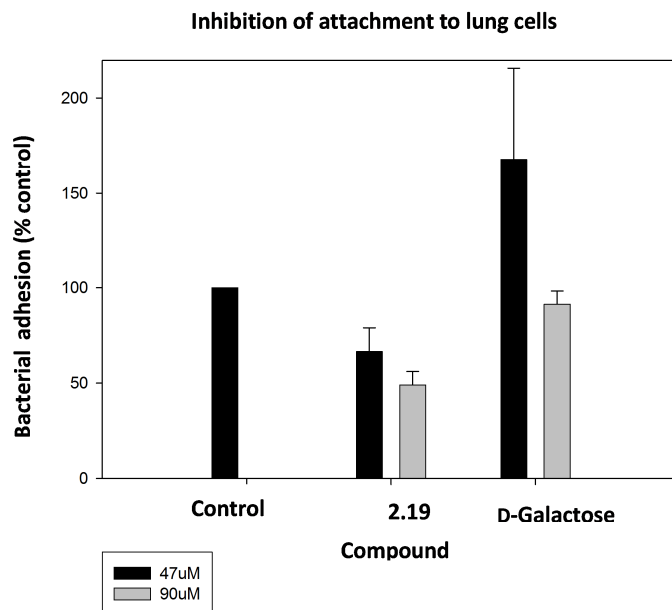


Figure 2.23 Study of inhibition of the attachment of *B. multivorans* to lung epithelial cells by *O*-glycolipid **2.19** and D-galactose. The results are presented from four independent experiments on two separate batches of *O*-glycolipid **2.19**.

A different technique was used for the biological evaluation of *N*-glycolipid **2.22**. The anti-adhesion approach for the L-aspartic acid derivative **2.22** was investigated on a specific strain of Bcc, *Burkholderia multivorans* (LMG13010) on cells extracted from immuno-compromised CF patients using a colony counting technique. Epithelial cells incubated with a bacterial strain were used as a control. The bacteria were pre-treated with the *N*-glycolipid **2.22** and the inhibition of the bacterial adhesion to the epithelial cells was evaluated. The results are presented in Figure 2.24. It was shown that the Bcc strain (LMG13010) adhesion to the epithelial cell was significantly reduced by treatment of the cells with the *N*-glycolipid **2.22** at higher concentrations (250 μM). Initially, at a concentration of 5 μM, the *N*-glycolipid **2.22** seemed to aid in the bacterial adhesion, presumably by acting as a “bridge” between bacteria and host cell, an observation previously reported in the literature.^[42, 95] At a higher concentration (250 μM), the *N*-glycolipid **2.22** inhibited the bacterial adhesion to the epithelial cell, with a 40% adhesion (compared to

100% of for control). This dramatic decrease in binding supports the hypothesis that the bacteria binds to the epithelial cell by a carbohydrate-protein interaction (described in Section 2.2); we can postulate that the free carbohydrates (*N*-glycolipid **2.22**) binds to the bacteria and renders the bacteria inactive to adhesion to the epithelial cell.

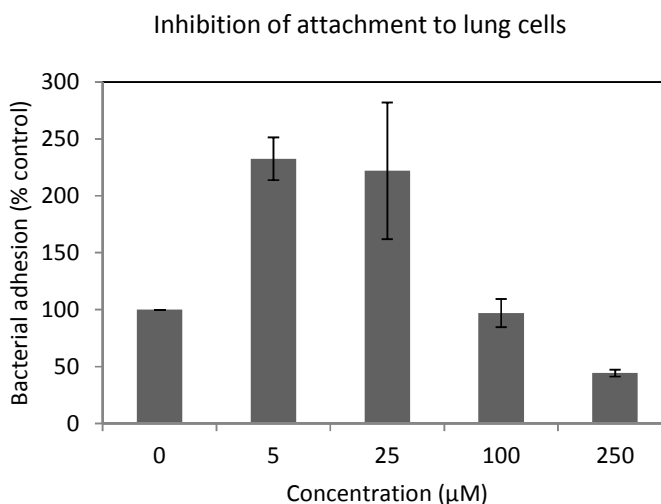


Figure 2.24 Bacterial adhesion of *Burkholderia cenocepacia* (LMG13010) to lung epithelial cell upon treatment with *N*-glycolipid **2.22**.

2.11. Summary

We described the successful syntheses of the *O*-glycolipids **2.18** and **2.19** using the Koenigs Knorr methodology. The solubility of the precursors and products proved to be the most challenging tasks. We completed the synthesis of an aromatic containing *N*-glycolipid **2.20** using a CuAAC cycloaddition reaction with little problems. Three enantiomerically pure L-aspartic acid derivatives **2.21-2.23** were successfully constructed, despite the initial problem of racemisation that occurred in the synthesis of the building block **2.45** (Section 2.8.1). Careful considerations and modifications in the synthetic sequence had to be taken into account, to preserve the optical purity of these *N*-aspartic acid derivatives. Undesired succinimide side products were also problematic in the synthetic strategies. However precipitation of the final *N*-glycolipids **2.21**, **2.22** and **2.23** alleviated this problem.

The amphiphilic properties of various different lipid species were probed and gelling studies were performed. We found that the L-serinyl derivative **2.66** and the L-aspartic acid derivative **2.62** acted as LMWGs, with potential biological applications as drug delivery vehicles or in material science. The self-assembly of these novel LMWGs leading to the formation of gels was investigated with the aid of FT-IR and SEM. We believe that the formation of EtOH and MeOH gels, induced by the self-assembly of **2.62** occurs primarily due to Van der Waal intermolecular interactions between the hydrophobic chains. Hydrogen-bonding does not seem to be prevalent in these competitive solvents, as suggested by the FT-IR data obtained. On the other hand, intermolecular hydrogen-bonding may be a more determinant factor in driving the self-assembly of L-serinyl lipid **2.66** in toluene, together with aromatic stacking interactions. Morphological studies performed on xerogels of these organogelators by SEM indicated their self-assembly patterns were very different to one another, whereby the L-aspartic acid derivative **2.62** displayed a more porous structure and the L-serinyl derivative **2.66** displayed dense three dimensional fibrous networks.

Two representative glycolipids were selected for preliminary evaluation of the potential of this type of compounds as anti-microbial agents. An anti-adhesion assay was performed on the *O*-glycolipid **2.19** using a PCR method and from the resulting data we can conclude that glycolipid **2.19** does inhibit *B. multivorans* binding to lung epithelial cells, although the poor solubility of the compound limited its further applications. A colony counting technique was employed to study the anti-adhesion properties of L-aspartic acid *N*-glycolipid **2.22** and preliminary results suggest it too inhibits bacterial binding to lung epithelial cells, albeit at concentrations higher than 100 μM . Our ultimate intention is to perform the anti-adhesion assays on the other glycolipids **2.18** and **2.20** and the *N*-glycolipid **2.21** mentioned in this chapter.

**Chapter 3: Synthesis of GI-X based glycolipid for biochemical
evaluation**

3.1. Introduction

This chapter presents work conducted by the author over a 6 month period in the laboratory of Assoc. Prof. Spencer Williams at the University of Melbourne, Australia, supported by an Endeavour Fellowship in 2010.

Tuberculosis (TB) is a disease that has infected one-third of the world's population.^[96] 2-3 million people develop active disease each year. Co-infection with human immunodeficiency virus (HIV) and the emergence of multi-drug resistant TB have brought this infectious disease to the attention of the medical and scientific research communities.

3.2. Current tuberculosis treatment

Current first-line treatments for TB involve the administration of multiple drugs, which consist of rifampicin (RIF), isoniazid (INH), pyrazinamide (PZA), ethambutol (EMB) and streptomycin (SM).^[97] Each anti-TB drug operates by different modes of action. For example, INH is a prodrug that disrupts the synthesis of the cell wall of the bacterium,^[97] and RIF inhibits prokaryotic RNA synthesis (Figure 3.1).^[97] Unfortunately, improper use or mismanaged treatments of this regimen can result in multidrug resistant tuberculosis (MDR-TB). Staggeringly, it has been reported that 500,000 cases of MDR-TB occur globally per annum.^[97] Many of these reported cases involve patients with TB and HIV coinfection; the combination of which results in high fatality rates. Extensively drug-resistant tuberculosis (XDR-TB) is a form of TB that is resistant to both first and second line drugs currently used in the treatment of TB. The emergence of XDR-TB is attributed to the mismanagement of individuals with MDR-TB,^[96] and only limited treatments are currently available for XDR-TB.^[98] Totally drug resistant tuberculosis (TDR-TB) is a form of TB that is incurable. It was first identified in Italy, subsequently in Iran^[99] and more recently in India.^[99] It is again accredited to the misuse of first and second line drugs, and thus remains one of the most pressing problems in TB control today.

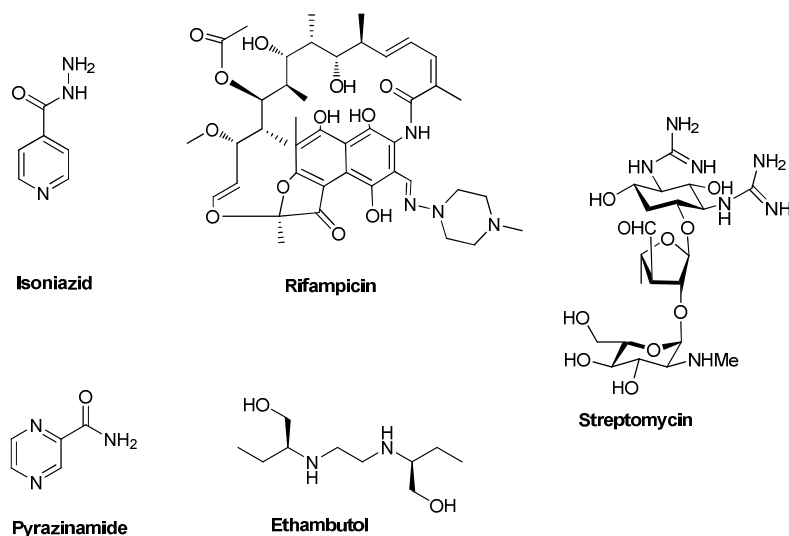


Figure 3.1 Structures of isoniazid (INH), rifampicin (RIF), pyrazinamide (PZA), ethambutol (EMB) and streptomycin (SM): current first line treatment for TB.^[97]

As a consequence of drug resistance, the urgency and need for alternative drugs is evident. Promising drug candidates include a 1,2-ethyldiamine derivative SQ109,^[100] which exhibited activity against drug-resistant strains of *M. tuberculosis*, OPC-67683,^[101] a nitro-dihydro-imidazooxazole derivative exhibiting a bioactivity similar to first-line drug RIF, PA-824, another nitroimidazooxazole which is believed to act as an intracellular NO donor^[102] and a diarylquinoline TMC207,^[103] whose clinical activity validates ATP synthase as a viable target for the treatment of tuberculosis.

The structures of these promising drug candidates are presented in Figure 3.2.

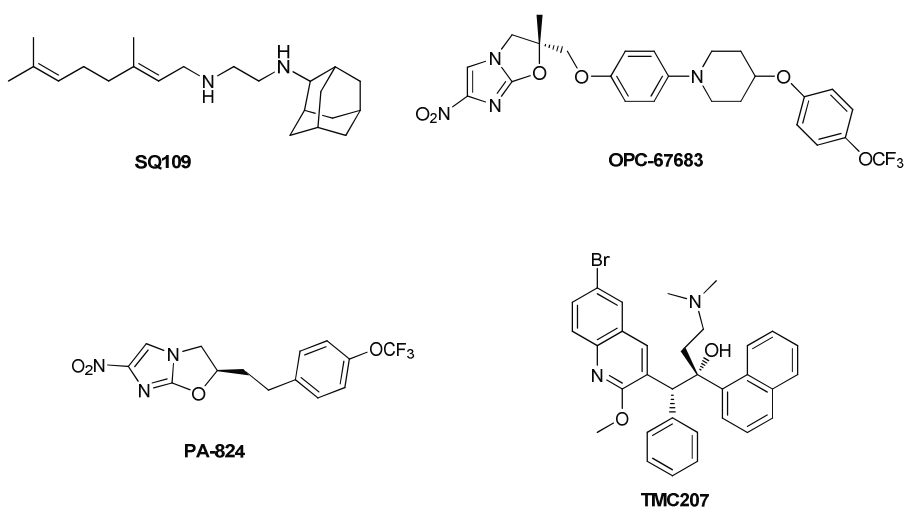


Figure 3.2 Promising drug candidates SQ109, OPC-67683, PA-824 and TMC207.^[100-103]

3.3. Mycobacterial cell wall associated glycolipids

Mycobacterium tuberculosis is the causative agent of TB in humans. *M. tuberculosis* possesses a unique and complex, multi-layered cell wall structure containing macromolecules of peptidoglycan, arabinogalactan and mycolic acids along with the membrane-associated lipids phosphatidyl-*myo*-inositol mannosides (PIMs), lipomannan (LM) and lipoarabinomannan (LAM). The structure of the cell wall complex is a major determinant of virulence for the bacterium; the structurally-related PIMs, LM and LAM play crucial roles in this virulence and are hence potential drug targets. As well, numerous studies have been devoted to the immunoregulatory effects of these glycolipids.^[104] Glycolipids based on D-glucuronic acid termed GI-A and GI-X (Figure 3.3) have been isolated from *C. glutamicum*, a non-pathogenic bacterium phylogenetically related to *M. tuberculosis*.^{[12],[105]} These glycolipids form the core of glycolipids termed GI-LM that are closely related to the phosphoglycolipids LM which possess a PI core (sometimes termed PI-LM). Compared to the PIMs, LM and LAM, little is understood of the biosynthesis and immunological properties of these glycolipids. The lack of availability of these natural products makes it difficult to study their biological activity.

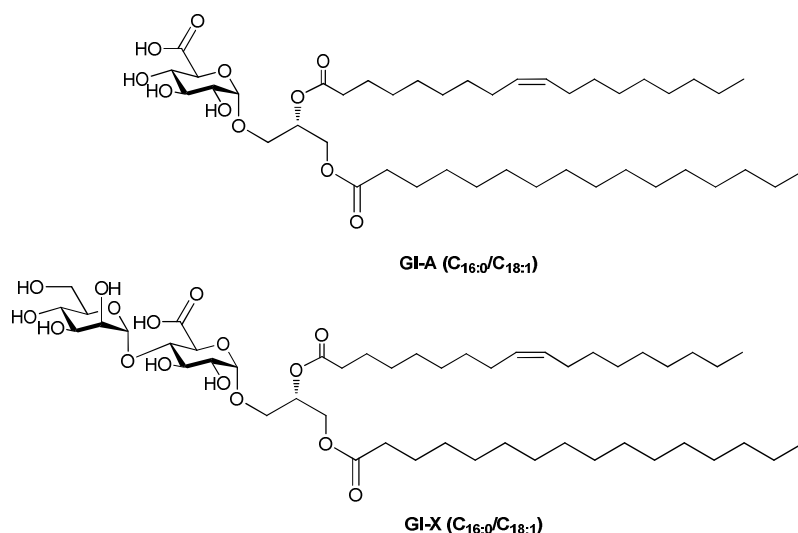


Figure 3.3 Structure of GI-A (C_{16:0}/C_{18:1}), and GI-X (C_{16:0}/C_{18:1}) isolated from *C. glutamicum*^{iv}

^{iv} C_{16:0}/C_{18:1} refers to the glycerol having palmitoyl (C_{16:0}) and oleoyl (C_{18:1}) residues at the *sn*-1 and *sn*-2 positions respectively. For the palmitoyl residue, the 16 represents the number of carbon atoms in the lipid chain and the 0 represents the degrees of unsaturation in the lipid.

3.4. PIMs, LM and LAM

PIMs, LM and LAM are found in the majority of bacteria from the *Corynebacterineae* family, including *M. tuberculosis*. Structural similarities of PIMs, LM and LAM are evident; PIM is the common anchor motif of LM and LAM, both of which are derived from the same biosynthetic pathway. The basic structure of phosphatidyl-*myo*-inositol mannosides (PIMs) consists of an acylated phosphatidyl-*myo*-inositol (PI) anchor extended by $\alpha(1\rightarrow6)$ - or $\alpha(1\rightarrow2)$ -linked D-Manp units,^v with further elongation at the C-6 position with D-Manp residues (Figure 3.4). They range from monomannosylated (PIM₁) to hexamannosylated (PIM₆) sugars with varying acylation patterns. The main fatty acids are palmitic (C₁₆) and tuberculostearic acids (C₁₉); however myristic (C₁₄) and octadecanoic acids (C₁₈) are also present in significant amounts.^[106]

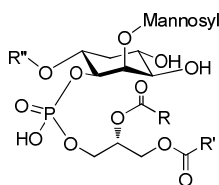


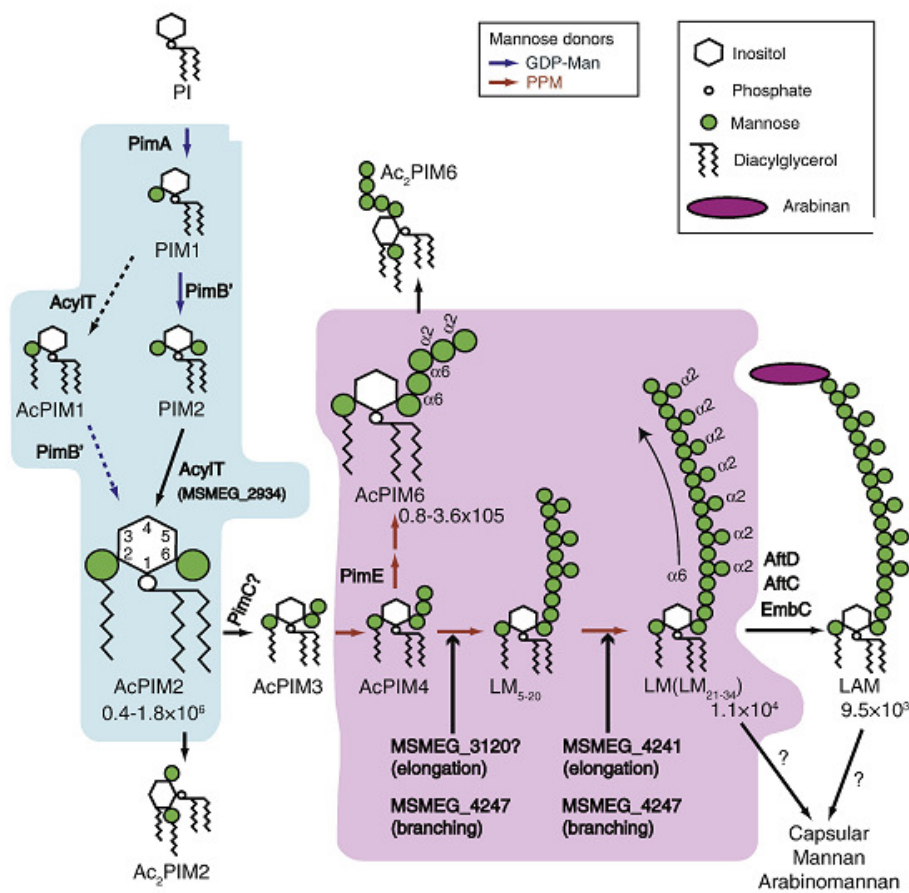
Figure 3.4 General schematic of PIM₁₋₆ (R, R' = acyl chains, R'' = 0-5 D-Manp residues), LM (R, R' = acyl chains, R'' = approx. 40 D-Manp residues), LAM (R, R' = acyl chains, R'' = approx. 40 residues of D-Manp and approx. 70 residues of D-Araf).^{vi}

LM contain a PIM backbone elongated with $\alpha(1\rightarrow6)$ -linear and single $\alpha(1\rightarrow2)$ -branched D-Manp residues. LAM contains the LM backbone and is further elaborated with up to 70 highly branched D-Araf residues.^[104a] Additional variability in the LAM structures arises from “capping” of the non-reducing termini of the arabinan core with D-Manp residues.^[107] Although the chemical structures of PIMs, LM and LAM are well established, the enzymes and sequence of events leading to their biosynthesis and regulation remains incomplete. Scheme 3.1 provides an overview of the biosynthesis of these lipoglycans in *M. smegmatis*, a fast-growing

^v D-Manp indicates D-mannopyranose and D-Araf indicates D-arabinofuranose.

^{vi} Details of arabinan attachments are unknown to date.

non-pathogenic mycobacterium that is often used as a model for *M. tuberculosis*.^[108]



Scheme 3.1 Metabolic pathway of PIMs, LM and LAM in *M. smegmatis*.^[108] vii,viii,ix,x

3.5. Introduction to GI-X, GI-A, GI-LM

Drugs such as isoniazid and ethambutol operate by altering/modifying the bacterial cell wall composition of *M. tuberculosis*, the causative agent of TB, which results in the death of the bacteria. Whether GI-X and GI-A glycolipids are present in *M. tuberculosis* is of interest to scientists, whereby the understanding of their bacterial

^{vii} Illustration procured from Morita and co-workers is edited by authors.

^{viii} The blue and pink areas indicate reactions taking place in different membrane compartments, respectively.

^{ix} Numbers next to some of the molecules indicate the cellular abundance in molecules per cell.

^x Sites of mannose and arabinan branches on LM/LAM are unknown.

cell wall roles, if any, may aid in the understanding of TB and the developments of novel drugs.

Biochemical analyses performed by Tatituri and co-workers suggest that a novel glycolipid termed Gl-X (diacylglyceryl α -D-mannopyranosyl-1,4- α -D-glucuronoside) serves as an alternative glycolipid core to LM-like molecules in *C. glutamicum*.^[12] Gene knockout studies in *C. glutamicum* revealed that disruption of a specific gene NCg10452 (MgtA; formally known as PimB) had no effect on LAM levels or the biosynthesis of AcPIM₂ (Scheme 3.1).^[12] Instead, loss of glycolipid Gl-X was observed. In addition, there was an accumulation of a glycolipid precursor to Gl-X, termed Gl-A which lacks the mannosyl residue (Figure 3.3). The absence of Gl-X led to a reduction in LM, a result that suggests that Gl-X is a biosynthetic precursor to LM-like molecules. As a result of these findings, the authors reassigned NCg10452 as MgtA, an α -mannosyl-glucopyranosyluronic acid-transferase that catalyses the formation of Gl-X from Gl-A.

Similar findings were reported for *C. glutamicum* by Lea-Smith and co-workers.^[109] Deletion of the gene NCg12106 from *C. glutamicum* revealed a reduction in AcPIM₂ with a concomitant accumulation of AcPIM₁, but had no effect on Gl-X. As expected, the pool of LAM was reduced as a direct result, but, surprisingly, the LM pool remained unaffected. Additional studies on this knock-out strain were performed by Mishra.^[110] Collectively, these studies indicated that, in *C. glutamicum*, LM is assembled from two cores: a minor one assembled on a PI core that extends to LAM (called PI-LM) and a major one assembled on a Gl-A core (called Gl-LM).^[110]

Gl-A and Gl-X have not been identified in *M. tuberculosis*; however there is evidence that the biosynthetic machinery required for their biosynthesis is present. The orthologous genes *mgtA*, *mptA* and *mptB* in *M. tuberculosis* complemented the production of LM in *C. glutamicum*, which demonstrates their existence in functional form in *M. tuberculosis*.^[105] Two Gl-A isoforms have been isolated from *M. smegmatis*,^[111] a related bacterial species of the *Corynebacterina* family. The

structures were proposed to contain tuberculostearic acid (C_{19:0}) and oleic acid (C_{18:1}) at the *sn*-1 position and palmitic acid (C_{16:0}) at the *sn*-2 position (Figure 3.5). Based on these findings, and those reported by Mishra,^[110] a proposed biosynthetic pathway for GI-LM from diacyl glycerol in *M.tuberculosis* is presented in Scheme 3.2.

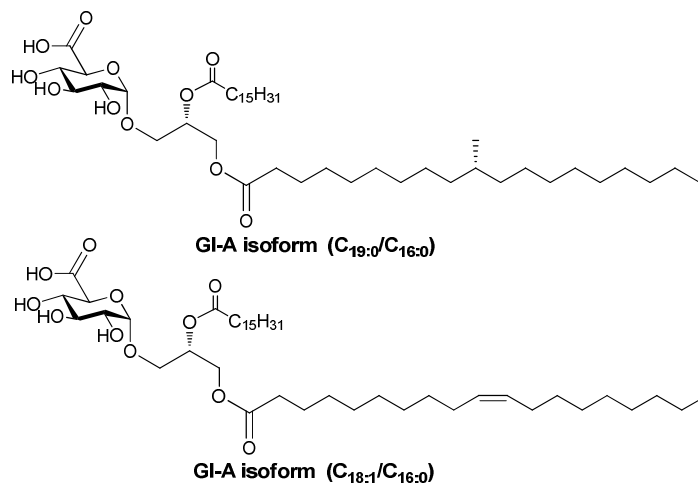
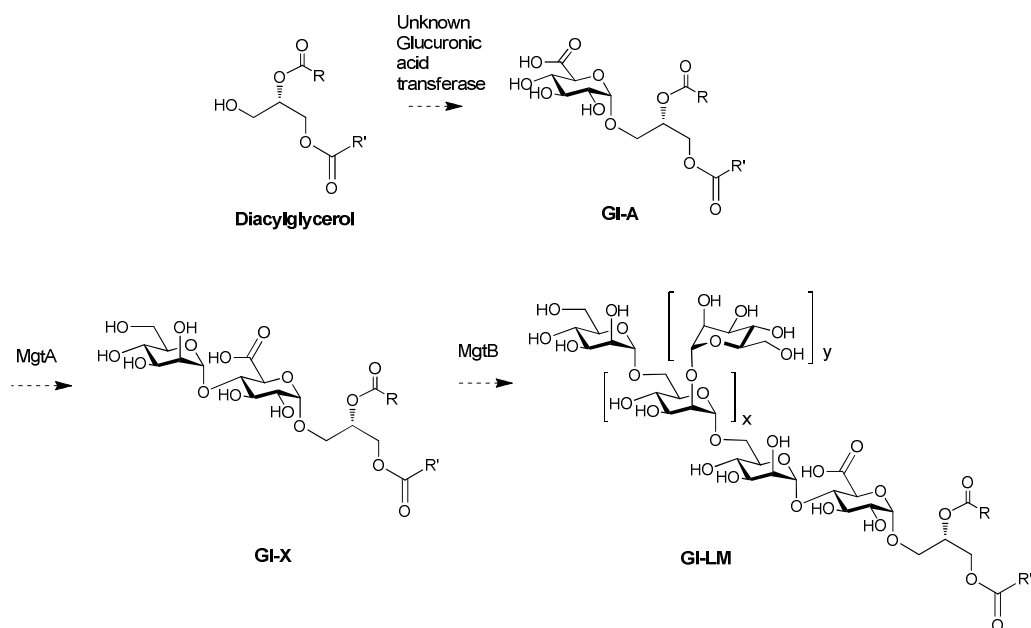


Figure 3.5 Structures of GI-A isoform (C_{19:0}/C_{16:0}) and isoform (C_{18:1}/C_{16:0}) isolated from *M. smegmatis*.^[111]



Scheme 3.2 Proposed biosynthetic pathway of GI-LM in *M. tuberculosis*.

3.5.1. Biological function of GI-X, GI-A, GI-LM

The antigenicity of purified GI-A was studied by Wolucka and co-workers.^[111] They observed purified GI-A bound to anti-*M. avium* and anti-*M. tuberculosis* rabbit sera by western blot-type TLC. Recently, synthetic GI-A (C_{19:0}/C_{16:0}) was shown to stimulate a novel subtype of NKT cell in a CD1d dependent manner.^[14] GI-A loaded CD1d tetramer were selective for V α 10 NKT over the canonical V α 14 NKT cell and induced a dose dependent cytokine response biased towards T_H2 cytokines (cytokines are discussed in detail in Chapter 4). Importantly the authors also demonstrated that the lipid composition and position of the glycerol was essential for bio-activity, as the regioisomeric variant iso-GI-A (C_{16:0}/C_{19:0}) and a desmethyl analogue nor-GI-A (C_{18:0}/C_{16:0}) were less active.

The potency of GI-LM and PI-LM were investigated by Mishra and colleagues to stimulate the release of TNF- α using a human macrophage line.^[112] Interestingly GI-LM was found to be as stimulatory as the PI-anchored LM. This evidence suggested that the PI moiety does not play a key role in lipoglycan pro-inflammatory activity. To the best of our knowledge, no known immunological studies have been carried out on GI-X.

3.6. Research objective

Study of the immunological properties and biosynthesis of the structurally-complex GI-X is hindered due to limited sources of the natural product. We aimed to undertake the synthesis of GI-X analogue **3.1** as a synthetic model for the natural product GI-X isolated from *C. glutamicum* (Figure 3.6). The targeted GI-X analogue **3.1** contains two important features present in the GI-X molecule: i) a 1 \rightarrow 4- α -D-Manp linkage to a glucuronic acid residue, and ii) an α -D-GlcAp^{xi} linkage to a dipalmitoyl glycerol moiety. The difference to the natural glycolipid is the replacement of the unsaturated alkyl chain by a saturated alkyl chain (Figure 3.6). The ultimate aim was to develop a synthesis of these compounds and to examine

^{xi} D-GlcAp indicates D-glucopyranosuronic acid.

their biochemical properties in cell free assays in *C. glutamicum*. We hoped that these biochemical studies would allow understanding of the role of GI-X in *C. glutamicum*, which in turn may give an insight into its potential role in TB, if present in *M. tuberculosis*.

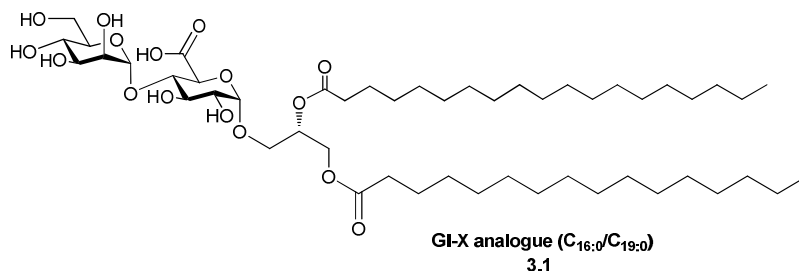


Figure 3.6 Structure of GI-X analogue **3.1** (C_{16:0}/C_{19:0}).

3.7. Design of GI-X analogue 3.1

The synthetic strategy to the target GI-X analogue **3.1** (Figure 3.6) involved careful considerations: a suitable method for constructing a difficult α -glucosidic linkage and the use of protecting groups that could be removed in the presence of benzyl esters in the desired product. Of special concern was the timing for the introduction of the acid functionality, and as glucuronosyl donors are known to exhibit poor reactivity, the acid functionality was to be introduced post-glycosylation. The building blocks for the synthesis of the GI-X analogue **3.1** are illustrated in Figure 3.7. In building block **3.2**, the ester protecting group at the C-2 position allows neighbouring group participation to afford a 1,2-*trans* mannoside linkage. Building block **3.3** is designed to serve as a glycosyl donor for intramolecular aglycon delivery (IAD; described in detail in Section 3.7.2) to provide a 1,2-*cis*-glucosidic linkage for the synthesis of glycolipid **3.1**. As well, the careful choice of the 4-bromobenzylidene group provides a means for accessing the C-6 position (by a regioselective reduction) for subsequent oxidation to the carboxylate group, and concomitantly installing a 4-*O*-(4-bromobenzyl) (PBB) ether, which can be removed in a two-step approach in the presence of unsubstituted benzyl ethers. Building block **3.4** acts as a glycosyl acceptor for the IAD glycosylation reaction with building block **3.3**.

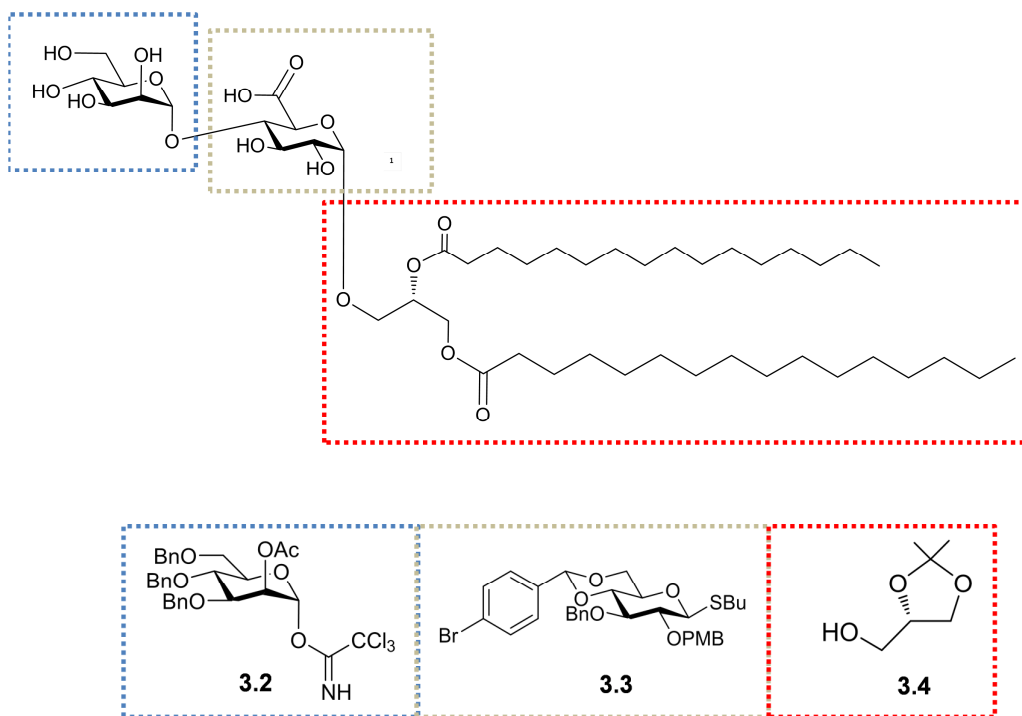
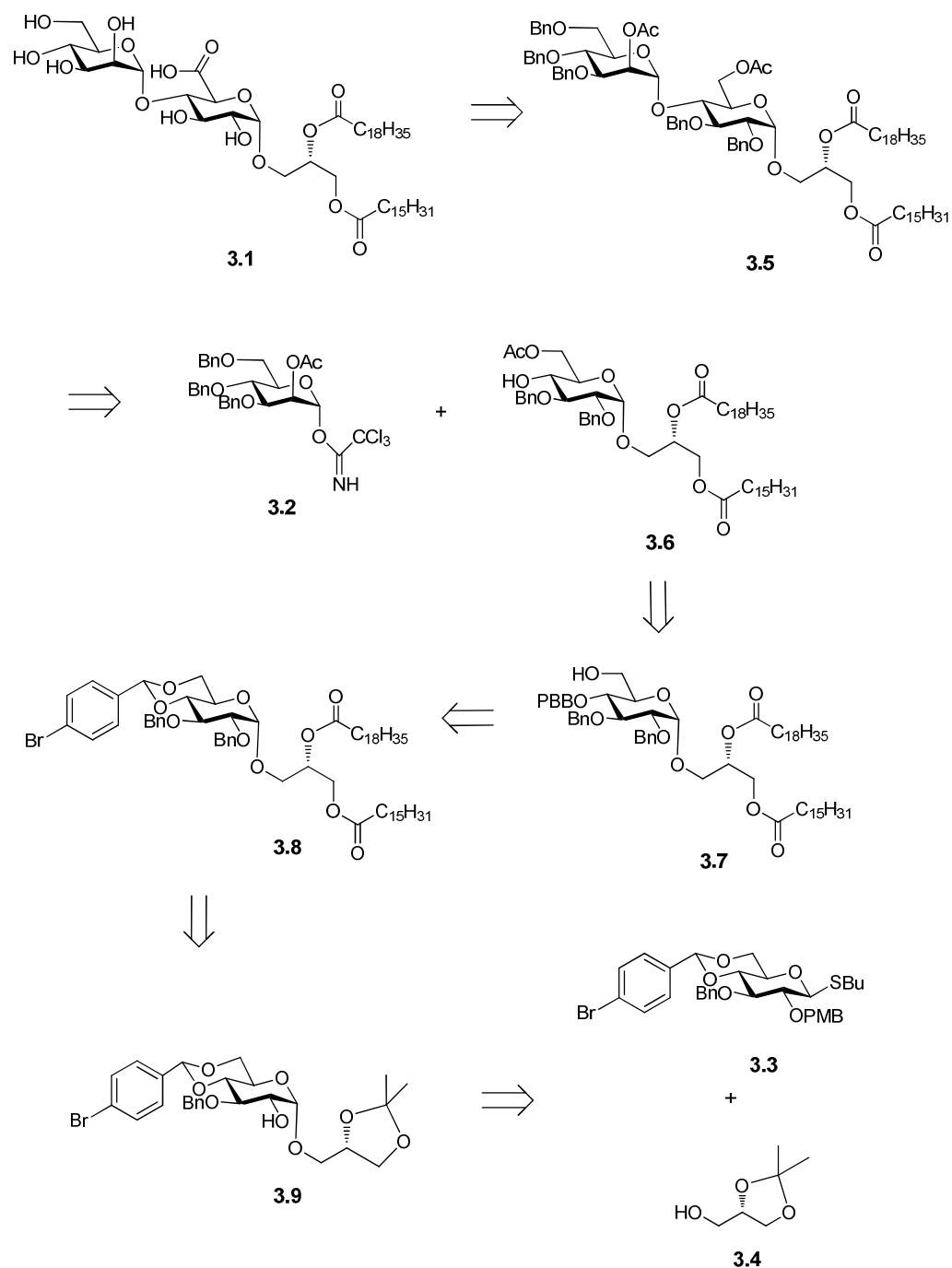


Figure 3.7 Proposed synthons for the synthesis of GI-X analogue **3.1**.

A retrosynthetic pathway is proposed in Scheme 3.3. A selective deacylation of C-2' and C-6 acetyl groups of glycolipid **3.5** in the presence of the diacylglycerol liberates the free hydroxyl groups, whilst maintaining the ester linkage of the diacylglycerol. Selective oxidation of the primary alcohol in the presence of the secondary alcohol using TEMPO, followed by global debenzylation allows the formation of the glycolipid **3.1**. Reaction of the mannosyl trichloroacetimidate **3.2** (bearing an acetyl group at the C-2 position to allow neighbouring group participation) with the glycosyl acceptor **3.6** stereoselectively forms a 1,2-trans linkage as in glycolipid **3.5**. Acetylation of the C-6 hydroxyl group on glycolipid **3.7**, followed by PBB deprotection (whereby PBB can be removed by conversion to a *p*-aminobenzyl group *via* a Pd-mediated amination reaction followed by oxidation)^[113] affords the desired glycosyl acceptor **3.6**.

Chapter 3: Synthesis of GI-X based glycolipid for biochemical evaluation



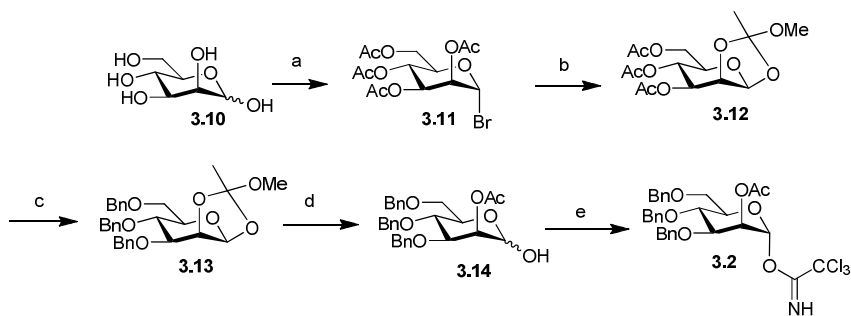
Scheme 3.3 Proposed synthetic pathway of GI-X analogue **3.1**.

Regioselective ring-opening of the 4,6-*p*-bromobenzylidene group of glycolipid **3.8** liberates a free hydroxyl group at the C-6 position, whilst the C-4 position is protected as a PBB ether as in glycoside **3.7**. The glycolipid **3.8** is formed by

protection of the hydroxyl group by a Williamson ether synthesis of glycoside **3.9**, followed by acidic cleavage of the isopropylidene protecting group and subsequent coupling to fatty esters. Since we considered the α -selective coupling of the D-glucose residue **3.3** to the suitably protected *sn*-glycerol^{xii} moiety **3.4** to be the most challenging glycosylation in the synthesis, the approach was designed where this linkage was constructed early in the synthesis (or late in the retrosynthesis). Thioglycoside **3.3** was designed to enable a 1,2-*cis*-glucosidic linkage using IAD methodologies. The *p*-methoxybenzyl (PMB) group at the C-2 position of this glycosyl donor **3.3** can be oxidatively coupled (DDQ) to the glycosyl acceptor **3.4** in the presence of the 4,6-*p*-bromobenzylidene group to produce the desired 1,2-*cis* linkage in glycoside **3.9** with a free hydroxyl group at the C-2 position.

3.7.1. Synthesis of α -mannosyl donor 3.2

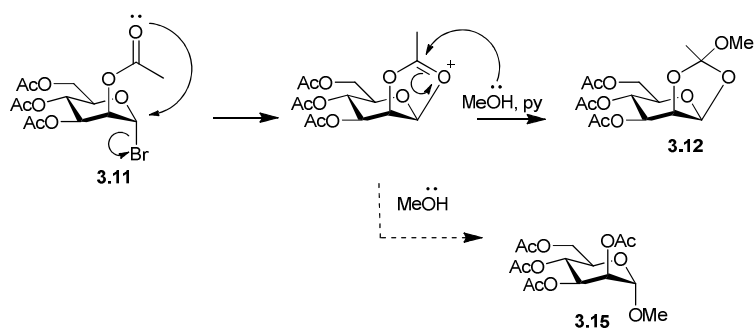
Schmidt and coworker's introduced glycosyl trichloroacetimidates, which are robust glycosyl donors suitable for glycosylation reactions of a wide variety of glycosyl acceptors (discussed in more detail in Chapter 4).^[114] The glycosyl donor **3.2** was readily prepared following a literature procedure (Scheme 3.4).^[115]



Scheme 3.4 Reagents and conditions. a) i) catalytic H_2SO_4 , Ac_2O , $0\text{ }^\circ\text{C}$ to rt, 3 h, 84% ii) HBr/AcOH , $0\text{ }^\circ\text{C}$ to rt, 18 h, 92%, α -anomer b) py/MeOH 2:1, rt, 18 h, 57% c) i) NaOMe , MeOH , 1 h ii) NaH , BnBr , DMF , $0\text{ }^\circ\text{C}$ to rt, N_2 , 18 h, quant. d) HOAc , rt, 18 h, 85% e) NCCl_3 , DBU , CH_2Cl_2 , $0\text{ }^\circ\text{C}$ to rt, N_2 , 2.5 h, 58%, α -anomer.

^{xii} the prefix '*sn*' (for *stereospecifically numbered*) is used for glycerol to indicate its prochiral stereochemistry.

Acetylation of D-mannose by treatment with Ac_2O and catalytic H_2SO_4 yielded the α -anomer as the major product.^[116] Anomeric bromination using 33% HBr/AcOH afforded the mannosyl bromide **3.11** exclusively as the α -anomer (88% over two steps). The α -stereoselectivity is attributed to the anomeric effect.^[69] The mannosyl bromide **3.11** was treated with Pyr/MeOH mixture to afford the glycosyl orthoacetate **3.12** as a mixture of diastereoisomers (1:4 endo/exo) in a 57% yield. The proposed reaction mechanism for the formation of the orthoester **3.12** is shown in Scheme 3.5. Nucleophilic participation by the neighbouring acetyl group by the neighbouring acetyl group (discussed in Chapter 2) forms a dioxolenium ion, which is attacked at the electrophilic carbon by MeOH to form the orthoester **3.12**.^[69]



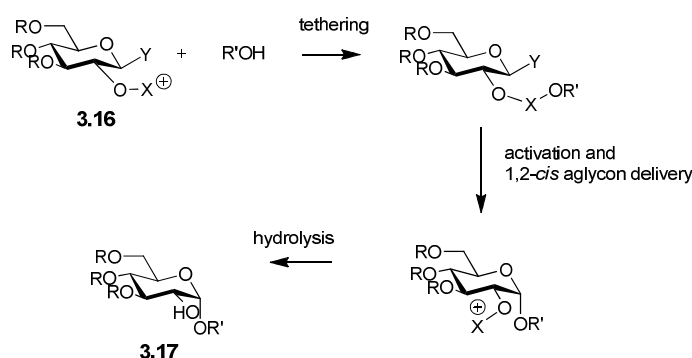
Scheme 3.5 Mechanism for the formation of orthoacetate **3.12**.^[69]

Deacetylation of **3.12** under standard Zemplén conditions followed by a Williamson ether synthesis afforded the benzyl orthoacetate **3.13** in quantitative yield (Scheme 3.4). The orthoacetate group was cleaved using AcOH to afford the mannosyl hemiacetal **3.14** in 85% yield. Treatment of the mannosyl hemiacetal **3.14** with trichloroacetonitrile in the presence of catalytic DBU yielded the α -mannosyl donor **3.2** in 58% yield. Characterisation of the trichloroacetimidate **3.2** was performed with the aid of ^1H NMR data, which was in agreement with data reported in the literature.^[115]

3.7.2. Intramolecular Aglycon Delivery

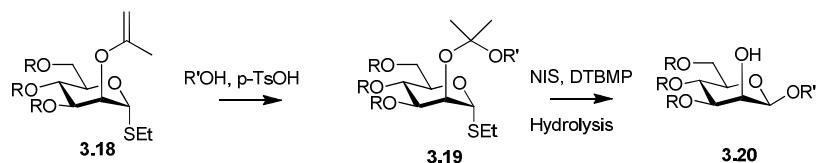
Controlling the stereochemical outcome of a glycosylation reaction is one of the most challenging tasks for carbohydrate chemists (discussed in detail in Chapter 2).

Intramolecular aglycon delivery (IAD) is an elegant approach designed to stereoselectively produce 1,2-*cis* glycosyl linkages (especially for β -mannosides) via a three-step process.^[117] First, the glycosyl donor **3.16** and acceptor are tethered together in such a manner to allow for 1,2-*cis* delivery of the tethered acceptor (Scheme 3.6).^[117a] Second, the glycosylation is performed by activation of the glycosyl donor. Finally, hydrolysis of the protecting group at the C-2 position of the 1,2-*cis* glycoside intermediate affords the C-2 hydroxy 1,2-*cis* glycoside **3.17**. In most cases steps 2 and 3 are combined, with the residual group at the C-2 position being cleaved during the glycosylation itself or workup.

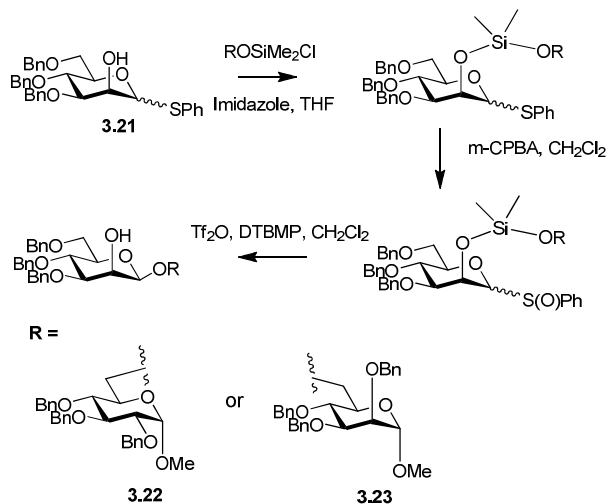


Scheme 3.6 The intramolecular aglycon delivery concept for the formation of 1,2-*cis* linkages in a glucopyranoside **3.17** involves tethering, activation, 1,2-*cis* aglycon delivery and hydrolysis.^[117a]

Barresi and Hindsgaul pioneered the concept of IAD.^[118] They utilised an acid-catalysed tethering approach from thioglycoside **3.18** to produce the mixed acetal **3.19** that was activated and hydrolysed to form the 1,2-*cis*- β -mannoside **3.20** (Scheme 3.7). Later, Stork introduced silicon-tethered IAD approaches.^[119] Stork utilised the thiomannoside **3.21** to tether alcohol acceptors derived from dimethylchlorosilyl ethers (Scheme 3.8).^[119] Oxidation of the anomeric substituent to give the glycosyl sulfoxide followed by glycosylation using Kahne's conditions (F_2O and DTBMP) afforded the intramolecular β -mannosides **3.22** and **3.23** in excellent yields.^[120]



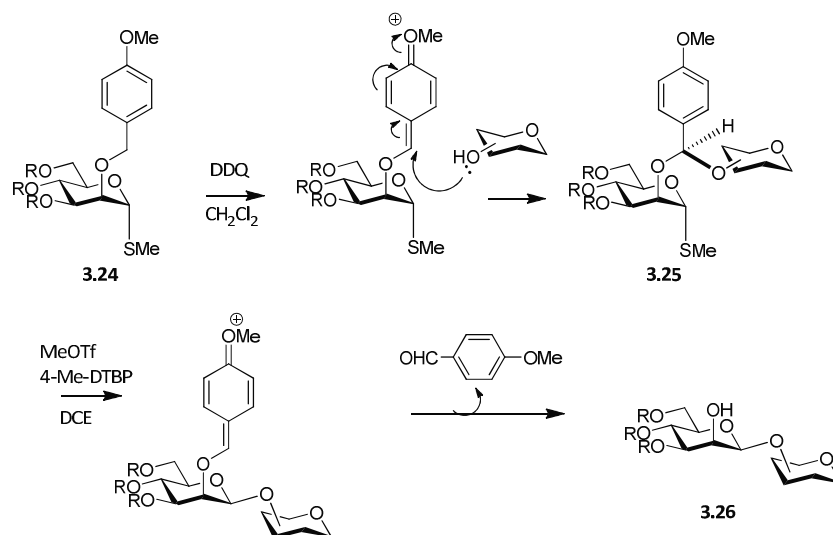
Scheme 3.7 Barresi and Hindsgaul IAD approach utilising acid-catalysed acetal tethering, glycosylation and hydrolysis to give 1,2-*cis* mannopyranoside **3.20**.^[119]



Scheme 3.8 Examples of Stork's silicon tethered IAD approach to produce 1,2-*cis* mannopyranosides **3.22** and **3.23**.^[119]

Perhaps the most useful IAD approach involves an oxidative tethering introduced by Ogawa and Ito,^[121] which is best explained using a mechanism proposed by their team (Scheme 3.9).^[122] This approach involves the tethering of the 2-*O*-PMB or 2-*O*-naphthylmethyl ether of a glycosyl donor (fluoride or thioglycoside) such as glycoside **3.24** to an acceptor using DDQ in CH₂Cl₂ to produce a mixed acetal intermediate **3.25**. Subsequent activation of the donor initiates the transfer of the tethered acceptor at the C-2 position of the glycosyl donor to the anomeric position to stereoselectively produce 1,2-*cis*-products after hydrolysis, such as the disaccharide **3.26**. Two distinct advantages lie in their method. First, the highly-efficient oxidative tethering ensures there is no need for chromatographic separation of the mixed acetal intermediate. Second, good overall yields (40% to 74%) and stereoselectivities were reported for both primary and secondary alcohols, indicating that a diverse range of acceptors could be used. Subsequent work carried out by Ito and Ogawa involved the use of thioglycosides as donors in

place of glycosyl fluorides, presumably due to the difficulties in controlling/curbing the highly reactive nature of glycosyl fluorides.^[123]

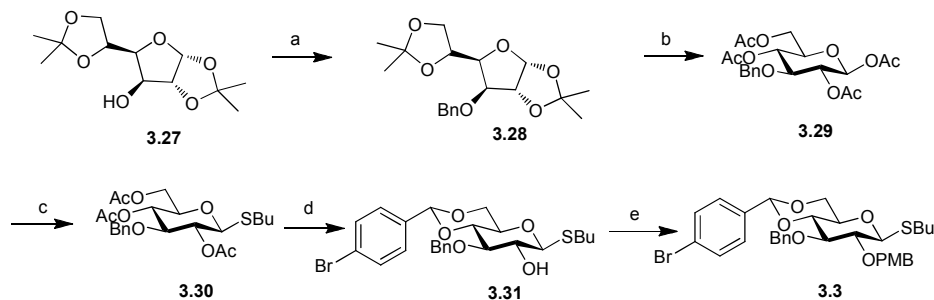


Scheme 3.9 Reaction mechanism proposed by Ogawa and Ito for IAD through 4-methoxybenzylidene-tethered intermediate to give desired product **3.26**.^[122]

3.7.3. Synthesis of Glycosyl Donor **3.3** for Intramolecular Aglycon Delivery

As discussed earlier (Section 3.7), the glycosyl donor **3.3** was designed with orthogonality in mind, enabling the selective cleavage of certain groups in the presence of others (Scheme 3.3). Commercially-available diacetone glucose **3.27** was chosen as the starting material for the synthesis of glycosyl donor **3.3** due to the accessibility of a free hydroxy group in the C-3 position (Scheme 3.10). This would subsequently allow for selective PMB protection of the C-2 position in the sequence. Benzylation of the diacetone glucose **3.27** afforded 3-*O*-benzyl diacetone glucose **3.28** in quantitative yield. Treatment of furanoside **3.28** with strongly acidic Dowex ion exchange resin (H⁺ form) at 70 °C resulted in hydrolysis of the acetonide protecting groups and simultaneous reversion to the more thermodynamically-stable pyranose form, giving 3-*O*-benzyl-D-glucopyranose. The crude glycoside was acetylated using Ac₂O and catalytic DMAP in Pyr to give the tetra-*O*-acetylated glucoside **3.29** as the β-anomer with a yield of 89% over two steps. The tetraacetate **3.29** was reacted with butanethiol and BF₃·OEt₂ to afford the thioglucoside **3.30** in a yield of 75%. Next, thioglucoside **3.30** was treated with catalytic Na metal in MeOH to give a triol intermediate, which was subsequently treated with *p*-

bromobenzylaldehyde dimethyl acetal and catalytic *p*-TsOH to afford the *p*-bromobenzylidene thioglycoside **3.31** in 88% (over two steps). The synthesis of glycosyl donor **3.3** was completed by treating glycoside **3.31** with NaH and *p*-methoxybenzyl bromide in a Williamson ether synthesis to yield the glycosyl donor **3.3** in 88%.



Scheme 3.10 Reagents and conditions a) NaH, BnBr, 0 °C to rt, quant. b) i) Dowex 50WX2-400 (H⁺ form), H₂O, 70 °C ii) cat. DMAP, Ac₂O, Pyr, rt, 89% (2 steps) c) BuSH, BF₃·OEt₂, rt, 75% d) i) cat. Na, MeOH ii) bromobenzylaldehyde dimethyl acetal, *p*-TsOH, MeCN, 88% (2 steps) e) NaH, PMBBBr, DMF, 88%.

Thioglycosides are versatile glycosyl donors (discussed in Chapter 4). They are stable to a range of chemical transformations.^[69] In the current scheme, the early introduction of the thioglycoside allows for further protecting group manipulations on the sugar that may not be possible with other anomeric substituents. The thioglycoside substituent also allows for a subsequent IAD glycosylation. To suit the criteria needed to design the glycolipid **3.1** (Scheme 3.3), the anomeric substituents of the glycosyl donor must be applicable to IAD and be orthogonal to the overall synthesis. These criteria are not met by other potential anomeric substituents, such as trichloroacetimidates or fluorides. Also worth noting is the choice of the anomeric substituent. We chose to use SBu in our synthetic methodology in place of the more commonly utilised SMe substituent more commonly used in oxidative IAD.^[123a, 123c] This action was taken to avoid the use of methanethiol as a starting material as it has an unpleasant odour relative to butanethiol. As well, it should be noted that arylthioglycosides have not been reported in IAD glycosylations, and it would appear that their reactivity is too low to be of use with the mild promoters used for IAD reactions.

As outlined in the synthetic strategy our route requires a means of accessing the C-4 position of the glucoside **3.3** for glycosylation with the mannosyl donor **3.2**. Benzylidene acetals can be ring opened to generate either 4-OH or 6-OH derivatives through careful choice of reagents. Garegg and co-workers were the first to report a regioselective ring opening of a benzylidene group to give the free C-4 hydroxyl product using a NaCNBH₃-HCl system.^[124] The same group later reported the use of a borane-Lewis acid combination (BH₃.NMe₃-AlCl₃) to yield the desired C-4 hydroxyl product. What they found was that the reaction was solvent dependent; the desired regioselectivity was observed in THF, however the free C-6 hydroxyl product was formed in toluene or CH₂Cl₂/ether solvent systems.^[125] Mechanistic studies exploring the regiochemical outcome of benzylidene protected sugars was carried out by Johnsson and colleagues.^[126] They propose that the regioselectivity that results in C-4 hydroxyl products is determined by the formation of an initial complex with the borane, activated by the Lewis acid in THF. This is converted into an oxocarbenium ion, which is reduced to give the free C-4 hydroxyl product. In the same publication, stereoelectronic effects were observed by competition studies using 1:1 mixtures of a benzylidene sugar and a *p*-bromobenzylidene sugar. They noted a weak influence in acetal cleavage outcome from the electron-withdrawing group on the *p*-bromobenzylidene, but no change in regioselectivity. Incidentally, the use of cyclic protected groups (such as benzylidene or *p*-bromobenzylidene) on glycosyl donors have also been reported to increase the glycosylation yields in oxidative IAD reactions.^[123a, 123c] It is believed that the increased rigidity of the system encourages an S_N2-like reaction to occur. As such, the choice of the *p*-bromobenzylidene protecting group serves many purposes in the synthesis of donor **3.3**.

Characterisation and assignment of the protons of the novel glycosyl donor **3.3** was achieved with a combination of ¹H NMR data, ¹³C NMR, 2D NMR data and EI-MS. A section of the ¹H NMR is shown below as a representative example (Figure 3.8). The conversion of the glycoside **3.31** into the desired glycosyl donor **3.3** involves the introduction of an PMB group into the structure. One defining feature of this new

substituent that indicates its presence in the glycosyl donor structure **3.3** is the appearance of a characteristic singlet at 3.8 ppm (3 H) representing the methyl protons of the PMB group. Signals corresponding to the methylene protons and the aromatic moiety of the PMB protecting group appear in regions of the ^1H NMR spectrum where significant overlap occurs with other signals. Important signals confirming the structure of glycosyl donor **3.3** include the anomeric proton at 4.53 ppm (d, $J = 9.8$ Hz, 1 H, H-1) and the benzyldene proton at 5.52 ppm (s, 1 H, CHArBr). Similarly, in the ^{13}C NMR, diagnostic signals which correspond to the coupling of the PMB substituent are present at 55.27 ppm (ArOCH_3) and 76.75 ppm (OCH_2ArOMe) including additional aromatic signals. HR-MS confirmed the m/z ratio of the glycosyl donor **3.3**.

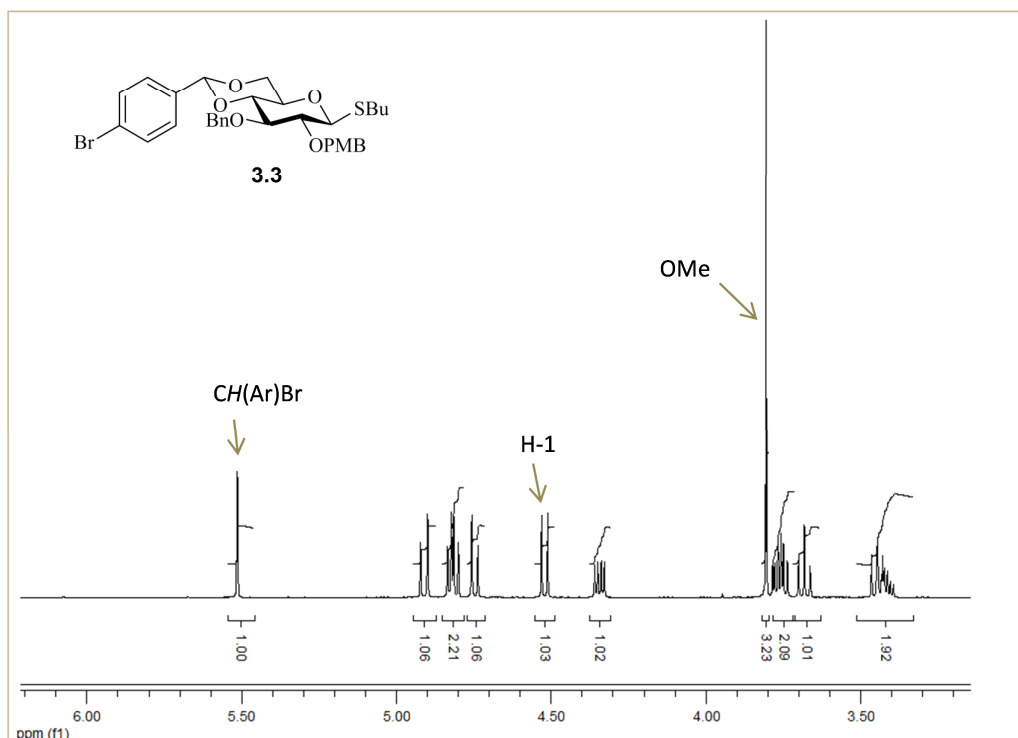
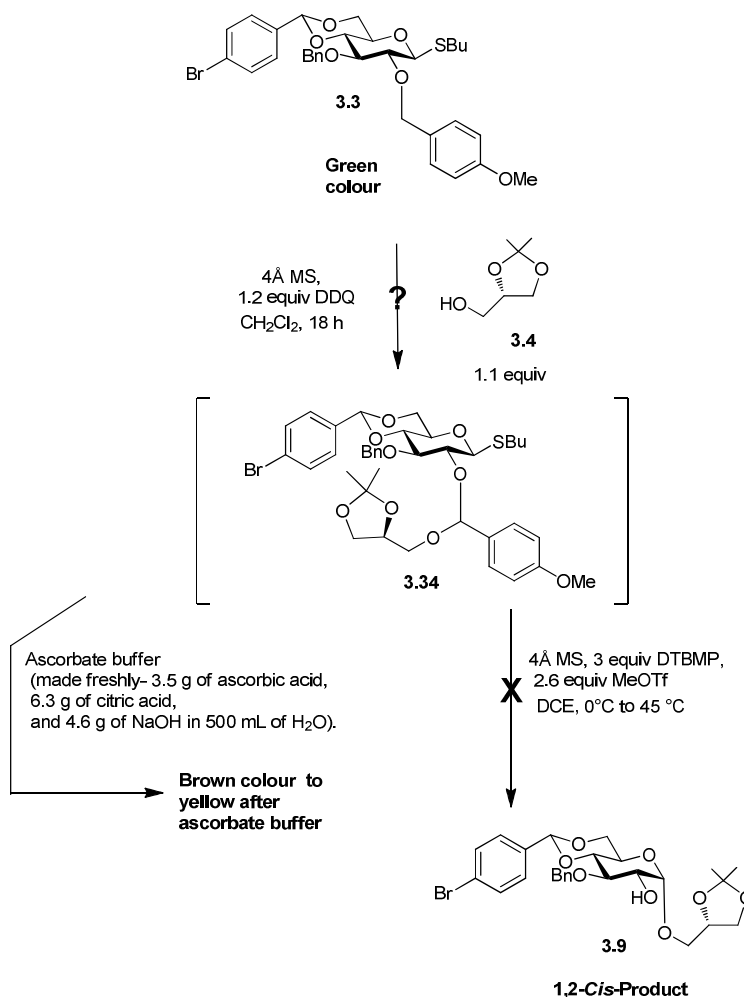


Figure 3.8 Section of ^1H NMR spectrum of glycosyl donor **3.3** for IAD. Characteristic signals are highlighted.

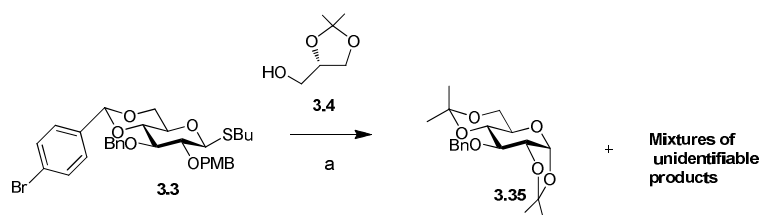
3.7.4. Initial Attempts at Intramolecular Aglycon Delivery Glycosylation

For the oxidative tethering and subsequent glycosylation, the procedure set out by Bertozzi and co-workers was followed.^[127] Under an inert atmosphere, the glycosyl

donor **3.3** and acceptor **3.4** were reacted with DDQ (freshly recrystallized from toluene) for 18 h in anhydrous CH_2Cl_2 containing 4Å MS to oxidatively tether the glycosyl acceptor **3.4** and the glycosyl donor **3.3** (Scheme 3.11). TLC analysis indicated the slow consumption of glycosyl donor **3.3** (over the 18 h period) and a corresponding appearance of a more polar product. No difference was observed at 18 h compared to 16 h with regard to consumption of the starting material and was therefore quenched.



Scheme 3.11 Attempted oxidative IAD conditions for formation of 1,2-cis product **3.9**.

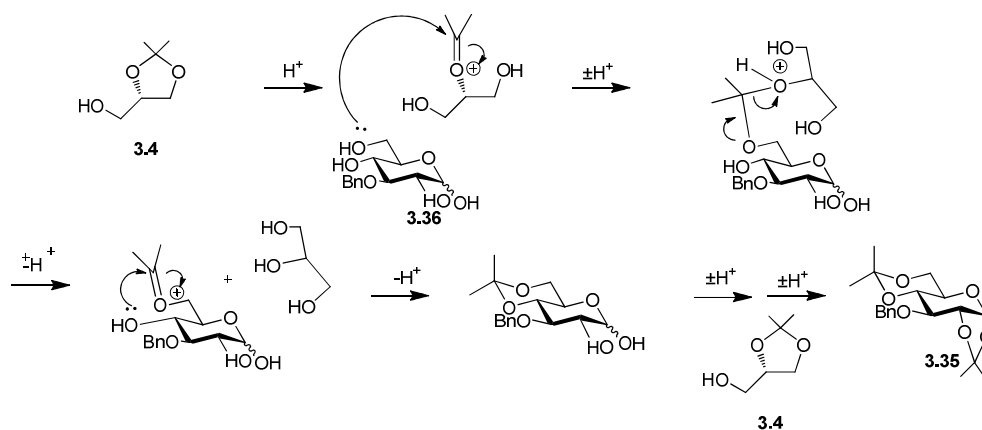


Scheme 3.12 Reagents and conditions a) DTBMP, MeOTf, DCE, 0 °C to rt, <10%.

The reaction was quenched with ascorbate buffer and extracted. The mixed acetal **3.34** was treated with MeOTf in the presence of DTBMP (which is added to diminish hydrolysis side-reactions) and allowed to stand for 18 h. A complicated mixture of products was evident from TLC analysis. The crude ^1H NMR analysis of the reaction mixture indicated the consumption of the glycosyl donor **3.3**. Flash column chromatography afforded the acetonide **3.35** (< 10% yield) along with a complicated mixture of unidentifiable compounds (Scheme 3.12), with no clear signs of formation of 1,2-*cis*- β -glucoside **3.9** (Scheme 3.11). The ^1H NMR spectrum of side product **3.35** appears in Figure 3.9. Diagnostic signals are highlighted; these signals and others verify the structure of the side product **3.35**.

A proposed mechanism for the formation of acetonide **3.35** is outlined in Scheme 3.13. The mechanism is based on the following assumptions: i) DDQ has fully oxidised the PMB group to give the free hydroxyl group at the C-2 position, ii) nucleophilic attack by water under Lewis acid conditions (MeOTf) has resulted in a free hydroxyl group at the anomeric position, and iii) ring opening of the *p*-bromobenzylidene group has occurred under acidic conditions to give the benzyl protected sugar **3.36**, which has free hydroxyl groups at the C-1, C-2, C-4 and C-6 positions. The mechanism is based on the fact that 1,2-*O*-isopropylidene glycerol **3.4** can undergo migration under acidic conditions that, in turn, can cause epimerisation of the glycerol.^[128] Under acidic conditions, the acetonide of the protected *sn*-glycerol **3.4** can ring open to give an oxocarbenium intermediate. One of the free hydroxyl groups on the sugar **3.36** can attack the electrophilic carbonyl to form a mixed acetal. Under acidic treatment, the *sn*-1 hydroxy of the glycerol can be protonated; the second carbenium intermediate can be formed with the

displacement of glycerol. The hydroxyl at the C-4 position of the sugar can then capture the oxocarbenium ion, which results in acetonide protection at the 4,6-positions of the glycoside. By a similar mechanism, 1,2-acetonide transfer can occur to result in the 1,2:4,6-diacetonide **3.35**.



Scheme 3.13 Proposed mechanism for formation of isolated side product **3.35**.

In order to achieve glycosylation products with high yields, isopropylidene migration from the aglycon must be prevented. The difficulties associated with isopropylidene migration can be avoided with the use of different protecting groups on the aglycon such as silyl ethers or benzyl ethers. A new strategy was therefore sought to synthesise a suitable aglycon, one that may not undergo isopropylidene migration and also, one that will be reactive enough to undergo IAD.

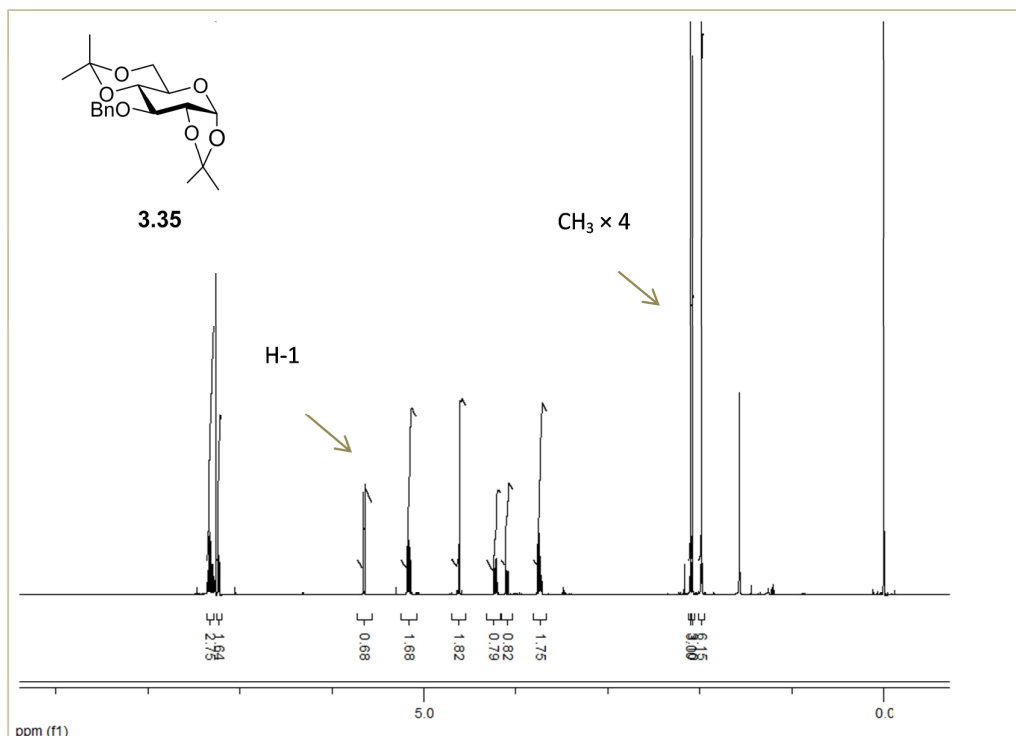
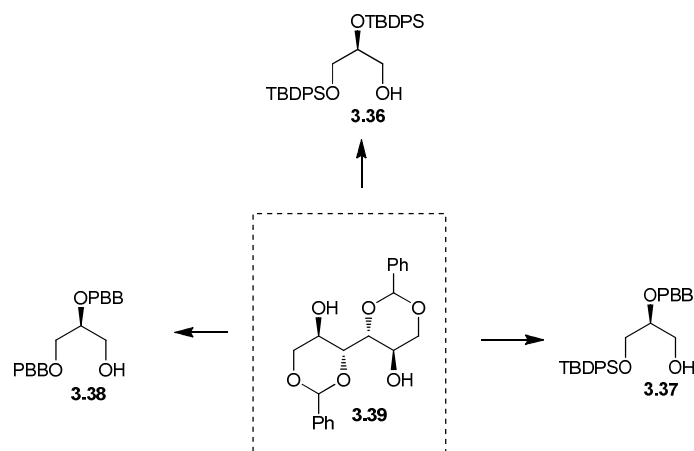


Figure 3.9 ^1H NMR spectrum of IAD side product **3.35**. Characteristic signals are highlighted.

3.7.5. Investigations into Alternative Aglycons for their use in Intramolecular

Aglycon Delivery

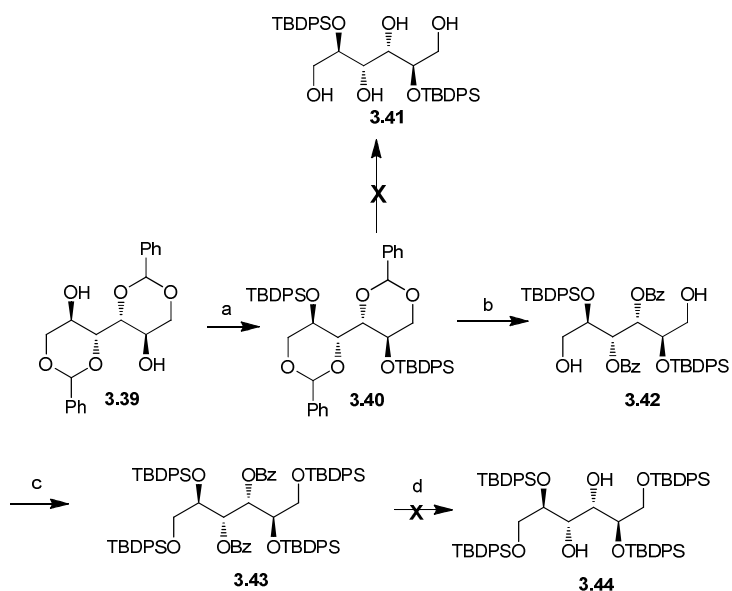
The building blocks **3.36**, **3.37** and **3.38** were investigated for their use as alternative glycosyl acceptors in IAD (Scheme 3.14). These building blocks were to be synthesised from 1,3:4,6-di-*O*-benzylidene mannitol **3.39**, which can be obtained from D-mannitol. With a view to maintaining orthogonality in the synthesis of GI-X analogue **3.1** (Figure 3.7), the most suitable glycosyl acceptor is *sn*-glycerol derivative **3.36** because the hydroxyl groups are protected as *tert*-butyldiphenylsilyl (TBDPS) protecting groups. These protecting groups are orthogonal to both the PMB and *p*-bromobenzylidene groups functional groups present on the glycosyl donor **3.3**.



Scheme 3.14 Suitable *sn*-glycerol derivatives **3.36**, **3.37** and **3.38** synthesised from D-mannitol derivative **3.39** for IAD glycosylation reaction.

An attempt to synthesise *sn*-glycerol derivative **3.36** was undertaken as in Scheme 3.15. 1,3:4,6-Di-*O*-benzylidene mannitol **3.39** was synthesised by a colleague from D-mannitol and benzaldehyde catalysed by H₂SO₄ in DMF, and purified by recrystallisation. Silylation of the secondary alcohols on *sn*-glycerol derivative **3.39** with TBDPSCI using imidazole in DMF proceeded smoothly to give **3.40** in a yield of 82%. Attempts at benzylidene hydrolysis to give the tetraol **3.41** failed under acidic conditions (HCl or TFA). Similarly, the hydrolysis did not proceed using pyridinium 4-toluenesulfonate, a weak acid catalyst that is commonly used to deprotect tetrahydropyran protecting groups.^[129] Alternatively an approach involving regioselective oxidative cleavage of the bis-benzylidene acetals was attempted.^[130] The D-mannitol derivative **3.40** was treated with KBrO₃ and Na₂S₂O₄ in a biphasic system of EtOAc/H₂O to yield the diol **3.42** in a yield of 34%. The isolated yield of the desired regioisomer **3.42** was lower than the 88% yield reported by Senthilkumar *et al.* under the same reaction conditions.^[130] The formation of the regioisomer **3.45** (Figure 3.10) was not observed in our work, despite its reported isolation by Senthilkumar *et al.*^[130] Another inconsistency was the isolation of the mixed diol **3.46** (19%), which was not observed by Senthilkumar *et al.* (Figure 3.10). Silylation of the primary alcohols of D-mannitol derivative **3.42** using TBDPSCI and imidazole afforded 51% of the protected D-mannitol derivative **3.43**. Surprisingly, standard Zemplén conditions (NaOMe) failed to remove the benzoate ester groups

to give silyl protected D-mannitol derivative **3.44**. The synthetic methodology was abandoned owing to a limited time frame.



Scheme 3.15 Reagents and conditions. a) Imidazole, TBDPSCI, DMF, 0 °C to 50 °C, 82%; b) KBrO_3 , $\text{Na}_2\text{S}_2\text{O}_4$, EtOAc, H_2O , 34%; c) imidazole, TBDPSCI, DMF, 0 °C to rt, 51%; d) cat. Na metal, MeOH.

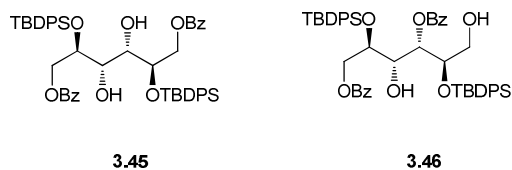
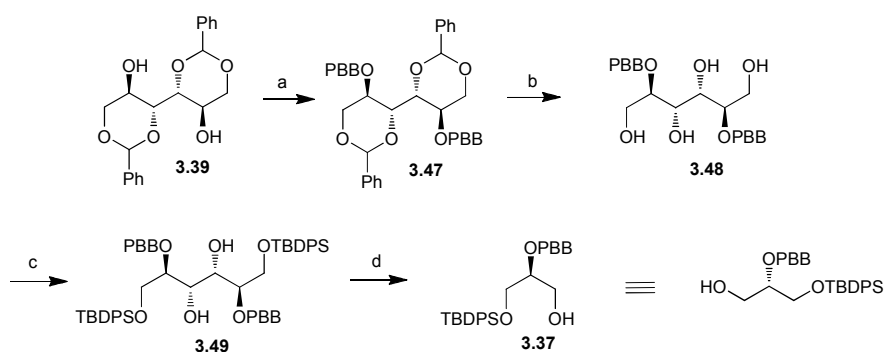


Figure 3.10 Potential side products **3.45** and **3.46** using Sentkilkumar regioselective ring opening reaction.^[130]

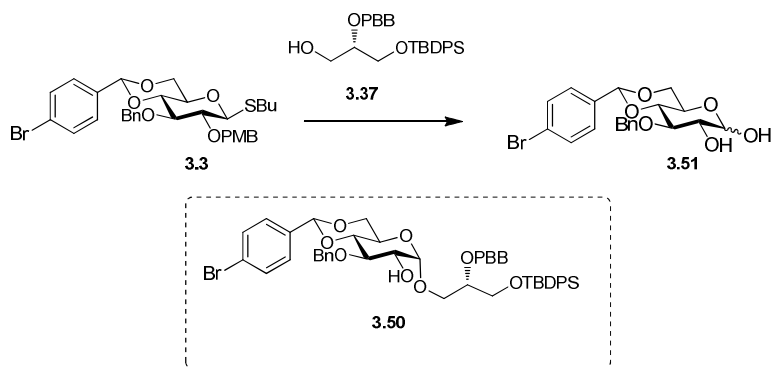
The PBB protected *sn*-glycerol **3.37** (Scheme 3.14) is not a suitable substrate for an IAD reaction with glycosyl donor **3.3**. Deprotection of the *p*-bromobenzyl ether group of the intermediate glycoside for subsequent reaction with Schmidt's trichloroacetimidate **3.2** would result in simultaneous cleavage of the PBB ether on the *sn*-glycerol backbone. However, to obtain a potential indication of the IAD approach for an α -selective *sn*-glycerol glycosylation, it was decided to pursue the synthesis of the aglycon **3.37**. The synthesis of the PBB protected glycerol **3.37** is shown in Scheme 3.16. An approach previously executed in the laboratory was

pursued, whereby 1,3:4,6-di-*O*-benzylidene D-mannitol **3.39** was etherified with *p*-bromobenzyl bromide using NaH in DMF, to give derivative **3.47** in a yield of 88%. Hydrolysis of the benzylidene protecting groups, in contrast to the attempted hydrolysis in the synthesis of the silyl protected glycerol **3.41** (Scheme 3.15), was successful. Treatment of the PBB-protected D-mannitol derivative **3.47** with 4 N HCl in EtOH afforded the tetraol **3.48** in 79% yield. Silylation of the primary alcohols of tetraol **3.48** with TBDPSCI and imidazole in DMF smoothly proceeded in 91% yield to give the *cis* diol **3.49**. The *cis* diol **3.49** then underwent oxidative cleavage with NaIO₄ to give an aldehyde intermediate that was subsequently reduced with NaBH₄ to afford the PBB-protected glycerol **3.37** in 62% yield (over two steps).



Scheme 3.16 Reagents and conditions. a) NaH, *p*-BrBnBr, DMF, 0 °C to rt, 88%; b) 4 N HCl, EtOH, 79%; c) Imidazole, TPDPSCI, DMF, 0 °C to rt, 93%; d) i) NaIO₄, THF/H₂O 4 :1 ii) NaBH₄, EtOH/H₂O 9:1, 62%.

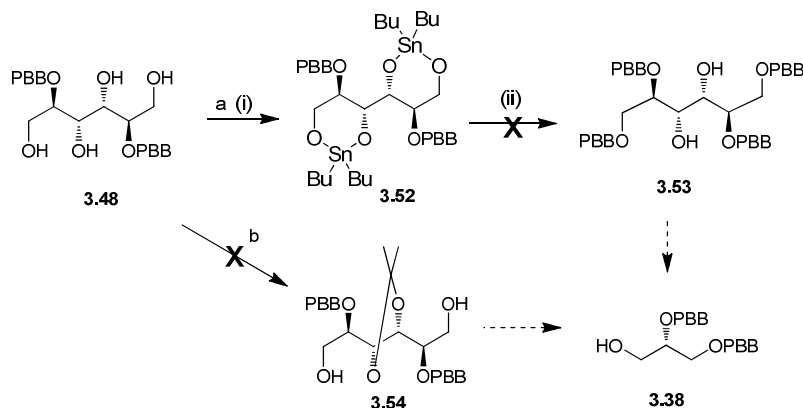
An IAD reaction was attempted using the glycoside **3.3** and PBB glycerol acceptor **3.37** (Scheme 3.17) using the reaction conditions described earlier in Scheme 3.11. After 18 h, neither the acceptor **3.37** nor the donor **3.3** were fully consumed in the reaction based on TLC analysis. However, it was quenched because the reaction did not seem to progress further after 6 h. Formation of a new product was observed by TLC analysis, which was presumably the mixed acetal. After workup, activation of the thioalkyl group of the mixed acetal product was attempted using MeOTf and afforded a complicated mixture of products. Disappointingly, none of the desired 1,2-*cis* product **3.50** was isolated. Only the diol **3.51** was isolated in a 10% yield.



Scheme 3.17 Reagents and conditions. a) i) DDQ, CH₂Cl₂, 4Å MS, rt b) DTBMP, 4Å MS, CH₂Cl₂, MeOTf, 0 °C to 45 °C, 10%. Desired glycoside **3.50** is highlighted.

As a final attempt to demonstrate a successful IAD reaction using the glycosyl donor **3.3**, the PBB protected glycerol derivative **3.38** (Scheme 3.14) was considered. This glycerol derivative contains only robust PBB groups at the *sn*-1 and *sn*-2 positions of *sn*-glycerol. The proposed synthesis is shown in Scheme 3.18. Dibutyltin oxide can be used to form *O*-stannylene acetals on polyfunctional molecules containing vicinal and 1,3-diol systems. Subsequent regioselective alkylations/acylations at the stannylated oxygen atoms have successfully been employed in many syntheses.^[131] A rationale for the regioselectivity seen in alkylations is as follows. The oxygen atoms of the corresponding stannylene acetals are more nucleophilic than the other hydroxyl groups in the molecule owing to donation of electron density to oxygen. Secondly, addition of excess soluble halide shorten reaction times of stannylene acetal reactions from sluggish (3-4 days) reactions to tolerable (18 h) reactions.^[131] The halide ions are believed to break up polymeric aggregates of the stannylene acetals and results in the formation of halide coordinated monomers or dimers. In these monomers, the oxygen atoms of the *cis*-diol function typically adopt apical and equatorial positions with respect to the coordinating tin atom, which adopts a trigonal bipyramidal geometry. Typically, primary oxygen atoms in a 1,2- or 1,3-diol occupy the apical position, which is more electron rich owing to electron channelling in the complex to the apical positions; thus, a selective alkylation/acylation can occur at this position. A regioselective stannylation of the primary alcohols in the tetraol **3.48** (previously synthesised in Scheme 3.16) was attempted using dibutyltin oxide in refluxing toluene, using a Dean-Stark apparatus for the continuous removal of water, to produce a

coordinated dibutyltin acetal as in *O*-stannylene acetal **3.52** (Scheme 3.18). The stannylene acetal presumably formed was reacted *in situ* with excess BrBnBr and TBAB, and the reaction mixture was heated to reflux at 18 h. The formation of the *p*-bromobenzylated species **3.55** (Figure 3.11) together with the fact that none of compound **3.38** was isolated, strongly indicated a failure in this approach from the polyol **3.48** (Scheme 3.18).



Scheme 3.18 Reagents and conditions. a) i) Bu_2SnO , toluene, reflux ii) BrBnBr, TBAB, toluene, reflux b) 2,2-dimethoxypropane, *p*-TsOH, rt.

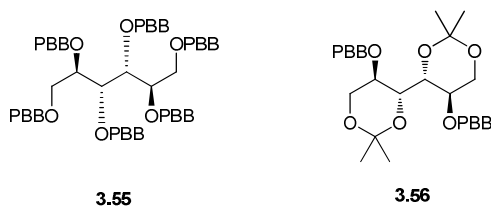


Figure 3.11 Undesired side products **3.55** and **3.56** in synthesis of desired *sn*-glycerol derivative **3.38**.

Reaction of a polyol containing several different hydroxyl groups with an aldehyde or ketone under acidic conditions result in the formation of cyclic acetals. Generally, ketones (or dimethyl acetals) preferentially form 5-membered rings due to thermodynamic factors (unfavourable diaxial interactions in the 6-membered cyclic acetal), whereas aldehydes preferentially form 6-membered rings (previously discussed in Section 2.7.3). In addition, if the two hydroxyl groups are *cis* to one another, they are more likely to form an acetonide as too much ring strain exists in

an alternative *trans* configuration. Thus, in theory, selective protection of certain hydroxyl groups can be achieved. A reaction of D-mannitol derivative **3.48** with 2,2-dimethoxypropane in *p*-TsOH was attempted (Scheme 3.18). Compound **3.54** was not isolated; instead complicated mixtures of products were observed. However the compound **3.56** (Figure 3.11) was isolated and its structure was identified by ¹H NMR and ¹³C NMR. Due to the unfavourable results achieved to date in our syntheses, along with unfavourable IAD results reported in the laboratory using glycerol acceptors, the IAD approach to GI-X was abandoned.

3.8. Summary

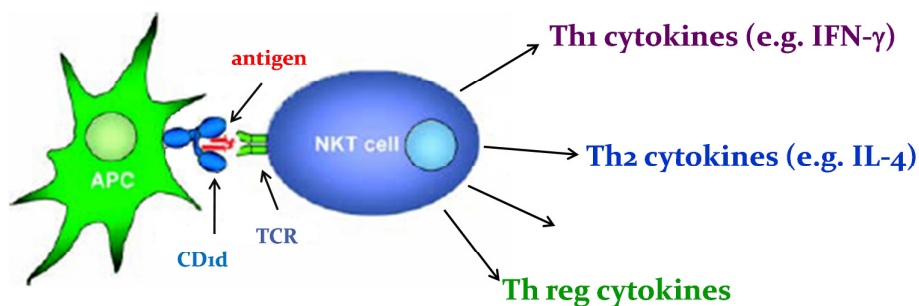
The successful syntheses of Schmidt's trichloroacetimidate **3.2**, the novel IAD glycosyl donor **3.3** and the glycosyl acceptor **3.4** for the synthesis of GI-X analogue **3.1** was described (Figure 3.7). We report unsuccessful IAD glycosylation reactions with glycosyl donor **3.3** and acceptors **3.4** and **3.37** and discussed various attempts to synthesise glycosyl acceptors from D-mannitol derivatives suitable for the IAD approach. The difficulties associated with the IAD approach and problems arising from incompatible protecting group strategies were highlighted. Time constraints did not allow the completion of this project, however subsequent efforts in the laboratory led to the overall synthesis of GI-A (a precursor to GI-X) and its analogues from *M. smegmatis* by halide ion catalysis using glycosyl iodides.^[132] It is hoped that GI-X will be synthesised by similar methods in the future within the laboratory.

Chapter 4: Synthesis of L-serinyl based glycolipid analogues of the immunostimulant KRN7000

4.1. Introduction

4.1.1. Immunological functions of *i*NKT cells

Natural killer T (NKT) cells are a sublineage of T cells that share properties of both T lymphocytes and Natural Killer (NK) cells.^[133] $V\alpha 14i$ NKT cells are the most abundant NKT cells in mice; they express an invariant TCR α chain (i TCR α chain) with $V\alpha 14$ - $J\alpha 18$ rearrangement. Humans have a similar population that mostly expresses an invariant $V\alpha 24$ - $J\alpha 18$ rearrangement ($V\alpha 24i$ NKT cells). Collectively, these populations are referred to as *i*NKT cells.^[134] *In vivo* activation of *i*NKT cells involves the binding of a binary complex formed by the loading of an antigen (such as KRN7000) onto the CD1d protein to the *i*NKT cell (Scheme 4.1).^[135] Cytokines are released as a result and depending on the different types and amounts of cytokines released, different immunological responses are induced.



Scheme 4.1 The immunological function of *i*NKT cells: presentation of CD1d-antigen binary complex to *i*NKT cell produces a ternary complex, which results in secretion of different types of cytokines to elicit different immunological effects.^[135]

The CD1d is a member of the CD1 family, along with four other isoforms termed Cd1a, CD1b, CD1c and CD1e. These proteins present lipidic antigens to NKT cells.^[136] Upon binding, a rapid secretion of cytokines will take place. Cytokines are small cell-signalling proteins that are secreted by numerous cells; they are used extensively in intercellular communication. A variety of cytokine types can be produced,^[137] but only T helper 1(T_H1) and T helper 2(T_H2) will be discussed in the context of this thesis. Pro-inflammatory cytokines (such as IFN- γ , IL-2) characterise a T_H1 type response and are implicated in the treatment of tumours, bacterial and viral

infections.^[22, 133a, 135] The release of immunomodulatory cytokines (IL-4, IL-5) leads to a T_H2 type response; a role for these T_H2 cytokines has been reported in the management of autoimmune diseases.^[22]

4.1.2. KRN7000

Agelasphin-9b was isolated from the extract of a marine sponge called *Agelas Mauritanus* in 1993, and this glycosphingolipid was found to exhibit anti-tumour and immunostimulatory properties.^[138] KRN7000 (or commonly termed α -GalCer) was developed soon after by researchers at Kirin Brewery Co., following structure-activity relationship studies on agelasphins.^[21] The structures of KRN7000 and agelasphin-9b are depicted in Figure 4.1.

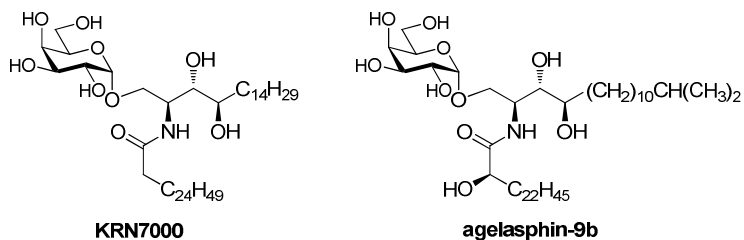


Figure 4.1 Structure of KRN7000 and agelasphin-9b.^[21]

KRN7000 was identified as a ligand for *i*NKT cells, and in pre-clinical trials, it exhibited anti-tumour properties in mice inoculated with B16 melanoma or EL-4 lymphoma.^[4] Not alone did they successfully achieve a relatively high rate of cured mice, but these mice were resistant to subsequent tumour challenge, indicating immune memory.^[139] Phase 1 clinical trials were undertaken on 24 patients suffering from refractory solid tumours.^[139] It was observed that the effects of KRN7000 on patients seemed to be reliant on their expression levels of *i*NKT cells, which was later confirmed by Kawano and colleagues in mice studies.^[140] Many of the patients tested in the clinical trials had low levels of *i*NKT cells prior to testing, indicating that the number of *i*NKT cells could be a marker for tumour activity. As a result, no partial or complete tumour responses were observed in this trial and clinical trials were terminated. Several clinical trials have been conducted since

using a combination of KRN7000 and dendritic cells (DC) and more promising results have ensued.^[141] Of special consideration also is that KRN7000 produces both T_H1 and T_H2 responses upon presentation to *i*NKT cells. The biological effects of the T_H2 response (immunosuppressant) can counteract the desired T_H1 response (proinflammatory) in cancer treatments. This accounts for another plausible reason why KRN7000 has not reached the marketplace as a suitable drug candidate for tumour treatment. Analogues of KRN7000 which could bias either response prompted an interest in the scientific community. Some of these examples will be discussed in Section 4.2.

A breakthrough in the understanding of the immunological functions of KRN7000 occurred when X-ray crystal structures of the human CD1d antigen presenting protein and the CD1d-KRN7000 binary complex were obtained (Figure 4.2).^[142] From the X-ray crystal structure of the CD1d-KRN7000 complex, it was discerned that the protein contained two large hydrophobic pockets (A' and C') which accommodated the alkyl chains of KRN7000. The hydrogen-bond network was elucidated, whereby the hydroxyl groups on the sugar moiety (except the hydroxyl group at the C-6 position) and the hydroxyl groups on the ceramide moiety were participating in hydrogen-bonding with the amino acid residues in the CD1d protein. It has been proposed that the affinity of antigens for CD1d contributes to the robust immunological response they produce. It has been proposed that the more stable the binary complex, the more bias towards a T_H1 response and, conversely, the less stable the complex, the more bias towards a T_H2 response.^[22, 143] Therefore the synthesis of analogues of KRN7000 which can stabilise/destabilise the binary complex has been a challenge for many chemists.

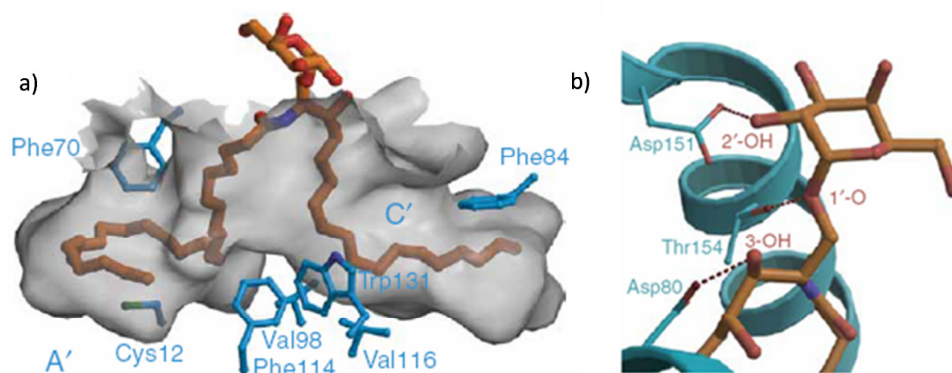


Figure 4.2 Antigen binding and recognition of KRN7000 in CD1d. (a) Side view of bound KRN7000. The hydrophobic antigen-binding groove, with pockets labeled A' and C' is gray; KRN7000 is orange; residues of CD1d are blue. (b) Hydrogen-bonds between residues of CD1d and KRN7000.^[142]

4.2. KRN7000 Analogues

Since its discovery, numerous analogues of KRN7000 have been synthesised with a view that structural alterations will tune the stability of the CD1d-antigen binary complex. Biological evaluations have been performed, with varying success.^[22, 144] The main sites for modifications in KRN7000 are highlighted in Figure 4.3, and representative examples will be discussed in the following sections. These include i) variations at the anomeric centre including β -anomeric linked, S- and C-glycolipid analogues; ii) changes at the polar head group such as the use of glucose or functionalization at different positions on the carbohydrate; iii) functionalization's to the ceramide moiety including changes at the stereocentres and variations in the length of the alkyl chains and/or different degrees of saturation, or by introducing different functional groups in the chains, like aromatic groups. Some striking modifications (with increased/ decreased T_H1 or T_H2 bias compared to KRN7000) will be discussed in more detail in the following section.

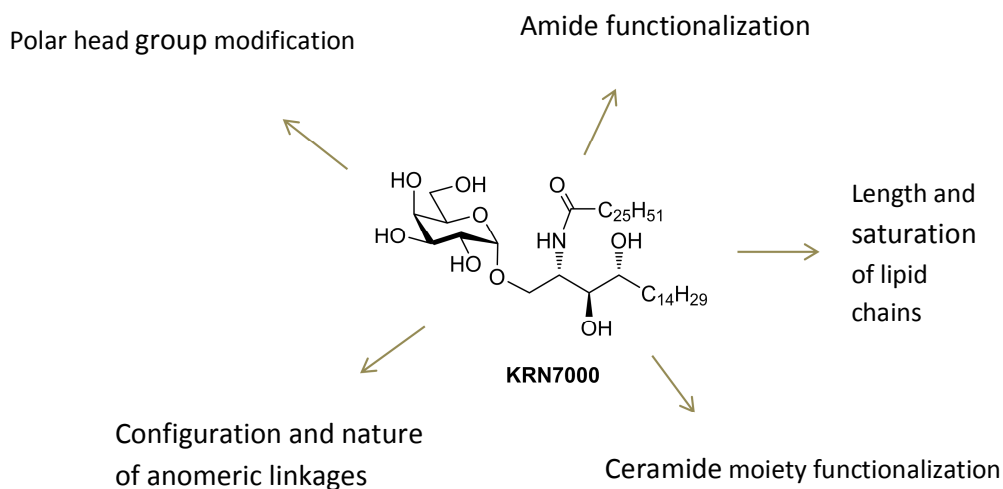


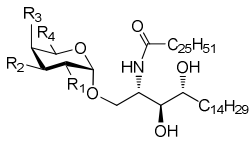
Figure 4.3 Different types of modifications on KRN7000.

4.2.1. Sugar modifications on O-glycoside analogues of KRN7000

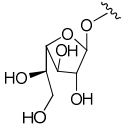
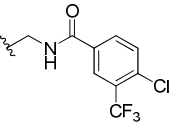
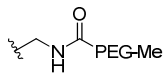
Variations to the carbohydrate residue have been investigated, and some have shown biased cytokine production. While it is well known that α -D-mannosylceramide and β -D-galactosylceramide exhibit no immunological effects to date in the context of *i*NKT cell activation, α -D-glucosylceramide was reported to have similar bioactivities to α -D-galactosylceramide (KRN7000) by Kawano and colleagues.^[145] These immunogenic results were in line with affinity studies of the glycolipid/CD1d binary complex for the TCR on an *i*NKT cell.^[146] It has recently been shown that β -D-mannosylceramide induced strong protection against cancer metastasis and it was reported to act in an *i*NKT cell-dependent manner, opening a window of opportunity for synthesis of a range of mannopyranosyl analogues of KRN7000.^[147] The immunogenic properties of KRN7000 analogues bearing alternative glycosyl moieties to galactopyranosides have been met with limited success. Despite showing promising bioactivities, no examples of sugar modified O-glycoside analogues display superior anti-tumour/autoimmune properties to KRN7000 to the best of our knowledge, thus cementing the importance of the galactose head group in the quest to synthesise a more efficient KRN7000 analogue. Several analogues have been described in which modifications on the different positions of the D-galactose moiety have been performed. Some of the

compounds were obtained by replacement of the hydroxyl groups on the sugar with other functional groups, indicated as R¹, R², R³ and R⁴ are shown in Table 4.1.

Table 4.1 KRN7000 analogues obtained by substitutions on the sugar moiety KRN7000.



KRN 7000 (2S', 3S', 4R')
R¹, R², R³ = OH, R⁴ = CH₂OH

Entry	R ¹	R ²	R ³	R ⁴	Activity compared to KRN7000	Ref.
1	F	OH	OH	CH ₂ OH	No <i>i</i> NKT cell activation ^m	[147a]
2	OMe	OH	OH	CH ₂ OH	No <i>i</i> NKT cell activation ^m	[147b]
3	OH		OH	CH ₂ OH	decreased <i>i</i> NKT cell activation ^m	[144]
4	OH	OH	OH		Increased T _H 1 bias ^{m+}	[148]
5	OH	OH	OH	COOH	Increased TH1 bias ^{m+,h}	[149]
6	OH	OH	OH	CH ₂ OMe	Increased T _H 1 bias ^{m+}	[150]
7	OH	OH	OH		Increased T _H 2 bias ^{m+}	[151]

⁺ *in vivo* test on mice; ^m *in vitro* test on mice cells; ^h *in vitro* test on human cells.

In vitro studies on mice *i*NKT cells performed with KRN7000 analogues, with replacement of the hydroxyl group at R¹ with fluorine or methoxy substituents resulted in a complete loss of bioactivity compared to KRN7000 (Entries 1, 2 in Table 4.1), with no *i*NKT cell activation reported for either glycolipid.^[148] Substitution at the R² position of the galactose moiety resulted in a decreased *i*NKT cell activation compared to KRN7000 (Entry 3 in Table 4.1).^[145]

Modifications at the R⁴ position of the sugar moiety lead to interesting immunogenic results. The replacement of the hydroxyl group with an aromatic moiety (Entry 4 in Table 4.1) gave a slight bias towards a T_H1 response compared to KRN7000,^[149] presumably because of favourable aromatic π - π stacking occurring between the glycolipid and the Trp153 amino acid residue of the CD1d protein,

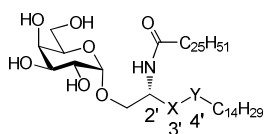
stabilising the ternary complex. Similarly, a good T_H1 bias was reported for the replacement of the C-6 hydroxyl group with either a carboxylic acid ^[150] or a methoxy substituent (Entries 5 and 6 in Table 4.1).^[151] Perhaps these results are not surprising since the crystallographic studies discussed earlier (Section 4.1.2.) showed that the C-6 hydroxyl group did not participate in hydrogen-bonding. The introduction of an amide functionality at the R⁴ position (Entry 7 in Table 4.1) resulted in an unexpected T_H2 bias compared to KRN7000.^[152] As the biological process of *i*NKT cell activation is very intricate and many of the molecular details are yet to be understood, it is unknown precisely how the T_H2 bias occurs in this situation. The increased water solubility of the PEG glycolipid may play a role in the bioavailability of the antigen, in agreement with what was reported for other T_H2 ligands.^[22] These reports seem to indicate functionalization at the C-6 position (R⁴) is superior to analogues with functionalizations at the other positions of the glycosyl moiety to date.

4.2.2. Modifications on the ceramide backbone of the O-glycoside analogues of

KRN7000

As the hydroxyl groups on the ceramide moiety were found to be involved in the hydrogen-bond network of the CD1d-KRN7000 binary complex, according to X-ray crystallographic studies,^[142] modifications of these functional groups would have a significant influence on the stabilisation/destabilisation of the binary complex, which in turn may lead to improved bias towards either T_H1 or T_H2 responses. Structure-activity relationship studies have been carried out in this regard and the structure of some of these analogues are shown in Table 4.2.

Table 4.2. KRN7000 analogues obtained by modifications to the ceramide backbone.



KRN7000 (2'S, 3'S, 4'R)
X, Y = CHOH

Entry	Configuration 2'	X (Configuration 3')	Y (Configuration 3')	Activity compared to KRN7000	Ref.
1	S	CH ₂	CH ₂	No <i>i</i> NKT cell activation ^m	[152]
2	S	CH-OH (S)	CH-OH (S)	Increased T _H 1 bias ^{m,h}	[153]
3	R	CH-OH (S)	CH-OH (S)	Decreased <i>i</i> NKT cell activation ^{m,h}	[153]
4	S	CH-NH ₂ (S)	CH-OH (S)	Decreased T _H 1 bias ^{m+}	[154]
5	S	CH-NH ₂ (R)	CH-OH (S)	Decreased T _H 1 bias ^{m+}	[154]
6	S	CH-OH (S)	CH-NH ₂ (S)	Decreased T _H 1 bias ^{m+}	[154]
7	S	CH-OH (S)	CH-NH ₂ (R)	Decreased T _H 1 bias ^{m+}	[154]

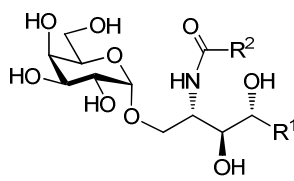
^m *in vitro* test on mice cells; ^{m+} *in vivo* test on mice; ^h *in vitro* tests on human cells.

Unsurprisingly perhaps, the removal of the hydroxyl groups at the X and Y positions (Entry 1 in Table 4.2) and replacement with methylene groups (with no hydrogen-bond donation ability) resulted in a complete loss of *i*NKT cell activation ability.^[153] Park and colleagues carried out biostudies on stereoisomers of KRN7000.^[154] They found that changing the stereochemistry at the 4' position (Entry 2 in Table 4.2) had little or no effect on the T_H1 bias compared to KRN7000. However, a dramatic loss of *i*NKT cell activation activity was reported with an inversion of stereochemistry at the 2' position (Entry 3 in Table 4.2). Trappenier and co-workers focused on the replacement of hydroxyl groups with amines, and compared these analogues with their stereoisomers (Entries 4-7 in Table 4.2).^[155] The biological effects were evaluated and, in all the cases studied, dramatic decreases in T_H1 bias were observed compared to KRN7000. The authors believe these results are due to protonation of the amine functional groups at physiological pH, which destabilises the CD1d-antigen binary complex by repulsion with the positively charged Arg95. In summary, the chiral integrity of KRN7000 seems to be important in the synthesis of KRN7000 analogues in order to exhibit good bioactivities.

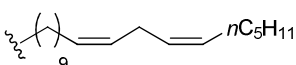
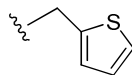
4.2.3. Modifications and/or functionalization of the lipid chains

Modifications of the lipid chain length and/or functionalization at the amino acid/sphingosine base positions have been explored, and for the most part have resulted in promising immunological outcomes. Table 4.3 summarises some of these findings in the literature.

Table 4.3 Modifications and/or functionalisation to the lipid chain.



KRN7000
 $R^1 = nC_{14}H_{29}$
 $R^2 = nC_{25}H_{51}$

Entry	R^1	R^2	Activity compared to KRN7000	Ref.
1	$nC_{14}H_{29}$	CH ₃	Decreased T _H 2 bias ^m , Increased T _H 2 bias ^h	[155]
2	nC_5H_{11}		Similar T _H 2 ^m	[158]
3	$nC_{14}H_{29}$	(CH ₂) ₇ Ph	Increased T _H 1 bias ^{m+,h}	[149]
4	$nC_{14}H_{29}$		Increased T _H 2 bias ^h	[30]

^{m+} in vivo tests on mice; ^m in vitro test on mice cells; ^h in vitro tests on human cells.

Goff and colleagues altered the lipid lengths of KRN7000 and found that truncation of the lipid chain at the amino acid functionality (Entry 1 in Table 4.3) resulted in a decrease in T_H2 bias, compared to KRN7000, by performing *in vitro* tests in mice.^[156] Interestingly, they observed the opposite outcome when testing the glycolipid *in vitro* with human cells, with an increased T_H2 bias compared to KRN7000, however the authors provide no explanations for this observation. Oki and colleague set out to provide a rationale for the T_H2 bias observed for truncated analogues of KRN7000, and proposed that shorter alkyl chain analogues failed to engage the TCR for a long enough period of time to induce IFN- γ secretion (T_H1 bias).^[157] Conflicting evidence is provided by Wu and co-workers,^[158] whereby crystal structures of a

truncated analogue of KRN7000 bound to CD1d was very similar to that obtained by Koch and colleagues, discussed earlier in Section 4.1.2.^[142] Introducing unsaturation in the alkyl chains and shortening of the sphingosine base alkyl chain (Entry 2 in Table 4.3) resulted in similar T_H2 responses to those of KRN7000.^[159]

The introduction of aromatic groups at the amino acid functionality (Entry 3 in Table 4.2), together with a long alkyl chain resulted in an increased bias for T_H1 responses compared to KRN7000.^[150] This result further highlights the influence of aromaticity on a T_H1 bias, as described in Section 4.2.1 whereby the presence of aromatic functional groups at the C-6 position of the sugar moiety increased the IFN- γ secretion (T_H1 response) compared to KRN7000. However, it seems that the long alkyl chain plays a dominant role in this selectivity also, as the 2-thienylacetyl analogue (Entry 4 in Table 4.3) resulted in a T_H2 bias.^[30]

Replacement of the amide functionality of the phytosphingosine backbone with long chain triazole rings was performed by Lee and colleagues.^[160] Triazoles can act as bio-isosteres to amide bonds (discussed later in this chapter), with hydrogen-bonding donation occurring from the proton on the triazole ring. Additionally, hydrolytic cleavage is less problematic with triazole linkages compared to their amide bond counterparts also. Lee *et al.* observed that glycolipids **4.1** and **4.2** (Figure 4.4) exhibited improved T_H2 biased cytokine production *in vitro* on mice cells compared to KRN7000. However, the long alkyl chains were necessary for this bias to occur, as shorter analogues tested by the same group did not exhibit this effect.

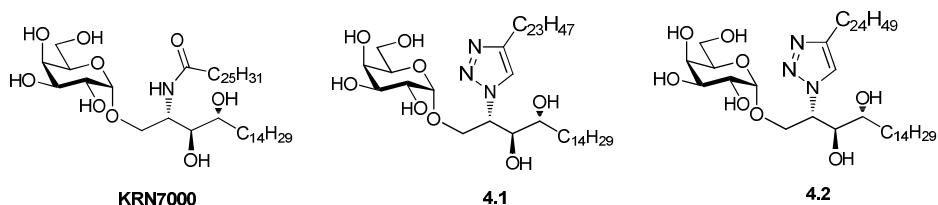


Figure 4.4 Structure of KRN7000 and triazole-containing analogues **4.1** and **4.2**.

4.2.4. Miscellaneous analogues of KRN7000

Many structurally diverse analogues of KRN7000 have been synthesised and their immunogenic properties have been assessed. The structures of representative glycolipids are shown in Figure 4.5. By changing the nature of the glycosidic bond, different physiological responses are anticipated. For example, changing from the native *O*-linkage to a *C*-, *N*- and *S*-glycosidic linkage limits the *in vivo* metabolism of the glycolipid by endogenous glycosidases.^[161]

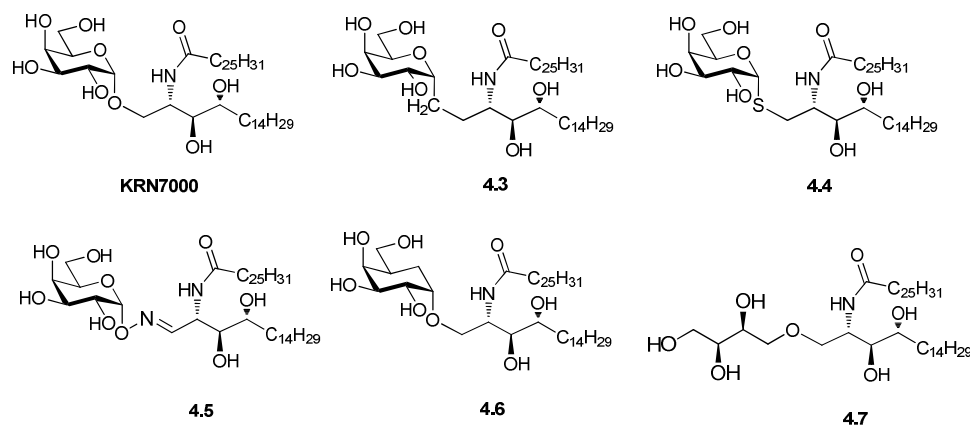


Figure 4.5 Structure of KRN7000 and selected miscellaneous analogues **4.3**, **4.4**, **4.5**, **4.6** and **4.7**.^[162]

The synthesis and *in vitro* mice studies of the *C*-glycoside **4.3** (Figure 4.5) was carried out by Kotobuki Pharmaceutical Co., and the analogue showed a stronger T_H1 response compared to KRN7000.^[162a] However, since this pioneering *C*-glycoside, no *C*-analogues have exhibited improved immunogenic properties compared to KRN7000 in the literature. *S*-glycosidic analogues of KRN7000 emerged in 2008 by Dere and co-workers, with the synthesis of glycolipid **4.4**.^[162b] Shortly after, Blauvelt and colleagues performed *in vitro* and *in vivo* tests on this analogue, whereby no activation whatsoever of *i*NKT cells was observed.^[163] A plausible reason for this inactivation is the length of the carbon-sulfur bond (182 pm), which is longer than the carbon-oxygen bond length, which could destabilise the ternary complex. The synthesis of the oxime derivative **4.5** was undertaken by Harrak and colleagues.^[162c] Despite the expected improved bioactivities due to the physiologically stable oxime linkage, a total loss of *i*NKT activation was observed, which was attributed to the additional length due to the oxime nitrogen atom.

More promising results were observed for the bioactivities of the carbasugar **4.6** and the threitolceramide analogue **4.7**.^[162d, 162e] The carbasugar **4.6** exhibited improved T_H1 biased *in vivo* cytokine production compared to KRN7000, whilst the threitolceramide **4.7** exhibited good bioactivities. These results are attributed to the greater metabolic stabilities compared to KRN7000. Many other different types of KRN7000 analogues are discussed in the literature such as cyclitol, inositol and non-glycoside analogues but will not be discussed in the present thesis.^[22]

4.2.5. β -glycoside analogues

The synthesis and biological evaluation of β -linked KRN7000 analogues are rarer compared to the corresponding α -glycoside counterparts, despite the fact that it is believed that the endogenous *i*NKT cell ligand contains a β -glycosidic linkage if, in fact, it possesses an endogenous ligand at all. Much debate is on-going in this regard. The rationale for this belief stems from the fact that there are no known α -glycosylated glycolipid antigens found in mammalian species to date. It has been recently reported that an abundant endogenous lipid, β -D-glucopyranosylceramide (β -GlcCer), was found to be a potent *i*NKT cell self-antigen in mice and humans.^[164] Koezuka and colleagues were the first to synthesise and study the bioactivity of the β -anomer of KRN7000.^[165] They observed a distinct reduction in anti-tumour activity compared to KRN7000. They similarly reported a decrease in anti-tumour activity of the β -glucosyl analogue of KRN7000 compared to the parent compound. Several groups have reported similar reductions in bioactivities when comparing β -analogues to their α -counterparts.^[166]

One promising literature example described the immunogenic evaluation of a β -C-glycoside analogue of KRN7000 **4.8** (Figure 4.6).^[167] The *in vitro* studies showed glycolipid **4.8** as a promising anti-tumour agent. However, no *in vivo* studies have been performed on the glycolipid to date. So, despite the limited scientific interest in the synthesis and evaluation of β -glycolipid analogues of KRN7000, evidence suggests that they too have potential as immune regulating compounds.

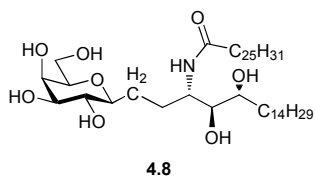


Figure 4.6 Structure of β -C-KRN7000 analogue **4.8**.

4.2.6. L-Serine glycosides as KRN7000 analogues

One emerging type of KRN7000 analogue of interest to our research group contains an L-serine residue in place of the phytoshingosine backbone of KRN7000. Fan and co-workers were the first team to investigate L-serine derivatives as potential KRN7000 analogues. They carried out *in vitro* mice studies on the proliferation of mouse spleenocytes using KRN7000 and several L-serine based analogues.^[168] They observed that the L-serine based analogue **4.9** (Figure 4.7) stimulated both IFN- γ (T_H1) and IL-4 (T_H2), albeit to a lesser degree compared to KRN7000. Interestingly, the longer chain analogue **4.10** did not exhibit any immunogenic properties.

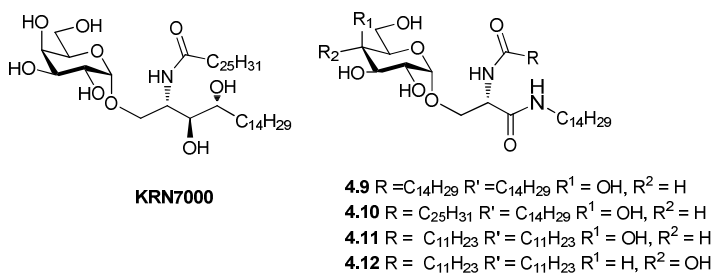


Figure 4.7 Structure of KRN7000 and L-serine analogues **4.9**, **4.10**, **4.11** and **4.12**.^[168-169]

Another L-serine based glycolipid **4.11** (Figure 4.7), reported by Huang *et al.* was found to induce macrophage activation by a TLR4-signalling pathway.^[169a] The effects of KRN7000 on TLR4 activation were also investigated, but proved to be inactive in that study. In a subsequent study by the same group, a series of L-serine analogues of KRN7000 were synthesised and tested for their ability to act as TLR4 activators.^[169b] The glucosyl glycolipid **4.12** was found to be the best TLR4 activator, only marginally better than the corresponding galactosyl glycolipid **4.11** (Figure 4.7). Thus, these compounds serve as potential drug candidates with

immunostimulator properties. No *i*NKT cell activation experiments were carried out by Huang and colleagues to investigate their potential usage as *i*NKT cell ligands.

4.2.7. Perspective

It seems obvious that minor changes to the structure of KRN7000 can have a major influence on the bioactivities exhibited. However, a few tentative conclusions can be drawn from the literature. First, modifications at the C-6 position of the sugar seems to be permitted and, in some cases, give desirable outcomes. Similarly, changes to the stereochemistry of the phytosphingosine backbone give undesirable results in many cases. Truncation and/or unsaturation of the alkyl chains seem to elicit a T_H2 response, whilst introduction of aromaticity elicits strong T_H1 or T_H2 biased cytokine production. β -analogues of KRN7000, although relatively unexplored, remain possible *i*NKT cell ligands. Lastly, L-serine provides an alternative simple core for phytosphingosine in a relatively unexplored classification of KRN7000 analogues, one in which is exploited in the current thesis.

4.3. Research objective

In this chapter, the discussion is focussed on the synthesis of an L-serine-based building block suitable for the construction of L-serinyl-based KRN7000 glycolipid analogues. Our interest in synthesising L-serine based analogues stemmed from a few important considerations. First, L-serine is more readily available and cheaper than phytosphingosine. Second, a simpler synthetic approach was envisaged, as the L-serine backbone contains only one stereogenic centre compared to three stereogenic centres present in the sphingosine backbone of KRN7000. Limited biological evaluations are reported in the literature regarding L-serine based KRN7000 analogues, despite the isosteric relationship that exists between L-serine and part of the phytosphingosine backbone.

Glycosylation reactions were executed using various different glycosyl donors and suitable L-serinyl acceptors to produce the corresponding α - or β -glycoside building blocks (Figure 4.8). The glycosyl donors include per-acetylated galactosides, galactosyl bromides, galactosyl trichloroacetimidates, thiogalactosides and

galactosyl iodides. These donors are suitably protected with ester, ether or silyl ether protecting groups. The glycosyl acceptors contain an L-serine backbone with amine protecting groups including *N*-Boc, *N*-Fmoc and azides. The carboxylic acid is functionalised as a benzyl ester, methyl ester or tetradecylamide. L-Serine acceptors with silyl ethers also serve as glycosyl acceptors.

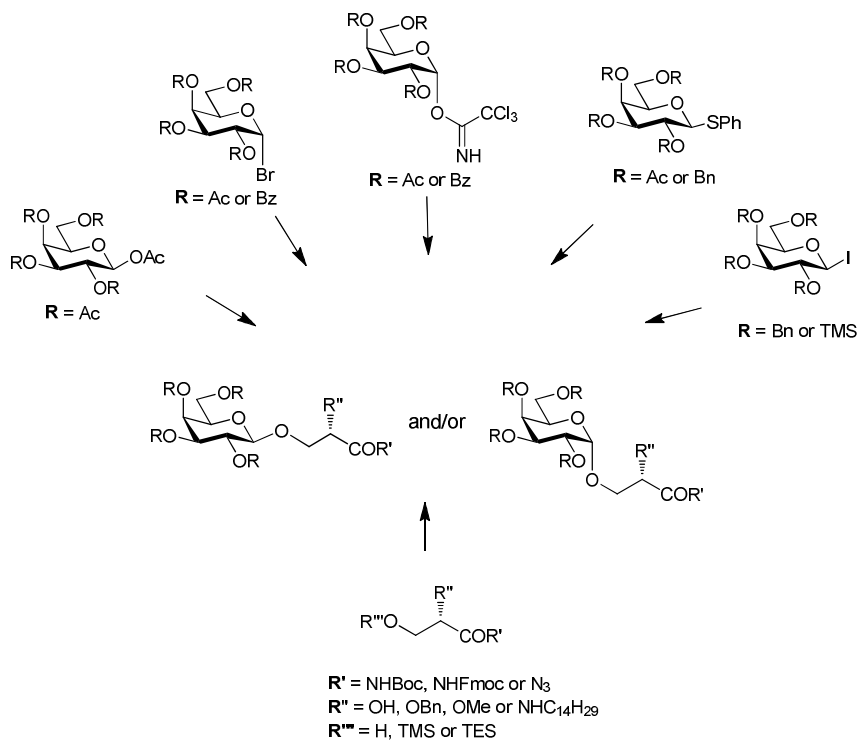


Figure 4.8 Galactosyl donors and L-serinyl acceptors for formation of L-serinyl building block.

With a suitable building block in place, we aimed to undertake the synthesis of L-serinyl galactosyl analogues of KRN7000 such as glycolipids **4.13-4.16** (Figure 4.9) with a view to study their immunological properties as CD1d antigens for *i*NKT cell stimulation. This work will be carried out under the supervision of Dr. Derek Doherty in St. James hospital on human *i*NKT cells.

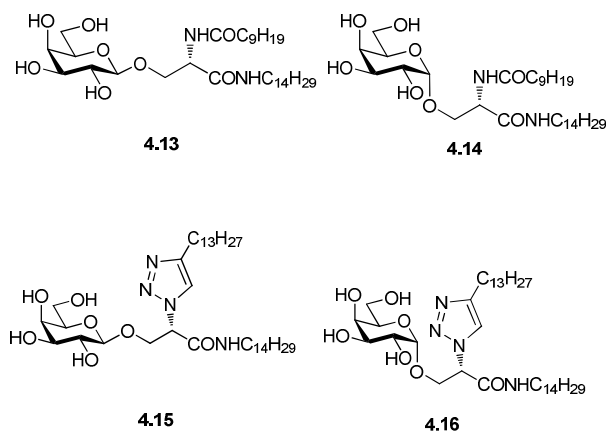


Figure 4.9 L-Serinyl KRN7000 analogues 4.13-4.16.

4.4. Stereoselective synthesis of β -galactoside building blocks for KRN7000

analogues

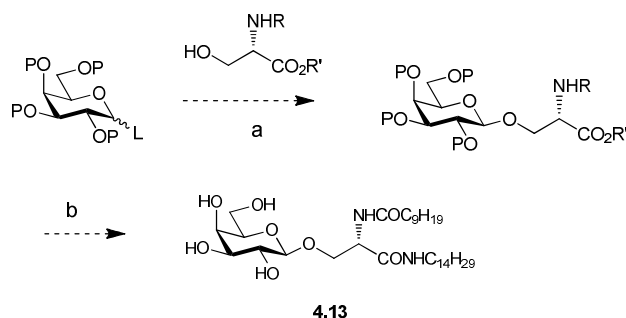
Initially, we envisaged that the synthesis of a desired β -galactosyl building block would involve a simpler methodology than the corresponding α -derivative building block. With an ester group at the C-2 position of the galactosyl donor, neighbouring group participation can stereoselectively allow the formation of a 1,2-*trans* anomeric linkage to produce a β -galactosyl building block (as discussed in detail in Chapter 2). The design of a suitable building block for the synthesis of KRN7000 analogue 4.13 (Figure 4.9) was first explored.

4.4.1. Design considerations for stereoselective β -galactosyl building block

formation

A synthetic approach for the formation of a β -galactosyl building block (Scheme 4.2) was designed based on the following considerations: i) the use of orthogonal protecting groups, ii) the need for an ester protecting group at the C-2 position of the galactosyl donor to give the desired 1,2-*trans* product and iii) the cost and availability of the starting materials and reagents. The proposed synthesis allows scope for the use of different ester protecting groups (P) on the sugar moiety, on the amino group (R) and on the carboxylic acid group (R') of the L-serine amino

acid. Also, a variety of glycosyl donors with different leaving groups (L) were investigated.



Scheme 4.2 General scheme for the synthesis of KRN7000 analogue **4.13** from a β -galactosyl donor and L-serinyl acceptor. Step a) involves the formation of a building block galactoside and step b) involves the synthesis of glycolipid **4.13**.

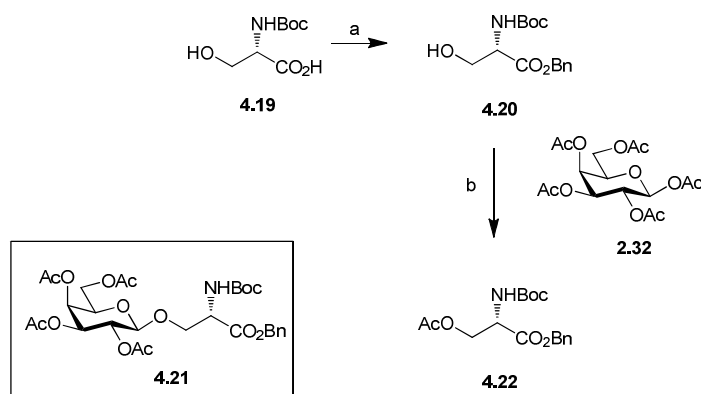
4.4.2. Use of galactosyl acetate donors for β -galactosyl building block formation

The use of glycosyl acetate donors was first discovered by Helferich and Schmitz-Hillerbrecht,^[170] and their use has maintained steady occurrence in the literature ever since. The anomeric acetate can be activated under Lewis acid conditions, displaced in an S_N1 fashion (as discussed in Chapter 2) and attacked by the incoming nucleophile stereoselectively to yield the desired 1,2-*trans* glycosidic product. The great advantage of their use is the relative ease of preparation and stability of the donor. Glycosyl acetate donors have been applied to many synthetic methodologies. For example, the 2,3-unsaturated-4-keto glycosyl donor **4.17** and *N*-acetylglucosamine donors **4.18** have been utilised as glycosyl donors (Figure 4.10).^[171] Also, glycosyl acetates are commonly employed as precursors in the synthesis of other types of glycosyl donors, including glycosyl bromides (discussed in Chapter 2), thioglycosides (discussed in Section 4.6.1.) and glycosyl trichloroacetimidates (discussed in Section 4.4.4.).



Figure 4.10 Examples of glycosyl acetate donors.^[171]

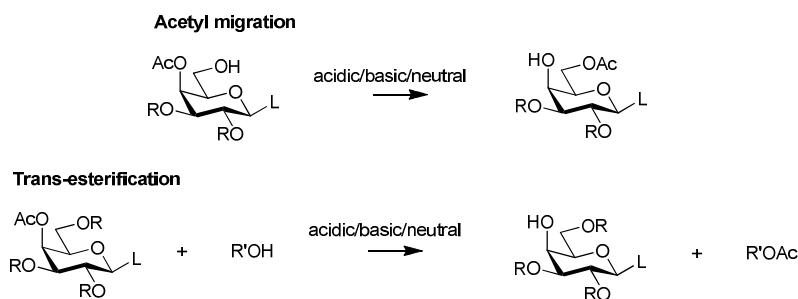
Initial investigations led us to synthesise the building block **4.21** illustrated in Scheme 4.3. The reaction of *N*-Boc-L-serine **4.19** with NEt_3 and BnBr afforded the L-serinyl acceptor **4.20** in a 70% yield. A subsequent glycosylation reaction between galactosyl donor **2.32** and L-serinyl derivative **4.18** was performed using $\text{BF}_3 \cdot \text{OEt}_2$ as a Lewis acid following a literature procedure.^[172] After 18 h, some galactosyl donor **2.32** remained unreacted in the reaction mixture (by TLC analysis), however due to the consumption of the glycosyl acceptor **4.18** and the indication of degraded material present in the reaction mixture, the reaction was terminated. ^1H NMR analysis confirmed the presence of the recovered glycosyl donor **2.32** in a 30% isolated yield and an acetylated side product **4.22** in a 10% isolated yield. The remainder of the reaction mixture consisted of unidentifiable compounds. No desired product **4.21** was identified in the ^1H NMR spectrum. Similarly, HR-MS reaffirmed this finding.



Scheme 4.3 Reagents and conditions a) NEt_3 , BnBr , DMF, 4 Å MS, rt, N_2 , 3h, 70 °C b) $\text{BF}_3 \cdot \text{OEt}_2$, CH_2Cl_2 , 4 Å MS, rt, N_2 , 18 h, 10%. Glycoside **4.21**, the desired product in step b was not isolated.

The isolation of the side product **4.22** is evidence that a trans-esterification reaction is occurring during the glycosylation step. Undesired trans-esterification reactions

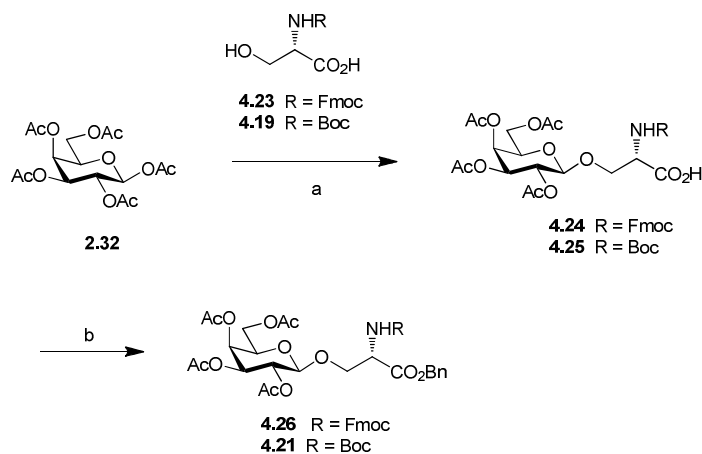
commonly occur in carbohydrate chemistry under acid,^[173] basic^[174] and sometimes neutral conditions.^[175] Acyl migration is an intramolecular trans-esterification reaction where an acyl group moves from one functional group to another on the molecule. Acetyl esters are particularly susceptible to acyl migration. Extensive studies have been carried out on acyl migration reactions occurring in D-galactopyranosides, and migration of the 4-acyl protecting groups is particularly common.^[174-176] It is probable that the acetyl protecting group at the C-4 position of the galactosyl donor **2.32** participated in the trans-esterification reaction, despite the fact that galactopyranoside containing a free hydroxyl group was not isolated in the reaction. Examples of a general trans-esterification reaction and an acetyl migration reaction are shown in Scheme 4.4.



Scheme 4.4 Example of an intramolecular acyl migration occurring in a galactopyranoside and an intermolecular trans-esterification reaction occurring between a galactopyranoside and an alcohol. R indicates protecting groups on the galactopyranosyl starting materials, Ac indicates an acetyl group, L indicates a leaving group and R' indicates an organic group.

The glycosylation reactions using commercially available L-serine carboxylic acids **4.19** and **4.23** with galactosyl donor **2.32** were also carried out, and involved the use of $\text{BF}_3 \cdot \text{OEt}_2$ as a promoter (Scheme 4.5). TLC analysis of the glycosylation reaction of the *N*-Fmoc protected L-serine derivative **4.23** with the *per*-acetylated galactose **2.32** showed consumption of the starting materials after only 3 h. The glycosylation reaction involving the *N*-Boc protected L-serine derivative **4.19** did not show full conversion after 3h. However, for comparison studies, both reactions were terminated after 3 h. In order to analyse whether the glycosylations were successful and for ease of purification, the products containing the free carboxylic

acids were benzylated with BnBr and NEt₃ as described earlier, in an attempt to yield the corresponding benzyl ester galactosides **4.26** and **4.21** respectively.



Scheme 4.5 Reagents and conditions a) BF₃·OEt₂, CH₂Cl₂, 4 Å MS, rt, N₂, 18 h; b) NEt₃, BnBr, DMF, rt, N₂, 18 h. For compound **4.26**, 31% over two steps. For compound **4.21** no desired glycoside was isolated.

More promising results were observed for the formation of the *N*-Fmoc galactoside **4.26** than for the corresponding *N*-Boc protected galactoside **4.21**. The desired β-galactosyl building block **4.26** was isolated along in 31% yield over two steps with traces of contaminants. The ¹H NMR data was in agreement with literature data.^[177] The contaminants were difficult to separate by chromatographic methods. The undesired hemiacetal product **4.27** was isolated in 9% yield (Figure 4.11) suggesting the presence of competing H₂O molecules in the reaction. The remainder of the reaction consisted of an unidentified mixture of compounds.

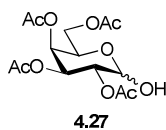
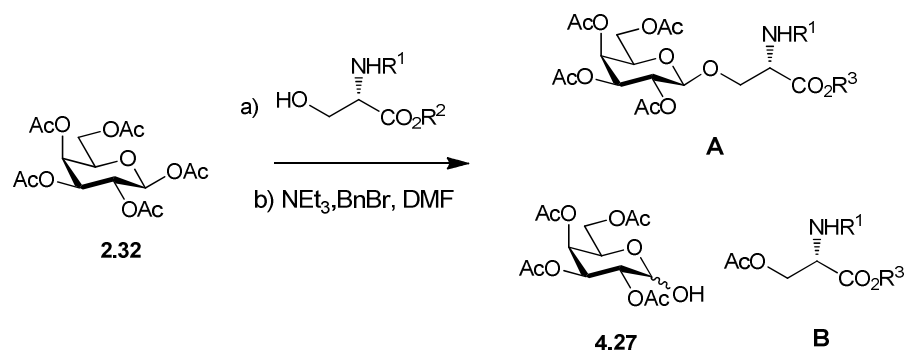


Figure 4.11 Structure of hemiacetal product **4.27** in glycosylation reaction.

In contrast to the *N*-Fmoc protected galactoside **4.26**, no desired glycosylated product **4.21** was isolated. The ¹H NMR spectra of the isolated fractions after flash chromatography were difficult to interpret, as mixtures of compounds were

present. HR-MS analysis however confirmed the presence of the undesired acetylated L-serine **4.22** and the galactosyl hemiacetal **4.27**. It seemed that the *N*-Fmoc protected L-serine acceptor **4.23** was a better choice for the formation of a building block suitable for synthesis of KRN7000 analogues. However, subsequent basic deprotection of the *N*-Fmoc protecting group on the building block **4.26** could cleave the base-labile acetyl groups present on the sugar moiety. This lack of orthogonality, together with the low yield of the reaction encouraged us to explore other strategies. A summary of the findings described above are shown in Table 4.4.

Table 4.4 Glycosylations utilising penta-*O*-acetyl- β -D-galactopyranoside **2.32** and L-serine acceptors **4.20**, **4.23** and **4.19**.



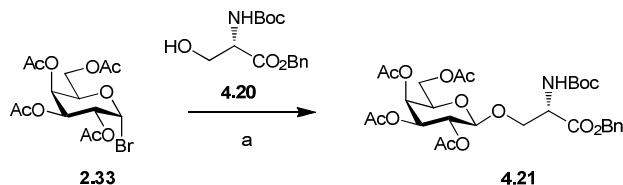
	R ¹	R ²	R ³	Time [‡]	Yield A (%)	Yield 4.27 (%)	Yield B (%)
1	Boc	Bn*	Bn	18 h	-	-	10
2	Fmoc	H	Bn	3 h	31	9	-
3	Boc	H	Bn	3 h	-	Traces**	Traces**

*no benzylated reaction performed for Entries 1; [‡] 1 equiv of donor **2.32**, 1.2 equiv of acceptor, 3 equiv of BF₃·OEt₂ activator in all glycosylation reactions; ** Presence confirmed by HR-MS.

4.4.3. A Koenigs-Knorr glycosylation for formation of a β -galactosyl building block

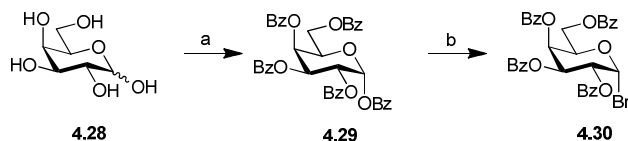
We reasoned that the use of a galactosyl halide donor could overcome some of the problems encountered with the use of *per*-acetylated donor **2.32**. A classic Koenigs-Knorr reaction was performed by Yoshiizumi *et al.* using a galactosyl halide **2.33** and *N*-Boc protected L-serinyl derivative **4.20** using a combination of halophilic

activators of Ag_2CO_3 and AgClO_4 (Scheme 4.6).^[178] The low yield (20%) reported for their synthesis of the *N*-Boc glycoside **4.21** suggested that undesirable side reactions were occurring during the glycosylation step.^[178] A trans-esterification reaction (discussed in Section 4.4.2) is one of the probable causes of this low yield. One of the plausible solutions to this problem involves the use of the more acid stable benzoyl ester in place of the acetyl ester on the galactosyl bromide donor.



Scheme 4.6 Reagents and conditions a) Ag_2CO_3 , AgClO_4 , CH_2Cl_2 , 4 Å MS, dark, rt, N_2 , 18 h, 20%.^[178]

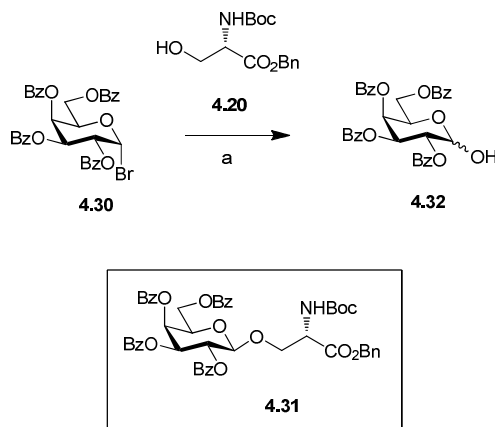
An alternative glycosyl donor **4.30** was prepared following a literature procedure as shown in Scheme 4.7.^[179] The reaction of D-galactose with benzoyl chloride in Pyr afforded 64% of the benzoyl protected α -D-galactopyranoside **4.29**. Treatment of the galactosyl precursor **4.29** with a solution of HBr/AcOH and Ac_2O in CH_2Cl_2 yielded the galactosyl bromide **4.30** in a 96% yield.



Scheme 4.7 Reagents and conditions. a) BzCl, Pyr, 0 °C to rt, 18 h, 64%; b) HBr/AcOH, Ac_2O , CH_2Cl_2 , 0 °C, N_2 , 2 h, 96%.

The glycosylation reaction of glycosyl halide **4.30** with the L-serine acceptor **4.20** was studied using two different halophilic activators (Ag_2CO_3 or AgOTf) as seen in Scheme 4.8. To our disappointment, neither reaction conditions yielded desirable results. Again, as in the case for reaction of the galactosyl acetyl donor **2.32** (Section 4.4.2), mixtures of unidentifiable side products were obtained, with little or no evidence of desired product formation of **4.31**. The corresponding benzoylated

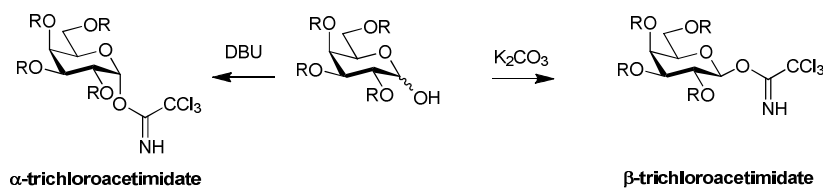
galactosyl hemiacetal **4.32** was identified from ^1H NMR and HR-MS analysis. It seemed that the use of benzoyl esters in place of acetyl esters seemed to reduce the reactivity of the galactosyl halide towards glycosylation, an observation that has precedence in the literature.^[180]



Scheme 4.8 Reagents and conditions. Ag_2CO_3 or AgOTf , CH_2Cl_2 , rt, 18 h or 48 h. Desired product **4.31** was not isolated.

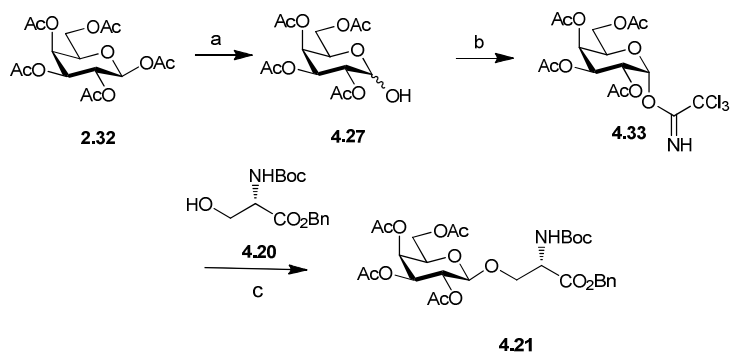
4.4.4. Schmidt's trichloroacetimidate glycosylation for the formation of β -galactosyl building block

The trichloroacetimidate donors were first reported in 1980 by Schmidt and colleagues,^[114, 181] and they are well regarded and extensively utilised in carbohydrate chemistry. The versatility of glycosyl trichloroacetimidates is illustrated by their use in various different syntheses and excellent yields and stereoselectivities are reported in the literature.^[182] One advantage pertaining to the use of glycosyl trichloroacetimidates over glycosyl halides, thioglycosides and glycosyl acetate donors involves the use of a catalytic amount of the Lewis acid promoter in trichloroacetimidate activation, compared to stoichiometric amounts needed for the later donors. Glycosyl trichloroacetimidates are conveniently prepared by the reaction of a hemiacetal with trichloroacetonitrile in the presence of a base. The anomeric stereoselectivity is controlled by the type of base used in the reaction, with weak bases (such as K_2CO_3) affording the kinetically favoured β -trichloroacetimidate and strong bases (such as DBU) affording the thermodynamically favoured α -trichloroacetimidates (Scheme 4.9).^[69]



Scheme 4.9 Base promoted stereoselective formation of α - and β -trichloroacetimidates.

The galactosyl trichloroacetimidate donor **4.33** was prepared as described in the literature from 1,2,3,4,6-penta-*O*-acetyl- β -D-galactose **2.32** by selective deacetylation at the anomeric centre upon treatment with Me_2NH , to give the galactosyl hemiacetal **4.27**.^[183] The reaction of this intermediate with trichloroacetonitrile and DBU (strong base) gave the desired α -galactosyl trichloroacetimidate **4.33** in a good overall yield of 92% over two steps (Scheme 4.10).^[183] The reaction of galactosyl trichloroacetimidate **4.33** and *N*-Boc-L-serine benzyl ester **4.20** was then performed under Lewis acid (TMSOTf) activation, to give the desired galactoside **4.21** in a 33% yield. The effects of time and different stoichiometric quantities of galactosyl donor **4.33** were explored to optimise the reaction yields, which are summarised in Table 4.5.



Scheme 4.10 Reagents and conditions. a) Me_2NH , CH_3CN , rt, 24 h, quant.; b) CCl_3CN , DBU, CH_2Cl_2 , 3Å MS , N_2 , 3.5 h, 83%; c) 0.04 N TMSOTf, 4Å MS , CH_2Cl_2 , -10°C to rt, N_2 , 18 h, 33%.

Table 4.5 Attempts to optimise reaction conditions used in the synthesis of β -galactoside building block **4.21** using trichloroacetimidate donor **4.33**.

The reaction scheme shows the glycosylation of acceptor **4.20** (a serinyl derivative with a hydroxyl group and a Boc-protected amine) with donor **4.33** (a galactosyl trichloroacetimidate). The reaction yields four products: **4.21** (the desired β -galactoside building block), **4.27** (an undesired hemiacetal), **4.34** (the *N*-Boc deprotected L-serinyl derivative), and **4.22** (a trans-esterification side product).

Entry	Equiv of glycosyl donor 4.33 *	Time	Yield 4.21 (%)	Yield 4.27 (%)	Yield 4.34 (%)	Yield 4.22 (%)
1	1.2	18 h	33	-	7	34
2	1.2	3 h	30	20	-	-
3	1.3	3 h	28	25	-	-

* 1 equiv of acceptor, 0.1 equiv of 0.04 N TMSOTf, -10°C –rt in CH₂Cl₂ in all glycosylations.

An initial glycosylation was carried out as in Scheme 4.10, with an excess of galactosyl donor **4.33** (1.2 equiv) for 18 h (Entry 1 in Table 4.5). This resulted in a 33% yield of the desired galactosyl building block **4.21**. The trans-esterification side product **4.22** and the *N*-Boc deprotected L-serinyl derivative **4.34** were isolated in 34% and 7% yield respectively. A shorter reaction time of 3 h (Entry 2 in Table 4.5) resulted in the formation of the product **4.21** with a reduced yield of 30%. The undesired hemiacetal **4.27** was isolated in 20% yield under these reaction conditions. Increasing the stoichiometric equivalents of the galactosyl donor **4.33**

(Entry 3 in Table 4.6) resulted in a poorer 28% yield of the building block **4.21** and a concomitant increase in the undesired hemiacetal product **4.27** formation (25% yield). These results suggested the best Schmidt glycosylation conditions involved a slight excess of galactosyl donor **4.33** (1.2 equiv) and a reaction time of 18 h (Entry 1 in Table 4.5).

In the ^1H NMR spectrum of the crude reaction mixture of **4.21** (Scheme 4.10), a signal present at 6.3 ppm was indicative of an orthoester product. In a ^1H NMR spectrum, a signal corresponding to an anomeric proton of an orthoester would have a higher chemical shift than the corresponding signal of the anomeric proton of a β -glycoside due to its different chemical environment. The coupling constant would also have a value closer to that of an α -glycoside as it has a similar diaxial angle to an α -glycoside. The anomeric proton of the purified β -glycoside **4.21** was found to resonate at 5.7 ppm.

Extensive studies have been carried out on the formation of orthoesters as side products in glycosylation reactions; one of the domineering factors attributed to their formation is the presence of base in the glycosylation step.^[184] Low temperature ^1H and ^{13}C NMR was utilised by Crich and his colleagues with ^{13}C -labelled compounds in order to probe the mechanism by which they form in glycosylations with and without base. They provided evidence for the existence of orthoesters in buffered solutions but no evidence in the corresponding base-free glycosylation was given.^[184c] Upon analysis of the reaction conditions in Scheme 4.10, the presence of base is not immediately evident; however one suggestion is the possibility that the nucleophilic hydroxyl group of the L-serine acceptor **4.20** is also acting as a Lewis base as in Figure 4.12. Intramolecular hydrogen-bonding of the hydrogen atom of the hydroxyl group to the nitrogen atom of the NHBoc protecting group increases the Lewis basicity of the oxygen atom.

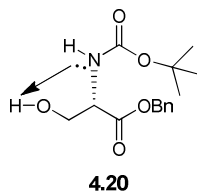
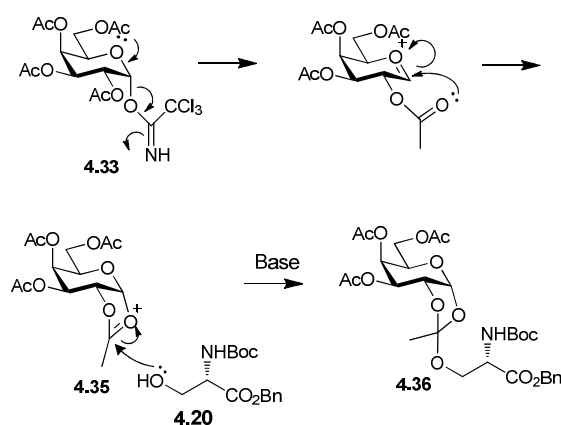


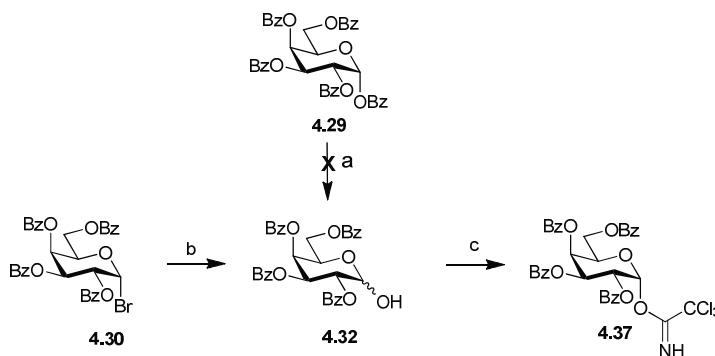
Figure 4.12 Hydrogen bonding in L-serine derivative **4.20** increases the Lewis basicity of the primary alcohol.

Thus the orthoester formation may have occurred due to the Lewis basic hydroxyl group of L-serine derivative **4.20**. A proposed mechanism for this orthoester formation is shown in Scheme 4.11 whereby the nucleophilic acceptor **4.20** can attack the intermediate cyclic oxonium ion **4.35**, leading to the formation of an orthoester **4.36**. The presence of the base retards the acid catalysed decomposition of the cyclic oxonium ion into the oxycarbenium ion for formation of *O*-glycosides. The orthoester **4.36** was not observed after purification by flash chromatography in the glycosylation reaction described above. A rearrangement of the orthoester may have occurred to give the desired *O*-glycoside **4.21**. If this was the case, this type of rearrangement is often accompanied by side reactions such as hydrolysis and transesterification from the hydroxyl group at the C-2 position of the donor to a free hydroxy group on the acceptor.^[185] This would account for the presence of the acetylated side product **4.22**.



Scheme 4.11 Proposed reaction mechanism for orthoester **4.36** formation.

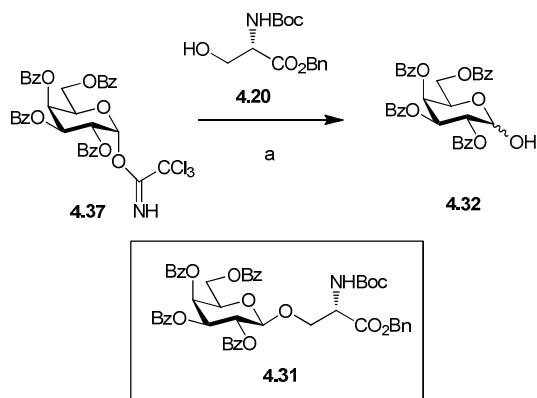
The use of benzoyl esters in place of acetyl esters in glycosyl donors retards the formation of orthoesters due to the greater stability (and thus lesser reactivity) of the intermediate oxonium ion of the benzoate, therefore potentially improving yields as a result. Thus, the synthesis of the benzoyl protected galactosyl trichloroacetimidate donor **4.37** was undertaken (Scheme 4.12). Initial attempts to hydrolyze the anomeric benzoyl ester of *per*-benzoylated-D-galactose **4.29** (described in Section 4.4.3) using Me₂NH to produce the corresponding benzoylated hemiacetal **4.32** failed. The starting material **4.29** remained unconsumed in the reaction. This was attributed to the fact that benzoyl protecting groups are more stable to basic conditions than acetyl groups. However, when harsher basic conditions were employed, the selective anomeric deprotection was not achieved, with all or some of the benzoyl groups being removed. Therefore, the galactosyl benzoylated hemiacetal **4.32** was formed by the reaction of the glycosyl bromide **4.30** (described in Section 4.4.3.) with Ag₂CO₃ in an acetone/H₂O mixture (4:1) in 90% yield. This was followed by reaction of hemiacetal **4.32** with trichloroacetonitrile and DBU to obtain the desired galactosyl trichloroacetimidate **4.37** in an 89% yield (Scheme 4.12).^[186]



Scheme 4.12 Reagents and conditions. a) Me₂NH, CH₃CN, rt, 24 h; b) Ag₂CO₃, acetone/H₂O 4:1, rt, 2.5 h, 90%; c) CCl₃CN, DBU, CH₂Cl₂, 3Å MS, 0°C, N₂, 2 h, 89%.

The glycosylation reaction of the benzoylated galactosyl donor **4.37** with the protected L-serine acceptor **4.20** was then carried out, however none of the desired β-galactosyl building block **4.31** was isolated, although its presence was detected by HR-MS analysis (Scheme 4.13). As in previous glycosylation attempts, unreacted

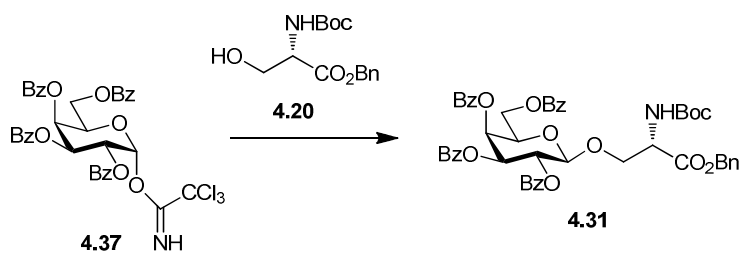
glycosyl acceptor **4.20** and the hemiacetal **4.32** were isolated from the reaction mixture as major components. A range of reaction conditions were explored in order to synthesise the desired *O*-glycoside **4.31** in a reasonable yield. A summary of these appear in Table 4.6.



Scheme 4.13 Reagents and conditions. a) TMSOTf, CH₂Cl₂, 3Å MS, N₂, 4 h. Desired product **4.31** was not isolated.

Some of the reaction parameters investigated were the amounts of glycosyl donor **4.37** and acceptor **4.20** used (Entries 1-3 in Table 4.6), the concentration of the Lewis acid promotor (Entries 1,3-5 in Table 4.6), the temperature used ranging from -40° C to 28 °C (all entries in Table 4.6), the reaction time ranging from 30 s to 5 h (all entries in Table 4.6), the reaction solvent (Entries 1,4 in Table 4.6). Microwave glycosylation conditions were also investigated (Entries 6, 7 in Table 4.6). Microwave assisted glycosylations are prevalent in the literature in recent times due to their potential to being clean, cheap and convenient reactions.^[187] In the literature, reaction times and yields can be improved using microwave irradiation compared to conventional methods, sometimes drastically.^[188] However in the case of the glycosylations mentioned, no changes were observed compared to the conventional glycosylation reactions. The desired compound **4.36** was not isolated in any of the reactions carried out.

Table 4.6 Different reaction conditions explored to synthesise β -glycoside **4.31**.



Entry	Equiv of glycosyl donor 4.37	Equiv of glycosyl acceptor 4.20	Activator	Equiv	Temperature	Time	Solvent*
1	1	1.1	0.04 N TMSOTf	0.25	rt	4 h	CH ₂ Cl ₂
2	1.1	1	0.04 N TMSOTf	0.25	-10 °C - rt	5 h	CH ₂ Cl ₂
3	3	1	neat TMSOTf	0.25	-10 °C - rt	5 h	CH ₂ Cl ₂
4	1	1	neat TMSOTf	0.25	-10 °C - rt	2 h	Diethyl ether
5	1	1	0.04 N TMSOTf	0.1	-40 °C	3 h	Diethyl ether
6	1	1	0.04 N TMSOTf	0.1	28 °C	5 min	CH ₂ Cl ₂
7	1	1	0.04 N TMSOTf	0.1	28 °C	30 sec	CH ₂ Cl ₂

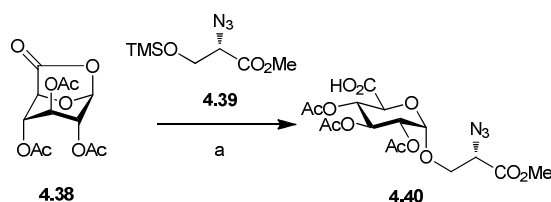
* glycosylation product **4.31** detected by HR-MS analysis.

4.4.5. Use of silylated glycosyl acceptors for the formation of a β -galactosyl

building block

The outcome of glycosylation reactions can depend on many factors and the choice of the glycosyl donors and glycosyl acceptors are vitally important. In the previous sections, we discussed the use of different galactosyl donors and acceptors for the synthesis of a desired β -galactosyl building block. We observed in the reaction of the galactosyl trichloroacetimidate donor **4.33** that the unreacted L-serine acceptor **4.20** was recovered, together with a series of side products, as discussed earlier in Section 4.4.4. This suggested that an alternative and more reactive acceptor was needed in order for the glycosylation to be more effective. We postulated that the reaction between the trichloroacetimidate galactosyl donor **4.33** with silylated L-serine derivatives could yield more promising results.

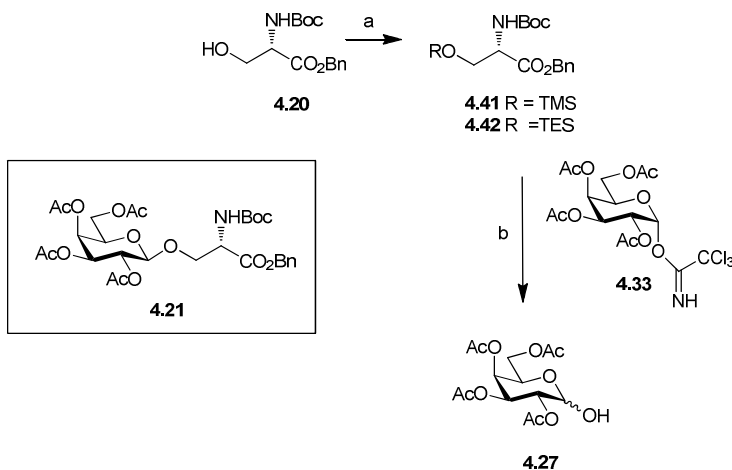
The use of silyl ether glycosyl acceptors was reported by Murphy and co-workers.^[189] They were involved in a stereoselective synthesis of glycosides and 2-deoxyglycosides by SnCl_4 catalysed coupling of a lactone derivative with various silyl ether glycosyl acceptors. Scheme 4.14 illustrates one such example whereby the coupling of lactone **4.38** with L-serine derivative **4.39** resulted in a 51% yield of the α -glucuronoside **4.40**. Nakamura reasoned that the use of silyl ether protected alcohols as nucleophiles could minimize the build-up of H_2O , which in turn could lead to higher glycosylation yields compared to alcohol acceptors.^[190]



Scheme 4.14 Reagents and conditions. a) SnCl_4 , CH_2Cl_2 , 4\AA MS, rt, N_2 , 15 h, 51%.

Two different silylated L-serine acceptors **4.41** and **4.42** were synthesised, which contained the labile TMS group and the more stable TES protecting group respectively (Scheme 4.15). Treatment of *N*-Boc-L-serine benzyl ester **4.20** with

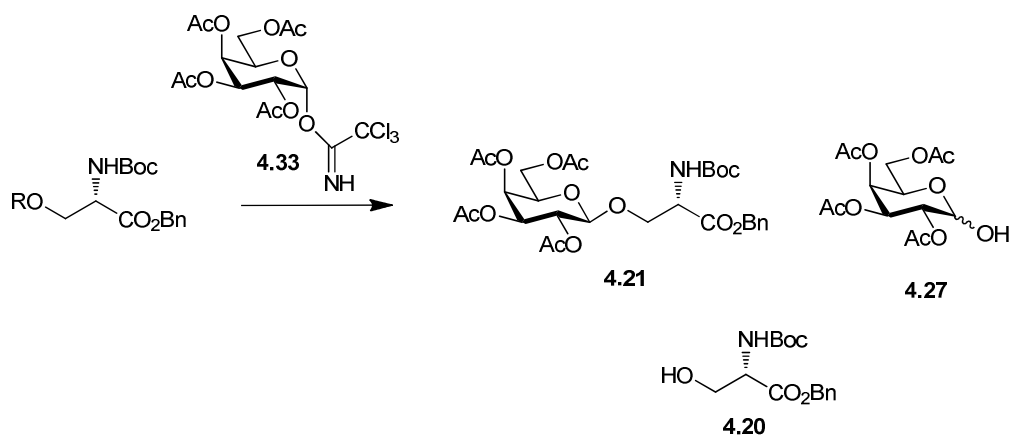
TMSCl and NEt_3 afforded TMS L-serine derivative **4.41** in a yield of 69%, and treatment of *N*-Boc-L-serine benzyl ester **4.20** with TESCl and NEt_3 afforded L-serine derivative **4.42** in a yield of 67%. Glycosylation reactions were then carried out with the trichloroacetimidate donor **4.33** in Lewis acid promoted reactions (TMSOTf). The results are summarised in Table 4.7.



Scheme 4.15 Reagents and conditions. a) For compound **4.41**: TMSCl, NEt_3 , CH_2Cl_2 , N_2 , 2 h, 69%; For compound **4.42**: TESCl, NEt_3 , CH_2Cl_2 , N_2 , 3 h, 67%; b) TMSOTf, CH_2Cl_2 , 4Å MS , -10°C to rt, N_2 , 2 h or 3 h. Desired product **4.21** was not isolated.

The glycosylation involving the use of the TMS functionalised L-serine **4.41** (Entries 1, 2 in Table 4.7) resulted in no formation of the desired compound **4.21**. Similarly, the TES protected L-serine acceptor **4.42** (Entry 3 in Table 4.7) resulted in none of the desired glycoside **4.21**. Only the hemiacetal **4.27** (1:100 α/β) and the desilylated L-serine derivative **4.20** were isolated along with starting materials in this case. In hindsight, these results are in line with those obtained in competition studies between an alcohol acceptor and the corresponding silyl ether acceptor carried out by Kahne and colleagues.^[191] The team observed that the silyl ether acceptor remained unreacted in the presence of the alcohol acceptor. This indicated that silyl ethers react more slowly than unprotected alcohols as glycosyl acceptors presumably because they must be unmasked first in the Lewis acid conditions of a glycosylation.^[191] The use of silylated L-serine acceptors were abandoned as a result of our findings and observations.

Table 4.7 Reaction conditions of glycosyl donor **4.33** and two L-serine acceptors **4.41** and **4.42**.



Entry	Equiv of glycosyl donor 4.33	R	Time	Yield 4.21 (%) *	Yield 4.27 (%)	Yield 4.20 (%)
1	1	TMS	2 h	-	- [‡]	-
2	1.5	TMS	2 h	-	26	35
3	1	TES	3 h	-	23	-

* 1 equiv of acceptor, 0.1 equiv of 0.04 N TMSOTf, -10°C -rt, CH₂Cl₂ as solvent in all glycosylations; [‡] product has R_f value identical to hemiacetal **4.27** on TLC plate and cannot identify individual signal in ¹H NMR spectrum.

4.4.6. Investigation of nucleophilicity of L-serine acceptor for β -galactosyl building block formation

In our attempt to understand why the glycosylation reactions involving the L-serine derivative **4.20** with various different donors were failing, we decided to investigate the nucleophilicity of the L-serine acceptor **4.20**. Polt *et al.* had reported that the nucleophilicity of L-serine and some of its derivatives was poor due to unfavourable hydrogen bonding between the amino residue of the L-serine backbone and the

hydroxyl group at the C-4 position as shown in Figure 4.13.^[192] The oxygen atom on the hydroxyl group can be deactivated by the proton of the amide bond, thus decreasing its nucleophilicity. Conversely, they postulated that if a favourable hydrogen bonding pattern could be generated via the use of different protecting groups on the amino residue of the L-serine, then the nucleophilicity of the hydroxyl group of the *N*-protected L-serine could be increased. They chose L-serine ester Schiff bases to induce hydrogen bonding favourable in glycosylation reactions. However, we were interested in utilising an azide moiety as the amino protecting group on L-serine. Azides can be considered to be masked amino groups since they can easily be reduced to give the free amine after the glycosylation step in the synthesis of a β -galactosyl building block which could improve the yield of the glycosylation reaction. Azide derivatives of ceramides are commonly used as building blocks in the synthesis of KRN7000 analogues, as exemplified by the work of Gervay-Hague *et al.*^[193] We believed that an azido functionalized L-serinyl compound would undergo favourable hydrogen-bonding similar to that observed by Polt for Schiff bases which would increase the nucleophilicity of the acceptor (Figure 4.13). Finally, the introduction of the azido functionality at this point in the synthesis of a galactosylated L-serinyl building block would be convenient towards the preparation of the target triazole containing glycolipids **4.15** and **4.16**.

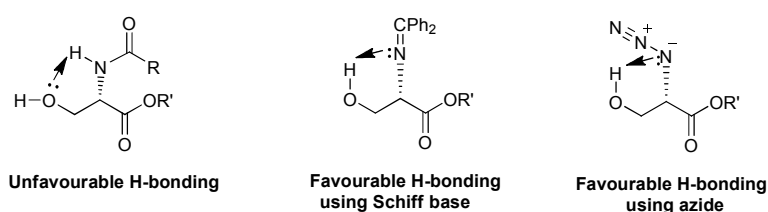
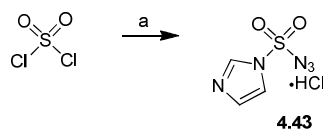


Figure 4.13 Unfavourable hydrogen bonding in L-serine derivative due to amide bond and favourable hydrogen bonding in L-serine derivative due to azide functionality.

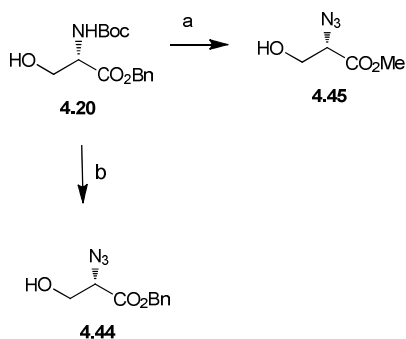
The synthesis of an azide glycosyl acceptor **4.44** was thus undertaken as in Scheme 4.17. The conversion of a primary amine into an azide is usually aided by a diazo-transfer reagent; TfN₃ being one of the most popular choices in the literature.^[194] However the explosive properties of TfN₃ when anhydrous and its relatively short shelf life challenged us to explore other methods reported in the literature.

Goddard-Borger and colleagues reported an alternative diazo-transfer reagent, imidazole-1-sulfonyl azide **4.43**, which was claimed to be shelf stable and safe to use at temperatures well below its decomposition point, rt preferably.^[195] We undertook the synthesis of the diazo-transfer reagent **4.43** as shown in Scheme 4.16 following a literature procedure.^[195] Treatment of sulfonyl chloride with NaN₃ in MeCN afforded chlorosulfonyl azide, which was then reacted *in situ* with imidazole, and treated with acid to give the hydrochloride salt **4.43** in a 39% yield.



Scheme 4.16 *Reagent and conditions.* a) i) NaN₃, MeCN, rt, 18 h ii) Imidazole, 0 °C to rt, 3 h
iii) HCl in EtOH, 0 °C, 1 h, 39%.

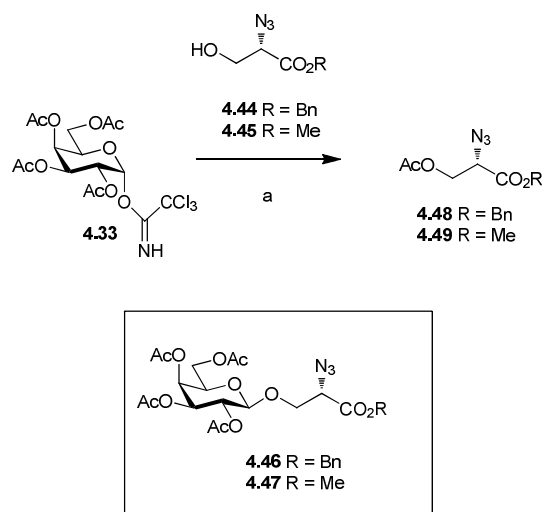
The formation of the L-serinyl azide derivative **4.44** was attempted following a procedure pioneered by Goddard-Borger and co-workers as shown in Scheme 4.17.^[195] The previously synthesised L-serine derivative **4.20** was *N*-Boc deprotected with 1 M HCl in a CH₂Cl₂/H₂O biphasic system to give the corresponding free amine hydrochloride salt. Subsequent reaction with the diazo-transfer reagent **4.43** using a Cu(II) catalyst in basic conditions in MeOH resulted in the desired azide transfer but also complete trans-esterification of the benzyl ester, to give a quantitative yield of the L-serine methyl ester **4.45**. Trans-esterification reactions typically occur under basic conditions with a reactive alcohol, such as MeOH. However bulkier alcohols, such as *t*-BuOH, are less likely to undergo this type of transformation. The reaction was thus carried out in *t*-BuOH with a Cu(II) catalyst in basic conditions to afford the desired compound **4.44** in a yield of 61%, as in Scheme 4.17.



Scheme 4.17 Reagents and conditions. a) i) 1 M HCl, CH₂Cl₂ ii) **4.43**, K₂CO₃, CuSO₄·5H₂O, MeOH, rt, 6 h, 100% or b) i) 1 M HCl, CH₂Cl₂ ii) **4.43**, K₂CO₃, CuSO₄·5H₂O, *t*-BuOH, rt, 6 h, 61%.

4.4.7. L-Serine azido acceptor **4.43** for β -galactosyl building block formation

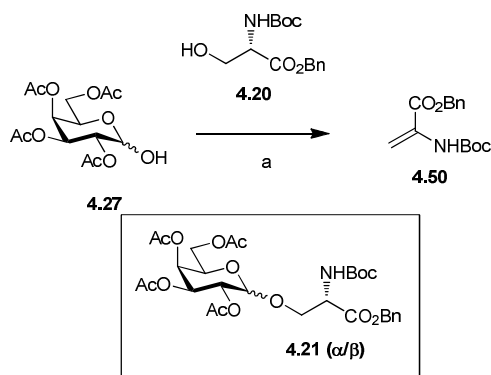
The glycosylation reaction between the trichloroacetimidate donor **4.33** and the azide L-serine acceptor **4.44** was attempted using Schmidt glycosylation conditions as in Scheme 4.18. For comparison purposes, the side product methyl ester glycosyl acceptor **4.45** (from the diazo-transfer reaction in MeOH described above) was also reacted with the trichloroacetimidate donor **4.33**, and both reactions were analysed and compared. The galactosyl donor **4.33** was activated under Lewis acid conditions and reacted with the acceptors **4.44** and **4.45** respectively as in Scheme 4.18. After 3 and 4 h, respectively, they were quenched based on the consumption of the galactosyl donor **4.33** as indicated by TLC analysis, and the reaction mixtures were analysed by ¹H NMR spectrometry. Neither reaction yielded the desired compounds **4.45** or **4.46** respectively. Mixtures of products which could not be separated were formed, and only the corresponding acetylated side products **4.48** and **4.49** (2% and 14% respectively) were identified. These results again indicated that the replacement of the protected amine function for an azide did not result in the expected increase in reactivity for L-serinyl acceptors **4.44** and **4.45**.



Scheme 4.18 Reagents and conditions. a) For **4.48**, 0.04 N TMSOTf, 4Å MS, CH₂Cl₂, rt, N₂, 3 h, 2%; For **4.49**, 0.04 N TMSOTf, 4Å MS, CH₂Cl₂, rt, N₂, 4 h, 14%. Desired products **4.46** and **4.47** were not isolated.

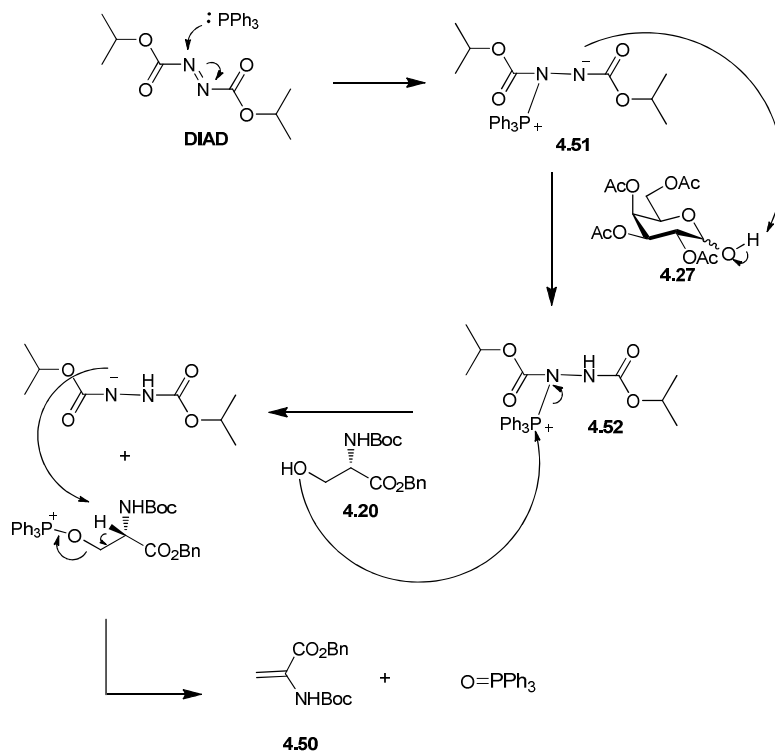
4.5. Mitsunobu conditions in formation of α/β -galactosyl building blocks

In light of the fact that the glycosylation reactions explored so far gave unsatisfactory results for the most part, possibly due to the reduced nucleophilicity of the L-serinyl acceptors, a different synthetic approach was investigated. The proposed glycosylation strategy involved the use of a Mitsunobu reaction. Mitsunobu reactions are commonly used in organic chemistry and have been used successfully to form glycosidic linkages.^[196] However, little control is held over the stereoselective formation of the products, because the hemiacetal starting material is found, in most cases, as a mixture of anomers. The hemiacetal participates as the nucleophile in the reaction, and thus the products retain the original stereochemistry. Hemiacetal **4.27** (as a 1:100 α/β mixture of anomers) and L-serine derivative **4.20** were reacted in the presence of PPh₃ and DIAD in CH₂Cl₂, as shown in Scheme 4.19. After 5 h, the starting material **4.20** had been consumed, as monitored by TLC analysis, and the reaction was terminated. However, no desired product **4.21**(α/β) was isolated. Instead we believe the L-serine derivative **4.20** underwent a β -elimination reaction to produce the dehydroalanine derivative **4.50**, isolated in a 50% yield, whose ¹H NMR data was in agreement with literature values.^[197] The unreacted hemiacetal **4.27** was recovered.



Scheme 4.19 Reagents and conditions a) PPh_3 , DIAD, CH_2Cl_2 , 4 \AA MS , rt, N_2 , 5 h, 50%.
Desired product **4.21** was not isolated.

We believe that the L-serine was dehydrated due to the acidity of the H- α in the proposed reaction mechanism (Scheme 4.20). The PPh_3 performs a nucleophilic attack on DIAD producing a betaine intermediate **4.51**. As in a Mitsunobu reaction, the betaine intermediate **4.51** attacks the hydroxyl proton on the hemiacetal **4.27** to produce the carbocation **4.52**. The L-serine derivative **4.20** then attacks the electrophilic phosphorous atom on the carbocation **4.52** to displace a DIAD derivative. At this point, the DIAD derivative is sufficiently basic to deprotonate the H- α of the L-serine derivative **4.20**, with the driving force of the formation of triphenylphosphine oxide to give the β -elimination product dehydroalanine **4.50**. This forms preferentially over nucleophilic attack from the deprotonated hemiacetal to give the desired building block **4.21(α/β)**.

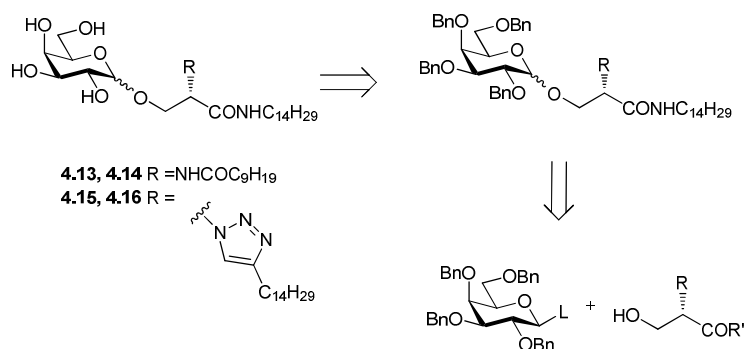


Scheme 4.20 Proposed reaction mechanism for E1_{sb} elimination reaction of L-serine derivative **4.20** to give dehydroalanine **4.49**.

It is also possible that the reaction did not proceed according to this mechanism. It is possible that the glycosylation occurred and a subsequent *retro*-Michael reaction occurred thereafter. However, it is unlikely that it may have occurred in this manner as no desired product was evident by TLC at any stage of the reaction and no trace of desired compound **4.21(α/β)** was observed by HR-MS. However *O*-serinyl galactosides are known to undergo this reaction, so it is not beyond the realm of possibility.^[192, 198] These observations highlight the base sensitivity of L-serine derivatives due to the acidic α-proton, an important note for the continuing work on *O*-serinyl compounds. The formation of dehydroalanine **4.50**, although undesired in our present circumstances could be useful in other applications such as in drug design. For example, dehydroamino acids are currently used as the basis for antibiotics.^[197] For the present study, no further investigations were carried out in this area.

4.6. Design considerations for the synthesis of α/β -galactoside building blocks for KRN7000 analogues

These results cemented our understanding of the electronic sensitivities of these reactions and the importance of matching donor and acceptor reactivity to achieve successful glycosylation reactions. With this in mind, we decided that a radical change in the glycosyl donor structure was needed to increase its armed character. The “armed-disarmed” terminology was coined by Fraser-Reid and co-workers in 1988.^[199] They observed that the protecting groups on glycosyl donors had a large impact on the resulting glycosylation yield, in particular the protecting group at the C-2 position of the glycosyl donor. Both esters and ether protecting groups are electron withdrawing; esters due to resonance and inductive effects and ethers due to inductive effects alone. Esters are more electron-withdrawing than ethers. Therefore they are more deactivating than the corresponding ethers and are less likely to induce the formation of an oxacarbenium ion. Thus they are less reactive and are termed disarmed. Ether containing glycosyl donors are more likely to induce the formation of an oxacarbenium ion. They are thus more reactive and are termed armed donors. This concept is fundamental to reactivity tuning of glycosyl donors used in one-pot oligosaccharide syntheses, as exemplified by Zhang *et al.*^[200] Their strategy involved the use of the most reactive donor at the non-reducing end, and an unreactive donor was used for the reducing end of the given oligosaccharide target. With this in mind, we decided to alter the structure of the glycosyl donor to increase its armed character and achieve higher glycosylation yields. As an ester protecting group would no longer be present at the C-2 position of the sugar, neighbouring group participation could no longer occur, and a mixture of anomers should be expected. A retrosynthetic analysis is presented in Scheme 4.21.



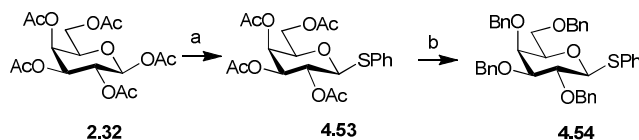
Scheme 4.21 Retrosynthetic analysis of KRN7000 analogues **4.13-4.16** from their corresponding α - or β -galactoside building blocks, which are in turn synthesised from an armed donor.

4.6.1. Armed thioglycosides for α/β -galactosyl building block formation

A benzylated thioglycoside such as **4.54** could be a suitable armed donor for a subsequent glycosylation with L-serinyl acceptors (Scheme 4.22). Both α - and β -building blocks necessary for the synthesis of KRN7000 analogues would now be accessible due to the presence of a non-participating ether protecting group at the C-2 position of the galactosyl donor **4.54**. However, as an important drawback in this approach, we envisaged that chromatographic separations of the mixture of anomers may be difficult. Thioglycosides are a type of glycosyl donor commonly used in carbohydrate chemistry. One of the reasons they are so frequently utilised is due to their high stability to a range of different reaction conditions.^[201] This would allow for chemical modifications on the glycosyl donor without activation of the anomeric leaving group. Thioglycosides have been employed in the work concerning three different chapters of this thesis: initially, for the synthesis of an IAD glycosyl donor (discussed in Chapter 3) and for the synthesis of *O*-serinyl building blocks for KRN7000 analogues (discussed in this chapter and in Chapter 5).

The synthesis of the thioglycoside **4.54** began with the glycosylation of the acetyl protected galactosyl donor **2.32** with thiophenol under Lewis acid activation to yield 79% of the thioglycoside **4.53** (Scheme 4.22). Subsequent Zemplén deprotection, followed by a Williamson ether synthesis, using BnBr and NaH, afforded the

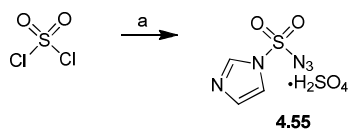
benzylated galactosyl donor **4.54** in an overall yield of 79% (over two steps). The spectroscopic data were in agreement with those reported in the literature.^[202]



Scheme 4.22 Reagents and conditions a) HSPH, $\text{BF}_3 \cdot \text{OEt}_2$, rt, 18 h, 79%; b) i) NaOMe, MeOH, 0 °C to rt, 1.5 h; ii) NaH, BnBr, DMF, 0 °C to rt, 18 h, 79% (2 steps).

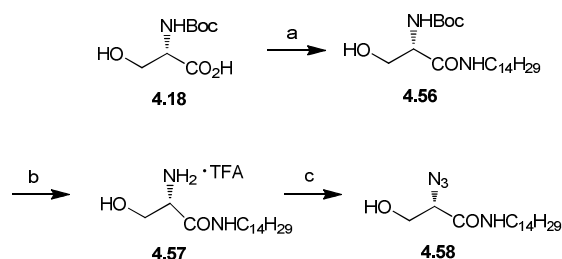
4.6.2. Revised syntheses of L-serine azido acceptors

The synthesis of L-serine azido acceptors **4.44** and **4.45** (previously described in Section 4.4.6) was revised. A correction to the original report regarding the use of the diazo-transfer reagent **4.43** was published by the authors.^[195] They outlined the explosive nature of the mother liquor of the hydrochloride salt **4.43**, amongst other notable problems. We decided the synthesis and use of the diazo-transfer reagent **4.43** was no longer appropriate, in particular on larger scale, which is a criterion necessary for building block formation. A publication superseding the efforts by Goddard-Borger and colleagues was presented by the same group whereby different acidic salts of the triazole transfer reagent **4.43** were precipitated and evaluated as diazo-transfer reagents.^[203] They did not exhibit the same hazardous effects as the previously described hydrochloride compound **4.43** and were not as explosive when friction tested. The sulfuric acid salt of the transfer reagent compound **4.55** was synthesised as shown in Scheme 4.23. The only difference from the previous experimental procedure lay in the addition of sulphuric acid to precipitate to give the corresponding sulphuric acid salt **4.55**. In our case, the salt **4.55** did not precipitate out instantly as described in the literature. However, with the addition of petroleum spirits and gentle scratching with a spatula, the imidazolium salt **4.55** precipitated in a yield of 32%. The remaining filtrate, containing potential azido containing materials were carefully quenched by oxidation with NaIO_4 and acidified with H_2SO_4 prior to disposal.



Scheme 4.23 Reagent and conditions. a) i) NaN_3 , MeCN, rt, 18 h; ii) imidazole, 0 °C to rt, 3 h; iii) H_2SO_4 , 0 °C, 1 h, 32%.

Since the glycosylation reactions involving non-participating protecting groups (such as the benzyl ethers present in thioglycoside donors like donor **4.54**) normally result in a mixture of stereoisomeric products, a number of strategies were investigated to bias the stereochemical outcome of these reactions. For this reason, we decided to synthesise the L-serine glycosyl acceptor **4.58**. This derivative features the presence of a long hydrocarbon chain (C_{14}), and this may impart stereoselective preferences due to steric bulk. The use of lipidic L-serinyl acceptors such as compound **4.58** will be discussed in more detail in Section 4.7.4. The synthesis of donor **4.58** began with the amide bond formation between the commercially available *N*-Boc-L-serine **4.18** and tetradecylamine, carried out with TBTU, HOBT and NEt_3 to give the desired lipidic compound **4.56** in a 59% yield (Scheme 4.24). *N*-Boc deprotection of L-serinyl derivative **4.56** and recrystallisation afforded the free amine TFA salt **4.57** quantitatively, which was subsequently treated with the diazo-transfer reagent **4.55** in basic conditions to give the desired L-serinyl acceptor **4.58** in less than a 54% conversion. The resulting oil contained both the desired compound **4.58** and an undesired side product which could not be separated by chromatographic separation. The ^1H NMR spectrum of the reaction mixture showed two signals corresponding to amide protons, one of them with an unusually high downfield resonance for an amide proton (7.5 ppm). This led us to believe that the unknown compound was a sulfonamide, with chemical shifts observed in agreement with those reported in the literature for this class of compounds.^[204] The side product was proposed to be the sulfonamide derivative **4.58a** (Figure 4.14).



Scheme 4.24 Reagents and conditions. a) $\text{NH}_2\text{C}_{14}\text{H}_{29}$, TBTU, HOBT, NEt_3 , 4Å MS , rt, 18 h, 59%; b) TFA, CH_2Cl_2 , 0 °C to rt, 18 h, quant.; c) **4.55**, K_2CO_3 , $\text{CuSO}_4 \cdot 5\text{H}_2\text{O}$, MeOH, rt, 18 h, <54%.

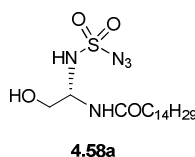
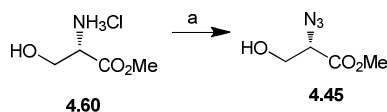
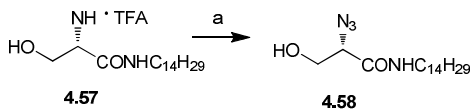


Figure 4.14 Undesired side product **4.58a** formed in the synthesis of L-serine azide **4.58**.

The unsuspected side reactions leading to the formation of compound **4.58a** was indeed unsettling and led us to abandon the imidazolium based diazo-transfer reagents for the TfN_3 route instead, which has been extensively reported in the literature, in order to achieve the formation of the desired L-serinyl azido derivative **4.58**.^[194a] We revisited the synthesis of the L-serine methyl ester derivative **4.45** (previously described in Section 4.4.6) and the long chain L-serine derivative **4.58** (described above) by this method. The synthesis of L-serine methyl ester derivative **4.45** proceeded smoothly from the reaction of commercially available L-serine methyl ester **4.60** with TfN_3 (which was made *in situ* by reaction of Tf_2O and NaN_3) catalysed by $\text{CuSO}_4 \cdot 5\text{H}_2\text{O}$ and NEt_3 in $\text{H}_2\text{O}/\text{MeOH}/\text{CH}_2\text{Cl}_2$ (3:10:3; Scheme 4.28).^[194a] This ratio of solvents ensured that the reaction was carried out as a homogeneous solution and stopped the precipitation of TfN_3 salts. As a precautionary measure, instead of large scale production, three separate reactions were carried out in parallel, which were combined, worked up and purified together. This synthesis allowed good access to glycosyl acceptor **4.45**, available for glycosylation. A similar procedure was followed for the preparation of the long chain L-serine acceptor **4.58**, as shown in Scheme 4.26, which afforded quantitative conversion to give the novel glycosyl acceptor **4.58**.



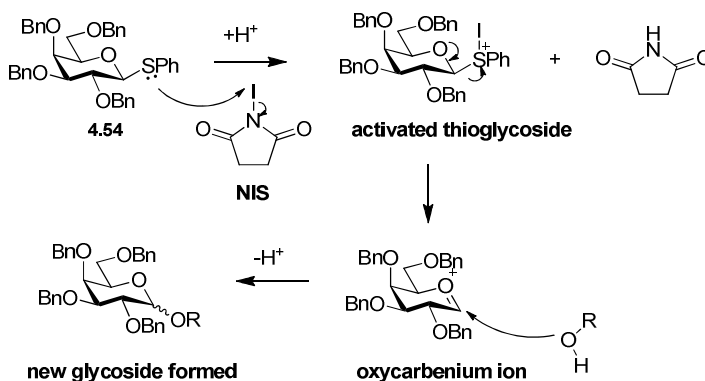
Scheme 4.25 Reagents and conditions. a) i) CH₂Cl₂, H₂O, 0 °C, N₂, 2 h, approx. 60% of TfN₃; ii) NEt₃, CuSO₄·5H₂O, CH₂Cl₂/MeOH/H₂O (3:10:3), rt, N₂, 18 h, 57%.



Scheme 4.26 Reagents and conditions. a) TfN₃, NEt₃, CuSO₄·5H₂O, CH₂Cl₂/MeOH/H₂O (10:3:3), rt, 18 h, 100%.

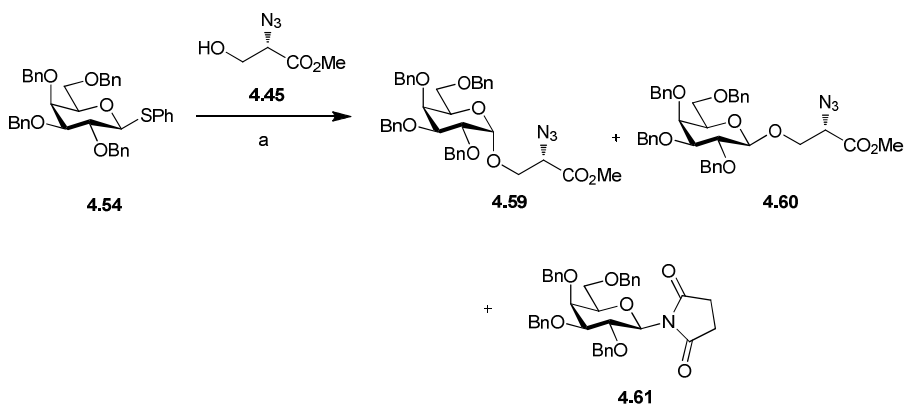
4.6.3. Glycosylation of armed thioglycosides with various acceptors for α/β -galactosyl building block formation

Thioglycoside activation with NIS and TfOH was first reported by Van Boom and co-workers.^[205] A general reaction mechanism for thioglycoside **4.54** glycosylation using NIS/TfOH is proposed in Scheme 4.27. Activation of the anomeric leaving group occurs by attack of the sulphur atom onto the thiophilic reagent NIS under acidic conditions. This activated thioglycoside drives the formation of an oxycarbenium ion in an S_N2 fashion. The glycosyl acceptor (ROH) can then attack the anomeric position at either the top or the bottom face and produce the glycosylation product forming a new glycosidic bond.



Scheme 4.27 Reaction mechanism for thioglycoside activation of **4.54** with NIS and TfOH results in formation of new glycoside formation.

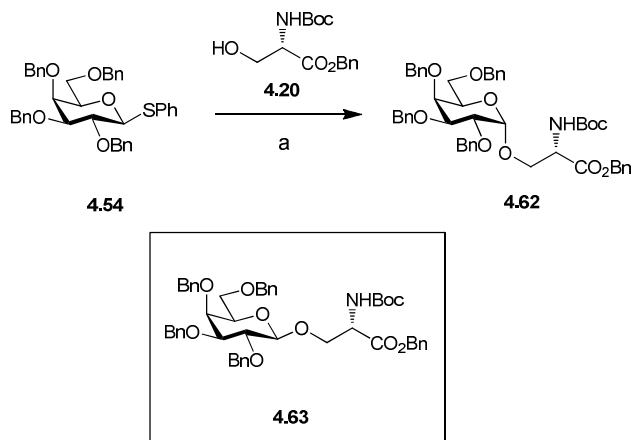
Using this system, the galactosyl thioglycoside donor **4.54** (acting as a limiting reagent) was reacted with the glycosyl acceptor **4.45**, using stoichiometric amounts of NIS and catalytic TfOH (Scheme 4.28). By analysis of the crude ^1H NMR spectrum a mixture of α -anomer building block **4.59** and β -anomer building block **4.60** were identified (77%, $\alpha/\beta = 2:1$). Careful flash chromatography afforded both the desired α -anomer **4.59** (32% yield) and the β -anomer **4.60** (25% yield). A glycosyl succinimide side product **4.61** was isolated in 21% yield). This side product reported by *Zhang et al.* can arise due to the formation of succinimide upon reaction of the galactosyl donor **4.54** with NIS.^[200] The succinimide can act as a nucleophile, albeit a poor one and compete with the glycosyl acceptor **4.45** to form the galactosyl succinimide side product **4.61**. This problem is evident in glycosylations involving unreactive glycosyl acceptors. These results corroborate that the presence of the azide functionality in the L-serine derivative **4.45** does not result in a significant increase the nucleophilicity of the L-serine acceptor, as discussed earlier.



Scheme 4.28 Reagents and conditions. a) NIS, TfOH, CH₂Cl₂, 4 Å MS, rt, N₂, 18 h, **4.59** (32%) and **4.60** (25%), and **4.61** (21%).

To clarify whether the azide functionality on the protected L-serine acceptor **4.45** had increased the nucleophilicity of the acceptor, and thus lead to an increase in the yield of the subsequent glycosylation, the thioglycoside **4.54** was reacted with the *N*-Boc glycosyl acceptor **4.20**. The reaction of the *N*-Boc protected acceptor

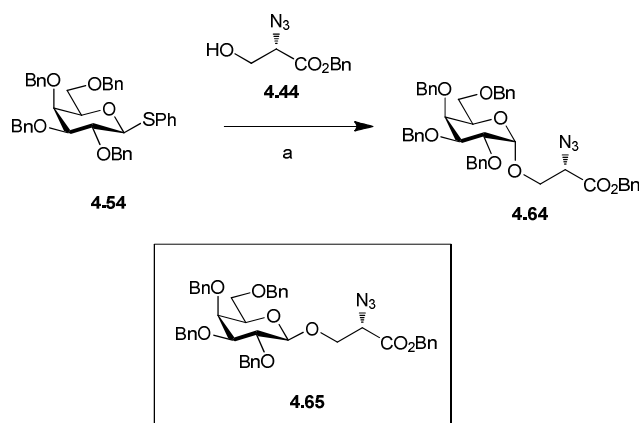
4.20 (deemed to be a poorer nucleophile due to unfavourable hydrogen-bonding) with the galactosyl donor **4.54** was performed (Scheme 4.29).



Scheme 4.29 Reagents and conditions. a) NIS, TfOH, CH₂Cl₂, 4Å MS, rt, N₂, 18 h, **4.62** (44%). No β -anomer **4.63** isolated in the reaction.

Poorer yields were achieved in this reaction, as anticipated. Careful flash chromatography afforded only the α -anomer **4.62** in a 44%. It is probable that the corresponding β -anomer **4.63** was also formed, as TLC analysis indicated a product with an R_f value almost identical to the α -anomer **4.62**. It was not possible to isolate it by chromatographic separation or to unambiguously identify it in the analysis of the remainder of the reaction products. Unreacted acceptor **4.20** and glycosyl succinimide **4.61** were also identified in this material. This result may indicate that the introduction of the azide functionality on L-serine derivative **4.45** moderately increases the yield of the glycosylation reaction.

The reaction between the azido glycosyl acceptor benzyl ester **4.44** with the thioglycoside donor **4.54** was executed as shown in Scheme 4.30. In this case, the corresponding α -anomer **4.64** was the only product isolated in the reaction in a 26% yield. Again the chromatographic separation proved to be a challenging step, and despite our best efforts, the remainder of the mixture of products could not be separated or characterised. As in the previous case the desired β -product **4.65** was most likely present due to a spot identified in TLC analysis in a very similar R_f region to the α -anomer **4.64**.



Scheme 4.30 Reagents and conditions. a) NIS, TfOH, CH₂Cl₂, 4Å MS, rt, N₂, 3 h, **4.64** (26%). No β-anomer **4.65** was isolated in the reaction.

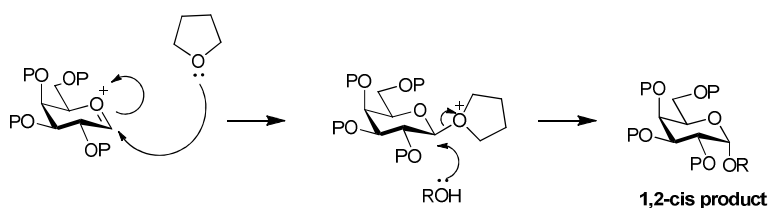
4.7. Stereoselective synthesis of α-galactoside building blocks for KRN7000

analogues

With these results in mind we decided that the most promising glycosylation reaction so far involved the thioglycoside donor **4.54** and the L-serine methyl ester acceptor **4.45** (see Scheme 4.28), whereby separation of the various components of the reaction was more achievable than in the other glycosylation reactions explored (Scheme 4.29 and 4.30). In order to increase the yield of the reaction and improve the α/β stereoselectivity, optimisation of the reaction conditions was carried out, with a bias to synthesise the more immunogenically relevant α-building block **4.59**. The fact that a higher percentage of the α-anomer was isolated (α/β ratio 2:1), as discussed in Section 4.6.3, may indicate that the main mechanism by which the reaction proceeds is via an S_N1 mechanism. It is possible also that it proceeded through of a mixture of S_N1 and S_N2 mechanism and as a result a mixture of anomers were isolated. As discussed in Chapter 2, an S_N1 reaction can be affected by various parameters. In our study, we explored the effect of temperature and solvent choice on the stereochemical selectivity of the reaction. We preferentially wanted to synthesise α-building blocks as we anticipated better biological results. Therefore parameters that may increase the α-selectivity were investigated.

4.7.1. Effects of temperature and solvent on α -stereoselectivity of glycosylation reactions

Temperature can affect the stereochemical outcomes of a glycosylation reaction. Kinetically controlled glycosylation reactions carried out at lower temperatures generally favour 1,2-*trans* glycoside formation. Nishizawi *et al.* reported a preference for the formation of β -glycosides (1,2-*trans* glycoside) at lower temperatures and α -glycosides at higher temperatures.^[206] Wegmann and Schmidt had similar findings.^[207] However, conflicting results have also been reported.^[208] Different solvents can induce the stereoselective formation of 1,2-*trans* products or 1,2-*cis* products, depending on their physicochemical properties. Polar solvents generally favour 1,2-*trans* products while solvents such as CH₂Cl₂ or toluene generally favour 1,2-*cis* products due to solvation effects.^[209] For certain solvents, special participating effects, as well as solvating effects, can increase the stereoselectivity of desired 1,2-*trans* products (such as MeCN) or 1,2-*cis* products (such as Et₂O). We tailored our solvent choice towards α -glycoside formation, the 1,2-*cis* product in our glycosylation. Ether-type reaction solvents (such as Et₂O, THF and dioxane) are known to participate in glycosylation processes.^[210] Improved α -stereoselectivities in glycosylations have been reported when these solvents were used in comparison to other solvents.^[211] The ether-type solvent acts as a nucleophile and attacks the anomeric position of the oxycarbenium ion to form a 1,2-*trans* product, which is then subsequently attacked by the glycosyl acceptor in an S_N2 type fashion to form the inverted 1,2-*cis* product as shown in Scheme 4.31.

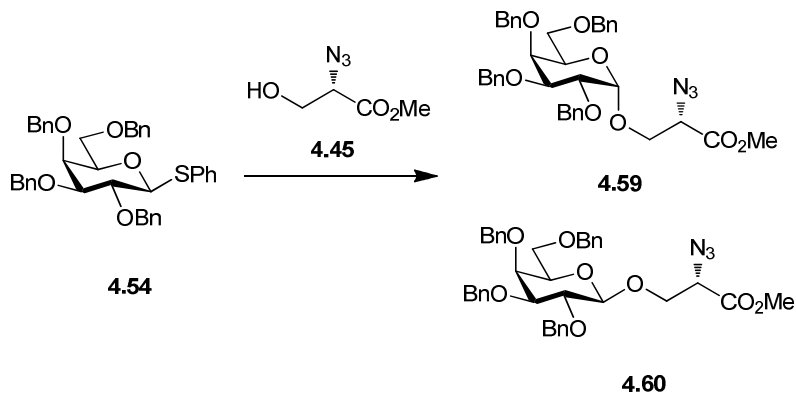


Scheme 4.31 Reaction mechanism for 1,2-*cis* glycosidic product formation induced by an ether-type solvent (THF).

The reaction conditions investigated in order to improve the stereoselectivity of the glycosylation between thioglycoside donor **4.54** and azido acceptor **4.44** are

summarized in Table 4.8. The effects of temperature and solvent on the glycosylation stereoselectivity were investigated.

Table 4.8 Summary of reaction conditions explored to optimise α -stereoselectivity in the formation of galactosyl building block **4.59**.



Entry	Temperature	Solvent	Yield 4.59 (%)*	Yield 4.60 (%)	α/β ratio
1	rt	CH ₂ Cl ₂	32	25	2:1
2	-20 °C	CH ₂ Cl ₂	- [‡]	- [‡]	1.8:1 [‡]
3	rt	THF	- [‡]	- [‡]	4:1 [‡]

* 1 equiv of glycosyl donor **4.54**, 2 equiv of glycosyl acceptor **4.45**, 2 equiv of NIS, 0.01 equiv of TfOH; [‡] α/β ratio was determined by ¹H NMR analysis.

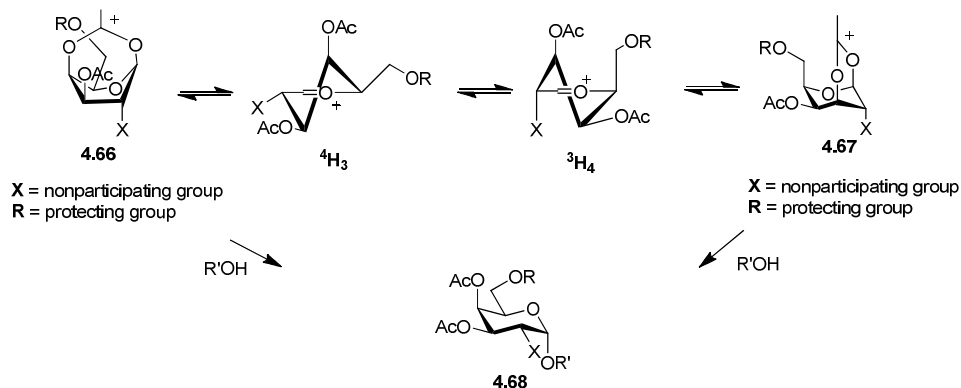
The effects of the temperature on the stereoselectivity of the glycosylation reaction were investigated (Entries 1 and 2 in Table 4.8). A decrease in temperature from rt to -20 °C resulted in a corresponding decrease in the α -stereoselectivity from a 2:1 α/β ratio to a 1.8:1 α/β ratio. Therefore, we can predict the reaction is under kinetic control, whereby 1,2-*trans* products are preferentially formed at decreased temperatures. Increased temperatures should encourage higher α -selectivities as a direct result of this observation. However, this may lead to degradation of the reactants, so rt was chosen as the optimum temperature for glycosylation in our system. The effect of solvent was explored (Entries 1 and 3 in Table 4.8) by comparison between CH₂Cl₂ and THF as the glycosylation solvent. An increase in α -selectivity was observed in THF compared to CH₂Cl₂, whereby the α/β ratio increased from 2:1 to 4:1. This observation was in agreement with the literature.^[210] Thus, optimised glycosylation conditions in terms of temperature and solvent involved the reaction of galactosyl donor **4.54** and glycosyl acceptor **4.45** in THF as a reaction solvent and at rt.

4.7.2. Effects of remote protecting group participation using Li's method on α -stereoselectivity of glycosylation reactions

The formation of a highly stereoselective 1,2-*cis* product is still one of the most challenging and daunting tasks in carbohydrate chemistry. In most cases, the formation of these stereoselective products involves very challenging methodologies. Gervay-Hague's glycosyl iodide chemistry, although yielding excellent α -stereoselectivities, can be difficult to reproduce due to the high reactivity of these glycosyl donors.^[143] IAD (discussed in detail in Chapter 3) is a method exemplified by Ito and Ogawa's work, which requires tedious protection and deprotection chemistry to deliver a tether suitable for activation and subsequent aglycon delivery.^[123a] These elaborate syntheses, although exhibiting beautiful chemistry lack the simplicity we desire in the synthesis of our building block. An ideal synthesis of an α -galactosyl building block would satisfy the following criteria: have very few synthetic steps, be accessibility to large scale, be

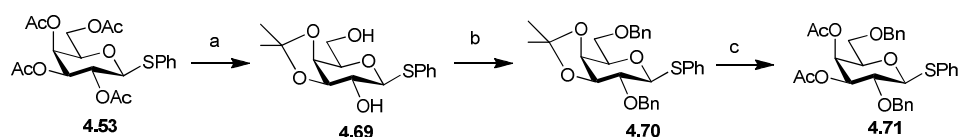
cheap and easy to handle, and also be highly stereoselective to minimise purification processes.

Despite an observed improvement in α -selectivity for the glycosylation reaction of α -galactosyl building block **4.59** described above, relatively difficult chromatographic separations were still encountered. In order to alleviate this problem, an investigation was begun whereby a more stereoselective glycosylation reaction was desired. Interestingly, Li and co-workers reported highly α -selective galactopyranosyl donors based on the influence of remote protecting groups.^[212] The α -selectivity reported by Li *et al.* is accredited to the influence of the remote protecting groups at the C-3 and C-4 positions of the glycosyl donor.^[212] If an S_N1 mechanism is in operation, a glycosyl oxycarbenium ion (described in Chapter 2) is the key intermediate. In general, two different conformations of glycosyl oxycarbenium ions, 4H_3 and 3H_4 favour different stereochemical outcomes. The 4H_3 glycosyl oxycarbenium conformations favour the formation of α -products as the chair-like transition state leading to the α -product is more stable than the corresponding one leading to the β -product (twist-boat transition state). Conversely, the 3H_4 conformation favours the formation of the β -products. Hence, mixtures of products are observed for many S_N1 glycosylations. In the case of the galactosyl oxycarbenium ion with remote acetyl protecting groups shown in Scheme 4.32,^[212] the carbonyl oxygen atoms can approach the anomeric carbon to form the participation intermediates **4.66** and **4.67**. In the case of 4H_3 oxycarbenium ion, an acetyl protecting group at the C-4 position can participate to give intermediate **4.66** while an acetyl group at the C-3 position can participate to give the intermediate **4.67**. The incoming nucleophile can only approach from the bottom face of these conformations and result in the stereoselective formation of the α -galactoside **4.68**. An important structural feature of these glycosyl donors is the non-participating group in the C-2 position of the conformations so neighbouring group participation cannot interfere.



Scheme 4.32 Mechanism of the remote protecting group directing effect.^[212]

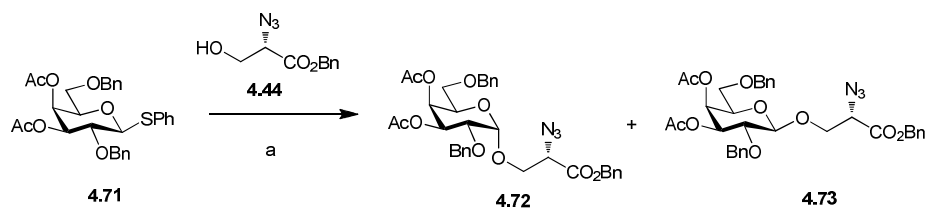
The synthesis of a novel galactosyl donor **4.71** was undertaken and it was initiated with the global deacetylation of thioglycoside **4.53** with NaOMe in MeOH as in Scheme 4.33. The crude thiol was selectively protected at the C-3 and C-4 positions by an isopropylidene group to give the acetonide **4.69** in 70% yield (over two steps). Benzoylation of the free C-2 and C-6 hydroxyl groups by treatment with NaH and BnBr in a Williamson ether synthesis yielded 75% of the glycoside **4.70**. Deprotection of the isopropylidene group under acidic conditions allowed acetylation at the C-3 and C-4 positions to yield the galactosyl donor **4.71** in a good overall yield of 77% over 5 steps.



Scheme 4.33 Reagents and conditions. a) i) cat. Na metal, MeOH, 0 °C to rt, 1.5 h; ii) H₂SO₄, acetone, rt, 18 h, 70% (2 steps); b) NaH, BnBr, DMF, 0 °C to rt, 18 h, 75%; c) i) AcOH, 80 °C, 4 h; ii) Ac₂O, DMAP, Pyr, rt, 1.5 h, 86% (2 steps).

Following the reaction conditions described by Li and colleagues,^[212] whereby the galactosyl donor **4.71** was reacted with L-serine acceptor **4.43** using a mixture of promoters (NIS/ TMSOTf) to give 66% of a mixture of diastereoisomers **4.72** and **4.73** (Scheme 4.34). Analysis by ¹H NMR spectroscopy of the crude reaction mixture indicated a 2:1 α/β stereoselectivity. After purification, only small amounts of the pure α-product **4.72** could be isolated (7%) for characterisation, and separation of

the β -product **4.73** proved to be impossible. Disappointed with the poor stereoselectivity observed, the methodology was abandoned.

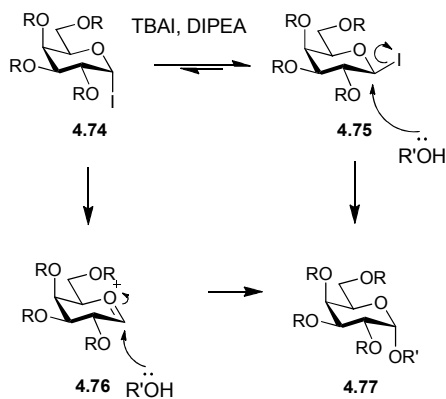


Scheme 4.34 Reagents and conditions. a) NIS, TMSOTf, CH₂Cl₂, 4Å MS, 0 °C, N₂, 1 h, 66% **4.72** and **4.73** (2:1 α / β).

4.7.3. Effects of halide-ion catalysis on α -stereoselectivity of glycosylation using glycosyl iodides

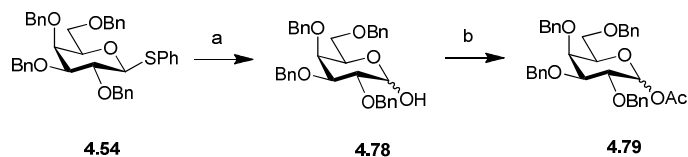
The use of glycosyl iodides as glycosyl donors has been reported to achieve excellent stereoselectivities.^[143, 213] However, due to their highly reactive nature, the preparation and handling of glycosyl iodides can be problematic. Since the desired α -stereoselectivity was not observed using Li's methodology, described above in Section 4.7.2, the preparation of 1,2-*cis* linkages using glycosyl iodides as glycosyl donors, as reported by Gervay-Hague and co-workers, was attempted.^[193]

Gervay-Hague capitalised on the effectiveness of halide-ion catalysis pioneered by Lemieux and colleagues, whereby α -glycosyl bromides were used to construct difficult 1,2-*cis* linkages.^[214] Gervay-Hague developed Lemieux's methodologies with the use of glycosyl iodide donors, TBAI and a hindered base to stereoselectively produce 1,2-*cis* glycosides in excellent yields.^[215] The addition of the halide ion (TBAI) facilitates *in situ* anomerisation of the α -halide **4.71** to the more reactive β -halide **4.72**. It is believed that the stereoselectivity arises from a Curtin-Hammett kinetic scheme whereby the glycosyl acceptor reacts in an S_N2 fashion to yield the 1,2-*cis* product **4.77**. A schematic representation is shown in Scheme 4.35.



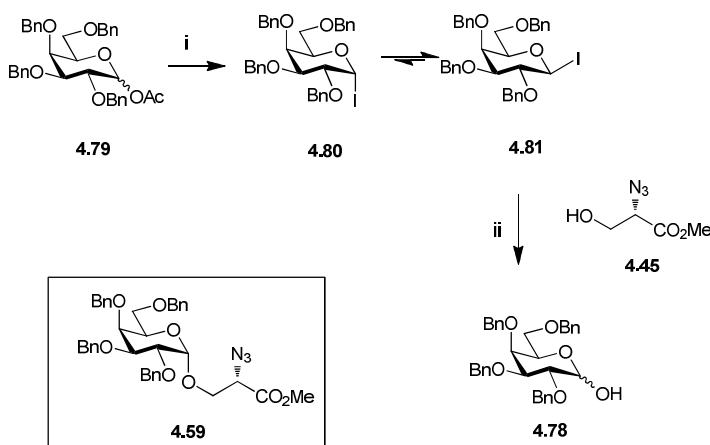
Scheme 4.35 Mechanism of glycosidic bond formation from glycosyl iodides in the presence of TBAI.^[213]

In the synthesis, the benzylated galactosyl acetate **4.79** was prepared by treatment of the thioglycoside **4.54** with NBS in wet acetone to give hemiacetal **4.78**, followed by acetylation using Ac_2O in Pyr, to give 41% of the acetylated donor **4.79** (Scheme 4.36).



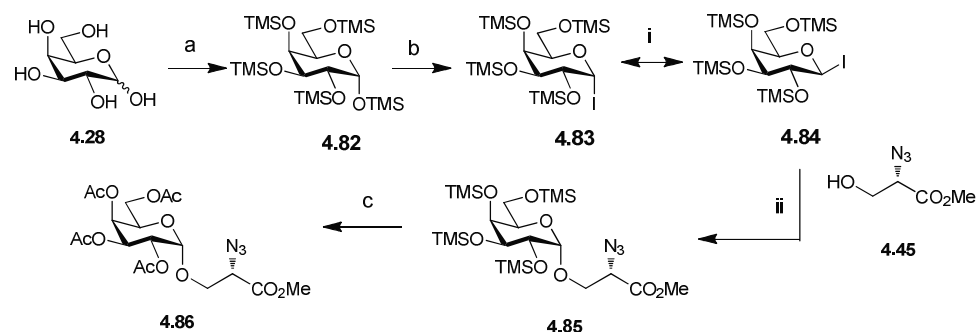
Scheme 4.36 Reagents and conditions. a) NBS, wet acetone, 75 °C, 18 h, 61% (based on recovered starting material); b) Ac_2O , Pyr, 0 °C, rt, 18 h, 41%.

The acetylated donor **4.79** was reacted under anhydrous conditions with TMSI in CH_2Cl_2 to form the α -glycosyl iodide **4.80**, which was then reacted with the L-serinyl acceptor **4.46** in the presence of TBAI and DIPEA, in order to produce the desired α -glycoside **4.81** following a literature procedure described by Wu and Gervay-Hague (Scheme 4.37).^[193] However, none of the desired product **4.59** was isolated. Instead, the unreacted L-serine acceptor **4.45** was recovered, along with hemiacetal product **4.78**. This observation indicates that, if the glycosyl iodide **4.81** had formed, it must have subsequently undergone hydrolysis to give the hemiacetal **4.78**.



Scheme 4.37 Reagents and conditions. i) TMSI, CH₂Cl₂, 0 °C, 20 min; ii) Benzene, TBAI, DIPEA, 65 °C, 1.5 h. Desired product **4.59** was not isolated.

In parallel with the conditions described above, the use of the fully TMS protected glycosyl donor **4.83** was investigated. The procedure for the formation and isolation of the silyl protected *O*-glycoside **4.83** were described by Besra and colleagues (Scheme 4.38).^[216] The synthesis began with the TMS protection of D-galactose **4.28** by reaction with TMSCl and NEt₃ to produce compound **4.82** in 89% yield. The precursor **4.82** was reacted with TMSI in CH₂Cl₂ at 0 °C, for a subsequent glycosylation reaction with glycosyl acceptor **4.45** with TBAI and DIPEA as described before. Attempts of purification with flash chromatography resulted in poor yields of α-anomer **4.85** (15%), possibly because the TMS protected compounds were acid labile. This prompted us to repeat the synthesis and remove the silyl protecting groups of glycoside **4.85** and acetylate the hydroxyl groups prior to flash chromatography of product **4.85**. This approach would give acetylated glycosyl donor **4.86**.^[193] Purification afforded an overall yield of 3% of the desired acetylated glycoside **4.86**. A complicated array of acetylated products were present also. This glycosyl iodide method was abandoned due to the poor yields obtained in our synthesis of glycoside **4.86**.



Scheme 4.38 Reagents and conditions. a) TMSCl, NEt₃, DMF, 4Å MS, 0 °C to rt, 4 h, 89%; b) i) TMSI, CH₂Cl₂, 0 °C, 20 min; ii) TBAI, DIPEA, benzene, rt, 48 h; c) i) Dowex (H⁺ form), MeOH, rt, 5 h; ii) Ac₂O, Pyr, rt, 18 h, 3% (overall yield).

4.7.4. Synthesis of glycolipids 4.14 and 4.16 using lipidic L-serine acceptors

Glycosylation conditions explored so far have resulted in moderate stereoselectivities and yields. Separation of the diastereoisomers proved to be even more problematic. We proposed that if a lipidic chain were introduced earlier in the synthesis, perhaps steric factors would influence the stereoselectivity of the glycosylation, with a preference towards the α -glycosyl product. Additionally, the separation of the diastereoisomers may be easier than for previous attempts. This method is also a more convergent approach to the previously explored building blocks synthesis. The disadvantage of this approach lies with the fact that, for different lipidic chain lengths on the acid residue, the stereochemical outcome may be different and the reaction conditions may need to be optimised every time. With the target KRN7000 analogues **4.14** and **4.16** in mind (shown in Figure 4.15), we focussed our attention on the synthesis of an L-serine donor functionalised with a C₁₄ hydrocarbon chain, such as protected glycolipid **2.67** (Scheme 4.39).

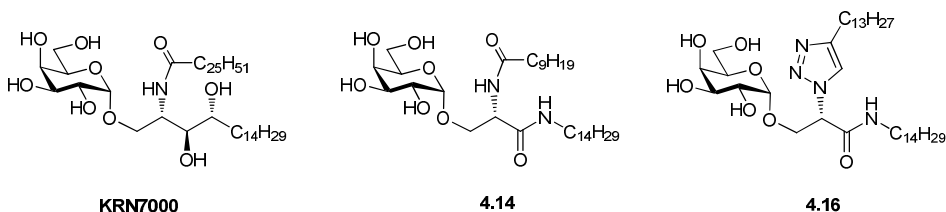
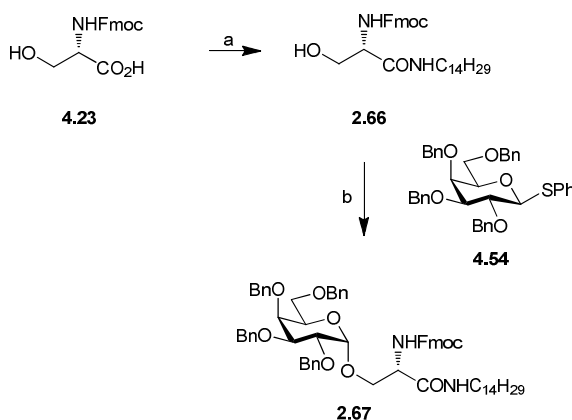


Figure 4.15 KRN7000 and L-serine analogue targets **4.14** and **4.16**.

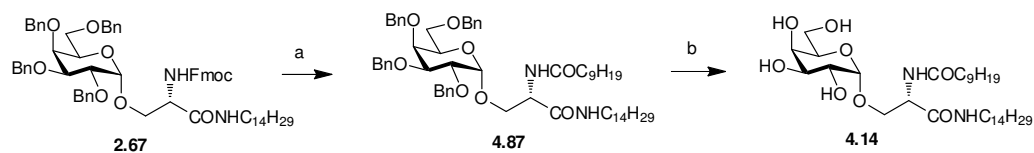
The synthesis of the *N*-Fmoc protected L-serine derivative **2.66** (mentioned in Chapter 2) was therefore undertaken by the reaction of *N*-Fmoc-L-serine **4.23** with tetradecylamine, using the TBTU/HOBT standard coupling methodology to give a yield of the amide **2.66** in 73% yield (Scheme 4.39). A glycosylation reaction was then performed with the glycosyl acceptor **2.66** and the previously synthesised thioglycoside **4.54**, using NIS and catalytic TfOH in THF under the optimised conditions described in Section 4.6.3. Analysis by TLC indicated that three compounds were present in the reaction mixture, namely the hemiacetal **4.78** (Scheme 4.36), the unreacted glycosyl acceptor **2.66** and a single glycosylation product, suggesting the stereoselective formation of a single diastereoisomer. Purification by flash chromatography afforded 49% of the novel α -glycoside **2.67**. No evidence of the formation of the corresponding β -glycoside was observed.



Scheme 4.39 Reagents and conditions. a) $\text{NH}_2\text{C}_{14}\text{H}_{29}$, TBTU, HOBT, DIPEA, 4\AA MS, $0\text{ }^\circ\text{C}$ to rt, 18 h, 73%; b) NIS, TfOH, 4\AA MS, THF, rt, 18 h, 49%.

Deprotection of the *N*-Fmoc protecting group of glycoside **2.67** under basic conditions (10% piperidine in CH_2Cl_2) afforded the free amine product, which was reacted without further purification with decanoic acid using TBTU/HOBT coupling methodology to yield the protected glycolipid **4.87** in a 74% yield (over two steps) as shown in Scheme 4.40. The ^1H NMR of the novel benzyl protected glycolipid **4.87** is shown as a representative example in Figure 4.16. Diagnostic signals are highlighted in the spectrum including the protons corresponding to the amide functionalities (at 7 and 6.8 ppm), and the anomeric proton (at 5.2 ppm, $J = 3.7$ Hz),

present at a chemical shift and containing a coupling constant characteristic for an α -galactoside.



Scheme 4.40 Reagents and conditions. a) i) 10% piperidine in CH_2Cl_2 , rt, 1 h, ii) $\text{C}_9\text{H}_{19}\text{CO}_2\text{H}$, TBTU, HOBT, DIPEA, DMF, rt, 18 h, 74% (2 steps); b) H_2 , Pd (C), EtOH, EtOAc, AcOH, rt, 20 h, 89%.

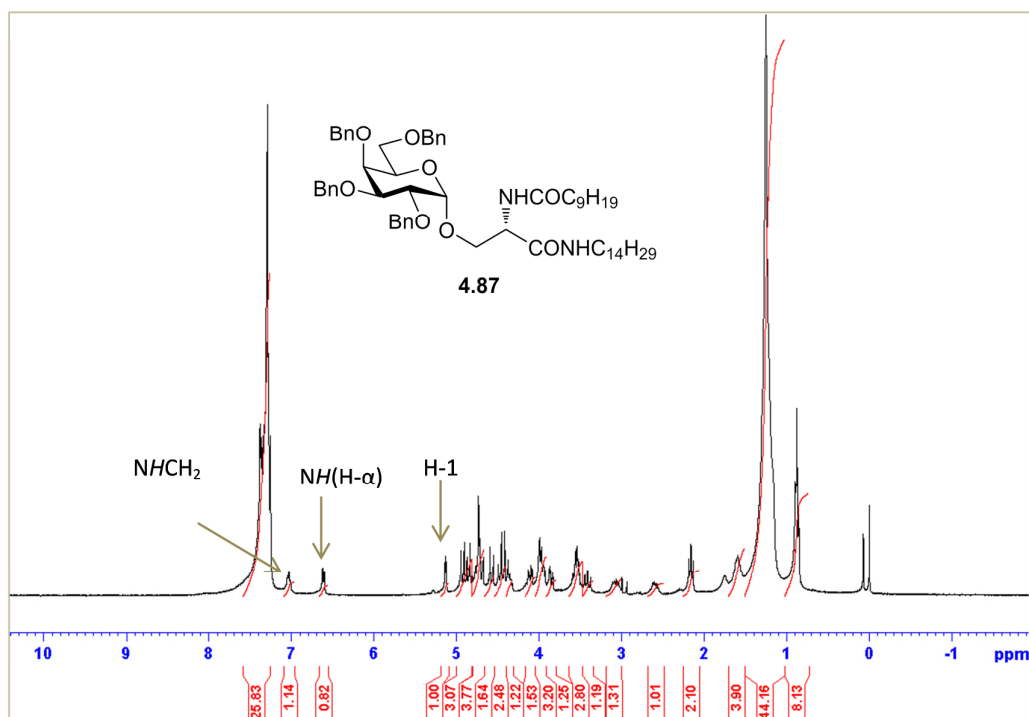


Figure 4.16 ^1H NMR spectrum of glycolipid **4.87**. Characteristic signals are highlighted.

Global debenzylation of glycolipid **4.87** was first attempted using $\text{H}_2(\text{g})$ and a 10% w/w loading of Pd(C) in EtOH/EtOAc (3:1) at 4 Barr pressure for 18 h in a hydrogenator shaker apparatus. However no hydrogenation of the benzyl ethers was observed. Upon addition of catalytic AcOH and a higher loading with 50% w/w of Pd(C), the deprotection of the benzyl ether protecting groups with H_2 at 4 Barr pressure yielded the literature known KRN7000 analogue **4.14** in 89% yield.^[169a]

Structural characterisation was carried out on the analogue **4.14** with the aid of NMR, IR and HR-mass spectrometry and a specific optical rotation value was obtained, as characteristic data was not reported for the literature example.^[169a] A representative example of the ¹H NMR spectrum is shown in Figure 4.17. Diagnostic signals include the H- α proton (4.6 ppm), the sugar protons (3.6-4.0 ppm) and the methylene protons of the long chains (1.3 ppm). No signals were identified for the amide protons due to deuterium exchange with residual D₂O in the d₄-MeOD.

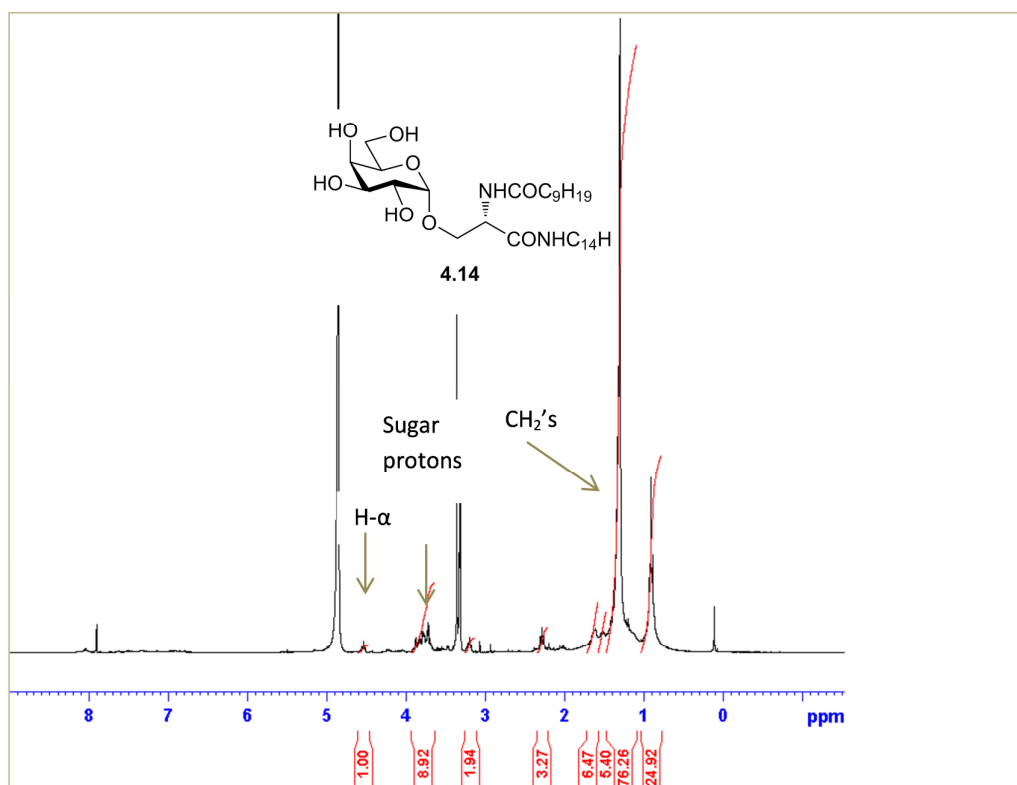
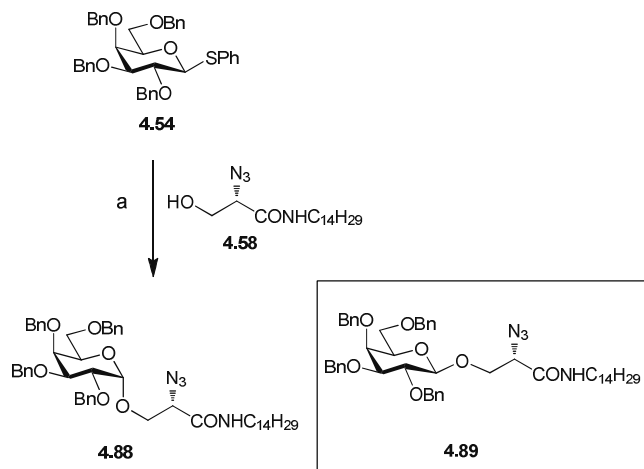


Figure 4.17 ¹H NMR spectrum of glycolipid **4.14** in d₄-MeOD. Characteristic signals are highlighted.

The synthesis of the triazole containing analogue, glycolipid **4.16** (Figure 4.15), required the use of the azido lipidic L-serinylacceptor **4.58** (previously described in Section 4.6.2). Reaction of the thioglycoside **4.54** and the L-serinyl acceptor **4.58** in THF, with NIS and TfOH as the promoter system, gave a mixture of diastereoisomers **4.88** and **4.89** (α/β ratio of 2.7:1 in a 63% combined yield), with

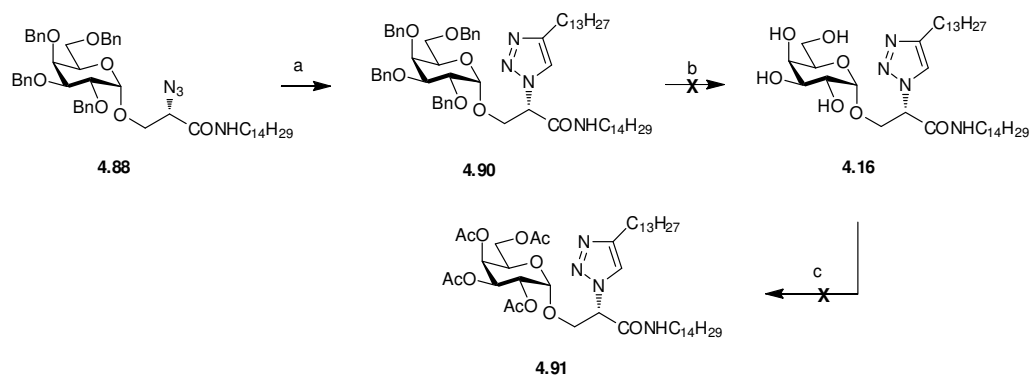
isolation of 35% of the 1,2-*cis* product **4.88** (Scheme 4.41). In this case, the easier separation of the desired α -anomer **4.88** during flash chromatography compensated for the decrease in the stereoselectivity in the glycosylation reaction. Fortunately also, recovery of the unreacted glycosyl acceptor **4.58** allowed for its use in subsequent glycosylation reactions to be carried out. On the other hand, attempts to isolate the β -glycoside **4.89** in a pure form failed.



Scheme 4.41 Reagents and conditions. a) NIS, TfOH, 4Å MS, THF, rt, 18 h, 63% (α/β ratio of 2.7:1), **4.88** (35%). No pure β -anomer **4.89** was isolated.

The galactosyl azide **4.88** was reacted with the commercially available pentadecyne in the presence of CuSO₄·5H₂O and sodium ascorbate in a CuAAC reaction (described in detail in Chapter 5), to afford 76% of the 1,4-disubstituted 1,2,3-triazole containing glycolipid **4.90** in a regioselective manner (Scheme 4.42). The ¹H NMR spectrum of the benzyl protected glycolipid **4.90** is shown in Figure 4.18, and diagnostic signals are highlighted. Interestingly, the coupling constant of the anomeric proton of the triazole glycolipid **4.90** ($J = 6.3$ Hz) is an unusually large coupling constant for an α -glycosidic linkage. However, the chemical shift of the anomeric proton (4.9 ppm) is characteristic of an α -product. Thus the formation of the triazole ring seems to have affected the conformation of the molecule. Also of significance is the signal corresponding to the H- α proton (5.4 ppm), appearing at a much higher chemical shift than expected for an H- α proton. However, this observation is in agreement with data reported for amino acid based derivatives containing a triazole moiety at the C- α , although it is not explicitly discussed.^[217]

Chapter 4: Synthesis of L-serinyl based glycolipid analogues of the immunostimulant KRN7000



Scheme 4.42 Reagents and conditions. a) Pentadecyne, $\text{CuSO}_4 \cdot 5\text{H}_2\text{O}$, Na ascorbate, THF/MeOH/ H_2O (2:2:1), rt, 18 h, 71%; b) H_2 , Pd (C), EtOAc/EtOH.

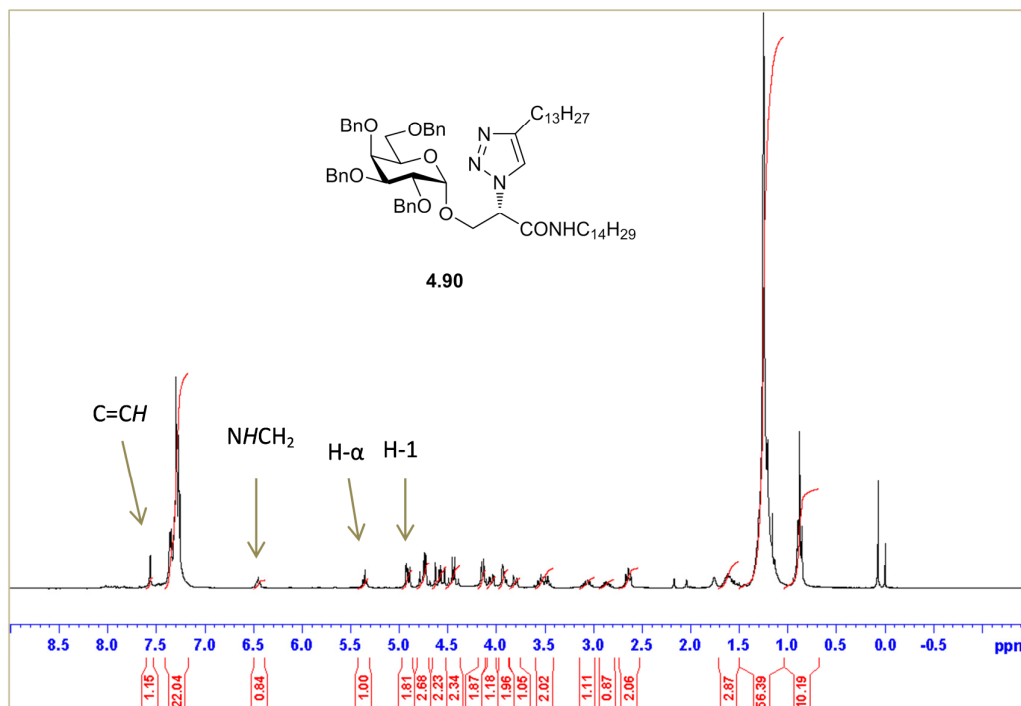


Figure 4.18 ^1H NMR spectrum of benzyl protected glycolipid **4.90**.

Difficulties arose with the global deprotection of the benzyl ether protecting groups of glycolipid **4.90**. Hydrogenolysis involving 10% w/w loading of Pd(C) at 4 Barr pressure in a hydrogenator shaker apparatus for 18 h did not result in complete hydrogenation of the benzyl ethers. The use of Pearlmans catalyst (Pd(OH)) in a 10% loading did not sufficiently catalyse the reaction as an alternative. Increased

quantities of Pd(C) ranging from 10% w/w up to 500% w/w loading were utilised in a systematic manner but complete deprotection was not achieved. The addition of AcOH, as performed for the glycolipid **4.14** did not yield favourable results either. Instead, degradation occurred with small amounts of partially protected compounds of glycolipid **4.90** detected in HR-MS analysis. In an attempt to further identify the possible degradation products in the reaction mixture or whether any of the desired glycolipid **4.90** had been formed, it was subjected to an acetylation reaction using Ac₂O in Pyr for 18 h as in Scheme 4.42. ¹H NMR analysis indicated hydrocarbon by-products with no signals indicative of a triazole containing product. HR-MS analysis confirmed traces of the desired compound **4.91** and some *per*-acetylated galactose **2.32** also. No other degradation products could be discerned. Due to a limited reservoir of the protected glycolipid **4.90** the debenzylolation conditions could not be optimised.

It was obvious that the forceful conditions necessary for the cleavage of the benzyl ethers resulted in a degradation of the product **4.90** to yield an unidentifiable mixture. Possible reasons for the need for such forceful conditions are outlined. The presence of residual CuSO₄·5H₂O from the previous CuAAC reaction may have hindered the rate of reaction, as Cu is known for poor hydrogenolytic activity,^[218] thus harsh conditions would be necessary for the hydrogenolysis. Alternatively, competing coordination of the triazole moiety to the Pd(C) in glycolipid **4.90** may also have been responsible for the sluggish reaction. The degradation observed may have been accelerated due to the increased acidity of the H-α in the protected glycolipid **4.90**. As a result of these observations, the synthesis of glycolipid **4.16** was not repeated using the synthetic strategy proposed above.

4.8. Concluding remarks

It seems that, after analysing a range of different reaction conditions for the synthesis of an L-serine building block for KRN7000 analogues **4.13-4.16**, the optimum glycosylation conditions involve the use of the thiogalactoside **4.54** with either the *N*-Fmoc protected L-serine acceptors **2.66** (Section 4.7.4) or the azido L-

serine glycosyl acceptor **4.58** (Section 4.4.7) to give KRN7000 α -analogues **4.14** and the benzyl protected analogue **4.90**, respectively.

The β -analogues of KRN7000 **4.13** and **4.15** were not synthesised. This was partially due to the problems arising from the diminished ability of galactosyl donors bearing ester protecting groups (discussed in Section 4.4) leading to poor glycosylation yields of β -galactosyl building blocks, coupled with the inherently low nucleophilicity of their L-serinyl acceptors. Secondly, the inability to separate sufficient quantities of β -galactosyl building blocks during glycosylations involving armed donors (discussed in Section 4.6 and 4.7) hindered the subsequent synthesis of the β -analogues of KRN7000 **4.13** and **4.15**.

In general, moderate yields were reported for the key synthetic step involving glycosylation to synthesise a suitable building block for KRN7000 analogues in this chapter. Most likely, the low nucleophilic nature of the L-serinyl glycosyl acceptors contributed to these moderate yields. However, excellent stereoselectivity was observed for the long chain *N*-Fmoc methodology (described in Section 4.7.4) and good separation of the azido glycolipid building block **4.88** (described in Section 4.7.4) was reported. These optimisation reaction conditions would serve as a suitable method for the synthesis of a C-6 functionalised L-serinyl KRN7000 analogue (described in Chapter 5). Isolation of the α -glycolipids **2.67** and **4.88** allowed for the synthesis of the KRN7000 analogue **4.14** and the benzyl protected precursor **4.90** respectively. The glycolipid **4.14** will be evaluated for its ability to serve as an *i*NKT cell stimulatory ligand. This *in vitro* study will be carried out by Dr. Derek Doherty in St. James hospital on human *i*NKT cells.

The difficulties encountered during the deprotection of glycolipid **4.90** indicated that an alternative approach is necessary for the synthesis of triazole containing glycolipid **4.16**. The use of PMB ethers in place of benzyl ethers in the synthetic strategy is one possible solution, whereby removal of the PMB ethers could occur with DDQ in the final deprotection step.

**Chapter 5: Synthesis of L-serinyl based macrocyclic analogues of
KRN7000**

5.1. Introduction

5.1.1. Carbohydrate macrocycles

A macrocyclic compound is defined as a molecule containing a ring of 12 or more atoms. Over the past decade, the development of carbohydrate containing macrocyclic compounds has received considerable attention due to their diverse structural characteristics and interesting biological profiles.^[219] The key design element in the formation of a carbohydrate containing macrocycle often involves a ring closing alkene metathesis (RCM) reaction, and some examples are shown in Figure 5.1.^[219-220]

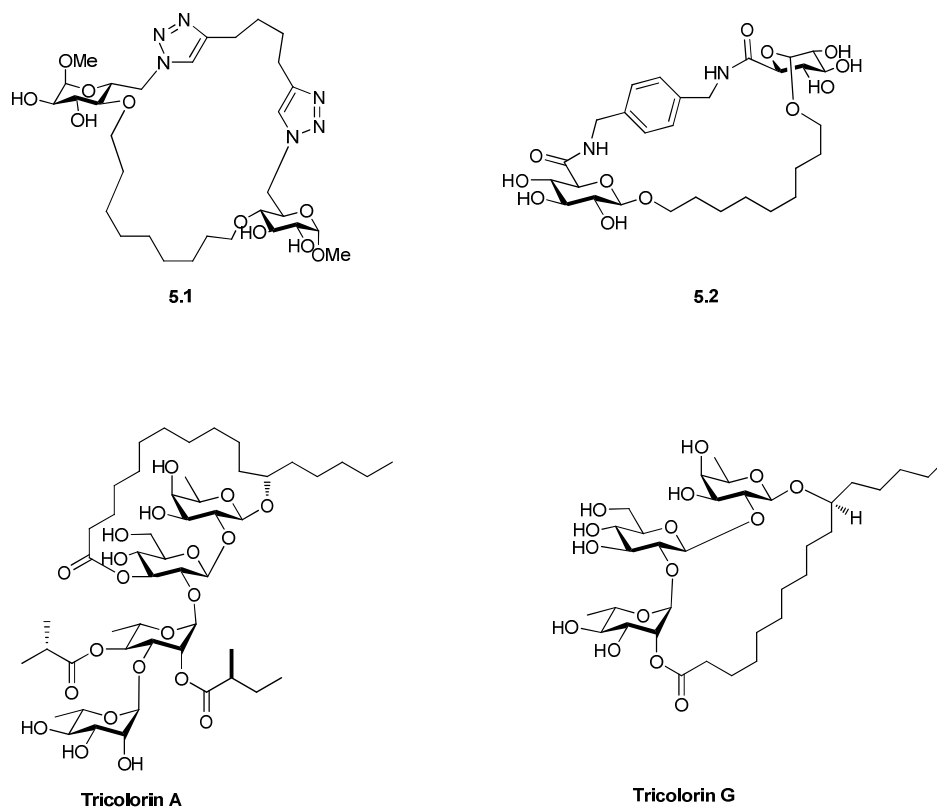


Figure 5.1 Carbohydrate macrocycles synthesised by a RCM reaction.^[219-220]

The synthesis of macrocycle **5.1** (Figure 5.1) was explored by Dorner and Westermann and it involved RCM as a key synthetic step. Macrocycle **5.1** was obtained in 95 % yield.^[219b] More recently, Doyle and Murphy synthesised a range of glycophanes using RCM (macrocycle **5.2** in Figure 5.1 is one such example) and ring closing alkyne metathesis (RCAM), to study host-guest interactions. However,

low aqueous solubility of these compounds restricted biological evaluation.^[221] Tricolorin A and G (Figure 5.1) were isolated from *Ipomoea tricolor Cav.*, a plant used in traditional medicine in Mexico to protect crops against invasive weeds (described in Chapter 1).^[220] Subsequent SAR studies on Tricolorin A highlighted the importance of the intact macrocyclic lactone ring of Tricolorin A on plant growth inhibition.^[222] The first total synthesis of Tricolorin G and the subsequent total synthesis of Tricolorin A were successfully achieved by Fuerstner and colleagues utilising RCM as the key synthetic step in the formation of both these macrocycles.^[10]

5.1.2. Carbohydrate macrocycles formed by CuAAC reactions

Since the discovery of the CuAAC click reaction (described in Section 5.1.3.), many applications in medicinal and biomedical chemistry have been explored utilising azides and alkynes. This is predominantly owing to the isosteric relationship of the 1,4-disubstituted 1,2,3-triazoles to the amide bond (Figure 5.2), making them attractive substrates for many biological applications.^[223] Examples of the formation of carbohydrate macrocycles involving the CuAAC reaction as a key synthetic step are scarce, most probably due to the difficulties involved in carbohydrate synthesis in general and the relative novelty of the CuAAC reactions to the scientific community (2002), not to mention the fact that macrocycles are difficult to prepare. Some examples in the literature are described below.

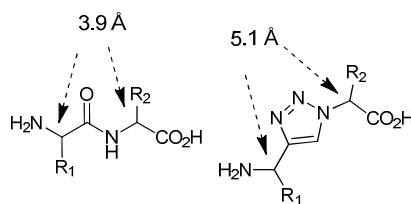
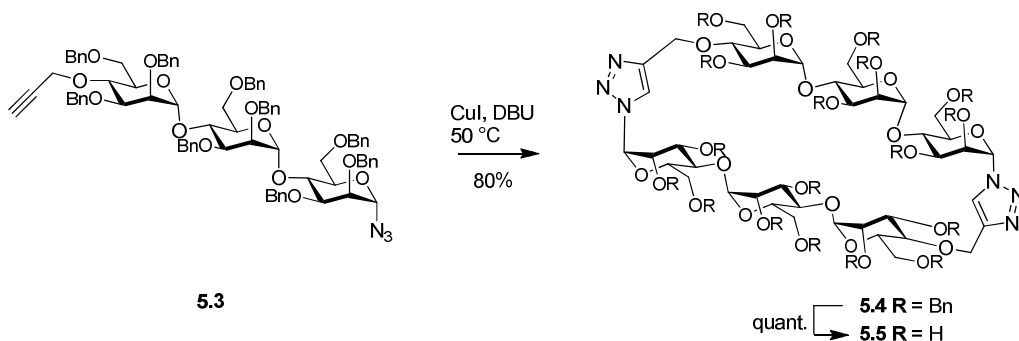


Figure 5.2 Structure of amide bond in a peptide (left) and a 1,4-disubstituted 1,2,3 triazole mimic (right). C- α distances, hydrogen-bonding abilities, dipole moment and structural planarity are comparable.^[223]

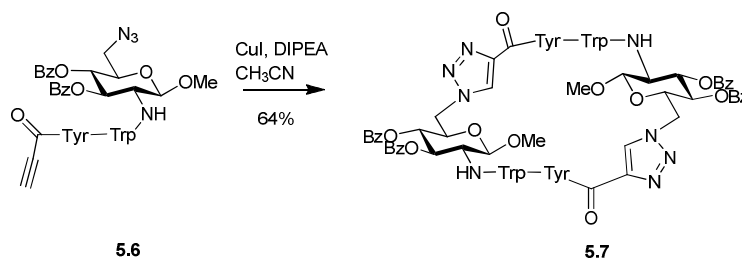
Much interest has been focussed on cyclodextrins (CD), which have applications in drug delivery systems^[224] and topical drug formulation^[225] amongst many others, due to their enhanced biocompatibility and water solubility compared to other multivalent constructs. The synthesis of CD mimics were performed by Bodine and

colleagues through the use of CuAAC chemistry as in Scheme 5.1.^[226] They reported a convergent click cyclodimerization of a bifunctionalised trimannoside using a CuI/DBU catalytic system to afford a 80% yield of the desired dimer **5.4**, with a concomitant formation of an undesired cyclic trimer (15%). After global deprotection of the benzyl ether protecting groups to give dimer **5.5** in quantitative yield, the CD mimic was found to serve as a host to inclusion of ANS, a small organic molecule in a similar manner to β -CD.



Scheme 5.1 Synthesis of macrocyclic dimer **5.5** from trimannoside **5.3**.^[226]

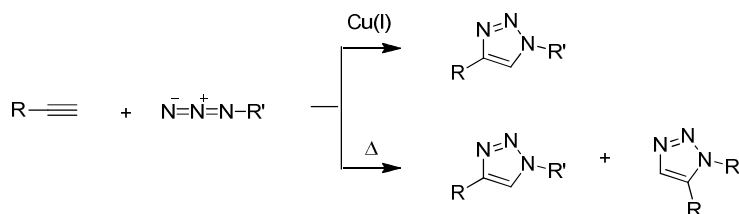
Macrocycles incorporating amino acids are important in the pharmaceutical industry. These conformationally constrained peptidomimetics possess unique properties that aid in their utility as important molecular probes of biological processes and as potential drug leads.^[227] Amino acid macrocycles combining carbohydrate moieties offer unique candidates as artificial receptors for small biomolecules as they possess functionalities that allow for most types of intermolecular interactions.^[228] Billing and Nilsson synthesised C_2 -symmetric macrocyclic carbohydrate/amino acid hybrids through CuAAC chemistry.^[228] One such example explored the reaction of the bifunctional precursor **5.6** with a CuI/DBU catalytic system to yield 64% of the desired C_2 -symmetric macrocycle **5.7** (Scheme 5.2). These novel carbohydrate based macrocycles were investigated as H₂O soluble artificial receptors using computational methods.



Scheme 5.2 Synthesis of macrocyclic carbohydrate/ amino acid hybrid **5.7**.^[228]

5.1.3. Cu catalysed azide-alkyne cycloaddition (CuAAC)

The Huisgen 1,3-dipolar cycloaddition reaction involves the reaction of an organic azide and a terminal alkyne to form a mixture of 1,2,3-triazole regioisomers upon thermal heating (Scheme 5.3).^[229] This classical cycloaddition has gained considerable attention since the introduction of the Cu(I) catalysed azide-alkyne cycloaddition (CuAAC), reported independently by the groups of Mendel^[230] and Sharpless.^[231] It involves the regioselective transformation of organic azides and terminal alkynes into 1,4-disubstituted 1,2,3-triazoles (Scheme 5.3).



Scheme 5.3 A CuAAC reaction involves the regioselective formation of a 1,4-disubstituted 1,2,3-triazole product in the presence of Cu(I) (top); a Huisgen 1,3-dipolar cycloaddition under thermal irradiation affords a mixture of 1,4 and 1,5-disubstituted 1,2,3-triazole regioisomers (bottom).

CuAAC reactions often satisfy the criteria for click chemistry, a term coined by Sharpless to describe a “near perfect” reaction that mimics nature by joining small modular units together.^[232] A click chemistry reaction must be modular, wide in scope, high yielding, produce inoffensive by-products (if any), be stereospecific, have high atom economy, produce compounds that are physiologically stable, and exhibit a large thermodynamic driving force. The resulting 1,4-disubstituted 1,2,3-

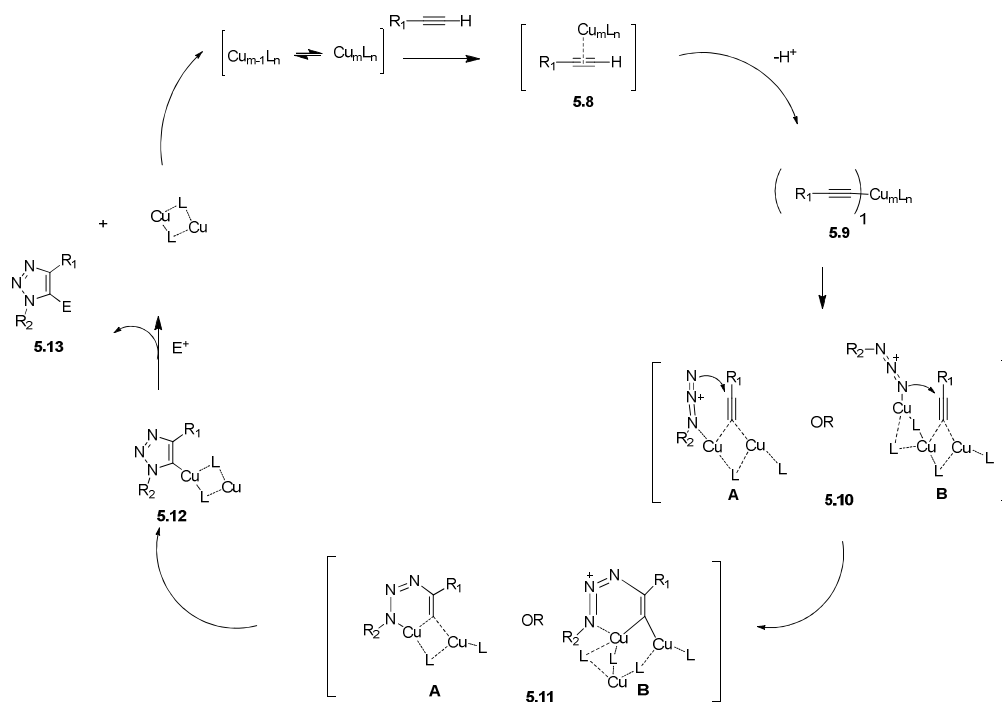
triazoles possess high chemical stability (generally inert to hydrolytic cleavage, oxidation or reduction), aromatic character and hydrogen bond accepting ability.^[233] For this reason, triazole containing molecules can serve as hydrolytically stable amide mimics, which can be exploited in the quest to synthesise biologically active KRN7000 analogues (as described in Chapter 4).

5.1.4. Mechanistic considerations of Cu(I) catalysed azide-alkyne cycloaddition

The mechanism proposed by Mendal and Tornøe^[234] for the CuAAC reaction is based on previous mechanistic studies whereby DFT calculations provided evidence for a stepwise mechanism, unlike the classical thermal cycloaddition which proceeds via a concerted mechanism.^[234] The catalytic cycle is initiated by π coordination of the terminal alkyne to a Cu(I) species to form Cu(I) acetylide complex **5.8** (Scheme 5.4). This causes the alkyne proton to be more acidic, facilitating its removal (generally under basic conditions) to form the δ -acetylide intermediate **5.9**. Mendal and Tornøe, with evidence from crystallographic structures, suggest that the acetylide carbon atom coordinates to three Cu atoms to form the Cu(I) species **5.9** (with $m=3$); however DFT calculations are needed to confirm such a hypothesis.^[234] The formation of Cu(I) species **5.9** was found to be endothermic in MeCN (0.6 kcal/mol), but exothermic in H₂O (11.7 kcal/mol).^[234] These findings were in good agreement with the literature, where it is well known CuAAC reactions proceed faster in aqueous media.^[235]

In the next step a Cu atom coordinates to the azide group as in transition states **5.10A** or **5.10B**. Kinetic studies by Rodionov and colleagues revealed that the CuAAC reaction proceeded following second order kinetics with respect to the Cu, indicating that activation of the alkyne and azide occurred by different metal centres.^[236] Structural evidence retrieved from X-ray crystallographic data and the kinetic studies described above seem to suggest that the acetylide and the azide are not necessarily bound to the same Cu atom as in **5.10A** but to two separate Cu atoms as in **5.10B**. Two possibilities for coordination and delivery of the azide to the alkyne during the transition state have been suggested (**5.10A** or **5.10B**), whereby the complexation of the azide to the Cu atom activates it towards nucleophilic

attack at the secondary carbon of the acetylide to generate the regioselective metallocene intermediates **5.11A** and **5.11B**. Experimental confirmation of this mechanistic step is given by the fact that electron-withdrawing substituted alkynes accelerate the CuAAC reaction.^[230] Ring contraction afforded by transannular association (of the nitrogen lone pair of electrons and the C(5)-Cu π^* orbital) yields the metallated triazole **5.12**. Electrophilic attack at the triazole (or protonation) yields the desired 1,2,3-triazole **5.13** and dissociation regenerates the Cu catalyst and ends the cycle.



Scheme 5.4 Outline of plausible mechanisms for the Cu(I) catalyzed reaction between organic azides and terminal alkynes.^[237]

5.2. Research objective

In this chapter, we focused our attention on the synthesis of novel macrocyclic L-serinyl glycolipid analogues of KRN7000, to probe whether they could be successfully synthesised using CuAAC reactions. The structures of the proposed macrocyclic targets **5.14** and **5.15** are presented in Figure 5.3. The idea of synthesising carbohydrate/amino acid macrocycles as KRN7000 analogues has not

been explored in the literature, to the best of our knowledge. The conformationally constrained analogues may prove to be interesting compounds for immunogenic studies. We aimed to investigate the effects that the introduction of rigidity and aromaticity on KRN7000 analogues would have on the activation of *i*NKT cells (discussed in Chapter 4), compared to KRN7000 and other acyclic analogues. The monomeric glycolipid **5.14**, containing a fused tricyclic scaffold, would serve as the most rigid antigen with only one alkyl chain for the hydrophobic groove pockets of the CD1d protein. The formation of higher order oligomers (cyclic and acyclic), is commonly observed in macrocyclization reactions.^[238] In this regard, the dimeric glycolipid **5.14** would serve as a more flexible cyclic system with two alkyl chains suitable for binding with the CD1d protein. The loading of such analogues to the CD1d protein would most likely result in an alteration in the presentation of the polar head groups to the TCR of the *i*NKT cell, which would alter the binding affinity of the ternary complex. This, in turn, may affect the subsequent cytokine release profile (as discussed in Chapter 4).

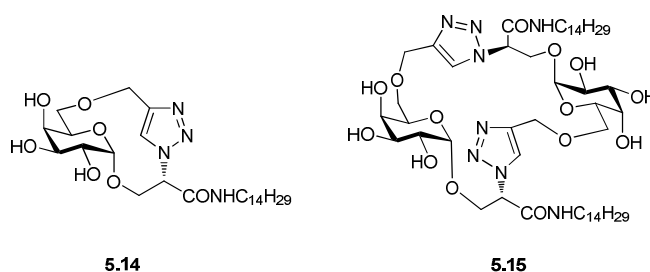


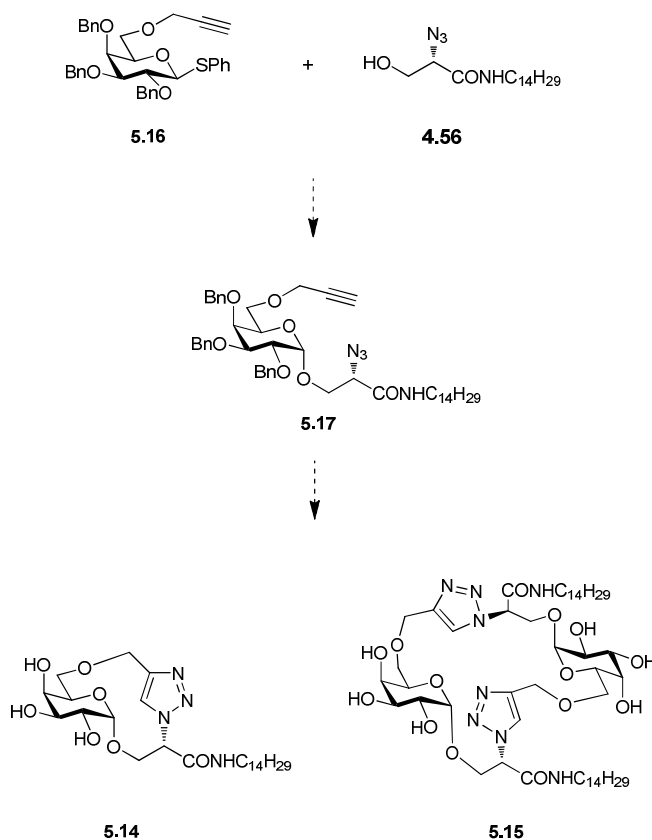
Figure 5.3 Structures of macrocyclic L-serinyl glycolipids **5.14** and **5.15** as KRN7000 analogues.

Accounting for the findings in Chapter 3, a building block for macrocycle formation leading to glycolipids **5.14** and **5.15** was selected, based on the use of a thioglycoside donor with alkyne functionalization at the C-6 position and an L-serinyl acceptor with an azide functionality. CuAAC chemistry would be utilised to form the corresponding 1,4-disubstituted 1,2,3-triazole in the macrocyclic compounds **5.14** and **5.15**, using different dilution conditions. As discussed in Chapter 4, we encountered problems in the removal of the benzyl ether protecting groups of triazole containing glycolipid **4.90**. For this reason, we were aware that

the use of a benzylated glycosyl donor such as thioglycoside **5.16** may lead to complications, upon final deprotection of the target macrocycles. However, due to their stability and compatibility with the conditions used in CuAAC, they were still employed. The ultimate aim would be to assess the ability of the macrocyclic glycolipids **5.14** and **5.15** to serve as *i*NKT cell stimulatory ligands.

5.3. Design strategy for the formation of macrocycles **5.14** and **5.15**

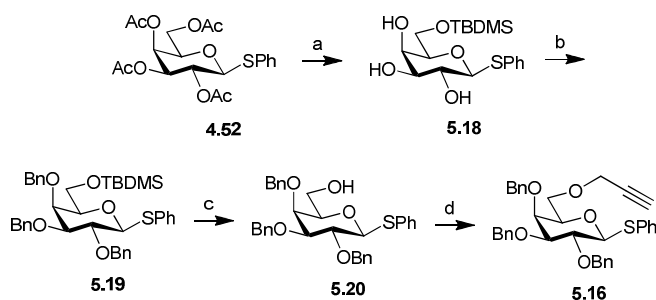
The synthetic pathway for the formation of the macrocycles **5.14** and **5.15** was designed as in Scheme 5.5. We envisaged an α -stereoselective coupling of glycosyl donor **5.16** and L-serinyl acceptor **4.56** to yield the L-serinyl galactosyl building block **5.17** containing both azide and alkyne functionalities. Subsequent CuAAC reactions under optimised conditions and global deprotection would yield the macrocycles **5.14** and **5.15** for biological evaluation.



Scheme 5.5 Proposed synthetic design of macrocyclic glycolipids **5.14** and **5.15**.

5.3.1. Synthesis of thiogalactosyl donor 5.16

The synthesis of the reported galactosyl donor **5.16**, differentially functionalised at the C-6 position, was undertaken as shown in Scheme 5.6.^[239] The synthesis began with the deacetylation of thioglycoside **4.52** (previously synthesised in Chapter 4) using Zemplén conditions to yield 81% of a crude thiogalactoside, which was reacted with TBDMSCl and NEt₃ to yield the thiogalactoside **5.18** protected at the C-6 position in a 79% yield. The use of bulky silyl protecting groups (such as TBDMSCl) is common practise in carbohydrate chemistry as they selectively react with the least hindered primary hydroxyl group at the C-6 position.^[69] A Williamson ether synthesis using NaH and BnBr was then undertaken following a literature procedure.^[240] The benzyl protected thiogalactoside **5.19** was isolated in a yield of 31%. This may be due to the hydrolysis of the TBDMS under the harshly basic (NaH) conditions.



Scheme 5.6 Reagents and conditions. a) i) cat. Na metal, MeOH, 0 °C to rt, 1.5 h, 81%; ii) Pyr, TBDMSCl, NEt₃, -10 °C to rt, 21 h, 79%; b) NaH, BnBr, DMF, 0 °C, 2 h, 31 %; c) TBAF, THF, 0 °C to rt, 6 h, 94%; d) NaH, TBAI, propargyl bromide, THF, 0 °C to rt, 18 h, 47%.

Deprotection of the bulky silyl ether (TBDMS) of galactoside **5.19** by treatment with TBAF was undertaken, following a literature procedure, to yield thioglycoside **5.19**.^[241] Nucleophilic attack of the small fluoride anion (in TBAF) leads to formation of a pentavalent silicon centre due to hybridisation with the vacant d-orbitals of silicon. In addition, the formation of the strong Si-F bond is the driving force for a fast cleavage. Treatment of the free hydroxyl group at the C-6 position of the thiogalactoside **5.20** with propargyl bromide using NaH and TBAI afforded 47% of the desired alkyne functionalised thiogalactoside **5.16** in a Finkelstein-Williamson

ether hybrid reaction. A Finkelstein reaction is an S_N2 reaction that involves the exchange of one halogen atom for another.^[242] Halide exchange is an equilibrium reaction (previously met in Chapter 4), and the reaction can be driven to completion by different solubilities of halide salts, or large excesses of halide salts. In our case, the exchange of BnBr with TBAI results in BnI and TBAB. The TBAB is not soluble in THF and in turn drives the Williamson ether reaction to completion to give the thiogalactoside **5.16**.

Structural elucidation was performed on the thiogalactoside **5.16**. Although it is a known compound,^[239] no experimental data or synthesis was provided by the authors. ^1H NMR, ^{13}C NMR, 2D NMR experiments (COSY and HSQC), IR and HR-MS were utilized to confirm the structure of the galactosyl donor **5.16**. A diagnostic stretch appears in the IR spectrum for galactosyl donor **5.16**, with the terminal alkyne C-H stretch appearing at 3287.6 cm^{-1} . This band is not present in the precursor thiogalactoside **5.20**. The ^1H NMR spectrum is presented in Figure 5.4 and characteristic signals are highlighted. Although the region of the ^1H NMR where the signal corresponding to the anomeric proton is obscured with other signals corresponding to the methylene protons of the benzyl ether protecting groups, HSQC directly correlates the signal corresponding to the anomeric carbon (87.7 ppm) to a signal in this proton overlap as shown in Figure 5.5. From analysis of the COSY spectrum (Figure 5.6), a signal in this region (4.5 to 5 ppm) directly correlates to a signal appearing at 4 ppm corresponding to H-2. These observations correlate well with the HSQC data acquired. Thus, by the chemical shift and direct coupling observed in both the HSQC and COSY spectra, we can highlight the anomeric proton and from the same method elucidate the other ring protons. The characteristic signals for the propargyl functional appear at 4.1 ppm. The benzylic protons appear at 4.1 ppm and the proton corresponding to the alkyne is present at 2.5 ppm. IR, ^{13}C NMR and HR-MS were in agreement with the ^1H NMR data obtained.

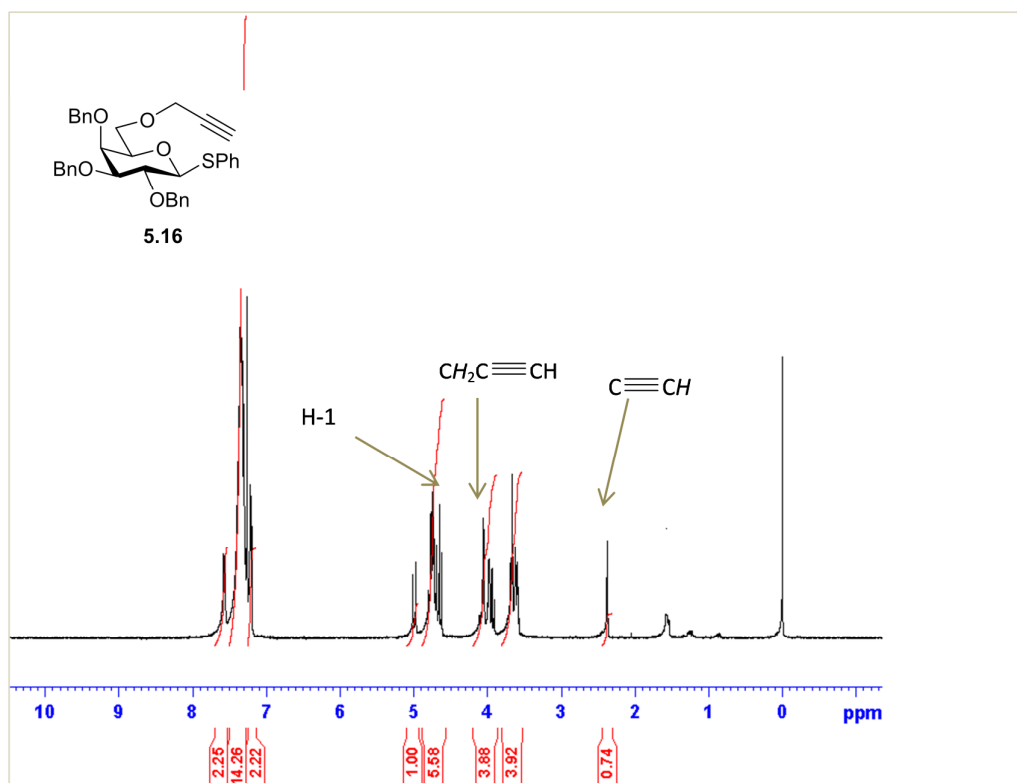


Figure 5.4 ^1H NMR spectrum of thiogalactoside **5.16**. Characteristic signals are highlighted.

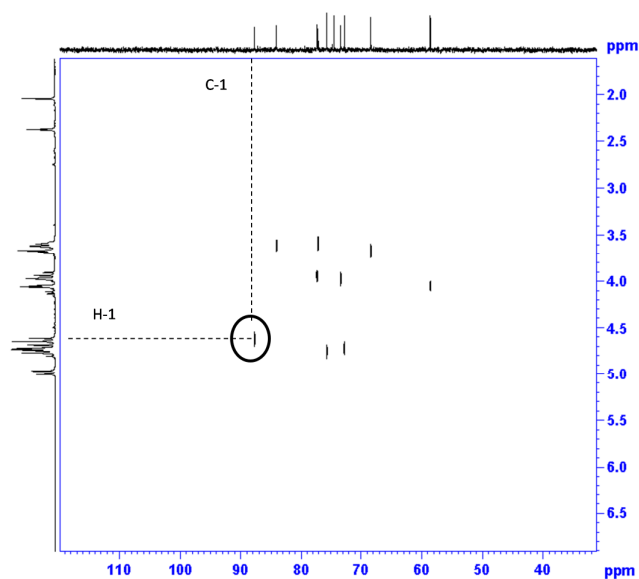


Figure 5.5 Zoom in of 2D HSQC experiment for thiogalactoside **5.16**. Direct coupling of signal corresponding to anomeric carbon to anomeric proton shown inset as a representative example.

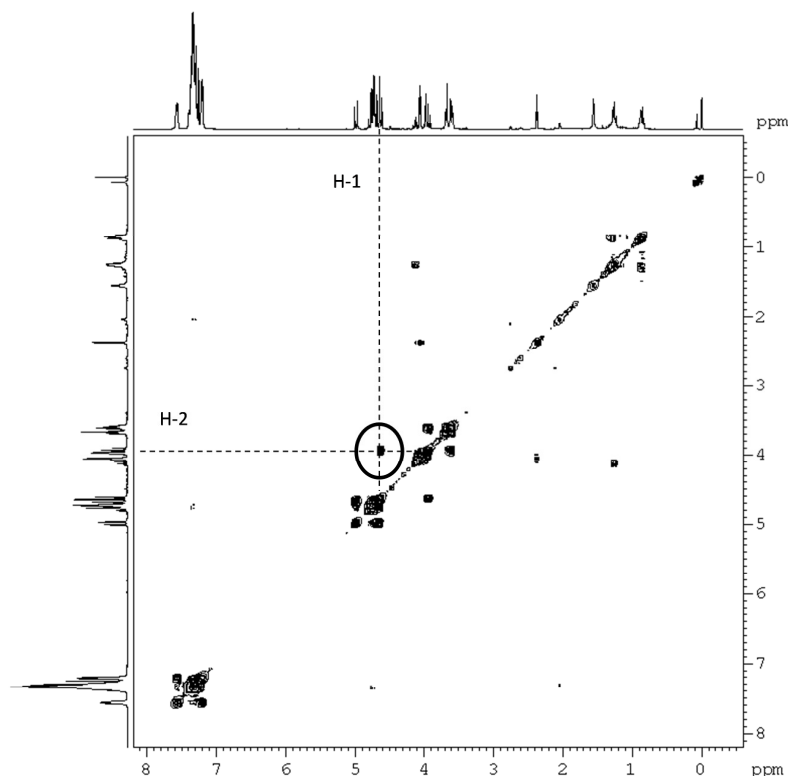
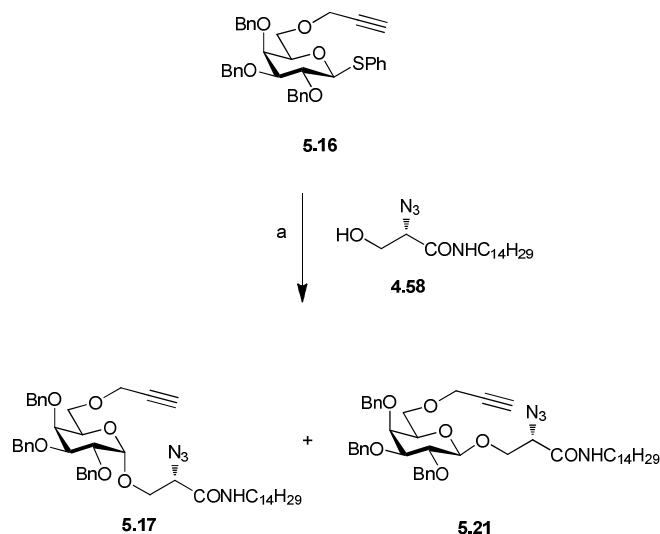


Figure 5.6 2D COSY experiment for thiogalactoside **5.16**. Direct coupling of signal corresponding to anomeric carbon to H-2 shown inset as a representative example.

5.3.2. Synthesis of bifunctional galactosyl building block **5.17**

The glycosylation of the galactosyl donor **5.16** with the L-serinyl acceptor **4.58** (prepared as described in Chapter 4) was performed using NIS and TfOH as a promoter system, at rt and in THF as a solvent (Scheme 5.7). After 18 h, the crude reaction mixture consisted of a mixture of diastereoisomers in a 2.3:1 ratio (α : β), which led to the desired α -anomer **5.17** in 16% isolated yield and the β -anomer **5.21** in 5% isolated yield. No further optimisation was performed in order to improve the stereoselectivity obtained in the reaction. It is noteworthy that a similar stereoselectivity was obtained in the glycosylation reaction of the fully benzylated thioglycoside **4.54** and the L-serinyl azide derivative **4.58** (α / β ratio of 2.7:1, as discussed in Chapter 4).



Scheme 5.7 Reagents and conditions a) NIS, TfOH, 4Å MS, THF, rt, 18 h, α/β (2.3: 1), **5.17** (16%) and **5.21** (5%).

Structural characterisation was carried out on the novel α -anomer **5.17** and the ^1H NMR spectrum is shown in Figure 5.7. The characteristic signals are highlighted: the amide proton (at 6.6 ppm), the anomeric proton (under the overlapping signals at 4.6-4.9 ppm), the alkyne proton (at 2.4 ppm) and the methylene protons (at 1.2 ppm). Assignment was performed with the aid of 2D NMR. As in the previous case, the anomeric proton resonance was obscured by the methylene protons of the benzyl ethers. ^{13}C NMR, IR, HR-MS and specific optical rotations were also performed on the novel glycoside **5.17**, which features both azide and alkyne functionality. The IR spectrum showed the disappearance of the S-C stretch (3030 cm^{-1}) found in the precursor C-6 functionalised thioglycoside **5.16**, and it now displayed characteristic stretches for alkyne and azide functionalities at 3777 and 2103 cm^{-1} respectively. The ^{13}C NMR showed a shift in the anomeric carbon atom from 87.7 ppm (in the precursor thioglycoside **5.16**) to 98.8 ppm (in the building block **5.17**).

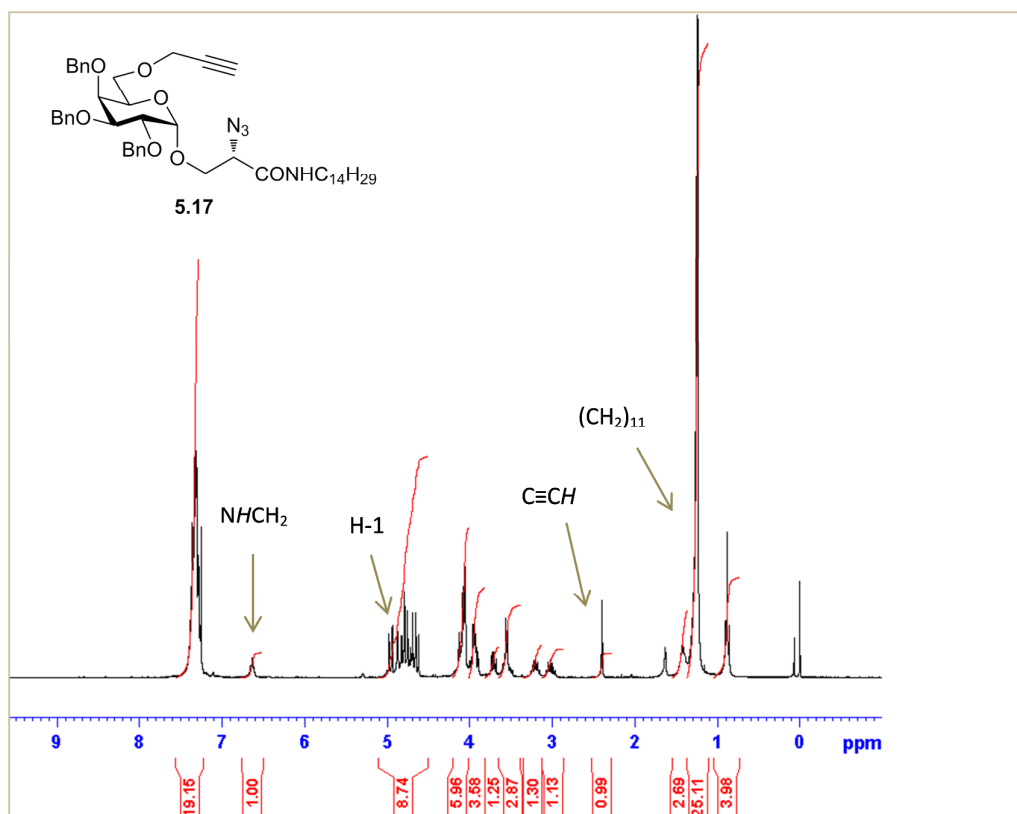


Figure 5.7 ^1H NMR spectrum of glycolipid **5.17**. Characteristic signals are highlighted.

Structural characterisation was performed on the β -anomer **5.21** and the ^1H NMR spectrum is shown in Figure 5.8. In the ^1H NMR spectrum some distinctive differences are observed compared to the spectrum of the α -anomer **5.17**. The signal corresponding to the anomeric proton resonates at a lower chemical shift value of 4.43 ppm and with a larger coupling constant of 7.8 Hz compared to the anomeric proton of the α -anomer **5.17**. Also, the signal for the methylene protons adjacent to the amide bond appear as a multiplet (at 3.1 ppm) in the β -anomer **5.21** compared to two sets of dd (at 3.0 and 3.2 ppm) in the case of the α -anomer **5.17**. This suggests that these methylene protons are in a similar chemical environment, in contrast to those of the α -anomer **5.17**. In the ^{13}C NMR spectrum, the β -anomeric carbon atom resonates at a higher chemical shift (104.0 ppm) relative to its α -anomer **5.17**. The corresponding IR spectrum of glycoside **5.21** was similar to the one of the α -anomer **5.17**.

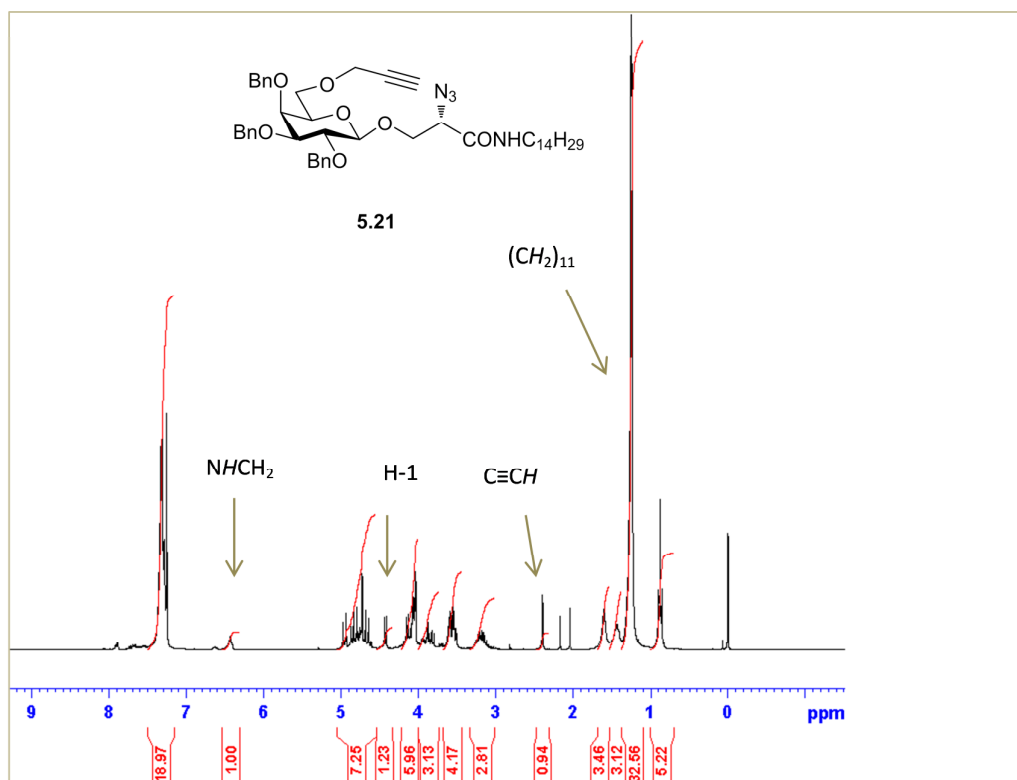


Figure 5.8 ^1H NMR spectrum of glycolipid **5.21**. Characteristic signals are highlighted.

5.3.3. Design Considerations of macrocycles **5.14** and **5.15**

If we consider the CuAAC reaction of the glycolipid building block **5.17**, various different possible products can be obtained indicating the difficulties and challenges associated with this particular reaction. One possible scenario involves the reaction of one azide functional group of the glycolipid **5.17** reacting with an alkyne group from another molecule of glycolipid **5.17** to form the dimeric molecule **5.22** (Figure 5.9). By the same vein, the free alkyne on the dimer **5.22** can react with another molecule of glycolipid **5.17** and form a trimeric molecule **5.23**. This reaction can proceed in a polymeric fashion and yield various different acyclic oligomers. Alternatively, the azide and alkyne moieties on the glycolipid building block **5.17** can react intramolecularly to form the corresponding fused tricyclic monomeric macrocycle **5.24**. Similarly, an intramolecular reaction can proceed between the azide and alkyne of the dimeric glycolipid **5.22** to form the corresponding dimeric

macrocycle **5.25**. In a similar manner the trimeric macrocycle **5.26** could be formed. In principle, various different sized macrocycles could be formed.

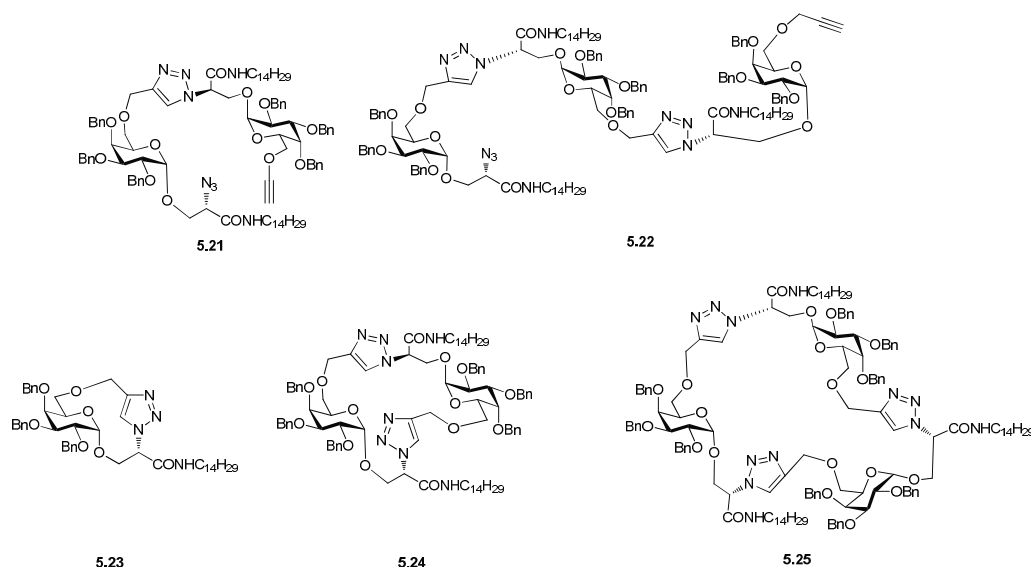


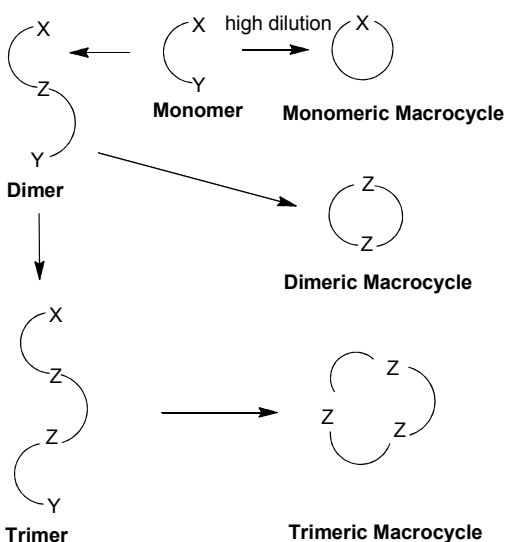
Figure 5.9 Structure of possible products from CuAAC of glycolipid **5.17** to give acyclic products **5.22** and **5.23** and macrocycles **5.24**, **5.25** and **5.26**.

Being aware of the possible formation of a mixture of products using the CuAAC reaction, we conducted the reaction under different conditions to investigate the effect that parameters such as concentration, temperature and the catalyst would have on the reaction outcome. One technique commonly employed in macrocyclic chemistry to obtain cyclisation products is a high dilution approach.^[243] High dilution involves using small quantities of reactants in large volumes of solvent. By using high dilution conditions, we could increase the probability to form macrocyclic products and minimise the formation of acyclic higher order oligomers, as shown in Scheme 5.8.

The rationale for the use of high dilution conditions in a CuAAC macrocyclisation is that, in dilute solutions the formation of the cyclic product by an intramolecular reaction is thermodynamically favoured. Thermodynamic factors are governed by the Gibbs-Helmholtz equation (Equation 5.1).

$$\Delta G = \Delta H - T\Delta S$$

Equation 5.1 Gibbs-Helmholtz equation where ΔG = change in gibbs free energy, ΔH = change in enthalpy, T = absolute temperature, ΔS = change in entropy.



Scheme 5.8 Formation of monomeric, dimeric and trimeric macrocycles.

If $\Delta G < 0$, then the reaction is favoured thermodynamically (as it is spontaneous). Thermodynamically favoured reactions depend on temperature, enthalpy and entropy changes. A reaction is entropically favoured if i) n precursor molecules are converted to $2n$ products, or ii) the number of degrees of freedom are increased in a system.^[244] The former point is not applicable in the case of an intramolecular CuAAC reaction as n molecules lead to n molecules. The latter is of special relevance under high dilution conditions. The entropy of a system is dependent on concentration changes because translational mobility increases with decreased viscosity.^[245] This is the case for high dilution conditions and thus renders the reaction entropically favoured. A minor entropic contributor is also the probability of encounter between reactive end groups in the same molecule, whereby the reaction is more likely and hence faster than the competing products resulting from intermolecular cycloadditions. The entropic effects can sometimes be offset by enthalpic effects, caused predominantly by ring strain in cyclisation reactions. Thus,

the importance of temperatures, entropic effects and enthalpic effects in creating a thermodynamic bias is central to the success of an intramolecular CuAAC reaction. Kinetic factors also influence the intramolecular cyclisation reaction, whereby the formation of the unimolecular cyclised product is favoured compared to the bimolecular oligomers. Another consideration is the choice of Cu source in the CuAAC reaction to encourage selective formation of either the monomer **5.24** or dimer **5.25**.

5.3.4. Synthesis of products possibly containing macrocycles 5.24 and 5.25

Initial investigations led us to execute the previously described CuSO₄ and sodium ascorbate methodology (discussed in Chapter 4). We hoped to minimize oligomerisation/polymerisation reactions by using high dilution conditions, so as to encourage the formation of smaller macrocycles. A 10% loading of CuSO₄·5H₂O, followed by a 20% loading of sodium ascorbate was added to a dilute solution (8.5 mM) of the precursor building block **5.17** in a homogeneous system (THF: H₂O: MeOH, 2:1:2). The reaction was analysed by TLC. After 18 h at rt, the reaction was not finished and CuSO₄·5H₂O and sodium ascorbate (same concentration as previously) was again added to the reaction mixture and the reaction was heated at 45 °C. TLC analysis showed consumption of the starting material **5.16** after 3 h.

After work up, the crude reaction mixture was analysed by ¹H NMR spectrometry (Figure 5.10). It displays a broad spectrum, indicative of macrocyclic formation. Most promisingly was the disappearance of the alkyne functionality of the precursor **5.17** (as highlighted in Figure 5.8), and the concomitant presence of a broad signal at 7.8-8.1 ppm, presumably corresponding to one or more triazole protons. Disappearance of the signal corresponding to the amide proton of building block **5.17**, and the appearance of a signal/s at 5.3 ppm indicated the formation of a new product. It was difficult to unambiguously conclude from the ¹H NMR spectrum whether a mixture of macrocyclic products were present, however the broad signal at 5.3 ppm and the multiple signals at 7.8-8.1 ppm certainly points towards the formation of a mixture of products. A signal resonating at 2.0 ppm, possibly

representative of an alkyne proton is indicative that a certain amount of undesired straight chain oligomers are present such as **5.22** and **5.23** (Figure 5.9).

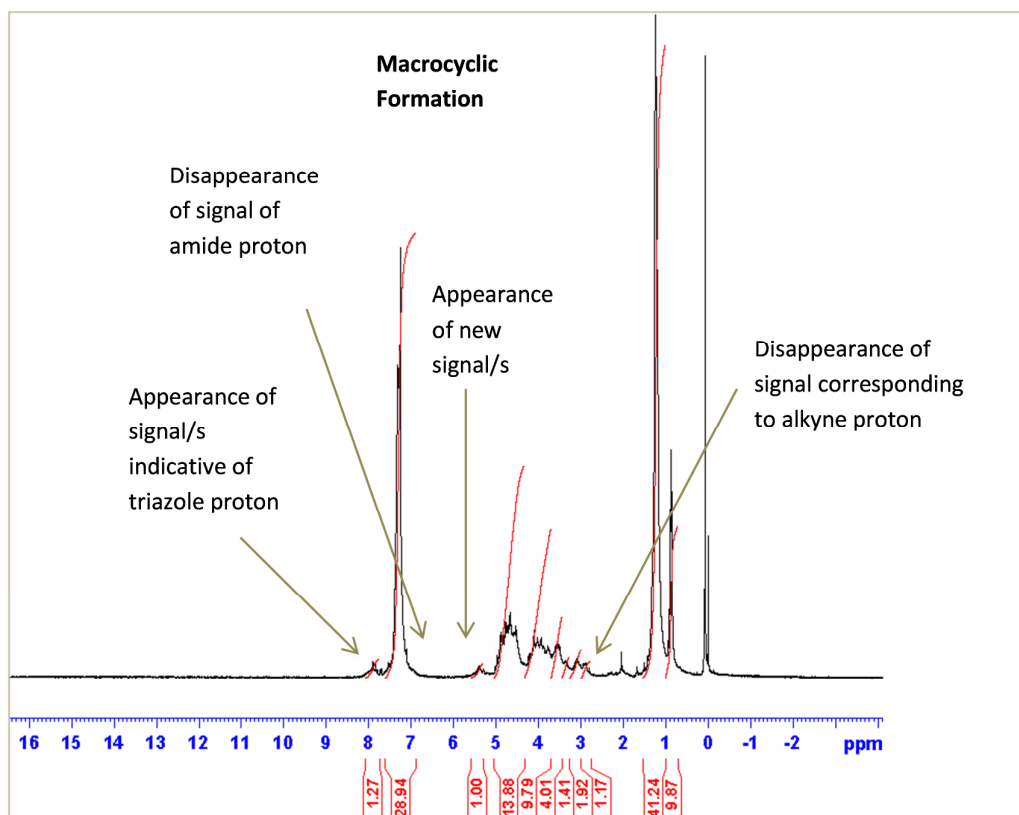


Figure 5.10 ^1H NMR spectrum of the crude reaction mixture of CuAAC intramolecular reaction under high dilution conditions.

TLC analysis of the reaction mixture did confirm the presence of two distinct compounds of similar R_f values (0.5-0.6 in PetEt:EtOAc 3:1), along with a very strongly UV absorbing baseline spot, that were clearly different in polarity to the starting material **5.17** (R_f value of 0.27 in PetEt:EtOAc 3:1). IR analysis of the crude reaction mixture gave little information on the macrocyclic formation (Figure 5.11). The disappearance of an azide signal (approx. 2100 cm^{-1}) in an IR spectrum has been used as an indicator of a success of various CuAAC reactions in the literature.^[246] However in the case of the reaction mixture, a signal is still present at 2033 cm^{-1} . This is not necessarily an indication of unreacted starting material as alkyne, azides and 1,2,3-triazole functionalities can all appear in this region. It may

also appear due to the straight chain oligomer products that may be present in the reaction mixture containing azide functionalities.

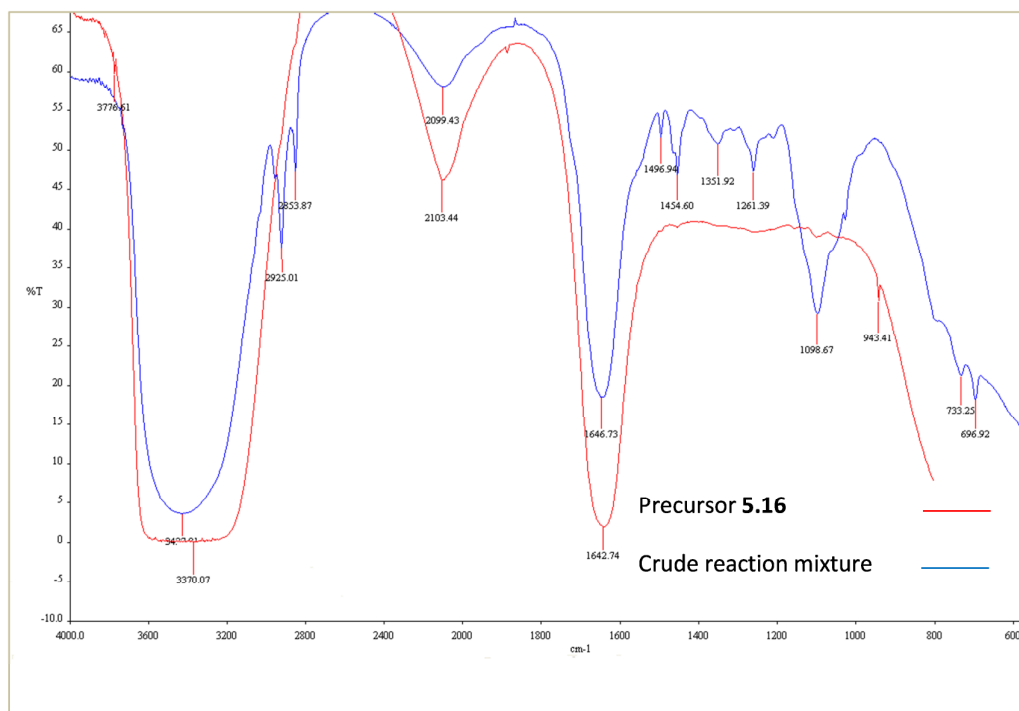


Figure 5.11 Comparison of the IR spectra of starting material **5.17** and the crude reaction mixture. The precursor **5.17** is shown in red and the crude reaction mixture is shown in blue.

The HR-MS mass spectrum for the CuAAC reaction mixture was recorded. Theoretically, the formation of the monomeric macrocycle **5.24** from the precursor **5.17** would have no loss/gain of atoms and thus would exhibit the same m/z signal in the ESI spectrum, making it difficult to discern whether the reaction had proceeded to completion by mass analysis. However, from the ^1H NMR data, we can assume that the precursor **5.17** was consumed in the reaction. The formation of the dimer macrocycle **5.25** and higher order macrocycles (or the straight chain oligomers) could be distinguished based on isotope pattern distributions in the Total Ion Chromatogram (TIC) of the HR-MS mass analyser.

The isotope distribution pattern of a compound (analysed by mass spectrometry) gives characteristic information about the molecule of interest. This is commonly utilised by chemists to aid in the structural elucidation of halogenated compounds,

macromolecules, peptides and proteins and unknown compounds.^[247] Each peak in the TIC corresponding to a distinct structural species will have a unique and characteristic isotopic pattern distribution. These are not to be mistaken with the peaks due to oligomerization of the sample (2M+1 or 3M+1) that may occur within the ionisation chamber of the electron spray. In our case, we were interested in the natural abundance of ^{13}C isotope in carbon containing molecules (the possible macrocycles), whereby the ^{13}C isotope generates a distinct m/z signal relative to the ^{12}C m/z signal. A naturally occurring $^{12}\text{C}/^{13}\text{C}$ ratio (98.89 % ^{12}C , 1.11 % ^{13}C) allowed us to monitor the amount of ^{13}C isotope present in our potential macrocycles compared to the ^{12}C isotope. This, in turn allowed us to differentiate between the monomer macrocycle **5.24**, dimer **5.25** and trimer **5.26** (or the corresponding straight chain oligomers) since they contain different amounts of naturally occurring ^{13}C isotopes and as a result different isotope patterns. Differentiation between the macrocycles and the acyclic compounds would not be discerned by this method.

In the TIC, two major isotopic clusters were detected, with base peaks at m/z 797 and m/z 1616. A minor isotopic cluster was also detected with a base peak at m/z 2391. These peaks possibly corresponded to the protonated monomer **5.24**, protonated dimer **5.25** and molecular trimer **5.26** respectively. It is also possible that they may correspond to the straight chain oligomers. However it is more likely to be the macrocycles due to the broad NMR spectrum (indicative of strained macrocycles). The isotopic distribution pattern of the possible protonated monomer **5.25** and the theoretical isotope pattern based on its elemental formula are depicted in Figure 5.12. The protonated monomeric macrocycle **5.24** (or corresponding straight chain oligomer) shows a unique isotope distribution pattern consistent with the theoretical pattern in the inset. In analysing the isotope pattern of the protonated macrocyclic compound **5.24** (or the corresponding straight chain oligomer) with an empirical formula of $\text{C}_{47}\text{H}_{65}\text{N}_4\text{O}_7$, the base peak at m/z 797 has the major abundance compared to the protonated ^{13}C isotope at m/z 798 in the isotope distribution pattern, as expected (Figure 5.12).

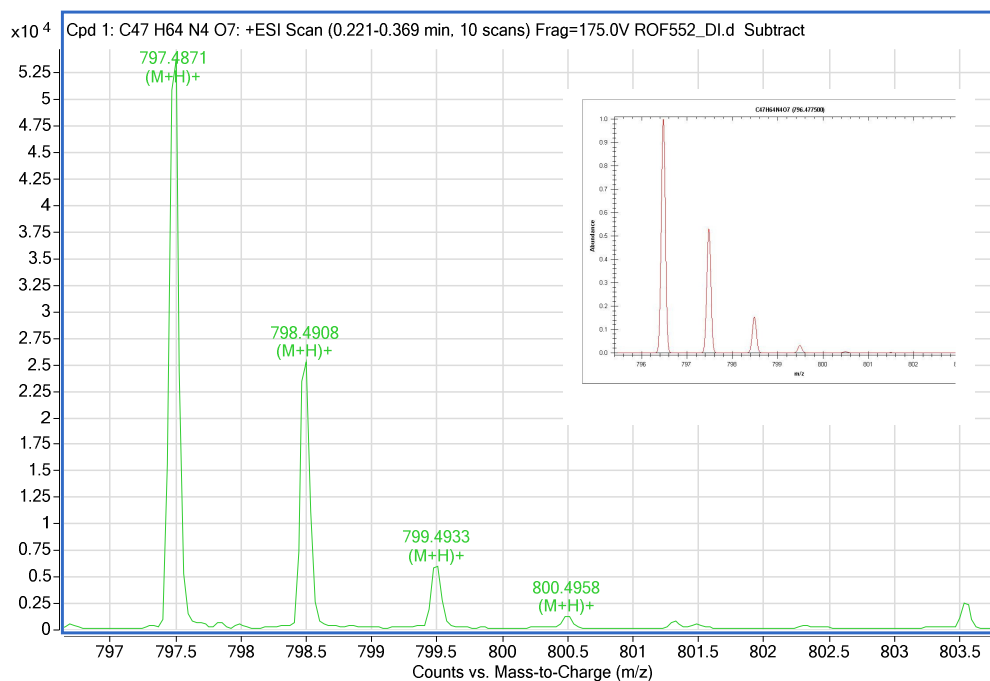


Figure 5.12 Isotope distribution pattern of the protonated monomer **5.24** (or corresponding straight chain oligomer), and the theoretical isotope pattern based on the elemental formula (inset).

The isotope pattern of the protonated dimer **5.25** (or corresponding straight chain dimer) and the theoretical isotope pattern based on the elemental formula are depicted in Figure 5.13. As in the previous example, the data are in good agreement. A different scenario (compared to the proposed monomer **5.24**) arises when analysing the isotope pattern of the potential protonated dimer **5.25**, with an empirical formula of $C_{94}H_{128}N_8O_{14}$ (Figure 5.13). Now the mass spectral peak representing the protonated monoisotopic mass of **5.25** (or corresponding straight chain dimer) is not the most abundant peak in the spectrum. Statistically there should be roughly one ^{13}C atom in the compound and this is observed with a base peak of m/z 1595. It is now the most abundant ion, as expected in the theoretical isotope pattern distribution (Figure 5.13, inset). This isotope pattern is only characteristic of the dimer **5.25** (or the corresponding straight chain dimer) formed in the cycloaddition, and not as a result of ionisation of a different species occurring in the chamber.

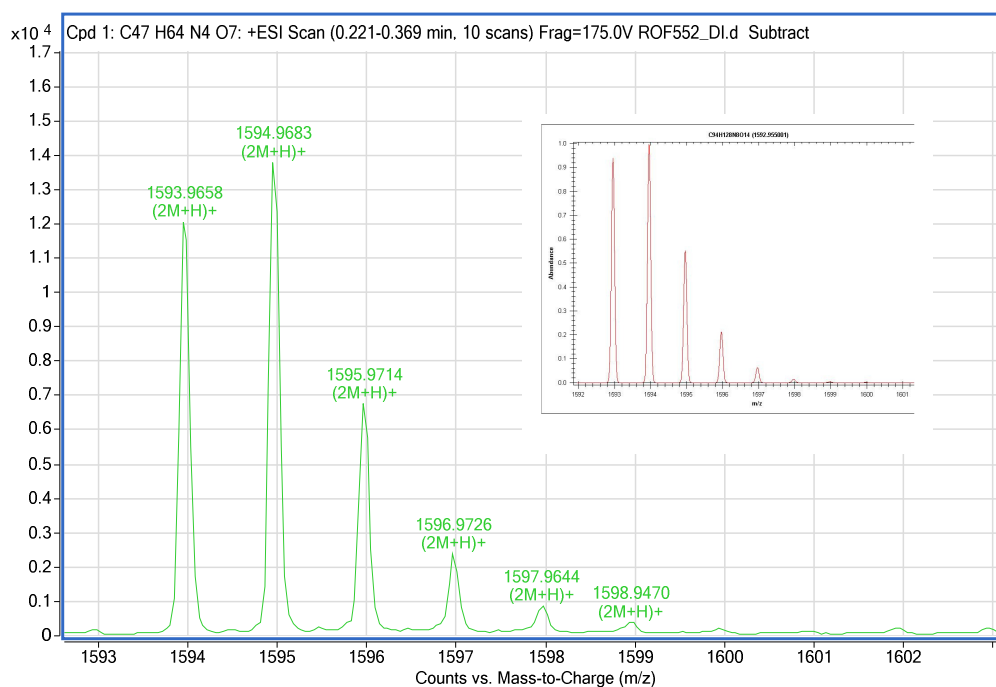


Figure 5.13 Isotope distribution pattern of the protonated dimer **5.25** (or corresponding straight chain dimer), and the theoretical isotope pattern based on the elemental formula (inset).

Similarly to the proposed dimeric macrocycle, the molecular ion for trimer **5.26** (or the corresponding straight chain trimer) displays an isotope distribution pattern characteristic of the empirical formula, $C_{141}H_{192}N_{12}O_{21}$ as predicted in the theoretical isotope pattern (Figure 5.14). Therefore, we suggest that the reaction mixture contains the monomer **5.24**, dimer **5.25** and the trimer **5.26** macrocycles and not the ionised products generated by the ionisation technique. It is also possible that the corresponding straight chain oligomers are responsible for the isotope distribution patterns.

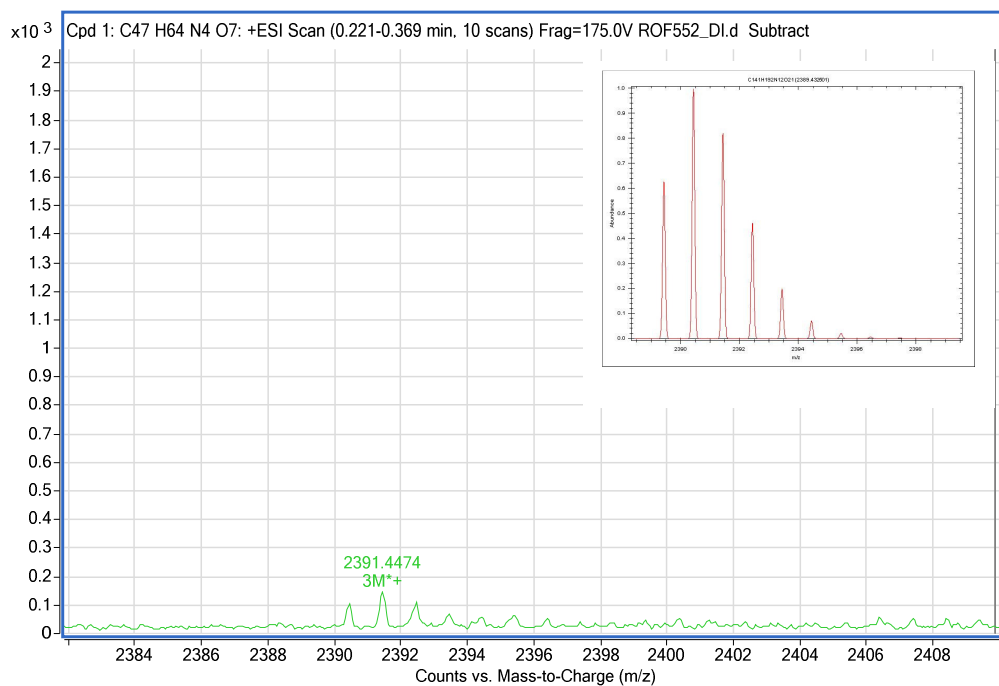


Figure 5.14 Isotope distribution pattern of the molecular trimer **5.26** (or the corresponding straight chain trimer), and the theoretical isotope pattern based on the elemental formula (inset).

To test whether different reaction conditions could result in the selective formation of either the fused monomeric macrocycle **5.24** or the dimeric macrocycle **5.25** (over oligomerisation reactions), we explored the use of different solvent concentrations, temperatures and different sources of Cu (I) in the CuAAC reaction at a 0.05 mmol scale. A summary of the findings are presented in Table 5.1. It seemed that macrocyclic formation occurred under high dilution conditions of 8.5 mM (Entries 1 and 3 in Table 5.1) but did not proceed in higher dilution conditions of 0.85 mM (Entries 2 and 4 in Table 5.1). Furthermore, it seemed, independently of the source of Cu(I) used, (CuSO₄ or CuI, Entries 1 and 3 in Table 5.1) the desired macrocycles **5.24** or **5.25** could not be obtained selectively, if in fact they were formed at all. Instead, both reactions resulted in mixtures of compounds, indicated by ¹H NMR spectroscopy and TLC analysis. It seemed that the reaction utilising CuSO₄ was a superior choice. In the reactions carried out using CuI, smaller amounts of product suggested to be the macrocycles (33% w/w) could be isolated compared to the CuSO₄ method (83% w/w).

Table 5.1 Optimisation conditions altering reaction concentrations and source of Cu(I) for CuAAC reaction.

	Solvent Ratio	Solvent Concentration	Time	Temperature	Cu(I) Source*	Additives [‡]	Possible macrocyclic Formation**
1	THF: MeOH: H ₂ O (2:2:1)	8.5 mM	23 h	rt to 45°C	CuSO ₄ ·5H ₂ O	Na ascorbate	Yes (88% w/w)
2	THF: MeOH: H ₂ O (2:2:1)	0.85 mM	23 h	rt to 45°C	CuSO ₄ ·5H ₂ O	Na ascorbate	No
3	THF	8.5 mM	20 h	rt	CuI	DIPEA	Yes (33% w/w)
4	THF	0.85 mM	20 h	rt	CuI	DIPEA	No

* 0.1 equiv of CuSO₄·5H₂O and 0.2 equiv of CuI; ‡ 0.2 equiv of sodium ascorbate and 2 equiv of DIPEA; ** Possible macrocyclic formation indicated by ¹H NMR spectroscopy.

The CuAAC reaction utilising CuSO₄·5H₂O and sodium ascorbate at 8.5 mmol was repeated on a larger scale (0.1 mmol). A similar ¹H NMR spectrum of the crude was recorded as in the smaller scale reaction (Figure 5.10). Flash chromatography was performed to separate polar products (an R_f value of 0.5 in 3:1 PetEt/EtOAc) possibly corresponding to the straight chain oligomers, and also to purify and separate the possible macrocycles (baseline spot in 3:1 PetEt/EtOAc mixture). The more polar products, the proposed straight chain oligomers were successfully separated from the baseline product, the proposed macrocycles. However, they were present in small quantities (20% w/w), and as a result, were difficult to characterise by ¹H NMR spectrometry. Also mixtures of the acyclic dimer **5.22**, trimer **5.23** and other potential linear oligomers would complicate the spectrum. However, the clear sharp signals observed suggested that these were not macrocyclic compounds. The ¹H NMR spectrum of the mixture of possible acyclic oligomers is presented in Figure 5.15. Various resonances for alkyne protons in the region of 2-3 ppm suggest that the dimer **5.22** and extended oligomers were

possibly formed. A ^{15}N HSQC experiment indicated N-H coupling of amide protons in the region of 6-7 ppm characteristic for these compounds, with at least 4 different couplings observed. Also, the distinctive triazole protons at 8.1 ppm were evident in the spectrum. HR-MS confirmed a m/z ratio corresponding to the empirical formula of the dimer **5.22**.

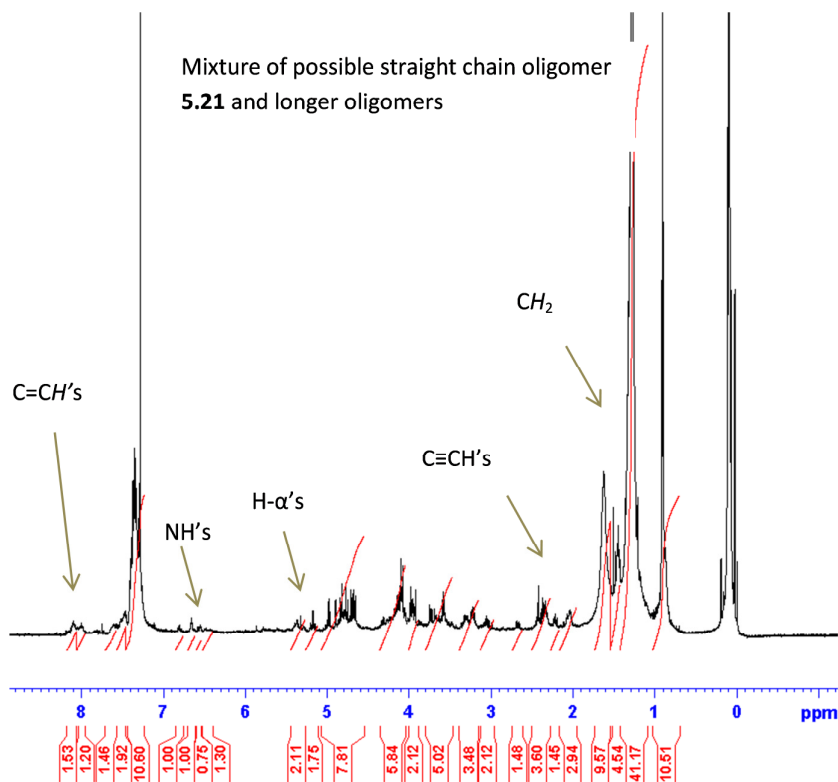


Figure 5.15 ^1H NMR spectrum of potential acyclic oligomers containing **5.22**. Characteristic signals are highlighted.

The individual compound, proposed to be macrocycles **5.24-5.26** could not be separated from one another using flash chromatography. Precipitation and recrystallization was also attempted with no success. Preparative Reverse Phase High Performance Liquid Chromatography (RP-HPLC) was performed to identify and separate the relatively polar suggested products **5.24-5.26**. A number of conditions were investigated, using isocratic or gradient based mobile phases, but no separation could be achieved. This was due to the precipitation of the proposed macrocycles with the introduction of H_2O in the mobile phase. It was evident that a major product elutes at 7 min, using 100% MeOH as the mobile phase. Mass analysis identified a m/z ratio indicative of the monomeric macrocycle **5.24**, but the

other possible macrocycles **5.25** and **5.26** were not identified. This was presumably due to the small quantities of sample recovered in the HPLC run for analysis. A minor product eluting at 5 min was an impurity present in the MeOH, as the HPLC chromatogram for MeOH alone displayed a similar peak at this retention time. Interestingly, using a gradient system of H₂O/MeOH to purify the proposed macrocycles resulted in no improvement in the resolution of the peaks. A solvent system of 100% H₂O (5 min) to a gradient system of 100% H₂O to 100 MeOH (over 10 min) to 100% MeOH was utilised. The proposed macrocyclic compounds only eluted when 100% MeOH was used and after 7 min, precisely as in the previous HPLC isocratic run. This demonstrated that the proposed macrocycles were water insoluble, even in H₂O/MeOH mixtures. Thus we concluded that Preparative Reverse Phase HPLC was not a suitable method for separation of proposed macrocycles **5.24-5.26**.

5.3.5. Elucidation of proposed macrocyclic mixture containing macrocycles 5.24, 5.25 and 5.26

Unable to separate and isolate the proposed macrocyclic mixture of **5.24** and **5.25**, we performed an array of NMR spectroscopic experiments in an attempt to assign and confirm the presence of these macrocyclic compounds. We also wanted to determine precisely the ratio of the proposed macrocyclic compounds if possible, despite the difficulties anticipated due to the broad ¹H NMR spectrum. A ¹⁵N HSQC experiment illustrated nitrogen-carbon couplings diagnostic of three different amide regions.

A small coupling was observed at 6.8 ppm, a larger coupling at 7 ppm and 2 adjacent couplings resonating at 7.5 ppm. We propose that two adjacent couplings at 7.5 ppm are indicative of the dimeric macrocycle **5.25**, with two amide bonds presumably in a similar chemical environment to one another resonating at a similar chemical shift. A signal at 7 ppm is most likely representative of the fused monomeric macrocycle **5.24** with a strong nitrogen-carbon coupling while the weak coupling at 6.8 ppm could represent one of the amide bonds of the trimeric

macrocycle **5.26**. Assignment of the proton signals of the reaction mixture was performed with the aid of COSY and selective TOCSY experiments and the ^1H NMR spectrum is shown in Figure 5.16. The H- α proton which resonates at a chemical shift of 5.5 ppm was coupled to a signal at 4 ppm, characteristic of the H- β protons, as indicated by a selective TOCSY experiment. In a separate selective TOCSY experiment, upon irradiation at 1.5 ppm, the amide protons at 7.0 ppm coupled to the NHCH₂ methylene protons at 3 ppm, which coupled to the methylene protons of the long chain at 1.2 ppm. Another TOCSY irradiated at 1.2 ppm showed coupling of these methylene protons to the terminal methyl group at 0.9 ppm. A selective ROESY irradiated at 8 ppm, the signal corresponding to the triazole proton, was performed in order to obtain insight into the structural conformation of these proposed macrocycles. Unsurprisingly, the triazole proton was found to be in close proximity to the aromatic benzyl ethers, with no other through space couplings observed.

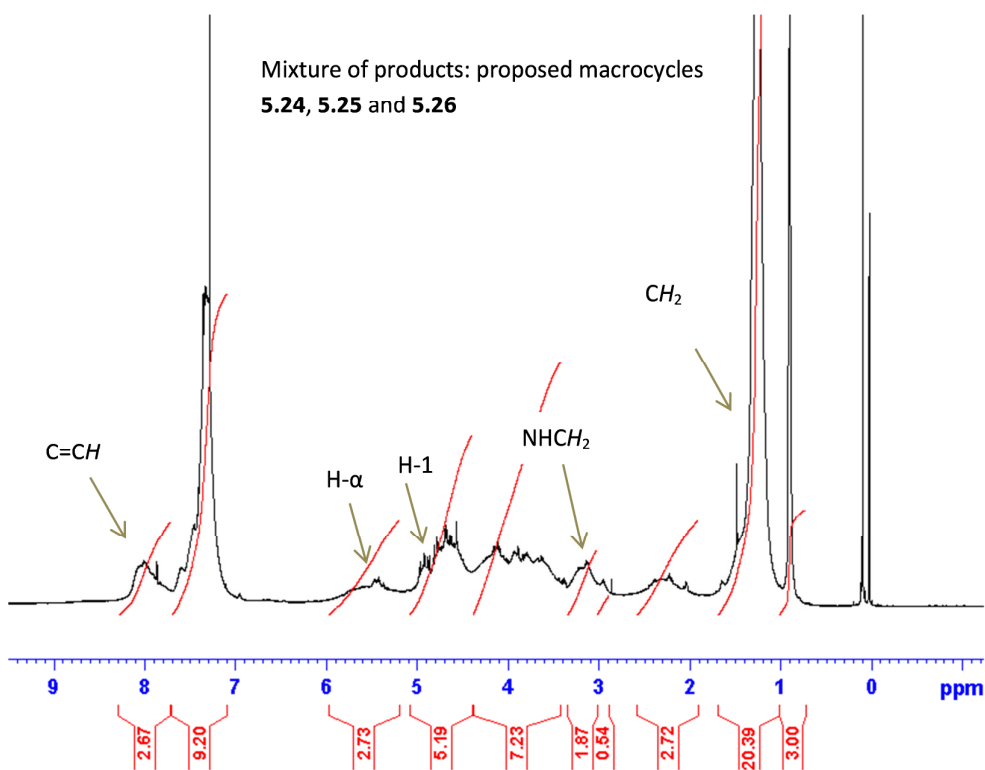


Figure 5.16 ^1H NMR spectrum of proposed macrocyclic mixture containing **5.24-5.26**. Characteristic signals are highlighted.

With regards to the ^{13}C NMR data extracted, poor spectral resolution was achieved and it is shown in Figure 5.17. Only methylene carbon atoms of hydrocarbon chains, a peak corresponding to a sugar carbon atom and aromatic carbons are identifiable. In an attempt to increase the sensitivity and resolution in the NMR experiment perdeuteration was performed on the proposed macrocyclic mixture as it is known that incorporation of ^2H into non-exchangeable positions in a molecule decreases the rate of ^{13}C T_2 relaxation and thus can increase the sensitivity and resolution in multidimensional NMR experiments.^[248]

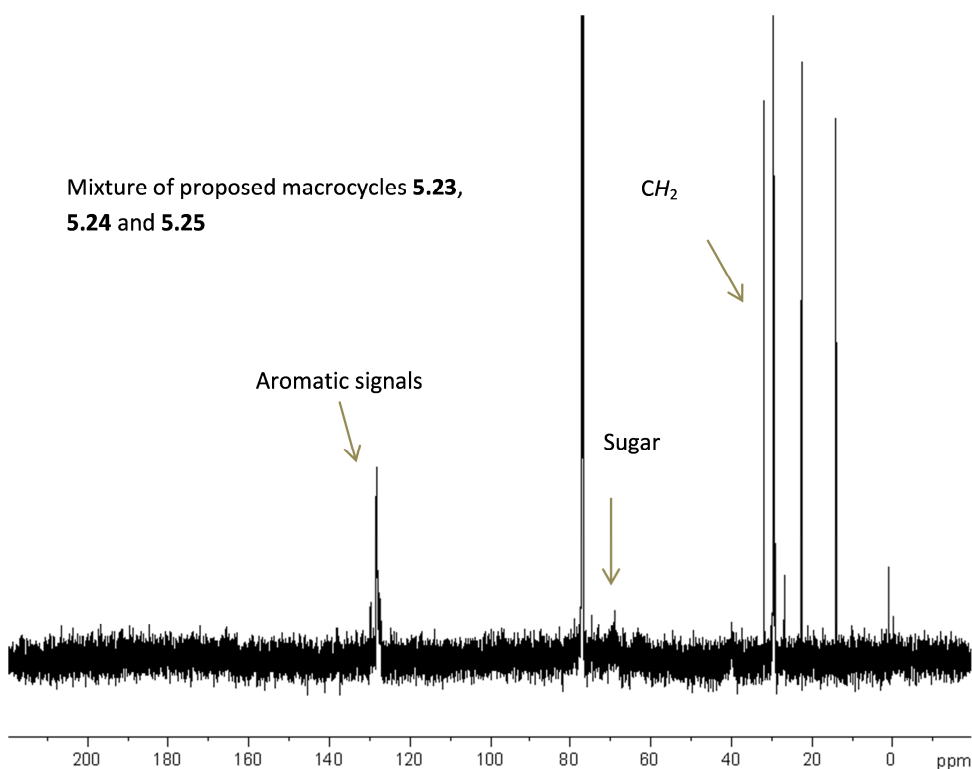


Figure 5.17 ^{13}C NMR spectrum of proposed macrocyclic mixture containing **5.24-5.26**. Characteristic signals are highlighted.

An ED-HSQC experiment shed more light on the structural assignment of the reaction mixture than the ^{13}C NMR spectrum and it is shown in Figure 5.18. Cross-peaks corresponding to the anomeric carbon, the methylene carbons of the benzyl ethers, and the sugar carbons are observed, further suggesting the mixture of

macrocycles. Unfortunately, the ratio of macrocycles present in the reaction mixture could not be determined, hindered by the small amount of material available for these studies and the inherent poor spectral resolution of the NMR spectra.

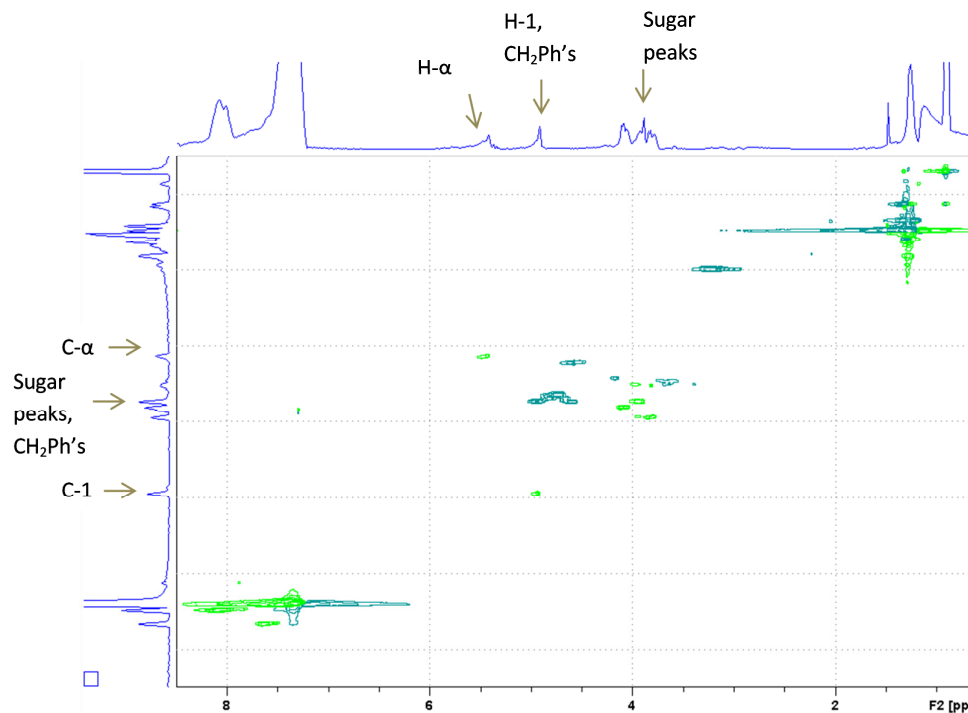


Figure 5.18 ED HSQC NMR experiment of proposed macrocyclic mixture containing **5.24**, **5.25** and **5.26**. Characteristic couplings are highlighted.

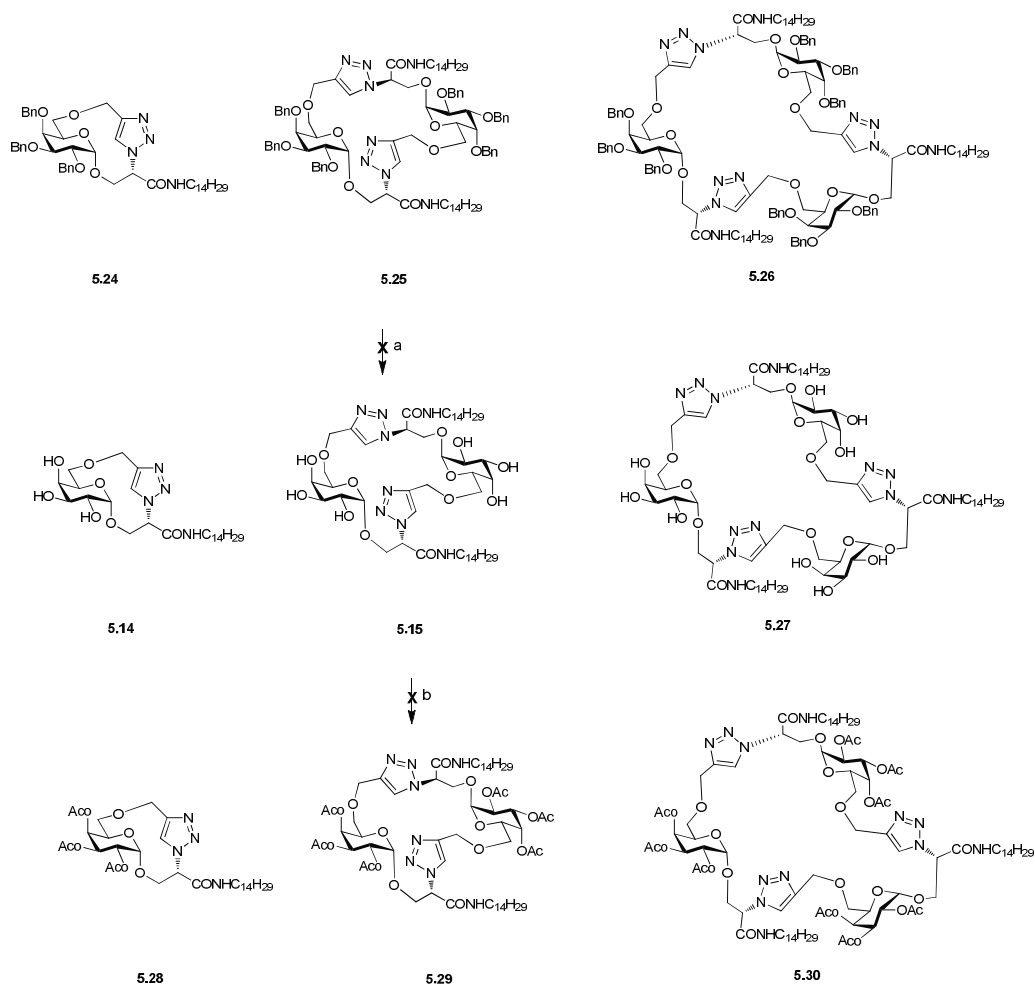
5.3.6. Global debenylation of proposed macrocycles **5.24**, **5.25** and **5.26**

Due to the inseparable mixture of benzyl protected products, postulated to macrocycles **5.24-5.26**, we proceeded to investigate the deprotection of the benzyl ethers which may facilitate future purification. We postulated that RP-HPLC may be more suitable to separate the deprotected polar compounds successfully. Conscious of the difficulties encountered in the removal of benzyl ethers (discussed in Chapter 4), a number of hydrogenolysis reaction conditions were used, in an attempt to afford the desired macrocycles **5.14**, **5.15** and **5.27**. Initially a 10% w/w

loading of Pd(C) was added to the proposed macrocyclic mixture dissolved in EtOH/EtOAc and subjected to a pressure of 4 Barr for 18 h on a hydrogenator shaker apparatus. However, no deprotected macrocycles were isolated. Next, the reaction mixture containing proposed macrocycles **5.24-5.26** was dissolved in a mixture of EtOH/EtOAc (3:1) containing catalytic AcOH, was deoxygenated, and then reacted with H₂ at 4 Barr pressure using a 50% Pd (C) loading for 24 h on a hydrogenator shaker apparatus (Scheme 5.9). The crude material was purified by washing through Celite with copious amounts of heated EtOH. TLC and ¹H NMR analysis indicated the presence of starting material in the reaction mixture. Thus, the reaction mixture was treated with a higher loading of the catalyst (500%) and the reaction was repeated for 18 h. As in the previous case, unreacted or partially debenzylated sugar formed the majority of the reaction mixture. After purification, this hydrogenolysis was performed at a lower loading of Pd (C) (50%) at 4 Barr pressure and was shaken for 18 h. TLC analysis showed consumption of the starting material. The ¹H NMR spectrum of the reaction mixture confirmed the consumption of starting material and presence of a small amount of partially deprotected compound, as indicated by the disappearance and reduction of the intensity of the benzyl ether aromatic signals. Trituerations were performed in order to remove the partially protected compounds from the reaction mixture, but were not fully successful.

Difficulties now arose relating to the solubility of the reaction mixture. ¹H NMR analysis was performed in CD₂Cl₂, d-MeOD and d₆-Pyr but did not indicate the presence of any of desired macrocycles. Instead the spectra constituted mainly of residual solvent and indicated degradation had occurred during the deprotection of the benzyl ethers. Little or no evidence of the desired products **5.14**, **5.15** or **5.27** could be observed. In an attempt to grasp an understanding of the degradation products that were present in the reaction mixture, and bearing in mind the difficulties of solubilising deprotected glycolipids, we performed the acetylation of the mixture of reaction products using Ac₂O in Pyr. After flash chromatography, none of the desired compound **5.28-5.30** were isolated, and no conclusive identification of by-products could be obtained. The methodology was abandoned

as a direct result. As discussed previously in Chapter 4, it is possible that the presence of the triazole groups in this class of L-serinyl derivatives hindered the removal of the benzyl ethers. An additional complication in this case arises due to the macrocyclic nature of compounds **5.24-5.26**, if indeed they are in fact macrocycles. The conformational strain inherent to macrocycles (specially fused tricyclic structures such as **5.24**), may significantly facilitate the occurrence of degradation reactions. It is also possible that steric factors complicated the debenzilylation, due to the presence of the long hydrophobic chains. Thus, the harsher conditions necessary for their removal ultimately led to the destruction of the reaction mixture.



Scheme 5.9 Reagents and conditions a) H₂, Pd (C), EtOH/ EtOAc, AcOH, rt, 4 Barr, 60 h b) Ac₂O, py, 18 h.

5.4. Conclusion and perspective

In conclusion, the glycoside **5.17** served as a suitable building block for formation of either the macrocycles **5.24-5.26** as an inseparable mixture or their corresponding straight chain oligomers. NMR studies, coupled with HR-MS analysis indicates the formation of the macrocycles **5.24**, **5.25** and **5.26**, however no conclusive evidence was found. The potential macrocyclic formation occurred via a CuAAC reaction, and the synthesis of products, most likely the macrocycles **5.24**, **5.25** and **5.26** was achieved successfully, albeit as an inseparable mixture. The selective formation of the monomeric macrocycle **5.14** or dimeric macrocycle **5.15** was not achieved under the conditions explored in our research.

The groundwork for the synthesis of a range of macrocyclic analogues of KRN7000 was put in place, where the difficult CuAAC reaction proved fruitful under dilute conditions. Most problematic in the current synthesis was the global deprotection of the benzyl ether protecting groups, discussed in Section 5.3.6, which had it been successful, would have allowed for the purification and biological evaluation of the glycolipids obtained. This would have led to an insight as to whether they would serve as effective iNKT cell ligands.

Various different approaches could be adapted in order to successfully synthesise the macrocycles **5.14** and **5.15**. The first approach would involve different conditions to cleave the benzyl ethers on the macrocycles. One such example involves the oxidation of the benzyl ethers followed by mildly basic deprotection to yield the desired alcohols.^[249] Another approach would involve the choice of different protecting groups on the glycosyl donor such as the use of PMB ethers (described in Chapter 3) which could be oxidatively cleaved. Another suitable protecting group would be the acid labile TMS protecting groups. However these changes could have dramatic influences on the glycosylation yield and stereoselectivity, and/or the selective formation of potential macrocyclic compounds **5.14** and **5.15**. Much more work is needed to synthesis these

aesthetically pleasing macrocycles **5.14** and **5.15** and to confirm their structure. However, important preliminary work towards their synthesis has been highlighted in this chapter.

Chapter 6: Conclusions and future work

6.1. Conclusions

In conclusion a range of glycolipids were synthesised using a plethora of glycosyl donors and glycosyl acceptors. Various different protecting groups, including acetyl and benzoyl esters, benzyl and PMB ethers and benzylidene acetals were utilised to carry out regioselective and stereoselective glycosylation reactions for building block formations. Different activating groups including TfOH, TMSOTf, AgOTf and NIS were utilised to form stable glycosidic linkages. The syntheses of several O- and N-glycolipids were explored (Figure 6.1).

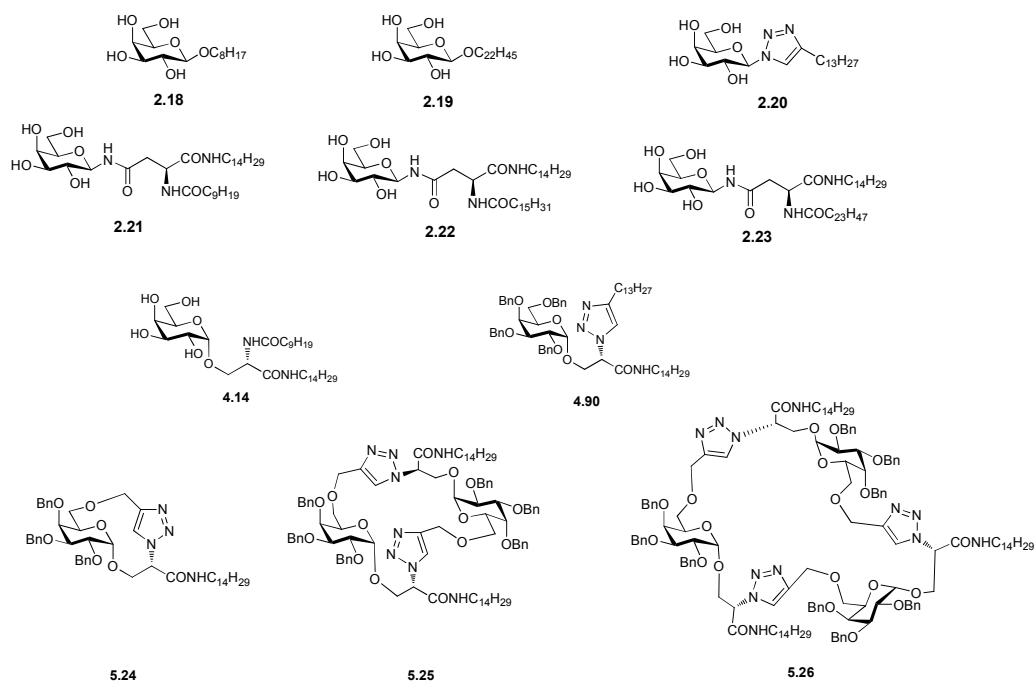


Figure 6.1 O- and N-glycolipids **2.18-2.23** were synthesised for anti-microbial evaluation.

The L-serine based glycolipid **4.14** was synthesised for *i*NKT cell activation studies. The benzyl protected glycolipid **4.90** and the suggested macrocycle structures **5.24-5.26** (or corresponding straight chain oligomers) were synthesised for ongoing synthetic work to be carried out with the eventual goal of *i*NKT cell activation studies on their deprotected glycolipids.

The O-glycolipids **2.18** and **2.19** were prepared to test their anti-microbial properties using an anti-adhesion methodology with a view to compare the effects

of alkyl chain length on anti-microbial adhesion. *N*-glycolipid **2.20** served as a means to test the effects of introducing aromaticity on anti-microbial adhesion studies. The synthesis of aspartic acid based *N*-glycolipids **2.21-2.23** was more challenging than the previous glycolipids discussed. Problems with racemisation and cyclisation side reactions hampered the progress of these reactions. However after careful considerations their synthesis was undertaken. As for the previous glycolipids, their ability to act as anti-microbial agents was of interest. Their increased hydrophobic character, compared to the other glycolipids, was the driving force for their synthesis and biological assessment.

The L-serine base glycolipids **4.14**, **4.90**, **5.24-5.26** (Figure 6.1) were prepared with a view to test their ability to act as *i*NKT cell stimulatory ligands. Many difficulties lay in the synthesis of these glycolipids, with particular problems arising due to poor stereoselective formation of the α -glycosidic linkages and the inherent low nucleophilicity of the L-serine glycosyl acceptors. However glycolipid **4.14** was successfully synthesised. The benzyl protected triazole derivative **4.90** was synthesised using CuAAC cycloaddition chemistry. However its subsequent deprotection resulted in degradation, indicating an alternative synthetic approach was necessary. It was suggested that the macrocycles **5.24-5.26** were synthesised as an inseparable mixture, however no conclusive evidence was given. Again, upon deprotection of the reaction mixture degradation occurred.

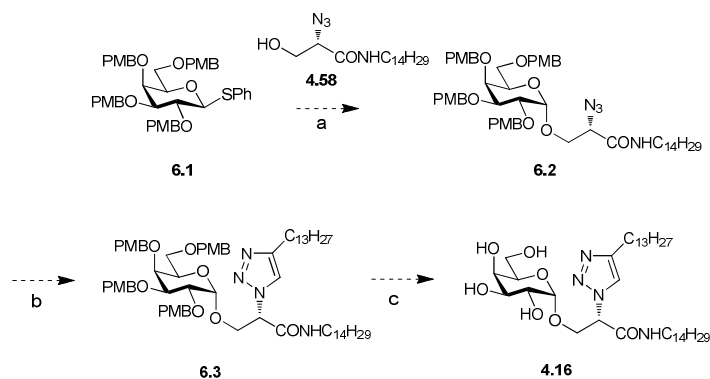
The synthesis of a GI-X analogue **3.1**, described in Chapter 3 was not completed. The key synthetic step involving the formation of a 1,2-*cis* glycosidic linkage of a glucosyl donor **3.3** and glycosyl acceptors **3.4** and **3.37** using an intramolecular aglycon delivery approach. Although the synthesis was not completed, this preliminary work aided in the completion of a GI-A analogue for NKT cell studies.

6.2. Future work

Preliminary anti-microbial evaluations were carried out on *O*-glycolipid **2.19** and *N*-glycolipid **2.22**, as described in Section 2.10. We wish to carry out the anti-adhesion studies of the *O*-glycolipid **2.18** and the *N*-glycolipids **2.20-2.23** to test their ability

to act as anti-microbial agents. We also wish to gain an insight into the parameters that may alter the anti-microbial results such as alkyl chain length, aromaticity and additional hydrophobic character of the glycolipids. In this regard, the anti-adhesion assays of the glycolipids would be compared and optimisation of the glycolipids would be performed, depending on the findings.

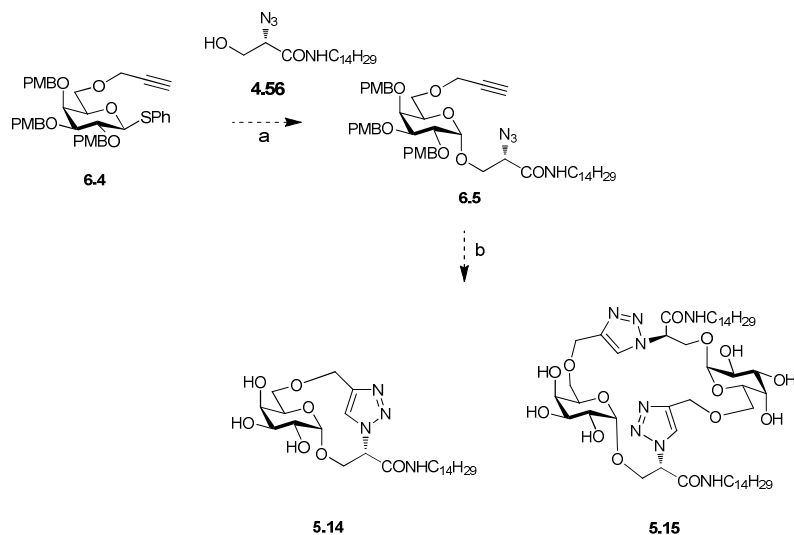
The L-serine based glycolipid **4.14** will be tested against *i*NKT cell human cells and the biological results will be compared to KRN7000. The synthesis of the desired glycolipid **4.16** will be repeated as in Scheme 6.1, with the use of PMB ethers in place of benzyl ethers as global protecting group. The synthesis will begin with the stereoselective coupling of the glycosyl donor **6.1** with the previously synthesised serine azido derivative **4.58**. A CuAAC reaction of the resulting *O*-glycoside **6.2** will then afford the 1,2-disubstituted 1,2,3-triazole product **6.3**. Finally, mild oxidative cleavage with DDQ will afford the desired glycolipid **4.16**. Its potential as an *i*NKT cell ligand will then be explored and compared to glycolipid **4.14**.



Scheme 6.1 Proposed synthesis of glycolipid **4.16** using PMB ether protecting groups on glycosyl donor **6.1**. Step a involves stereoselective glycosylation. Step b involves a CuAAC reaction. Step c involves oxidative cleavage to yield desired glycolipid **4.16**.

A similar approach could be followed for the synthesis of the desired macrocycles **5.14** and **5.15** (described in Section 5.2) also with the use of PMB ethers (Scheme 6.2), provided the synthesis of the glycolipid **4.16** proceeded without any major problems. As in the case for the benzyl protected potential macrocycles, we

anticipated the selective formation of either the monomer **5.14** or the dimer **5.15** to be the most challenging task in the synthetic design. We also hoped that degradation would not occur with the milder oxidative conditions and that structural elucidation, separation of the macrocycles would be easier as a result of the different protecting group in place, the PMB in place of the benzyl ether group.



Scheme 6.2 Proposed synthesis of glycolipid **5.14** and **5.15** using PMB ether protecting groups on glycosyl donor **6.4**. Step a involves stereoselective glycosylation. Step b involves a CuAAC reaction, followed by oxidative cleavage to yield desired glycolipid **5.14** and **5.15**.

Chapter 7: Experimental details

7.1. General Procedures and Instrumentation

All chemicals purchased were reagent grade and used without further purification unless stated otherwise. CH_2Cl_2 was distilled over CaH_2 or NaH , dichloroethane and toluene over CaH_2 , MeCN over P_2O_5 , MeOH over Na metal, THF over Na wire and benzophenone, Pyr over NaOH or was purchased from Sigma Aldrich. Anhydrous DMF was purchased from Sigma Aldrich. Molecular Sieves (MS) used for glycosylation were 8-12 Mesh and were ground and flame dried prior to use. Reactions were monitored with thin layer chromatography (TLC) on Merck Silica Gel F₂₅₄ plates, using mixtures of petroleum ether-EtOAc unless otherwise stated. Detection was effected by either visualisation in UV light and/or charring in a mixture of 5% H_2SO_4 -MeOH or phosphomolybdic acid in EtOH. Evaporation under reduced pressure was always effected with the bath temperature kept below 40 °C.

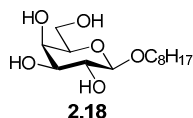
NMR spectra were obtained on a Bruker Avance 300 MHz spectrometer operated at 300 MHz for ^1H and 75 MHz for ^{13}C at 298 K or a Bruker Avance AV-600 MHz spectrometer (Trinity College Dublin) operated at 600 MHz for ^1H and 150 MHz for ^{13}C at 298 K. In University of Melbourne, NMR spectra were obtained on a Varian Inova 500 instrument (Melbourne, Australia) or a Varian Inova 400 instrument (Melbourne, Australia). Proton and carbon signals were assigned with the aid of 2D NMR experiments (COSY, HSQC, ED-HSQC, TOCSY, ^{14}N HSQC, ROESY or HCCOSW) and DEPT experiments. HCCOSW is a HSQC type of experiment. Deuterated CDCl_3 was used in NMR experiments unless otherwise stated. Flash column chromatography was performed according to the method of Still *et al.* with Merck Silica Gel 60, using adjusted mixtures of PetEt-EtOAc unless otherwise stated.^[250] Silica plug chromatography involved the use of small quantities of silica in a glass column, generally for separation of baseline impurities. Optical rotation data was obtained using a AA-100 polarimeter. In University of Melbourne, optical rotation data was obtained using a JASCO DIP-1000 Polarimeter. $[\alpha]_D^{25}$ values are given in $10^{-1}\text{cm}^2\text{g}^{-1}$. Melting points were determined on a Stuart Scientific SMP1 melting point apparatus and are uncorrected. In University of Melbourne, the melting points were obtained using a Gallenkamp melting point apparatus and are uncorrected. High resolution mass spectra (HR-MS) were performed on an Agilent -

LC 1200 Series coupled to a 6210 Agilent Time-Of-Flight (TOF) mass spectrometer equipped with an electrospray source both positive and negative (ESI+/-). In University of Melbourne, High resolution mass spectra (HR-MS) were performed on a Finnigan LCQ quadrupole ion-trap mass spectrometer equipped with a Finnigan electrospray ionisation source. Infra-red spectra were obtained in the region 4000–400 cm^{-1} on a Nicolet Impact 400D spectrophotometer or using a Perkin Elmer 2000 FTIR spectrometer. Either KBr disks or NaCl plates were used as templates. SEM was performed using a Hitachi S-3200-N with a tungsten filament and sample was coated in gold. UV-Vis spectra were recorded with a Jasco V-630BIO spectrophotometer at 25 °C. Hydrogenolysis reactions were performed on a Parr 3911 Hydrogenation Apparatus at 4 Barr pressure for removal of benzyl ether protecting groups.

7.2. Experimental procedures

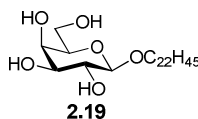
7.2.1. Experimental procedures for Chapter 2

Octadecyl-1-*O*- β -D-galactopyranoside **2.18**



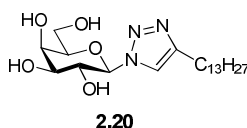
Na metal (1 mg approx., 0.02 mmol approx., 0.1 equiv approx.) was added to a solution of octadecyl-2,3,4,6-tetra-*O*-acetyl- β -D-galactopyranoside **2.34** (68 mg, 0.15 mmol) in MeOH (2 mL) at rt. It was stirred for 2 h; quenched with Amberlite ion-exchange resin (H^+ form), filtered and concentrated *in vacuo* to yield the title compound **2.18** (39 mg, 90%, crude yield) as a white solid; mp = 104-106 °C (lit 154 °C)^[251]; $^1\text{H-NMR}$ (300 MHz, drop D_2O in CDCl_3): δ 0.88 (t, J = 7.0 Hz, 3 H, CH_3), 1.26-1.28 (m, 10 H, $\text{OCH}_2\text{CH}_2(\text{CH}_2)_5\text{CH}_3$), 1.60-1.62 (m, 2 H, OCH_2CH_2), 3.41-3.43 (m, 1 H, OCHHCH_2), 3.42-3.96 (m, 7 H, OCHHCH_2H , H-2, H-3, H-4, H-5, H-6, H-6'), 4.23 (d, J = 8.0 Hz, 1 H, H-1).

The NMR data is in agreement with the reported values.^[72]

Dodecyl-1-O-β-D-galactopyranoside 2.19

NEt₃ (2 drops) was added to a solution of dodecyl-2,3,4,6-tetra-*O*-acetyl-β-D-galactopyranoside **2.35** (0.122 g, 0.18 mmol) in THF/H₂O/MeOH (5 mL, 2:2:1) at rt. It was stirred for 18 h; quenched with Amberlite ion-exchange resin (H⁺ form) and filtered. THF was added and the precipitate was filtered and dried to yield the title compound **2.19** (45 mg, 50%, crude yield) as a white solid; IR ν_{\max} (KBr disk): 3459.6, 2919.1, 2849.4, 1637.9, 1384.6, 1080.7, 753.8 cm⁻¹; ¹H-NMR (300 MHz, d₆-Pyr): δ 0.88 (t, *J* = 6.4 Hz, 3 H, CH₃), 1.31-1.34 (m, 36 H, OCH₂CH₂(CH₂)₁₉), 1.66-1.71 (m, 2 H, OCH₂CH₂), 3.67-3.75 (m, 1 H, OCHHCH₂), 4.09-4.23 (m, 3 H, H-5, H-6, OCHHCH₂), 4.48-4.53 (m, 3 H, H-2, H-3, H-6'), 4.61-4.63 (m, 1 H, H-4), 4.81 (d, *J* = 7.7 Hz, 1 H, H-1); ¹³C-NMR (75MHz, d₆-Pyr): δ_c 16.2 (CH₃), 24.9, 28.5, 31.6, 31.80, 31.9, 31.9, 32.3, 34.1 (O(CH₂)₂₀), 64.5 (OCH₂), 71.7, 72.3, 74.6, 77.4, 78.9 (C-2, C-3, C-4, C-5, C-6), 107.3 (C-1).

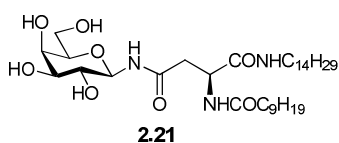
The NMR data is in agreement with the reported values.^[252]

1-(β-D-galactopyranosyl)-4-tridecyl-1,2,3-triazole 2.20

Na metal (1 mg approx., 0.012 mmol approx., 0.1 equiv approx.) was added to a solution of 1-(2,3,4,6-tetra-*O*-acetyl-β-D-galactopyranosyl)-4-tridecyl-1,2,3-triazole **2.37** (72 mg, 0.12 mmol) in MeOH (2 mL) at 0 °C. It was stirred for 1 h; quenched with Amberlite ion-exchange resin (H⁺ form), filtered and concentrated *in vacuo* to yield the title compound **2.20** (45 mg, 88%, crude yield) as a white foam; [α]²⁵_D = +8.82 (c, 0.68 in MeOH); IR ν_{\max} (NaCl plate, CH₂Cl₂): 3431.0, 2922.8, 2852.5, 2126.9, 1641.9, 1094.5 cm⁻¹; ¹H-NMR (300 MHz, d₄-MeOD): δ 0.92 (t, *J* = 6.8 Hz, 3 H, CH₂CH₃), 1.30-1.31 (m, 20 H, (CH₂)₁₀), 1.67-1.72 (m, 2 H, C=CCH₂CH₂), 2.72 (t, *J* = 7.6

Hz, 2 H, C=CCH₂CH₂), 3.69-3.87 (m, 4 H, H-3, H-5, H-6, H-6'), 3.99 (d, *J* = 2.3 Hz, 1 H, H-4), 4.15 (pt, *J* = 9.2 Hz, 1 H, H-2), 5.55 (d, *J* = 9.2 Hz, 1 H, H-1), 7.99 (s, 1 H, C=CH); ¹³C-NMR (75 MHz, d₄-MeOD): δ_c 13.1 (CH₃), 22.3, 24.9, 28.9, 29.1, 29.1, 29.3, 29.4, 31.7 ((CH₂)₁₂), 61.0 (C-6), 69.0 (C-4), 70.0 (C-2), 73.9 (C-3 or C-5), 78.5 (C-3 or C-5), 88.8 (C-1), 120.5 (C=CH), 147.9 (C=CH); HRMS *m/z* (ESI+) 414.2961, (C₂₁H₃₉N₃O₅H: [M+H]⁺ requires 414.2962).

N*^γ-(β-D-galactopyranosyl)-*N*^α-(decanosyl)-L-asparagine 1-tetradecylamide **2.21*

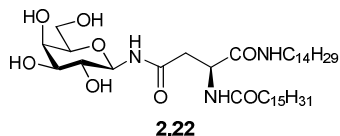


NEt₃ (0.05 mL) was added to a stirred solution of *N*^γ-(2,3,4,6-tetra-*O*-acetyl-β-D-galactopyranosyl)-*N*^α-(decanosyl)-L-asparagine 1-tetradecylamide **2.58** (43 mg, 0.05 mmol) dissolved in CH₂Cl₂: MeOH: H₂O (5 mL, 1:2:1) at 40 °C. The reaction mixture was vigorously stirred for 18 h. The precipitate formed was filtered through a vacuum to afford the title compound **2.21** as white crystals (7 mg, 21%, crude yield). The filtrate was reacted for a further 18 h under the same conditions whereby degradation occurred; [α]²²_D = -6.67 (c 0.6, Pyr); ¹H-NMR (300 MHz, d₅-Pyr): δ 0.81-0.88 (m, 6 H, CH₃ × 2), 1.15-1.24 (m, 34 H, CO(CH₂)₂(CH₂)₆CH₃, NH(CH₂)₂(CH₂)₁₁CH₃), 1.50-1.58 (m, 2 H, NHCH₂CH₂), 1.70-1.75 (m, 2 H, COCH₂CH₂), 2.33 (t, *J* = 7.5 Hz, 2 H, COCH₂), 3.25-3.27 (m, 2 H, H-β, H-β'), 3.44-3.35 (m, 2 H, NHCH₂), 4.11 (pt, *J* = 6.0 Hz, 1 H, H-5), 4.17 (dd, *J* = 3.0 Hz, 9.2 Hz, 1 H, H-3), 4.35-4.38 (m, 2 H, H-6, H-6'), 4.53 (pt, *J* = 9.2 Hz, 1 H, H-2), 4.57 (d, *J* = 2.9 Hz, 1 H, H-4), 5.43 (dd, *J* = 6.8, 14.3 Hz, 1 H, H-α), 5.85 (t, *J* = 9.2 Hz, 1 H, H-1), 8.51 (t, *J* = 5.7 Hz, 1 H, NHC₁₄H₂₉), 8.94 (d, *J* = 7.9 Hz, 1 H, NHCOC₉H₁₉), 10.15 (d, *J* = 9.1 Hz, 1 H, NHC1); ¹³C NMR (d₅-Pyr, 75 Hz): δ_c 14.2 (CH₃^{xiii}), 22.9, 22.9, 26.0, 27.25, 29.5, 29.6, 29.6, 29.6, 29.7, 29.9, 29.9, 32.0, 32.1 (CO(CH₂)₂(CH₂)₆CH₃, NH(CH₂)(CH₂)₁₂CH₃), 36.5 (COCH₂), 39.0 (C-β), 39.9 (NHCH₂), 51.1 (C-α), 62.4 (C-6), 70.4 (C-4), 71.9 (C-2), 76.2

^{xiii} Overlapping signals at 14.2 ppm for two methyl carbon atoms.

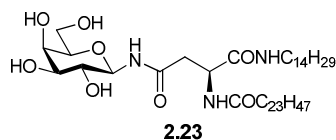
(C-3), 78.4 (C-5), 81.7 (C-1), 171.8 (C=O) , 171.9 (C=O) , 173.4 (C=O); HRMS m/z (ESI+) 666.4689, (C₃₄H₆₅O₈N₃Na: [M+ Na]⁺ requires 666.4664).

N*^β-(β-D-galactopyranosyl)-*N*^α-(tetradecanoyl)-L-asparagine 1-tetradecylamide **2.22*



NEt₃ (0.05 mL) was added to a vigorously stirred solution of *N*^β-(2,3,4,6-tetra-*O*-acetyl-β-D-galactopyranosyl)-*N*^α-(tetradecanoyl)-L-asparagine tetradecylamide **2.62** (54 mg, 0.06 mmol) in CH₂Cl₂: MeOH: H₂O (5 mL, 1:2:1) at 40 °C. The reaction mixture was stirred for 18 h. The precipitate formed was filtered through a vacuum to afford the title compound **2.22** as white crystals (22 mg, 50%, crude yield). The filtrate was reacted for a further 18 h under the same conditions and degradation occurred; [α]²⁷_D = -8.00 (c 0.5, Pyr); ¹H-NMR (300 MHz, *d*₅-Pyr): δ 0.85-0.87 (m, 6 H, CH₃ × 2), 1.24-1.26 (m, 46 H, CO(CH₂)₂(CH₂)₁₂CH₃, NH(CH₂)₂(CH₂)₁₁CH₃) , 1.54-1.56 (m, 2 H, NHCH₂CH₂), 1.71-1.73 (m, 2 H, COCH₂CH₂), 2.32-2.34 (m, 2 H, COCH₂), 3.26-3.28 (m, 2 H, H-β, H-β'), 3.40-3.41 (m, 2 H, NHCH₂), 4.12-4.16 (m, 2 H, H-3, H-5), 4.35-4.38 (m, 2 H, H-6, H-6'), 4.44-4.58 (m, 2 H, H-2, H-4), 5.58-5.62 (m, 1 H, H-α), 5.88-5.88 (m, 1 H, H-1), 6.94-6.96 (m, 2 H, OH × 2), 7.01 (s, 1 H, OH), 7.02 (s, 1 H, OH), 8.46-8.49 (m, 1 H, NHC₁₄H₂₉), 8.91-8.93 (m, 1 H, NHCOC₁₅H₃₁), 10.10-10.12 (m, 1 H, NHC1); ¹³C NMR (*d*₅-Pyr, 75 Hz): δ_c 14.2 (CH₃)^{xiv}, 22.9, 26.1, 27.3, 29.6, 29.6, 29.6, 29.8, 29.9, 29.9, 32.0, 32.1 (CO(CH₂)₂(CH₂)₁₁CH₃, NH(CH₂)(CH₂)₁₂CH₃), 36.5 (COCH₂), 39.1 (C-β), 39.9 (NHCH₂), 51.1 (C-α), 62.4 (C-6), 70.4 (C-4), 71.9 (C-2), 76.21 (C-3), 78.4 (C-5), 81.7 (C-1), 171.7 (C=O), 171.9 (C=O), 173.4 (C=O); HRMS m/z (ESI+) 728.5747, (C₄₀H₇₇O₈N₃H: [M+H]⁺ requires 728.5783).

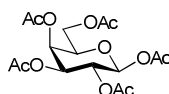
N*^β-(β-D-galactopyranosyl)-*N*^α-(tetracosyl)-L-asparagine 1-tetradecylamide **2.23*



^{xiv} Overlapping signals at 14.2 for two methyl carbon atoms.

NEt₃ (0.05 mL) was added to a stirring solution of N^γ-(2,3,4,6-tetra-*O*-acetyl-β-D-galactopyranosyl)-N^α-(tetracosyl)-L-asparagine 1-tetradecylamide **2.65** (35 mg, 0.04 mmol) dissolved in CH₂Cl₂: MeOH: H₂O (5 mL, 1:2:1) at 40 °C. It was stirred for 18 h. The precipitate formed was filtered through a vacuum to afford the title compound **2.23** as white crystals (23 mg, 79%, crude yield); ¹H-NMR (300 MHz, *d*₅-Pyr): δ 0.85-0.89 (m, 6 H, CH₃ × 2); 1.22-1.32 (m, 62 H, CO(CH₂)₂(CH₂)₂₀CH₃, NH(CH₂)₂(CH₂)₁₁CH₃), 1.54-1.59 (m, 2 H, NHCH₂CH₂), 1.73-1.77 (m, 2 H, COCH₂CH₂), 2.35 (t, *J* = 7.5 Hz, 2 H, COCH₂), 3.21-3.29 (m, 2 H, H-β, H-β'), 3.38-3.49 (m, 2 H, NHCH₂), 4.13-4.20 (m, 1H, H-5), 4.36-4.56 (m, 3 H, H-6, H-6', H-3), 4.60 (d, *J* = 2.9 Hz, 1 H, H-2), 4.73 (d, *J* = 6.1 Hz, 1 H, H-4), 5.61-5.65 (m, 1 H, H-α), 5.90 (dd, *J* = 8.9 Hz, 17.9 Hz, 1 H, H-1), 8.50 (t, *J* = 5.5 Hz, 1 H, NHC₁₄H₂₉), 8.90-9.02 (m, 1 H, NHCOC₂₃H₄₇), 10.14-10.20 (m, 1 H, NHC1).

1,2,3,4,6-Penta-*O*-acetyl-β-D-galactopyranose **2.32** ^[253]



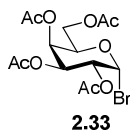
2.32

A suspension of anhydrous NaOAc (4.55 g, 56 mmol, 1 equiv) in Ac₂O (52 mL, 560 mmol, 10 equiv) was heated to reflux temperature in a round bottom flask. To this solution, D-galactose **4.28** (10 g, 56 mmol) was added in portions, until the reaction mixture went colourless. The reaction mixture was poured onto crushed ice (400 mL) and stirred for 2 h. The precipitated product was filtered off, washed with water and recrystallised from EtOH to yield the β-anomer **2.32** (11.50 g, 39%) as white crystals; R_f = 0.30 (hexane/EtOAc 2:1); [α]_D²⁰ = +24.00 (c, 0.01 in CH₂Cl₂); mp = 139-140 °C (lit 140 °C)^[254]; ¹H NMR (300 MHz): δ 2.00 (s, 3 H, OC(O)CH₃), 2.05 (s, 3 H, OC(O)CH₃), 2.12 (s, 3 H, OC(O)CH₃), 2.16-2.17 (m, 6 H, OC(O)CH₃ × 2), 4.05-4.09 (m, 1 H, H-5), 4.13-4.20 (m, 2 H, H-6, H-6'), 5.07-5.11 (dd, *J* = 3.1 Hz, 9.5 Hz, 1 H, H-3), 5.31-5.37 (dd, *J* = 6.0 Hz, 9.4 Hz, 1 H, H-2), 5.42-5.44 (m, 1 H, H-4), 5.71 (d, *J* = 6.0 Hz, 1 H, H-1); ¹³C NMR (75 Hz): δ_C 20.5 (OC(O)CH₃), 20.6 (OC(O)CH₃), 20.6 (OC(O)CH₃), 20.8 (OC(O)CH₃), 30.9 (OC(O)CH₃), 61.0 (C-6), 66.8 (C-4), 67.8 (C-2), 70.8 (C-3), 71.7 (C-5), 92.1 (C-1), 168.9 (OC(O)CH₃), 169.3 (OC(O)CH₃), 169.9

(OC(O)CH₃), 170.1 (OC(O)CH₃), 170.3 (OC(O)CH₃); HRMS m/z (ESI+) 413.1000, (C₁₆H₂₃O₁₁ [M+H]⁺ requires 413.1060).

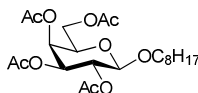
The NMR data are in agreement with the reported values.^[255]

2,3,4,6-Tetra-*O*-acetyl-1-bromo- α -D-galactopyranose **2.33**



HBr in AcOH (33%) (5 mL, 138 mmol, 27 equiv) was added to 1,2,3,4,6-penta-*O*-acetyl- β -D-galactopyranose **2.32** (2 g, 5.12 mmol) at 0 °C. The reaction mixture was stirred for 18 h at rt. The reaction mixture was concentrated *in vacuo* and re-dissolved in EtOAc (50 mL) and a red/orange solid was removed by filtration. The reaction mixture was diluted with CH₂Cl₂ (50 mL) and washed with satd. aq. Na₂CO₃ (30 mL \times 3) followed by brine (30 mL). The organic layers were dried over MgSO₄, filtered, concentrated *in vacuo*, high-vacuum dried and stored in the fridge to yield the α -anomer **2.33** as a white foam (1.58 g ,75%, crude yield); R_f =0.5 (hexane/EtOAc 2:1); $[\alpha]_D^{20} = +142.96$ (c, 0.03 in CH₂Cl₂); ¹H-NMR (300 MHz): δ 1.99 (s, 3 H, OC(O)CH₃), 2.02 (s, 3 H, OC(O)CH₃), 2.11 (s, 3 H, OC(O)CH₃), 2.16 (s, 3 H, OC(O)CH₃), 4.09-4.24 (m, 2 H, H-6, H-6'), 4.52 (pt, *J* = 6.4 Hz, 1 H, H-5), 5.04 (dd, *J* = 3.9 Hz, 10.6 Hz, 1 H, H-2), 5.38 (dd, *J* = 3.2, 10.6 Hz, 1 H, H-3), 5.52 (d, *J* = 3.2 Hz, 1 H, H-4), 6.73 (d, *J* = 3.9 Hz, 1 H, H-1); ¹³C-NMR (75 MHz): δ_c 20.4 (OC(O)CH₃), 20.3 (OC(O)CH₃), 20.2 (OC(O)CH₃), 60.7 (C-6), 66.9 (C-2), 67.5 (C-4), 67.8 (C-3), 71.1 (C-5), 88.4 (C-1), 169.3 (OC(O)CH₃), 169.5 (OC(O)CH₃), 169.8 (OC(O)CH₃), 169.9 (OC(O)CH₃).

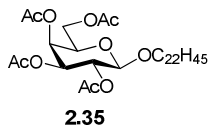
The NMR data are in agreement with the reported literature values.^[71]

Octadecyl-2,3,4,6-tetra-*O*-acetyl- β -D-galactopyranoside 2.34**2.34**

Ag₂CO₃ (0.72 g, 2.63 mmol, 2 equiv) and I₂ (33 mg, 0.13 mmol, 0.1 equiv) was added to 2,3,4,6-tetra-*O*-acetyl-1-bromo- α -D-galactopyranose **2.33** (0.54 g, 1.31 mmol) in CH₂Cl₂ (5 mL) at rt. Octanol (0.21 g, 1.31 mmol, 1 equiv) was added to the reaction mixture and was stirred for 22 h. The suspension was filtered through Celite, washing with CH₂Cl₂. The filtrate was washed with brine and the organic layer was dried over MgSO₄, filtered and rotary evaporated. Flash column chromatography (hexane/EtOAc 3:1) afforded the β -anomer **2.34** (0.11 g, 17%) as a white solid; R_f = 0.70 (hexane/EtOAc 3:1); ¹H-NMR (300 MHz): δ 0.86 (t, *J* = 6.0 Hz, 3 H, CH₃), 1.25-1.26 (m, 10 H, OCH₂CH₂(CH₂)₅CH₃), 1.53-1.59 (m, 2 H, OCH₂CH₂), 1.97 (s, 3 H, OC(O)CH₃), 2.02-2.03 (m, 6 H, OC(O)CH₃ × 2), 2.13 (s, 3 H, OC(O)CH₃), 3.41-3.50 (m, 1 H, OCHCH₂), 3.83-3.91 (m, 2 H, H-5, OCHCH₂), 4.08-4.46 (m, 2 H, H-6, H-6'), 4.45 (d, *J* = 7.8 Hz, 1 H, H-1), 5.00 (dd, *J* = 3.3 Hz, 10.4 Hz, 1 H, H-3), 5.19 (dd, *J* = 7.8 Hz, 10.4 Hz, 1 H, H-2), 5.37 (d, *J* = 3.3 Hz, 1 H, H-4); ¹³C-NMR (75 MHz): δ _c 14.0 (CH₃), 20.5 (OC(O)CH₃), 20.6 (OC(O)CH₃), 20.6 (OC(O)CH₃)^{xv}, 22.6, 25.8, 29.2, 29.2, 29.4, 31.8 ((CH₂)₆CH₃), 61.3 (C-6), 67.1 (C-4), 68.9 (C-2), 70.2 (OCH₂), 70.5 (C-5), 70.9 (C-3), 101.3 (C-1), 169.3 (OC(O)CH₃), 170.1 (OC(O)CH₃), 170.2 (OC(O)CH₃), 170.3 (OC(O)CH₃).

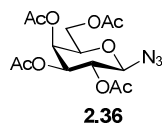
The NMR data are in agreement with the reported values.^[72]

^{xv} Two overlapping signals.

Dodecyl-2,3,4,6-tetra-O-acetyl- β -D-galactopyranoside 2.35

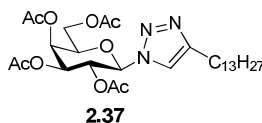
Ground docosonol (583 mg, 2.14 mmol, 1.2 equiv) was added to a suspension of Ag_2CO_3 (494 mg, 1.79 mmol, 1 equiv) and I_2 (45 mg, 0.18 mmol, 0.1 equiv) in CH_2Cl_2 (10 mL) at rt in the dark. A solution of 2,3,4,6-tetra-O-acetyl-1-bromo- α -D-galactopyranose **2.33** (0.54 g, 1.31 mmol) in CH_2Cl_2 (5 mL) was slowly added to the suspension and the reaction mixture and was stirred for 24 h. The suspension was filtered through Celite and washed with CH_2Cl_2 . The filtrate was washed with brine and the organic layer was dried over MgSO_4 , filtered and rotary evaporated. Flash column chromatography (hexane/EtOAc 4:1) afforded the β -anomer **2.35** (0.13 g, 11%) as a white solid; $R_f = 0.3$ (hexane/EtOAc 4:1); $[\alpha]_D^{20} = -8.25$ (c, 0.04 in CH_2Cl_2); IR ν_{max} (NaCl plate, CH_2Cl_2): 3059.6, 2919.2, 2850.9, 2119.0, 1751.3 cm^{-1} ; $^1\text{H-NMR}$ (300 MHz): δ 0.88 (t, $J = 6.9$ Hz, 3 H, CH_3), 1.24-1.25 (m, 38 H, $\text{OCH}_2\text{CH}_2(\text{CH}_2)_{19}\text{CH}_3$), 1.59 (bs, 2 H, OCH_2CH_2), 3.43-3.51 (m, 1 H, H-5), 3.87-3.92 (m, 2 H, H-6', OCHHCH_2), 4.09-4.22 (m, 2 H, H-6, OCHHCH_2), 4.45 (d, $J = 7.9$ Hz, 1 H, H-1), 5.02 (dd, $J = 3.4$ Hz, 10.5 Hz, 1 H, H-3), 5.21 (dd, $J = 7.9$ Hz, 10.5 Hz, 1 H, H-2), 5.39 (dd, $J = 0.9$ Hz, 3.4 Hz, 1 H, H-4); $^{13}\text{C-NMR}$ (75 MHz): δ_c 14.1 (CH_3), 20.6 (OC(O)CH_3), 20.7 (OC(O)CH_3), 20.7 (OC(O)CH_3)^{xvi}, 22.7 (CH_2CH_3), 25.8 ($\text{CH}_2\text{CH}_2\text{CH}_2\text{CH}_3$), 29.4 ($\text{OCH}_2\text{CH}_2(\text{CH}_2)_{16}$), 29.6 (CH_2CH_2), 31.9 ($\text{CH}_2\text{CH}_2\text{CH}_3$), 61.3 (OCH_2), 67.1 (C-4), 68.9 (C-2), 70.3 (C-6), 70.6 (C-5), 70.9 (C-3), 101.4 (C-1), 169.4 (OC(O)CH_3), 170.2 (OC(O)CH_3), 170.3 (OC(O)CH_3), 170.4 (OC(O)CH_3); HRMS m/z (ESI+) 657.4574, ($\text{C}_{36}\text{H}_{64}\text{O}_{10}\text{H}$ $[\text{M}+\text{H}]^+$ requires 657.4572).

^{xvi} Two overlapping signals.

2,3,4,6-Tetra-*O*-acetyl- β -D-galactopyranosyl-1-azido **2.36** ^[74]

TMSN₃ (2.56 mL, 19.48 mmol, 2.5 equiv) was added to a solution 1,2,3,4,6-penta-*O*-acetyl- β -D-galactopyranose **2.32** (3.04 g, 7.79 mmol) in CH₂Cl₂ (30 mL). SnCl₄ (3.90 mL, 3.90 mmol, 0.5 equiv) (1 M solution in CH₂Cl₂) was added to this solution and the reaction mixture was stirred for 18 h. Satd. aq. NaHCO₃ (50 mL) was added and the suspension was extracted with CH₂Cl₂ (2 × 50 mL). The combined organic extracts were dried over MgSO₄, filtered and concentrated *in vacuo* to afford the β -anomer **2.36** (2.28 g, 80%, crude yield) as a white solid; R_f = 0.55 (hexane/EtOAc 1:1); ¹H NMR (300 MHz): δ 1.93 (s, 3 H, OC(O)CH₃), 2.01 (s, 3 H, OC(O)CH₃), 2.04 (s, 3 H, OC(O)CH₃), 2.12 (s, 3 H, OC(O)CH₃), 3.98 (td, *J* = 5.6 Hz, 9.2 Hz, 1 H, H-5), 4.11-4.13 (m, 2 H, H-6, H-6'), 4.57 (d, *J* = 8.6 Hz, 1 H, H-1), 5.00 (dd, *J* = 3.3 Hz, 10.4 Hz, 1 H, H-3), 5.11 (dd, *J* = 8.6 Hz, 10.4 Hz, 1 H, H-2), 5.37 (dd, *J* = 1.0 Hz, 3.3 Hz, 1 H, H-4); HRMS *m/z* (ESI+) 396.1010, (C₁₄H₁₉O₉N₃Na: [M+Na]⁺ requires 396.1014).

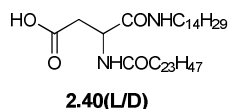
The NMR data is in agreement with the reported values.^[74]

1-(2,3,4,6-Tetra-*O*-acetyl- β -D-galactopyranosyl)-4-tridecyl-1,2,3-triazole **2.37**

CuSO₄·5H₂O (33 mg, 0.13 mmol, 0.1 equiv) was added to a solution of 2,3,4,6-tetra-*O*-acetyl- β -D-galactopyranosyl-1-azido **2.36** (500 mg, 1.34 mmol) and pentadecyne (279 mg, 1.34 mmol, 1 equiv) in THF/H₂O/MeOH (5 mL, 1:1:3) at rt. Sodium ascorbate (53 mg, 0.27 mmol, 0.2 equiv) was added and the reaction mixture was stirred for 48 h. The reaction mixture was filtered through Celite and rinsed with EtOAc. The reaction mixture was washed with brine (100 mL) and the organic layer was dried over Na₂SO₄, filtered and concentrated *in vacuo* to afford the β -anomer **2.37** (692 mg, 89%, crude yield) as a white solid; R_f = 0.25 (PetEt/EtOAc 3:1); [α]_D²⁵ = -1.67 (c, 1.2 in CH₂Cl₂); IR ν_{\max} (NaCl plate, CH₂Cl₂): 2924.9, 2854.2, 1754.9, 1369.8,

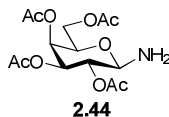
cm⁻¹; ¹H-NMR (300 MHz): δ 0.88 (t, *J* = 6.9 Hz, 3 H, CH₂CH₃), 1.24-1.26 (m, 20 H, (CH₂)₁₀), 1.68 (t, *J* = 8.2 Hz, 2 H, C=CCH₂CH₂), 1.88 (s, 3 H, OC(O)CH₃), 2.01 (s, 3 H, OC(O)CH₃), 2.05 (s, 3 H, OC(O)CH₃), 2.22 (s, 3 H, OC(O)CH₃), 2.72 (t, *J* = 8.1 Hz, 2 H, C=CCH₂CH₂), 4.13-4.23 (m, 3 H, H-5, H-6, H-6'), 5.24 (dd, *J* = 3.3 Hz, 10.3 Hz, 1 H, H-4), 5.53-5.59 (m, 2 H, H-2, H-3), 5.82 (d, *J* = 9.3 Hz, 1 H, H-1); ¹³C-NMR (75 MHz): δ_c 14.1 (CH₃), 20.2 (OC(O)CH₃), 20.5 (OC(O)CH₃), 20.6 (OC(O)CH₃)^{xvii}, 22.7, 25.7, 29.2, 29.2, 29.4, 29.6, 29.7, 30.3, 31.9 ((CH₂)₁₂CH₃), 61.2 (C-6), 66.9, 67.8 (C-2, C-3), 70.9 (C-4), 74.0 (C-5), 86.2 (C-1), 118.8 (C=CH), 149.2 (C=CH), 169.1 (C=O), 169.8 (C=O), 169.9 (C=O), 170.3 (C=O); HRMS *m/z* (ESI+) 582.3389, (C₂₉H₄₇N₃O₉H: [M+H]⁺ requires 582.3385).

N*^α-Tetradecanosyl-L/D-aspartic acid-tetradecylamide **2.40(L/D)*



H₂ gas was bubbled through a suspension of *N*^α-tetradecanosyl-L/D-aspartic acid-tetradecylamide 4-benzyl ester **2.47(L/D)** (96 mg, 0.13 mmol) and Pd (C) (10 mg, 10 % w/w) in EtOAc (5 mL) at 50 °C at 1 atm. The reaction mixture was stirred for 2 h. The suspension was filtered through Celite, washed with EtOAc and was concentrated *in vacuo* to yield the title compound **2.40(L/D)** (61 mg, 72%, crude yield) as a white solid; [α]²³_D = +0.10 (c 0.4, CH₂Cl₂); Data recorded for racemic mixture: ¹H NMR (300 MHz): δ 0.86-0.88 (m, 6 H, CH₃ × 2), 1.23-1.25 (m, 62 H, COCH₂CH₂(CH₂)₂₀CH₃, NHCH₂CH₂(CH₂)₁₁CH₃), 1.48 (t, *J* = 6.9 Hz, 2 H, NHCH₂CH₂), 1.63 (t, *J* = 7.2 Hz, 2 H, COCH₂CH₂), 2.17-2.25 (m, 2 H, COCH₂), 2.67 (dd, *J* = 7.1 Hz, 17.1 Hz, 1 H, H-β), 2.93 (dd, *J* = 3.6 Hz, 17.1 Hz, 1 H, H-β'), 3.19-3.25 (m, 2 H, NHCH₂), 4.72-4.78 (m, 1 H, H-α), 6.96 (t, *J* = 4.8 Hz, 1 H, NHCH₂), 7.01 (d, *J* = 7.6 Hz, 1 H, NH(H-α)); HRMS *m/z* (ESI+) 1376.2602, (C₄₂H₈₄O₄N₂NH₄: [M+NH₄]⁺ requires 1376.2614).

^{xvii} Two overlapping signals.

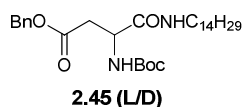
2,3,4,6-Tetra-O-acetyl-β-D-galactopyranosyl-1-amino 2.44

H₂ gas was bubbled through a suspension of 2,3,4,6-tetra-O-acetyl-β-D-galactopyranosyl-1-azido **2.36** (560 mg, 1.50 mmol) and Pd (C) (56 mg, 10% w/w) in EtOAc (5 mL) at 1 atm at rt. It was left to stir for 18 h. The suspension was filtered through Celite, washed with EtOAc and concentrated *in vacuo* to yield the β-anomer **2.44** (498 mg, 96%, crude yield) as a white foamy solid; ¹H NMR (300 MHz): δ 1.98 (s, 3 H, OC(O)CH₃), 2.04 (s, 3 H, OC(O)CH₃), 2.07 (s, 3 H, OC(O)CH₃), 2.14 (s, 3 H, OC(O)CH₃), 3.89-3.91 (m, 1 H, H-5), 4.08-4.10 (m, 2 H, H-6, H-6'), 4.16 (d, *J* = 8.0 Hz, 1 H, H-1), 5.02-5.04 (m, 1 H, H-3), 5.11 (dd, *J* = 8.0 Hz, 10.3 Hz, 1 H, H-2), 5.39 (d, *J* = 1.8 Hz, 1 H, H-4); HRMS *m/z* (ESI+) 348.1279, (C₁₄H₂₁O₉NH: [M+H]⁺ requires 348.1289).

The NMR data is in agreement with the reported values. ^[74]

***N*^α-tert-Butoxycarbonyl-L/D-aspartic acid-tetradecylamide 4-benzyl ester 2.45(L/D)**

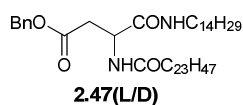
[82]



TBTU (1.09 g, 3.40 mmol, 1.1 equiv) and HOBt (0.460 g, 3.40 mmol, 1.1 equiv) were added to Boc-Asp(OBn)-OH **2.41** (1.00 g, 3.09 mmol) in DMF (15 mL) containing 4 Å MS under N₂ at rt. The reaction mixture was stirred for 30 min and tetradecylamine (0.660 g, 3.09 mmol, 1 equiv) was added. The reaction mixture was stirred for 2.5 h, then concentrated *in vacuo*; diluted with EtOAc (4 mL), washed with H₂O (4 mL), brine (4 mL), H₂O (4 mL), dried over MgSO₄, filtered and concentrated. Recrystallisation in *i*-PrOH afforded the title compound **2.45(L/D)** (1.40 g, 87%) as white crystals; Data recorded for racemic mixture: *R*_f = 0.67 (hexane/EtOAc 2:1); [α]_D²² = 0 (c 0.9, CHCl₃); IR *v*_{max} (KBr): 3339.8, 2910.3, 1736.6, 1664.8, 1519.1 cm⁻¹; ¹H NMR (300 MHz): δ 0.88 (t, *J* = 6.9 Hz, 3 H, CH₃), 1.22-1.25 (m, 22 H,

(CH₂)₁₁CH₃), 1.43-1.45 (m, 11 H, C(CH₃)₃, NHCH₂CH₂), 2.72 (dd, *J* = 6.5 Hz, 17.2 Hz, 1 H, H-β'), 3.04 (dd, *J* = 4.5 Hz, 17.2 Hz, 1 H, H-β), 3.15-3.25 (NHCH₂), 4.45-4.47 (m, 1 H, H-α), 5.13 (d, *J* = 3.3 Hz, 2 H, CH₂Ph), 5.65-5.65 (m, 1 H, NHCOOC(CH₃)₃), 6.43-6.44 (m, 1 H, NHCH₂), 7.26-7.37 (m, 5 H, Ph); ¹³C NMR (75 Hz): δ_c 14.1 (CH₂CH₃), 22.7, 26.8, 28.3, 29.3, 29.3, 29.4, 29.5, 29.6, 29.7, 31.9 ((CH₂)₁₂CH₃), 36.2 (C-β), 39.6 (NHCH₂), 50.7 (C-α), 66.8 (CH₂Ph), 80.5 (OC(CH₃)₃), 128.2, 128.4, 128.5, 128.6 (aromatics), 135.4 (C=O), 170.4 (C=O), 171.8 (C=O).

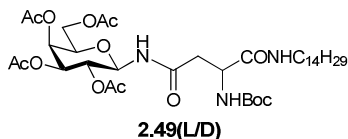
N*^α-Tetradecanosyl-L/D-aspartic acid-tetradecylamide 4-benzyl ester **2.47*



TFA (2.93 mL, 34.70 mmol, 10 equiv) in CH₂Cl₂ (3 mL) was added drop-wise to a solution of *N*^α-*tert*-butoxycarbonyl-L/D-aspartic acid-tetradecylamide 4-benzyl ester **2.45(L/D)** (1.80 g, 3.47 mmol) in CH₂Cl₂ (10 mL). The reaction mixture was stirred for 3 h and concentrated. It was diluted in CH₂Cl₂ (50 mL) and washed with satd. aq. NaHCO₃ solution (50 mL), brine (50 mL) and H₂O (50 mL). It was concentrated *in vacuo* to yield the crude amine **2.46(L/D)** (1.29 g, 77%, crude yield) as a white solid. The compound was used without further purification. In a separate pot, TBTU (479 mg, 1.49 mmol, 1.1 equiv) and HOBt (201 mg, 1.49 mmol, 1.1 equiv) were added to lignoceric acid (500 mg, 1.36 mmol) in DMF (10 mL) containing 4 Å MS under N₂ at rt. It was stirred for 30 min and the crude amine **2.46(L/D)** (706 mg, 1.36 mmol, 1 equiv) was added. The reaction mixture was stirred for 18 h. It was concentrated *in vacuo*; diluted with EtOAc (4 mL), washed with H₂O (4 mL), brine (4 mL), H₂O (4 mL), dried over MgSO₄, filtered and concentrated to yield the title compound **2.47(L/D)** (935 mg, 89%, crude yield) as a white solid. A small sample was recrystallized in toluene for characterisation; Data recorded for racemic mixture: R_f = 0.50 (hexane/EtOAc 2:1); [α]_D²³ = 0 (c 0.8, CHCl₃); mp = 82-84 °C; IR ν_{max} (KBr): 3298.3, 2918.8, 2850.1, 1732.9, 1643.3, 1546.3, 1469.1, 1412.6, cm⁻¹; ¹H NMR (300 MHz): δ 0.86-0.88 (m, 6 H, CH₃ × 2), 1.24-1.25 (m, 64 H, COCH₂CH₂(CH₂)₂₀CH₃, NHCH₂(CH₂)₁₂CH₃), 1.44 (t, *J* = 6.9 Hz, 2 H, COCH₂CH₂), 2.17-2.22 (m, 2 H, COCH₂), 2.64 (dd, *J* = 7.0 Hz, 16.9 Hz, 1 H, H-β), 2.98 (dd, *J* = 4.2 Hz, 16.9 Hz, 1 H, H-β'), 3.16-

3.23 (m, 2 H, NHCH_2), 4.78 (td, $J = 4.2$ Hz, $J = 7.0$ Hz, $J = 11.8$ Hz, 1 H, H- α), 5.15 (d, $J = 3.0$ Hz, 2 H, CH_2Ph), 6.51 (t, $J = 5.6$ Hz, 1 H, NHCH_2), 6.77 (d, $J = 7.9$ Hz, 1 H, $\text{NH}(\text{H}-\alpha)$), 7.35 (s, 5 H, Ph); ^{13}C NMR (75 Hz): δ_c 14.1 (CH_3)^{xviii}, 22.7, 25.6, 26.8, 29.3, 29.4, 29.5, 29.6, 29.7, 29.7, 31.9 ($\text{COCH}_2(\text{CH}_2)_{21}\text{CH}_3$, $\text{NHCH}_2(\text{CH}_2)_{12}\text{CH}_3$), 35.7 (C- β), 36.6 (COCH_2), 39.7 (NHCH_2), 49.1 (C- α), 66.9 (CH_2Ph), 128.3, 128.4, 128.6, 138.6 (aromatic), 170.1 (C=O), 172.2 (C=O), 173.4 (C=O); HRMS m/z (ESI+) 769.6815, ($\text{C}_{49}\text{H}_{88}\text{O}_4\text{N}_2\text{H}$: $[\text{M}+\text{H}]^+$ requires 769.6817).

N* ^{α} -*tert*-Butoxycarbonyl-*N* ^{γ} -(2,3,4,6-tetra-*O*-acetyl- β -D-galactopyranosyl)-L/D-asparagine tetradecylamide **2.49(L/D)*

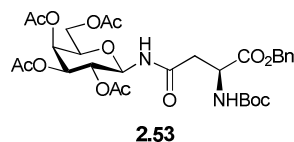


H_2 gas was bubbled through a suspension of *N* ^{α} -*tert*-butoxycarbonyl-L/D-aspartic acid-tetradecylamide 4-benzyl ester **2.45(L/D)** (500 mg, 9.65 mmol) and Pd (C) (50 mg, 10% w/w) in EtOAc (5 mL) at 1 atm at rt. The reaction mixture was left to stir for 18 h. The suspension was filtered through Celite, washed with EtOAc and concentrated *in vacuo* to yield the crude carboxylic acid **2.48(L/D)** (400 mg, 97%, crude yield) as a white solid. It was used without further purification. TBTU (43 mg, 0.13 mmol, 1.1 equiv) and HOBT (18 mg, 0.13 mmol, 1.1 equiv) were added to the carboxylic acid **2.48(L/D)** (52 mg, 0.12 mmol) in DMF (3 mL) under N_2 at rt. The reaction mixture was stirred for 30 min and 2,3,4,6-tetra-*O*-acetyl- β -D-galactopyranosyl-1-amino **2.44** (42 mg, 0.121 mmol, 1 equiv) was added. The reaction mixture was stirred for 18 h. It was concentrated *in vacuo*; diluted with EtOAc (4 mL), washed with H_2O (4 mL), brine (4 mL), H_2O (4 mL), dried over MgSO_4 , filtered and concentrated. Flash column chromatography (hexane/EtOAc 1:1) afforded the β -glycoside **2.49(L/D)** (55 mg, 59%) as a white solid as a mixture of diastereoisomers (1.57:1 ratio); Data recorded for racemic mixture: $R_f = 0.22$ (hexane/EtOAc 1:1); ^1H NMR (300 MHz): δ 0.86-0.88 (m, 6 H, $\text{CH}_3 \times 2$), 1.21-1.23 (m, 20 H, $(\text{CH}_2)_{10}\text{CH}_3 \times 2$), 1.40-1.43 (m, 22 H, $\text{C}=\text{OOC}(\text{CH}_3)_3 \times 2$, $\text{NHCH}_2\text{CH}_2 \times 2$), 1.97 (s, 3

^{xviii} Two overlapping signals.

H, OC(O)CH₃), 1.98 (s, 3 H, OC(O)CH₃), 2.02 (s, 3 H, OC(O)CH₃), 2.03 (s, 3 H, OC(O)CH₃), 2.05 (s, 3 H, OC(O)CH₃), 2.13 (s, 3 H, OC(O)CH₃), 2.13 (s, 3 H, OC(O)CH₃), 2.46-2.59 (m, 2 H, H-β × 2), 2.75-2.84 (m, 2 H, H-β' × 2), 3.14-3.20 (m, 4 H, NHCH₂ × 2), 3.97-4.14 (m, 6 H, H-5 × 2, H-6 × 2, H-6' × 2), 4.39-4.43 (m, 2 H, H-α × 2), 5.08-5.23 (m, 6 H, H-1 × 2, H-2 × 2, H-3 × 2), 5.41-5.42 (m, 2 H, H-4 × 2), 5.72 (d, *J* = 7.9 Hz, 1 H, NHC=OOC(CH₃)₃), 6.17 (d, *J* = 8.5 Hz, 1 H, NHC=OOC(CH₃)₃), 6.61-6.75 (m, 4 H, NH (C-1) × 2, NHCH₂ × 2); ¹³C NMR (75 Hz): δ_c 14.1 (CH₂CH₃), 20.5 (OC(O)CH₃), 20.6 (OC(O)CH₃), 20.6 (OC(O)CH₃), 20.7 (OC(O)CH₃), 22.6 (OC(CH₃)₃), 26.8, 28.2, 29.2, 29.3, 29.4, 29.5, 29.6, 29.6, 29.6, 29.6, 31.9 (CH₂)₁₃CH₃), 39.6 (C-β), 50.9 (C-α), 60.9 (C-6), 61.1 (C-4), 70.7 (C-2), 72.3 (C-3), 78.3 (C-5), 80.3 (C-1), 168.1 (C=O), 168.3 (C=O), 168.3 (C=O), 168.6 (C=O), 168.8 (C=O), 168.9 (C=O), 169.4 (C=O); HRMS *m/z* (ESI+) 780.4237, (C₃₇H₆₃O₁₃N₃Na: [M+Na]⁺ requires 780.4253).

N*^α-*tert*-Butoxycarbonyl-*N*^γ-(2,3,4,6-tetra-*O*-acetyl-β-D-galactopyranosyl)-L-asparagine 1-benzyl ester **2.53*

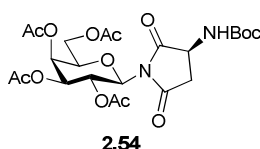


HOBt (1.30 g, 9.60 mmol, 2 equiv) was added to a stirred solution of *N*-*boc*-L-Asp-OBn **2.52** (1.55 g, 4.80 mmol) and TBTU (3.08 g, 0.72 mmol, 2 equiv) in DMF (25 mL) under N₂ at rt. The reaction mixture was stirred for 30 min and 2,3,4,6-tetra-*O*-acetyl-β-D-galactopyranosyl-1-amino **2.44** (2 g, 5.76 mmol, 1.2 equiv) dissolved in DMF (10 mL) was added drop-wise to the solution and was stirred for 18 h. The reaction mixture was concentrated *in vacuo*, diluted with EtOAc (20 mL), washed with H₂O (20 mL), 0.1 N aq. HCl solution (20 mL), satd. aq. NaHCO₃ (20 mL), dried over MgSO₄, filtered and concentrated. Flash column chromatography (hexane/EtOAc 1:1) afforded the β-anomer **2.53** (1.70 g, 71%) as a white solid. This was used without further purification. A small sample of *N*-glycoside **2.53** was recrystallised in CHCl₃/ hexane to give white crystals used for characterisation; *R*_f = 0.25 (hexane/EtOAc 1:1); [α]²²_D = +30.00 (c 1.2, CHCl₃); mp = 148-150 °C; IR ν_{max} (NaCl plate, CH₂Cl₂): 3348.7, 2965.2, 1749.6, 1499.7 cm⁻¹; ¹H NMR (300 MHz): δ 1.41

(s, 9 H, C(O)OC(CH₃)₃), 1.98 (s, 3 H, OC(O)CH₃), 1.99, (s, 3 H, OC(O)CH₃), 2.03 (s, 3 H, OC(O)CH₃), 2.13 (s, 3 H, OC(O)CH₃), 2.71 (dd, *J* = 3.4 Hz, 15.0 Hz, 1 H, H-β), 2.84-2.95 (m, 1 H, H- β'), 3.97-4.15 (m, 3 H, H-5, H-6, H-6'), 4.56-4.58 (m, 1 H, H-α), 5.04-5.21 (m, 5 H, CH₂Ph, H-1, H-2, H-3), 5.42 (d, *J* = 3.6 Hz, 1 H, H-4), 5.70 (d, *J* = 9.2 Hz, 1 H, NHC=OCH₂), 6.39 (d, *J* = 9.4 Hz, 1 H, NHC=OC(CH₃)₃), 7.33-7.34 (m, 5 H, Ph).

The NMR data is in agreement with the reported values.^[256]

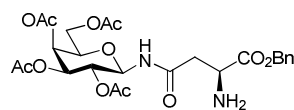
N*^α-*tert*-Butoxycarbonyl-2,4-dioxo-*N*^γ-(2,3,4,6-tetra-*O*-acetyl-β-D-galactopyranosyl)-L-pyrrolidone **2.54*



H₂ gas was bubbled through a suspension of *N*^α-*tert*-butoxycarbonyl-*N*^γ-(2,3,4,6-tetra-*O*-acetyl-β-D-galactopyranosyl)-L-asparagine 1-benzyl ester **2.53** (179 mg, 0.27 mmol) and Pd (C) (17 mg, 10% w/w) in EtOAc (10 mL) at 1 atm at rt. The reaction mixture was left to stir for 18 h. The suspension was filtered through Celite, washed with EtOAc and was concentrated *in vacuo* to yield the crude carboxylic acid (125 mg, 81%, crude yield) as a colourless oil. No further purification was performed. TBTU (0.321 g, 1.00 mmol, 1.1 equiv) and HOBT (0.135 g, 1.00 mmol, 1.1 equiv) were added to a stirring solution of the carboxylic acid (512 mg, 0.91 mmol) in DMF (40 mL) under N₂ at rt. It was stirred for 30 min and tetradecylamine (194 mg, 0.91 mmol, 1 equiv) was added to the reaction mixture. It was stirred for 4 h and was concentrated *in vacuo*, diluted with EtOAc (40 mL), washed with H₂O (40 mL), 0.1 N aq. HCl solution (40 mL), satd. aq. NaHCO₃ (40 mL), dried over MgSO₄, filtered and concentrated. Flash column chromatography (hexane/EtOAc 2:1) afforded the succinimide β-glycoside **2.54** (215 mg, 48%) as a white foamy solid; R_f = 0.17 (hexane/EtOAc 1:1); [α]²³_D = +11.43 (c 0.7, CH₂Cl₂); IR ν_{max} (NaCl plate, CH₂Cl₂): 3386.6, 2977.1, 1751.2, 1509.2 cm⁻¹; ¹H NMR (300 MHz): δ 1.44 (s, 9 H, C=OOC(CH₃)₃), 1.99 (s, 3 H, OC(O)CH₃), 2.01 (s, 3 H, OC(O)CH₃), 2.05 (s, 3 H, OC(O)CH₃), 2.21 (s, 3 H, OC(O)CH₃), 2.74 (dd, *J* = 5.8 Hz, 15.3 Hz, 1 H, H-β), 3.06-3.15 (m, 1 H, H- β'), 4.00-4.20 (m, 3 H, H-5, H-6, H-6'), 4.24-4.27 (m, 1 H, H-α), 5.08 (dd,

$J = 3.2$ Hz, 10.0 Hz, 1 H, H-3), 5.33-5.35 (m, 2 H, H-1, NH), 5.45-5.46 (d, $J = 3.2$ Hz, 1 H, H-4), 6.09-6.10 (m, 1 H, H-2); ^{13}C NMR (75 Hz): δ_{c} 19.6 (OC(O)CH₃), 19.7 (OC(O)CH₃), 19.7 (OC(O)CH₃),^{xix} 27.2 (OC(CH₃)₃), 34.4 (C- β), 48.4 (C- α), 60.5 (C-6), 64.1 (C-2), 65.9 (C-4), 70.9 (C-3), 72.5 (C-5), 77.3 (OC(CH₃)₃), 79.9 (C-1), 154.1, 168.7, 160.1, 169.4 (C=O); HRMS m/z (ESI+) 567.1773, (C₂₃H₃₂O₁₃N₂Na: [M+ Na]⁺ requires 567.1797).

N*'-(2,3,4,6-Tetra-*O*-acetyl- β -D-galactopyranosyl)-L-asparagine 1-benzyl ester **2.55*

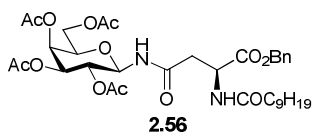


2.55

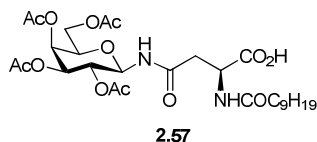
TFA (1.34 mL, 17.93 mmol, 10 equiv) in CH₂Cl₂ (1.34 mL) was added drop-wise to a solution of *N* ^{α} -*tert*-butoxycarbonyl-*N*'-(2,3,4,6-tetra-*O*-acetyl- β -D-galactopyranosyl)-L-asparagine 1-benzyl ester **2.53** (1.17 g, 1.79 mmol) in CH₂Cl₂ (10 mL) at 0 °C. The reaction mixture was allowed to warm to rt and stirred for 6 h. It was rotary evaporated. The reaction mixture was diluted in CH₂Cl₂ (50 mL) and washed with satd. aq. NaHCO₃ solution (50 mL), brine (50 mL) and H₂O (50 mL). It was concentrated *in vacuo* to yield the β -glycoside **2.55** (0.73 g, 74%, crude yield) as a white foam. The compound was used without further purification; ^1H NMR (300 MHz): δ 1.95 (s, 3 H, OC(O)CH₃), 1.99 (s, 3 H, OC(O)CH₃), 2.00 (s, 3 H, OC(O)CH₃), 2.10 (s, 3 H, OC(O)CH₃), 2.40 (dd, $J = 9.6$ Hz, 5.3 Hz, 1 H, H- β'), 2.63-2.67 (m, 1 H, H- β), 3.65-3.68 (m, 1 H, H- α), 3.97-4.11 (m, 3 H, H-5, H-6, H-6'), 5.07-5.12 (m, 4 H, CH₂Ph, H-2, H-3), 5.22 (t, $J = 9.3$ Hz, 1 H, H-1), 5.39 (d, $J = 1.4$ Hz, 1 H, H-4), 7.31-7.31 (m, 5 H, Ph), 8.09 (d, $J = 9.3$ Hz, 1 H, NH); HRMS m/z (ESI+) 553.2024, (C₂₅H₃₃O₁₂N₂: [M+ Na]⁺ requires 553.2033).

^{xix} Two overlapping signals.

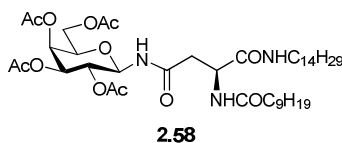
N*'-(2,3,4,6-Tetra-*O*-acetyl- β -D-galactopyranosyl)-*N* $^{\alpha}$ -(decanosyl)-L-asparagine 1-benzyl ester **2.56*



TBTU (56 mg, 0.18 mmol, 1.1 equiv) and HOBt (24 mg, 0.18 mmol, 1.1 equiv) were added to decanoic acid (27 mg, 0.16 mmol) in DMF (2 mL) containing 4 Å MS under N_2 at rt. It was stirred for 20 min and *N*'-(2,3,4,6-tetra-*O*-acetyl- β -D-galactopyranosyl)-L-asparagine 1-benzyl ester **2.55** (88 mg, 0.16 mmol, 1 equiv) in DMF (1 mL) was added drop-wise to the solution. It was stirred for 18 h. The reaction mixture was concentrated *in vacuo*; diluted with EtOAc (4 mL), washed with H_2O (4 mL), brine (4 mL), H_2O (4 mL), dried over $MgSO_4$, filtered and concentrated. Flash column chromatography (hexane/EtOAc 1:1) afforded the β -anomer **2.56** (60 mg, 54%) as a colourless oil; R_f = 0.36 (hexane/EtOAc 1:1); $[\alpha]_D^{22} = +27.27$ (c 1.76, $CHCl_3$); IR ν_{max} (NaCl plate, CH_2Cl_2): 3330.9, 2926.4, 1751.0, 1674.3, 1530.8 cm^{-1} ; 1H NMR (300 MHz): δ 0.86 (t, $J = 7.0$ Hz, 3 H, CH_3), 1.23-1.25 (m, 12 H, $(CH_2)_6CH_3$), 1.56-1.61 (m, 2 H, $COCH_2CH_2$), 1.98 (s, 3 H, $OC(O)CH_3$), 1.99 (s, 3 H, $OC(O)CH_3$), 2.03 (s, 3 H, $OC(O)CH_3$), 2.13 (s, 3 H, $OC(O)CH_3$), 2.19 (t, $J = 7.3$ Hz, 2 H, $COCH_2$), 2.70 (dd, $J = 4.4$ Hz, 16.4 Hz, 1 H, H- β'), 2.90 (dd, $J = 4.1$ Hz, 16.5 Hz, 1 H, H- β), 3.97-4.15 (m, 3 H, H-5, H-6, H-6'), 4.87-4.93 (m, 1 H, H- α), 5.04-5.20 (m, 5 H, H-1, H-2, H-3, CH_2Ph), 5.42 (d, $J = 2.0$ Hz, 1 H, H-4), 6.49 (d, $J = 8.7$ Hz, 1 H, $NHC1$), 6.73 (d, $J = 8.3$ Hz, 1 H, $NHCOC_9H_{19}$), 7.31-7.33 (m, 5 H, Ph); ^{13}C NMR (75 Hz): δ_c 14.1 (CH_2CH_3), 20.5 ($OC(O)CH_3$), 20.5 ($OC(O)CH_3$), 20.6 ($OC(O)CH_3$), 20.6 ($OC(O)CH_3$), 22.6, 25.5, 29.2, 29.2, 29.3, 29.4 ($(CH_2)_6CH_3$), 31.8 ($COCH_2CH_2$), 36.5 ($COCH_2$), 37.4 (C- β), 48.4 (C- α), 61.0 (C-6), 67.0 (C-4), 67.4 (CH_2Ph), 68.1 (C-2), 70.7 (C-3), 72.4 (C-5), 78.4 (C-1), 127.9, 128.3, 128.5, 135.2 (aromatics), 169.7 (C=O), 169.9 (C=O), 170.3 (C=O), 170.8 (C=O), 170.9 (C=O), 171.5 (C=O), 173.1 (C=O); HRMS m/z (ESI+) 707.3376, ($C_{35}H_{51}O_{13}N_2$: $[M+H]^+$ requires 707.3386).

N*^γ-(2,3,4,6-Tetra-*O*-acetyl-β-D-galactopyranosyl)-*N*^α-(decanosyl)-L-asparagine **2.57*

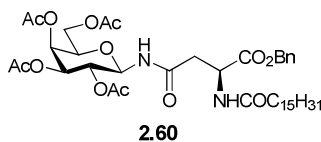
H₂ gas was bubbled through a suspension of *N*^γ-(2,3,4,6-tetra-*O*-acetyl-β-D-galactopyranosyl)-*N*^α-(decanosyl)-L-asparagine 1-benzyl ester **2.56** (56 mg, 0.08 mmol) and Pd (C) (6 mg, 10% w/w) in EtOAc (10 mL) at 1 atm. It was stirred for 3 h. The suspension was filtered through Celite, washed with EtOAc and concentrated *in vacuo* to yield the carboxylic acid **2.57** (30 mg, 61%, crude yield) as a colourless oil; ¹H NMR (300 MHz): δ 0.87 (t, *J* = 6.9 Hz, 3 H, CH₃); 1.23-1.26 (m, 12 H, (CH₂)₆CH₃), 1.60-1.65 (m, 2 H, COCH₂CH₂), 2.00 (s, 3 H, OC(O)CH₃), 2.05 (m, 6 H, OC(O)CH₃ × 2), 2.15 (s, 3 H, OC(O)CH₃), 2.30 (t, *J* = 8.0 Hz, 1 H, COCH₂), 2.77 (dd, *J* = 4.8 Hz, 16.5 Hz, 1 H, H-β'), 2.87 (dd, *J* = 3.6 Hz, 16.5 Hz, 1 H, H-β), 4.00-4.25 (m, 3 H, H-5, H-6, H-6'), 4.71-4.74 (m, 1 H, H-α), 5.10-5.16 (m, 2 H, H-2, H-3), 5.32-5.38 (m, 1 H, H-1), 5.52 (d, *J* = 1.7 Hz, 1 H, H-4), 6.56 (d, *J* = 9.4 Hz, 1 H, NHC1), 7.24 (d, *J* = 6.8 Hz, 1 H, NHCOC₉H₁₉); HRMS *m/z* (ESI⁺) 617.2900, (C₂₈H₄₄O₁₃N₂H: [M+ H]⁺ requires 617.2916).

N*^γ-(2,3,4,6-Tetra-*O*-acetyl-β-D-galactopyranosyl)-*N*^α-(decanosyl)-L-asparagine 1-tetradecylamide **2.58*

TBTU (14 mg, 0.05 mmol, 1.1 equiv) and HOBt (6 mg, 0.05 mmol, 1.1 equiv) were added to *N*^γ-(2,3,4,6-tetra-*O*-acetyl-β-D-galactopyranosyl)-*N*^α-(decanosyl)-L-asparagine **2.57** (25 mg, 0.04 mmol) in DMF (3 mL) containing 4 Å MS under N₂ at rt. The reaction mixture was stirred for 30 min and tetradecylamine (9 mg, 0.04 mmol, 1 equiv) was added to the solution under N₂. The reaction mixture was stirred for 3 h. It was subsequently concentrated *in vacuo*; diluted with EtOAc (4 mL), washed with brine (4 mL), H₂O (4 mL), dried over MgSO₄, filtered and concentrated. Flash

column chromatography (hexane/EtOAc 1:1) afforded the β -anomer **2.58** (18 mg, 55%) as a white solid; R_f = 0.10 (hexane/EtOAc 1:1); $[\alpha]_D^{25} = +20.00$ (c 0.75, CH_2Cl_2); IR ν_{max} (NaCl plate, CH_2Cl_2): 3286.1, 2924.1, 2853.8, 1751.2, 1642.6, 1546.1, 1466.7, cm^{-1} ; ^1H NMR (300 MHz): δ 0.87-0.87 (m, 6 H, $\text{CH}_3 \times 2$); 1.24-1.26 (m, 34 H, $\text{CO}(\text{CH}_2)_2(\text{CH}_2)_6\text{CH}_3$, $\text{NH}(\text{CH}_2)_2(\text{CH}_2)_{11}\text{CH}_3$), 1.42-1.46 (m, 2 H, NHCH_2CH_2), 1.63-1.66 (m, 2 H, COCH_2CH_2), 2.00 (s, 3 H, $\text{OC}(\text{O})\text{CH}_3$), 2.04 (s, 3 H, $\text{OC}(\text{O})\text{CH}_3$), 2.14 (s, 3 H, $\text{OC}(\text{O})\text{CH}_3$), 2.17 (s, 3 H, $\text{OC}(\text{O})\text{CH}_3$), 2.21-2.25 (m, 1 H, COCH_2), 2.45 (dd, $J = 5.6$ Hz, 15.5 Hz, 1 H, H- β'), 2.68 (dd, $J = 3.4$ Hz, 15.5 Hz, 1 H, H- β), 3.11- 3.18 (m, 2 H, NHCH_2), 3.99-4.16 (m, 3 H, H-5, H-6, H-6'), 4.67-4.71 (m, 1 H, H- α), 5.10-5.23 (m, 3 H, H-1, H-2, H-3), 5.44 (d, $J = 1.6$ Hz, 1 H, H-4), 6.74-6.79 (m, 2 H, NHC_1 , $\text{NHC}_{14}\text{H}_{29}$), 7.58 (d, $J = 7.6$ Hz, 1 H, $\text{NHCOC}_9\text{H}_{19}$); ^{13}C NMR (75 Hz): δ_c 14.1 (CH_2CH_3)^{xx}, 20.5 ($\text{OC}(\text{O})\text{CH}_3$), 20.6 ($\text{OC}(\text{O})\text{CH}_3$), 20.7 ($\text{OC}(\text{O})\text{CH}_3$), 20.9 ($\text{OC}(\text{O})\text{CH}_3$), 22.7, 22.7, 25.6, 26.9, 29.3, 29.3, 29.4, 29.4, 29.6, 29.6, 29.6, 29.7, 31.8 ($\text{CO}(\text{CH}_2)_2(\text{CH}_2)_6\text{CH}_3$, $\text{NH}(\text{CH}_2)(\text{CH}_2)_{12}\text{CH}_3$), 31.9 (COCH_2CH_2), 36.2 (COCH_2), 36.6 (C- β), 39.6 (C- β), 49.8 (C- α), 61.1 (C-6), 67.1 (C-4), 67.8 (C-2), 70.7 (C-3), 72.3 (C-5), 78.5 (C-1), 169.8 (C=O), 170.0 (C=O), 170.3 (C=O), 170.4 (C=O), 172.3 (C=O), 173.0 (C=O), 173.8 (C=O); HRMS m/z (ESI+) 834.5079, ($\text{C}_{42}\text{H}_{73}\text{O}_{12}\text{N}_3\text{Na}$: $[\text{M}+\text{Na}]^+$ requires 834.5086).

N*'-(2,3,4,6-Tetra-*O*-acetyl- β -D-galactopyranosyl)-*N* $^{\alpha}$ -(hexadecanosyl)-L-asparagine 1-benzyl ester **2.60*

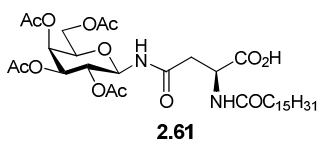


NEt_3 (57 μL , 0.411 mmol, 1 equiv) was added to *N*'-(2,3,4,6-tetra-*O*-acetyl- β -D-galactopyranosyl)-L-asparagine 1-benzyl ester **2.55** (227 mg, 0.411 mmol) in CH_2Cl_2 (8 mL) and the reaction mixture was stirred for 10 min at rt under N_2 . Hexadecanosyl chloride (125 μL , 0.411 mmol, 1 equiv) was added drop-wise to the solution and it was stirred for 18 h. The reaction mixture was concentrated *in vacuo*; diluted with EtOAc (4 mL), washed with 0.1 N aq. HCl (4 mL), satd. aq. NaHCO_3 (4 mL), brine (4 mL), dried over MgSO_4 , filtered and concentrated. Flash column chromatography

^{xx} Two overlapping signals.

(hexane/EtOAc 1:1) afforded the β -anomer **2.60** (136 mg, 42%) as a white solid; $R_f = 0.21$ (hexane/EtOAc 1:1); $[\alpha]^{22}_D = +21.33$ (c 0.75, CH_2Cl_2); IR ν_{max} (NaCl plate, CH_2Cl_2): 3440.0, 2095.1, 1750.3, 1644.9, 1226.3 cm^{-1} ; ^1H NMR (300 MHz): δ 0.86 (t, $J = 6.9$ Hz, 3 H, CH_3), 1.22-1.24 (m, 24 H, $(\text{CH}_2)_{12}\text{CH}_3$), 1.56-1.60 (m, 2 H, COCH_2CH_2), 1.97 (s, 3 H, $\text{OC}(\text{O})\text{CH}_3$), 2.00 (s, 3 H, $\text{OC}(\text{O})\text{CH}_3$), 2.03 (s, 3 H, $\text{OC}(\text{O})\text{CH}_3$), 2.12 (s, 3 H, $\text{OC}(\text{O})\text{CH}_3$), 2.19 (t, $J = 7.3$ Hz, 2 H, COCH_2), 2.70 (dd, $J = 4.4$ Hz, 16.4 Hz, 1 H, H- β'), 2.90 (dd, $J = 4.0$ Hz, 16.4 Hz, 1 H, H- β), 3.97-4.14 (m, 3 H, H-5, H-6, H-6'), 4.87-4.92 (m, 1 H, H- α), 5.07-5.19 (m, 5 H, H-1, H-2, H-3, CH_2Ph), 5.42 (d, $J = 2.0$ Hz, 1 H, H-4), 6.55 (d, $J = 8.7$ Hz, 1 H, NHC1), 6.75 (d, $J = 8.3$ Hz, 1 H, $\text{NHCOC}_{15}\text{H}_{31}$), 7.31- 7.32 (m, 5 H, Ph); ^{13}C NMR (75 Hz): δ_c 14.1 (CH_2CH_3), 20.5 ($\text{OC}(\text{O})\text{CH}_3$), 20.6 ($\text{OC}(\text{O})\text{CH}_3$), 20.6 ($\text{OC}(\text{O})\text{CH}_3$), 20.7 ($\text{OC}(\text{O})\text{CH}_3$), 22.7, 25.5, 29.2, 29.3, 29.3, 29.5, 29.6, 29.7 ($(\text{CH}_2)_{12}\text{CH}_3$), 31.9 (COCH_2CH_2), 36.5 (COCH_2), 37.5 (C- β), 48.5 (C- α), 61.0 (C-6), 67.0 (C-4), 67.4 (CH_2Ph), 68.2 (C-2), 70.7 (C-3), 72.4 (C-5), 78.5 (C-1), 127.9, 128.4, 128.6, 135.3 (aromatics), 169.8 (C=O), 169.9 (C=O), 170.3 (C=O), 170.9 (C=O), 170.9 (C=O), 171.5 (C=O), 173.1 (C=O); HRMS m/z (ESI+) 792.4389, ($\text{C}_{41}\text{H}_{62}\text{O}_{13}\text{N}_2\text{H}$: $[\text{M} + \text{H}]^+$ requires 792.4358).

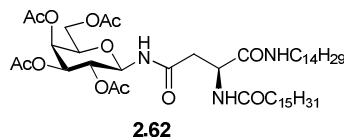
***N'*-(2,3,4,6-Tetra-*O*-acetyl- β -D-galactopyranosyl)-*N* $^\alpha$ -(hexadecanosyl)-L-asparagine
2.61**



H_2 gas was bubbled through a suspension of *N'*-(2,3,4,6-tetra-*O*-acetyl- β -D-galactopyranosyl)-*N* $^\alpha$ -(hexadecanosyl)-L-asparagine 1-benzyl ester **2.60** (136 mg, 0.17 mmol) and Pd (C) (14 mg, 10% w/w) in EtOAc (5 mL) at 1 atm at rt and was stirred for 18 h. The suspension was filtered through Celite, washed with EtOAc and the filtrate was concentrated *in vacuo* to yield the carboxylic acid **2.61** (104 mg, 86%, crude yield) as a white solid; ^1H NMR (300 MHz): δ 0.85 (t, $J = 6.9$ Hz, 3 H, CH_3), 1.21-1.24 (m, 24 H, $(\text{CH}_2)_{12}\text{CH}_3$), 1.58-1.63 (m, 2 H, COCH_2CH_2), 1.98 (s, 3 H, $\text{OC}(\text{O})\text{CH}_3$), 2.01 (s, 3 H, $\text{OC}(\text{O})\text{CH}_3$), 2.04 (s, 3 H, $\text{OC}(\text{O})\text{CH}_3$), 2.14 (s, 3 H, $\text{OC}(\text{O})\text{CH}_3$), 2.29 (t, $J = 8.0$ Hz, 2 H, COCH_2), 2.77-2.91 (m, 2 H, H- β , H- β'), 3.95- 4.25 (m, 3 H, H-

5, H-6, H-6'), 4.70-4.72 (m, 1 H, H- α), 5.09-5.11 (m, 2 H, H-2, H-3), 5.35-5.41 (m, 1 H, H-1), 5.50-5.52 (m, 1 H, H-4), 6.76 (d, $J = 9.5$ Hz, 1 H, NHC1), 7.18 (d, $J = 7.0$ Hz, 1 H, NHCOC₁₅H₃₁); HRMS m/z (ESI+) 701.3861, (C₃₄H₅₆O₁₃N₂H: [M+H]⁺ requires 701.3855).

N*'-(2,3,4,6-Tetra-*O*-acetyl- β -D-galactopyranosyl)-*N* ^{α} -(tetradecanosyl)-L-asparagine 1-tetradecylamide **2.62*

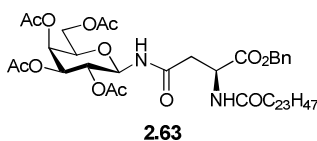


TBTU (51 mg, 0.16 mmol, 1.1 equiv) and HOBt (21 mg, 0.16 mmol, 1.1 equiv) were added to *N*'-(2,3,4,6-tetra-*O*-acetyl- β -D-galactopyranosyl)-*N* ^{α} -(hexadecanosyl)-L-asparagine **2.61** (27 mg, 0.03 mmol) in DMF (3 mL) under N₂ at rt. Tetradecylamine (61 mg, 0.29 mmol, 2 equiv) was added slowly to the solution and the reaction mixture was stirred for 18 h. The reaction mixture was concentrated *in vacuo*. Flash column chromatography (hexane/EtOAc 1:1) afforded the title compound **2.62** (120 mg, 98%) as a white solid; $R_f = 0.17$ (hexane/EtOAc 1:1); $[\alpha]_D^{28} = +5.71$ (c 1.05, CH₂Cl₂); IR ν_{\max} (NaCl plate, CH₂Cl₂): 3292.3, 2921.0, 2851.5, 1750.4, 1645.9, 1546.1, 1371.0, 1227.8, 1054.6 cm⁻¹; ¹H NMR (300 MHz): δ 1.20-1.22 (m, 46 H, CO(CH₂)₂(CH₂)₁₂CH₃, NH(CH₂)₂(CH₂)₁₁CH₃), 1.40-1.44 (m, 2 H, NHCH₂CH₂), 1.57-1.61 (m, 2 H, COCH₂CH₂), 1.97 (s, 3 H, OC(O)CH₃), 2.01 (s, 3 H, OC(O)CH₃), 2.11 (s, 3 H, OC(O)CH₃), 2.14 (s, 3 H, OC(O)CH₃), 2.16-2.22 (m, 1 H, COCH₂), 2.43 (dd, $J = 5.7$ Hz, 15.7 Hz, 1 H, H- β'), 2.68 (dd, $J = 3.6$ Hz, 15.7 Hz, 1 H, H- β), 3.01- 3.16 (m, 2 H, NHCH₂), 3.98-4.14 (m, 3 H, H-5, H-6, H-6'), 4.65-4.71 (m, 1 H, H- α), 5.11-5.25 (m, 3 H, H-1, H-2, H-3), 5.42 (d, $J = 1.3$ Hz, 1 H, H-4), 6.78 (t, $J = 5.6$ Hz, 1 H, NHC₁₄H₂₉), 6.89 (d, $J = 8.5$ Hz, 1 H, NHC1), 7.56 (d, $J = 7.7$ Hz, 1 H, NHCOC₁₅H₃₁); ¹³C NMR (75 Hz): δ_c 13.1 (CH₂CH₃)^{xxi}, 19.5 (OC(O)CH₃), 19.7 (OC(O)CH₃), 19.9 (OC(O)CH₃), 20.0 (OC(O)CH₃), 21.7, 24.6, 25.9, 28.3, 28.4, 28.5, 28.6, 28.6, 28.7, 28.7, (CO(CH₂)₂(CH₂)₁₂CH₃, NH(CH₂)(CH₂)₁₂CH₃), 30.9 (COCH₂CH₂), 35.3 (COCH₂), 35.6 (C- β), 38.6 (NHCH₂), 48.8 (C- α), 60.1 (C-6), 66.1 (C-4), 66.9 (C-2), 69.8 (C-3), 71.4 (C-5),

^{xxi} Two overlapping signals.

77.4 (C-1), 168.9 (C=O), 169.0 (C=O), 169.3 (C=O), 169.5 (C=O), 171.0 (C=O), 171.9 (C=O), 172.8 (C=O); HRMS m/z (ESI+) 896.6226, ($C_{48}H_{85}O_{12}N_3H$: $[M+H]^+$ requires 896.6206).

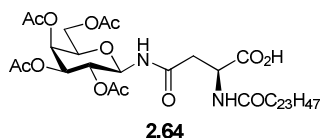
N^{ν} -(2,3,4,6-Tetra-*O*-acetyl- β -D-galactopyranosyl)- N^{α} -(tetracosyl)-L-asparagine 1-benzyl ester **2.63**



TBTU (59 mg, 0.18 mmol, 1.1 equiv) and HOBt (25 mg, 0.18 mmol, 1.1 equiv) were added to lignoceric acid (62 mg, 0.17 mmol) in DMF (3 mL) containing 4 Å MS under N_2 at rt. It was stirred for 30 min and then N^{ν} -(2,3,4,6-tetra-*O*-acetyl- β -D-galactopyranosyl)-L-asparagine 1-benzyl ester **2.55** (88 mg, 0.16 mmol, 1 equiv) in DMF (2 mL) was added drop-wise to the solution. It was stirred for 2 h at 50 °C. The reaction mixture was concentrated *in vacuo*; diluted with EtOAc (4 mL), washed with H_2O (4 mL), brine (4 mL), H_2O (4 mL), dried over $MgSO_4$, filtered and concentrated. Flash column chromatography (hexane/EtOAc 1:1) afforded the title compound **2.63** (93 mg, 62%) as a white solid; R_f = 0.23 (hexane/EtOAc 1:1); $[\alpha]_D^{25} = +18.95$ (c 0.95, EtOAc); IR ν_{max} (NaCl plate, CH_2Cl_2): 2918.7, 2850.5, 1750.5, 1371.1 cm^{-1} ; 1H NMR (300 MHz): δ 0.86 (t, $J = 7.0$ Hz, 3 H, CH_3), 1.23-1.25 (m, 40 H, $(CH_2)_{20}CH_3$), 1.56-1.61 (m, 2 H, $COCH_2CH_2$), 1.99 (s, 3 H, $OC(O)CH_3$), 2.03 (s, 3 H, $OC(O)CH_3$), 2.04 (s, 3 H, $OC(O)CH_3$), 2.13 (s, 3 H, $OC(O)CH_3$), 2.19 (t, $J = 7.5$ Hz, 2 H, $COCH_2$), 2.70 (dd, $J = 4.4$ Hz, 16.4 Hz, 1 H, H- β'), 2.90 (dd, $J = 3.9$ Hz, 16.4 Hz, 1 H, H- β), 3.97-4.15 (m, 3 H, H-5, H-6, H-6'), 4.88-4.93 (m, 1 H, H- α), 5.07-5.20 (m, 5 H, H-1, H-2, H-3, CH_2Ph), 5.42 (d, $J = 2.0$ Hz, 1 H, H-4), 6.49 (d, $J = 8.6$ Hz, 1 H, $NHC1$), 6.73 (d, $J = 8.3$ Hz, 1 H, $NHCOC_{23}H_{47}$), 7.31- 7.33 (m, 5 H, Ph); ^{13}C NMR (75 Hz): δ_c 14.1 (CH_2CH_3), 20.5 ($OC(O)CH_3$), 20.6 ($OC(O)CH_3$), 20.6 ($OC(O)CH_3$), 20.6 ($OC(O)CH_3$), 22.7, 25.5, 29.2, 29.3, 29.3, 29.5, 29.6, 29.7 ($(CH_2)_{20}CH_3$), 31.9 ($COCH_2CH_2$), 36.5 ($COCH_2$), 37.5 (C- β), 48.4 (C- α), 61.0 (C-6), 67.0 (C-4), 67.4 (CH_2Ph), 68.1 (C-2), 70.7 (C-3), 72.4 (C-5), 78.5 (C-1), 127.9, 128.4, 128.5, 135.2 (aromatics), 169.8 (C=O),

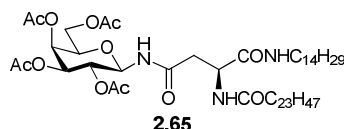
169.9 (C=O), 170.3 (C=O), 170.8 (C=O), 170.9 (C=O), 171.5 (C=O), 173.1 (C=O); HRMS m/z (ESI+) 904.5632, ($C_{49}H_{78}O_{13}N_2H$: $[M+H]^+$ requires 904.5610).

N*'-(2,3,4,6-Tetra-*O*-acetyl- β -D-galactopyranosyl)-*N* $^{\alpha}$ -(tetracosyl)-L-asparagine **2.64*



H_2 gas was bubbled through a suspension of *N*'-(2,3,4,6-tetra-*O*-acetyl- β -D-galactopyranosyl)-*N* $^{\alpha}$ -(tetracosyl)-L-asparagine 1-benzyl ester **2.63** (67 mg, 0.07 mmol) and Pd (C) (7 mg, 10% w/w) in EtOAc (5 mL) at 1 atm pressure and stirred for 18 h. The suspension was filtered through Celite, washing with EtOAc and concentrated *in vacuo* to yield the title compound **2.64** (60 mg, 55%, , crude yield) as a white solid; 1H NMR (300 MHz): δ 0.87 (t, $J = 6.9$ Hz, 3 H, CH_3), 1.23-1.25 (m, 40 H, $(CH_2)_{20}CH_3$), 1.58-1.67 (m, 2 H, $COCH_2CH_2$), 2.00 (s, 3 H, $OC(O)CH_3$), 2.05 (s, 3 H, $OC(O)CH_3$), 2.06 (s, 3 H, $OC(O)CH_3$), 2.15 (s, 3 H, $OC(O)CH_3$), 2.26-2.37 (m, 2 H, $COCH_2$), 2.74 (dd, $J = 5.0$ Hz, 16.5 Hz, 1 H, H- β'), 2.84-2.96 (m, 1 H, H- β), 4.02-4.22 (m, 3 H, H-5, H-6, H-6'), 4.71-4.76 (m, 1 H, H- α), 5.10-5.12 (m, 2 H, H-2, H-3), 5.28-5.34 (m, 1 H, H-1), 5.50 (d, $J = 1.2$ Hz, 1 H, H-4), 6.61 (d, $J = 9.2$ Hz, 1 H, $NHC1$), 7.20 (d, $J = 7.0$ Hz, 1 H, $NHCOC_{23}H_{47}$); HRMS m/z (ESI+) 813.5106, ($C_{42}H_{72}O_{13}N_2H$: $[M+H]^+$ requires 813.5107).

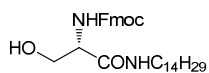
N*'-(2,3,4,6-Tetra-*O*-acetyl- β -D-galactopyranosyl)-*N* $^{\alpha}$ -(tetracosyl)-L-asparagine 1-tetradecylamide **2.65*



TBTU (12 mg, 0.04 mmol, 1.1 equiv) and HOBT (5 mg, 0.04 mmol, 1.1 equiv) were added to *N*'-(2,3,4,6-tetra-*O*-acetyl- β -D-galactopyranosyl)-*N* $^{\alpha}$ -(tetracosyl)-L-asparagine **2.64** (27 mg, 0.03 mmol) in DMF (3 mL) containing 4 Å MS under N_2 at rt. The solution was stirred for 20 min and tetradecylamine (7 mg, 0.03 mmol, 1 equiv) was added to the solution and was stirred for 18 h. The reaction mixture was

concentrated *in vacuo*; diluted with EtOAc (4 mL), washed with brine (4 mL), H₂O (4 mL), dried over MgSO₄, filtered and concentrated. Flash column chromatography (hexane/EtOAc 1:1) afforded the title compound **2.54** (15 mg, 45%) as a white solid; $R_f = 0.20$ (hexane/EtOAc 1:1); $[\alpha]_D^{25} = +9.23$ (c 0.65, CH₂Cl₂); IR ν_{\max} (NaCl plate, CH₂Cl₂): 3426.0, 2918.5, 2850.5, 1750.7, 1641.8, 1228.5 cm⁻¹; ¹H NMR (300 MHz): δ 0.87 (t, $J = 6.9$ Hz, 3 H, CH₃), 1.23-1.25 (m, 62 H, CO(CH₂)₂(CH₂)₂₀CH₃, NH(CH₂)₂(CH₂)₁₁CH₃), 1.42-1.46 (m, 2 H, NHCH₂CH₂), 1.64-1.67 (m, 2 H, COCH₂CH₂), 2.00 (s, 3 H, OC(O)CH₃), 2.04 (s, 3 H, OC(O)CH₃), 2.14 (s, 3 H, OC(O)CH₃), 2.17 (s, 3 H, OC(O)CH₃), 2.21-2.24 (m, 1 H, COCH₂), 2.43 (dd, $J = 5.6$ Hz, 15.7 Hz, 1 H, H- β'), 2.68 (dd, $J = 3.5$ Hz, 15.7 Hz, 1 H, H- β), 3.11- 3.26 (m, 1 H, NHCH₂), 3.98-4.17 (m, 3 H, H-5, H-6, H-6'), 4.66-4.71 (m, 1 H, H- α), 5.10-5.26 (m, 3 H, H-1, H-2, H-3), 5.44 (d, $J = 1.8$ Hz, 1 H, H-4), 6.73-6.78 (m, 2 H, NHC₁, NHC₁₄H₂₉), 7.57 (d, $J = 7.8$ Hz, 1 H, NHCOC₂₃H₄₇); ¹³C NMR (75 Hz): δ_c 14.1 (CH₂CH₃)^{xxii}, 20.5 (OC(O)CH₃), 20.6 (OC(O)CH₃), 20.6 (OC(O)CH₃), 20.9 (OC(O)CH₃), 22.7, 25.6, 26.9, 29.3, 29.7 (CO(CH₂)₂(CH₂)₂₀CH₃, NH(CH₂)₂(CH₂)₁₂CH₃), 31.9 (COCH₂CH₂), 36.2 (COCH₂), 36.6 (C- β), 49.7 (C- α), 39.6 (NHCH₂), 61.0 (C-6), 67.0 (C-4), 67.8 (C-2), 70.7 (C-3), 72.3 (C-5), 78.5 (C-1), 169.8 (C=O), 170.0 (C=O), 170.3 (C=O), 170.4 (C=O), 172.2 (C=O), 173.0 (C=O), 173.8 (C=O); HRMS m/z (ESI+) 1008.7429, (C₅₆H₁₀₁O₁₂N₃H: [M+H]⁺ requires 1008.7458).

N*-(9-Fluorenylmethyloxycarbonyl)-L-serine tetradecyl amide **2.66* ^[257]



2.66

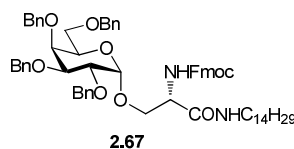
DMF (5 mL) was added to a mixture of *N*-(9-fluorenylmethyloxycarbonyl)-L-serine **4.23** (1 g, 3.06 mmol), TBTU (1.08 g, 3.37 mmol, 1.2 equiv) and HOBt (455 mg, 3.37 mmol, 1.2 equiv), DIPEA (1.07 mL, 6.12 mmol, 2 equiv) under nitrogen and was left to stir for 10 min. Tetradecylamine (652 mg, 3.06 mmol, 1 equiv) was then added under N₂ to the reaction mixture and was left to stir for 18 h. It was rotary evaporated, re-dissolved in CH₂Cl₂ (25 mL); washed with brine (30 mL) and 0.2 N aq.

^{xxii} Two overlapping signals.

HCl (30 mL). The aqueous layer was extracted with CH_2Cl_2 (25 mL x 3), and the combined organic layers were washed with satd. aq. NaHCO_3 (30 mL). The organic layer was dried over MgSO_4 , filtered and concentrated. A silica plug was performed (CH_2Cl_2) to give the title compound **2.66** as a white solid (1.16 g, 73%); $R_f = 0.36$ (PetEt/EtOAc 5:1); $^1\text{H NMR}$ (300 MHz): δ 0.86-0.90 (t, $J = 6.9$ Hz, 3 H, CH_3), 1.22-1.25 (m, 22 H, $\text{NHCH}_2\text{CH}_2(\text{CH}_2)_{11}\text{CH}_3$), 1.45 (s, 2 H, NHCH_2CH_2), 3.18-3.24 (m, 2 H, NHCH_2), 3.64-3.71 (m, 1 H, H- β), 4.03-4.06 (m, 1 H, H- β'), 4.16-4.21 (m, 2 H, H- α , $\text{CH}(\text{Fmoc})$), 4.37-4.40 (m, 2 H, $\text{CH}_2(\text{Fmoc})$), 6.08 (d, $J = 7.5$ Hz, 1 H, NHFmoc), 6.75 (s, 1 H, NHCH_2), 7.26-7.76 (m, 8 H, aromatics); HRMS m/z (ESI+) 522.3438 ($\text{C}_{32}\text{H}_{46}\text{N}_2\text{O}_4$: $[\text{M}^*]^+$ requires 522.3452).

The $^1\text{H NMR}$ data is in agreement with the literature.^[257]

N*-(9-Fluorenylmethyloxycarbonyl)-O-(2,3,4,6-tetra-O-benzyl- α -D-galactopyranosyl)-L-serine tetradecyl amide **2.67*

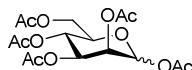


NIS (29 mg, 0.128 mmol, 2 equiv) was added to a solution of phenyl-2,3,4,6-tetra-*O*-benzyl-1-thio- β -D-galactopyranoside **4.54** (41 mg, 0.06 mmol), and *N*-(9-fluorenylmethyloxycarbonyl)-L-serine tetradecyl amide **2.66** (67 mg, 0.13 mmol, 2 equiv) in THF (3 mL) containing 4Å MS in the dark under N_2 . TfOH (1 μL , 0.0006 mmol, 0.01 equiv) was added and the reaction mixture was stirred for 20 h and MeOH was added. It was rotary evaporated and then was diluted with CH_2Cl_2 (20 mL) and washed with satd. aq. $\text{Na}_2\text{S}_2\text{O}_4$ (20 mL) followed by brine (20 mL). The organic layer was dried (Na_2SO_4), filtered and concentrated. Flash column chromatography (PetEt/EtOAc 5:1) afforded the α -diastereoisomer **2.67** (34 mg, 49%) as a white solid; $R_f = 0.15$ (PetEt/EtOAc 5:1); $[\alpha]_D^{25} = +75.79$ (c, 0.95 in CH_2Cl_2); IR ν_{max} (NaCl plate, CH_2Cl_2): 3300.1, 3031.5, 2923.6, 2853.5, 1686.0, 1644.9, 1535.4 cm^{-1} ; $^1\text{H NMR}$ (300 MHz): δ 0.87 (t, $J = 6.9$ Hz, 3 H, CH_3), 1.23-1.25 (m, 24 H, $\text{NHCH}_2(\text{CH}_2)_{12}\text{CH}_3$), 2.61-2.70 (m, 1 H, NHCHH), 3.05-3.10 (m, 1 H, NHCHH), 3.50-3.54 (m, 3 H- β , H- β' , H-6'), 3.84-3.89 (m, 1 H, H-3), 3.93-4.03 (m, 3 H, H-4, H-5, H-6), 4.08-4.16

(m, 2 H, H-2, H- α), 4.20 (t, $J = 6.7$ Hz, 1 H, CH(Fmoc)), 4.38 (m, 2 H, CH₂(Fmoc)), 4.34-4.96 (m, 8 H, CH₂Ph \times 4), 5.03 (d, $J = 3.0$ Hz, 1 H, H-1), 6.07 (d, $J = 6.4$ Hz, 1 H, NHFmoc), 6.95 (s, 1 H, NHCH₂), 7.25-7.40 (m, 24 H, aromatics), 7.59 (d, $J = 7.3$ Hz, 2 H, aromatics), 7.74 (d, $J = 7.4$ Hz, 2 H, aromatics); ¹³C NMR (75 Hz): δ_c 13.1 (CH₃), 21.7, 25.8, 28.3, 28.4, 28.6, 28.7, 28.7, 30.9, 38.5 (NH (CH₂)₁₃CH₃), 46.1 (CHFmoc), 51.9 (C- α), 65.9 (CH₂Fmoc), 67.9 (C- β), 68.0 (C-6), 68.9 (C-5), 71.7 (CH₂Ph), 72.5 (CH₂Ph), 73.5 (CH₂Ph), 73.7 (C-4), 73.7 (CH₂Ph), 76.2 (C-2), 78.4 (C-3), 97.5 (C-1), 118.9, 124.0, 124.1, 126.1, 126.3, 126.5, 126.6, 126.6, 126.7, 126.7, 126.8, 126.9, 126.97, 127.1, 127.2, 127.2, 127.3, 127.3, 127.4, 127.4, 127.4, 127.5, 136.5, 136.7, 137.3, 137.5, 140.3 (aromatics), 154.7 (C=O), 167.98 (C=O); HRMS m/z (ESI+) 1045.5971 (C₆₆H₈₀N₂O₄₉H: [M+H]⁺ requires 1045.5937).

7.2.2. Experimental procedures for Chapter 3

1,2,3,4,6-Penta-*O*-acetyl- α -D-mannopyranose

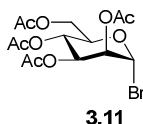


Ac₂O (5.29 mL, 55.5 mmol, 10 equiv) was added to D-mannose **3.10** (1.00 g, 5.55 mmol) in Pyr (10 mL) at 0 °C. The reaction mixture was stirred for 18 h at rt. The suspension was diluted with ice-water (20 mL) and extracted with EtOAc (20 mL). The organic layer was washed successively with H₂O (20 mL \times 3), satd. aq. NaHCO₃ solution (20 mL), satd. aq. CuSO₄ solution (20 mL) and H₂O (20 mL). The organic layer was dried over MgSO₄, filtered and concentrated under reduced pressure, yielding 1,2,3,4,6-penta-*O*-acetyl- α,β -D-mannopyranose (1.71 g, 78%, crude yield) (α/β 5:1) as a pale yellow oil; Data recorded for α -anomer: $R_f = 0.69$ (hexane/EtOAc 1:1); ¹H NMR (500 MHz, α -anomer): δ 1.86 (s, 3 H, OC(O)CH₃), 1.92 (s, 3 H, OC(O)CH₃), 1.93 (s, 3 H, OC(O)CH₃), 2.02-2.03 (m, 6 H, OC(O)CH₃ \times 2), 3.94-3.98 (m, 2H, H-5, H-6'), 4.15 (dd, 1 H, $J = 5.0$ Hz, 12.5 Hz, H-6), 5.13 (dd, 1 H, $J = 2.3$ Hz, 4.2 Hz, H-2), 5.22-5.23 (m, 1 H, H-3), 5.95 (d, $J = 2.2$ Hz, H-1). Ac₂O (52.5 mL, 0.56 mol, 10 equiv) was added to D-mannose **3.10** (10.0 g, 55.5 mmol) at rt. Catalytic H₂SO₄ (5 drops) was added slowly to this solution at 0 °C. The reaction mixture was stirred for 3 h and the suspension was diluted with ice-water (200 mL) and extracted with

EtOAc (200 mL). The organic layer was washed with H₂O (200 mL x 3), followed by aq. NaHCO₃ solution (200 mL). The organic layer was dried over MgSO₄, filtered and concentrated under reduced pressure, yielding 1,2,3,4,6-Penta-*O*-acetyl- α -D-mannopyranose (17.6 g, 82%) (α -anomer) as a pale yellow oil.

The NMR data are in agreement with the reported values. ^{[116],[258]}

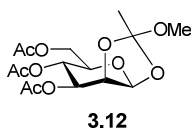
2,3,4,6-Tetra-*O*-acetyl- α -D-mannopyranosyl bromide **3.11**



33% HBr/AcOH (53 mL) was added to 1,2,3,4,6-penta-*O*-acetyl- α -D-mannopyranose (17.6 g, 45.0 mmol) at 0 °C. The solution was allowed to warm to rt and was stirred for 18 h at rt. The reaction mixture was concentrated, diluted with CH₂Cl₂ (300 mL), washed with brine (300 mL) followed by satd. aq. NaHCO₃ (300 mL x 2). The organic layer was dried over MgSO₄, filtered and concentrated *in vacuo* to yield the α -anomer **3.11** (16.6 g, 92%, crude yield) as a pale yellow oil; R_f = 0.55 (hexane/EtOAc 1:1); $[\alpha]^{22}_D = +111.7$ (c, 2.5 in CHCl₃); ¹H NMR (500 MHz) : 1.95 (s, 3 H, OC(O)CH₃), 2.02 (s, 3 H, OC(O)CH₃), 2.05 (s, 3 H, OC(O)CH₃), 2.12 (s, 3 H, OC(O)CH₃), 4.09 (dd, *J* = 10.2 Hz, 12.5 Hz, 1 H, H-5), 4.15-4.18 (m, 1 H, H-6), 4.27 (dd, *J* = 4.9 Hz, 12.5 Hz, 1H, H-6'), 5.31 (dd, *J* = 9.3 Hz, 10.2 Hz, 1 H, H-4), 5.38-5.39 (m, 1 H, H-2), 5.64-5.67 (m, 1 H, H-3), 6.25 (s, 1 H, H-1).

The NMR data is in agreement with the reported values. ^[258-259]

3,4,6-Tri-*O*-acetyl-1,2-*O*-(methoxyethylidene)- β -D-mannopyranoside **3.12**

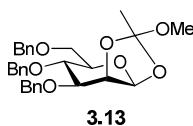


MeOH (1 mL) was added to a solution of 2,3,4,6-tetra-*O*-acetyl- α -D-mannopyranosyl bromide **3.11** (1.00 g, 2.43 mmol) in Pyr (2 mL) under an inert atmosphere and the reaction mixture was stirred for 18 h at rt. The reaction mixture was added to ice-water (20 mL) and extracted with CH₂Cl₂ (5 mL x 3). The

organic layers were combined and subsequently washed with H₂O. The organic layer was dried over MgSO₄, filtered and concentrated, azeotroping with toluene. Flash column chromatography (PetEt/EtOAc 3:1) yielded the title compound **3.12** (0.50 g, 57%) as a mixture of diastereoisomers (1:4 endo/exo); For the exo product: ¹H NMR (500 MHz): δ 1.70 (s, 3 H, CH₃), 2.01 (s, 3 H, OC(O)CH₃), 2.03 (s, 3 H, OC(O)CH₃), 2.01 (s, 3 H, OC(O)CH₃), 3.23 (s, 3 H, OCH₃), 3.64 -3.67 (m, 1 H, H-5), 4.09 (dd, *J* = 3.0 Hz, 12.5 Hz, 1 H, H-6'), 4.18-4.21 (m, 1 H, H-6), 4.57 (dd, *J* = 2.9 Hz, 4.0 Hz, 1 H, H-2), 5.12 (dd, *J* = 4.0 Hz, 10.0 Hz, 1 H, H-4), 5.23-5.27 (m, 1 H, H-3), 5.46 (d, *J* = 2.9 Hz, 1 H, H-1).

The NMR data is in agreement with the reported values.^[115]

3,4,6-Tri-*O*-benzyl-1,2-*O*-(methoxyethylidene)-β-D-mannopyranoside **3.13**

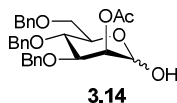


Na metal (1 mg approx., 0.064 mmol approx., 0.1 equiv approx.) was added to a solution of 3,4,6-tri-*O*-acetyl-1,2-*O*-(methoxyethylidene)-β-D-mannopyranoside **3.12** (0.23 g, 0.64 mmol) in MeOH (2 mL) at rt. The reaction mixture was stirred for 1 h; quenched with Amberlite ion-exchange resin (H⁺ form), filtered and concentrated *in vacuo*. The resulting solid was then dissolved in DMF (20 mL) and NaH (60% suspension in mineral oil) (1.16 g, 29.0 mmol, 6 equiv) was added in portions at 0 °C in an inert atmosphere. The reaction mixture was stirred for 30 min. BnBr (2.58 mL, 21.7 mmol, 4.5 equiv) was added to this suspension and the reaction mixture was stirred for 18 h at rt. MeOH (1 mL) was added to the reaction mixture. The suspension was added to ice-water (40 mL) and extracted with toluene (3 × 20 mL). The combined organic extracts were dried over MgSO₄, filtered and concentrated under reduced pressure. Flash column chromatography (PetEt/EtOAc 10:1 to 8:1) afforded the title compound **3.13** (2.44 g, 100%) as a mixture of diastereoisomers (1:4 endo/exo); R_f = 0.83 (hexane/EtOAc 3:1); For the exo product: ¹H NMR (500 MHz): δ 1.79 (s, 3 H, CH₃), 3.33 (s, 3 H, OCH₃), 3.46-3.48 (m, 1 H, H-5), 3.74-3.81 (m 2 H, H-6, H-6'), 3.96-3.97 (m, 1 H, H-4), 4.44 (dd, *J* = 2.5 Hz, 4.0 Hz, 1 H,

H-3), 4.58-4.60 (m, 2 H, CH_2Ph), 4.64-4.67 (m, 2 H, CH_2Ph), 4.82 (d, $J = 4.0$ Hz, 2 H, CH_2Ph), 4.94-4.95 (m, 1 H, H-2), 5.38 (d, $J = 2.5$ Hz, 1 H, H-1), 7.27-7.45 (m, 15 H, Ph $\times 3$).

The NMR data is in agreement with the reported values.^[260]

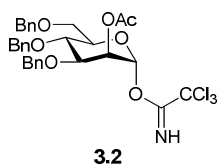
2-*O*-Acetyl-3,4,6-tri-*O*-benzyl- α,β -D-mannopyranoside **3.14**



80% AcOH in water (200 mL) was added to 3,4,6-tri-*O*-benzyl-1,2-*O*-(methoxyethylidene)- β -D-mannopyranoside **3.13** (6.22 g, 12.3 mmol) at rt and stirred for 18 h. The reaction mixture was added to a mixture of toluene (300 mL) and H₂O (200 mL) and the organic layer was separated, and successively washed with H₂O (200 mL), satd. aq. NaHCO₃ (200 mL) and H₂O (200 mL). NEt₃ was added drop-wise until a pH of approx. 7 was reached and the reaction mixture was concentrated *in vacuo*. Flash column chromatography (PetEt/EtOAc 3:1) yielded the title compound **3.14** (5.12 g, 85%) as a mixture of anomers (1:100 α/β); Data recorded for β -anomer: $R_f = 0.15$ (PetEt/EtOAc 3:1); ¹H NMR (500 MHz): δ 2.24 (s, 3 H, OC(O)CH₃), 3.74-3.75 (m, 1 H, H-5), 4.11-4.16 (m, 2 H, H-6, H-6'), 4.52-4.66 (m, 6 H, $CH_2Ph \times 3$), 4.75-4.77 (m, 1 H, H-4), 4.93 (d, $J = 11.0$ Hz, 1 H, H-1), 5.25 (dd, $J = 2.0$ Hz, 4.0 Hz, 1 H, H-3), 5.43 (dd, $J = 2.0$ Hz, 11.0 Hz, 1 H, H-2), 7.22-7.41 (m, 15 H, Ph $\times 3$).

The NMR data is in agreement with the reported values.^[260]

2-*O*-Acetyl-3,4,6-tri-*O*-benzyl- α -D-mannopyranosyl trichloroacetimidate **3.2**

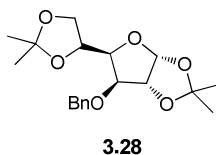


Trichloroacetonitrile (40 μ L, 0.40 mmol, 5 equiv) was added to a solution of 2-*O*-acetyl-3,4,6-tri-*O*-benzyl- α,β -D-mannopyranoside **3.14** (39 mg, 0.08 mmol) in CH₂Cl₂

(2 mL), followed by DBU (0.50 μ L, 0.01 mmol, 0.05 equiv) under an inert atmosphere at 0 °C. The reaction mixture was stirred for 2.5 h at rt and then concentrated *in vacuo*. Flash column chromatography was performed (PetEt/EtOAc 5:1) to α -anomer **3.2** (29 mg, 58%) as a colourless oil; R_f =0.80 (PetEt/EtOAc 5:1); ^1H NMR (500 MHz): δ 2.12 (s, 3 H, OCOCH_3), 3.72 (dd, J = 1.8 Hz, 11.2 Hz, 1 H, H-6'), 3.85 (dd, J = 3.7 Hz, 11.2 Hz, 1 H, H-6), 4.00-4.01, 4.04-4.05 (m, 3 H, H-3, H-4, H-5), 4.50-4.89 (m, 6 H, $\text{CH}_2\text{Ph} \times 3$), 5.50-5.51 (m, 1 H, H-2), 6.31 (d, J = 1.9 Hz, 1 H, H-1), 7.18-7.36 (m, 15 H, aromatics), 8.68 (s, 1 H, NH).

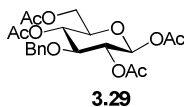
The NMR data is in agreement with the reported values.^[115]

3-*O*-benzyl-1,2:5,6-di-*O*-isopropylidene- α -D-glucopyranoside **3.28**

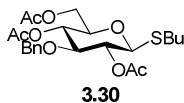


NaH (60% suspension in mineral oil) (3.02 g, 37.8 mmol, 2 equiv) was slowly added to a solution of diacetone-D-glucofuranose **3.27** (9.84 g, 37.8 mmol) in DMF (100 mL) in an inert atmosphere at 0 °C. The reaction mixture was stirred for 30 min and then BnBr (6.73 mL, 56.7 mmol, 1.5 equiv) was added to the suspension at 0 °C. The reaction mixture was stirred for 2.5 h at rt. MeOH (10 mL) was added to this suspension. The organic layer was diluted with brine (200 mL) and extracted with EtOAc (2 \times 200 mL). The organic layers were combined, dried over MgSO_4 , filtered and concentrated under reduced pressure. Flash column chromatography (PetEt/EtOAc 20:1 to 5:1) afforded the title compound **3.28** (10.2 g, 100%) as a waxy oil; R_f = 0.50 (PetEt/EtOAc 10:1); $[\alpha]_D^{25} = -32.87$ (c, 5.5 in CHCl_3); ^1H NMR (500 MHz) : δ 1.25 (s, 3 H, CH_3), 1.33 (s, 3 H, CH_3), 1.39 (s, 3 H, CH_3), 1.44 (s, 3 H, CH_3), 3.95-3.99 (m, 2 H, H-6, CHHPh), 4.03-4.08 (m, 2 H, H-6', CHHPh), 4.13 (dd, J = 3.2 Hz, 8.0 Hz, 1 H, H-4), 4.34 (td, J = 1.5 Hz, 8.0 Hz, 1 H, H-5), 4.49-4.63 (m, 2 H, H-3, H-2), 5.84 (d, J = 3.5 Hz, 1 H, H-1), 7.21-7.32 (m, 5 H, Ph).

The ^1H NMR data is in agreement with literature values.^[261]

1,2,4,6-Penta-*O*-acetyl-3-*O*-benzyl- β -D-glucopyranoside 3.29 ^[262]

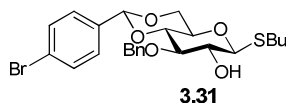
Dowex 50WX2-400 (H^+ form) was added to a suspension of 3-*O*-benzyl-1,2:5,6-di-*O*-isopropylidene- α -D-glucopyranoside **3.28** (1.71 g, 4.88 mmol) in H_2O (12 mL) and the reaction mixture was stirred for 18 h at 70 °C. The reaction mixture was concentrated *in vacuo*, azeotroped with toluene to afford a white solid. This crude product (1.29 g, 4.76 mmol) was dissolved in Pyr (40 mL) and DMAP (64 mg, 0.52 mmol, 0.11 equiv) was added followed by Ac_2O (5.40 mL, 57.10 mmol, 12 equiv). The reaction mixture was stirred for 24 h. The reaction mixture was diluted with EtOAc (40 mL) and washed with ice-cold water (35 mL), 1 N aq. HCl (35 mL), satd. aq. $CuSO_4$ solution (35 mL), H_2O (35 mL), satd. aq. $NaHCO_3$ solution (35 mL) and dried over $MgSO_4$ and filtered. It was concentrated *in vacuo* and recrystallised in EtOH to afford the β -anomer **3.29** (1.0 g, 89% over 2 steps) as a white solid; $R_f = 0.49$ (PetEt/EtOAc 1:1); $[\alpha]_D^{22} = -0.86$ (c, 0.4 in $CHCl_3$) (lit $[\alpha]_D^{25} = -1$ (c, 1.2 in $CHCl_3$))^[262]; mp = 104-106 °C (lit 107-108 °C)^[262]; 1H NMR (500 MHz): δ 1.98 (s, 3 H, $OC(O)CH_3$), 1.98 (s, 3 H, $OC(O)CH_3$), 2.08 (s, 3 H, $OC(O)CH_3$), 2.10 (s, 3 H, $OC(O)CH_3$), 3.71-3.77 (m, 2 H, H-3, H-5), 4.10 (dd, $J = 2.4$ Hz, 12.5 Hz, 1 H, H-6'), 4.22 (dd, $J = 4.9$ Hz, 12.5 Hz, 1 H, H-6), 4.61 (s, 2 H, CH_2Ph), 5.14-5.19 (m, 2 H, H-2, H-4), 5.65 (d, $J = 8.2$ Hz, 1 H, H-1), 7.22-7.35 (m, 5 H, Ph); HRMS m/z (ESI+) 456.1864 ($C_{21}H_{26}O_{10}NH_4$ $[M+NH_4]^+$ requires 456.1903)

Butyl 2,4,6-tri-*O*-acetyl-3-*O*-benzyl-1-thio- β -D-glucopyranoside 3.30

Butanethiol (90 μ L, 1.44 mmol, 1.2 equiv) was added to a solution of 1,2,4,6-Penta-*O*-acetyl-3-*O*-benzyl- β -D-glucopyranoside **3.29** (0.53 g, 1.20 mmol) in CH_2Cl_2 (5 mL) followed by $BF_3 \cdot OEt_2$ (181 μ L, 1.44 mmol, 1.2 equiv) and the reaction mixture was stirred for 3 h. NEt_3 (199 μ L, 1.44 mmol, 1.2 equiv) was added and the reaction mixture was washed with ice-cold H_2O (5 mL), satd. aq. $NaHCO_3$ (5 mL), H_2O (5 mL)

and brine (5 mL), dried over MgSO_4 , filtered and concentrated *in vacuo*. Flash column chromatography (PetEt/ EtOAc 4:1) afforded the β -anomer **3.30** (0.42 g, 75%) as a colourless oil; $R_f = 0.75$ (PetEt/EtOAc 7:3); $[\alpha]_{\text{D}}^{22} = -32.96$ (c, 0.55 in CHCl_3); ^1H NMR (400 MHz): δ 0.90 (t, $J = 7.3$ Hz, 3 H, CH_3), 1.34-1.44 (m, 2 H, CH_2CH_3), 1.53-1.61 (m, 2 H, $\text{CH}_2\text{CH}_2\text{CH}_3$), 1.95 (s, 3 H, OC(O)CH_3), 2.00 (s, 3 H, OC(O)CH_3), 2.04 (s, 3 H, OC(O)CH_3), 2.60-2.73 (m, 2 H, $\text{CH}_2\text{CH}_2\text{CH}_2\text{CH}_3$), 3.61-3.65 (m, 1 H, H-5), 3.73 (t, $J = 9.3$ Hz, 1 H, H-3), 4.09 (dd, $J = 1.9$ Hz, 12.2 Hz, 1 H, H-6'), 4.19 (dd, $J = 5.4$ Hz, 12.2 Hz, H-6), 4.43 (d, $J = 10.0$ Hz, 1 H, H-1), 4.59-4.66 (d x 2, $J = 11.8$ Hz, $J = 16.0$ Hz, 2 H, CH_2Ph), 5.03-5.11 (m, 2 H, H-4, H-2), 7.22-7.33 (m, 5 H, Ph); ^{13}C NMR (100 MHz): δ_{C} 13.2 ($\text{CH}_2\text{CH}_2\text{CH}_2\text{CH}_3$), 20.3 (OC(O)CH_3), 20.5 (OC(O)CH_3), 21.4 ($\text{CH}_2\text{CH}_2\text{CH}_2\text{CH}_3$), 29.2 ($\text{CH}_2\text{CH}_2\text{CH}_2\text{CH}_3$), 31.3 ($\text{CH}_2\text{CH}_2\text{CH}_2\text{CH}_3$), 62.2 (C-6), 69.4 (C-4), 71.0 (C-2), 73.9 (CH_2Ph), 75.7 (C-5), 81.2 (C-3), 83.4 (C-1), 127.3 (Ph), 127.4 (Ph), 128.0 (Ph), 137.5 (Ph), 168.8, 168.9, 170.1 (C=O x 3); HRMS m/z (ESI+) 959.3528 ($\text{C}_{46}\text{H}_{64}\text{O}_{16}\text{S}_2\text{Na}$ $[\text{M}+\text{Na}]^+$ requires 959.3533).

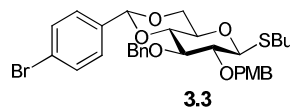
Butyl 4,6-*O*-(*p*-bromobenzylidene)-3-*O*-benzyl-1-thio- β -D-glucopyranoside **3.31**



Na metal (13 mg approx., 0.58 mmol approx., 0.1 equiv approx.) was added to a solution of butyl 2,4,6-tri-*O*-acetyl-3-*O*-benzyl-1-thio- β -D-glucopyranoside **3.30** (2.56 g, 5.83 mmol) in MeOH (20 mL) at rt. It was stirred for 1 h; quenched with Amberlite ion-exchange resin (H^+ form), filtered and concentrated *in vacuo*. The resulting white solid was then dissolved in MeCN (10 mL) and *p*-bromobenzaldehyde dimethyl acetal (0.90 mL, 5.41 mmol, 1.2 equiv) was added to the solution followed by *p*-TsOH (16 mg, 0.09 mmol, 0.02 equiv) in an inert atmosphere. It was stirred for 3 h, NEt_3 was added and the reaction mixture was concentrated *in vacuo*. Recrystallisation in MeOH afforded the title compound **3.31** (2.29 g, 88% over 2 steps) as a white solid; $R_f = 0.57$ (PetEt/EtOAc 3:1); $[\alpha]_{\text{D}}^{22} = -283.85$ (c, 0.5 in CDCl_3); mp = 101-102 °C; ^1H NMR (500 MHz): δ 0.93 (t, $J = 7.4$ Hz, 3 H, CH_3), 1.39-1.47 (m, 2 H, CH_2CH_3), 1.60-1.65 (m, 2 H, $\text{CH}_2\text{CH}_2\text{CH}_3$), 2.55 (d, $J = 2$ Hz, 1 H, OH), 2.71-2.74 (m, 2 H, $\text{CH}_2\text{CH}_2\text{CH}_2\text{CH}_3$), 3.46-3.48 (m, 1 H, H-5), 3.56-3.60 (m, 1

H, H-2), 3.65-3.72 (m, 2 H, H-4, H-3), 3.77 (pt, $J = 10.3$ Hz, 1 H, H-6'), 4.36 (dd, $J = 5.0$ Hz, 10.3 Hz, 1 H, H-6), 4.44 (d, $J = 9.7$ Hz, 1 H, H-1), 4.83, 4.94 (d x 2, $J = 11.7$ Hz, $J = 11.7$ Hz, 2 H, CH_2Ph), 5.53 (s, 1 H, CHArBr), 7.30-7.53 (m, 9 H, aromatics); ^{13}C NMR (125 MHz): δ_{C} 13.6 ($\text{CH}_2\text{CH}_2\text{CH}_2\text{CH}_3$), 21.9 ($\text{CH}_2\text{CH}_2\text{CH}_2\text{CH}_3$), 30.1 ($\text{CH}_2\text{CH}_2\text{CH}_2\text{CH}_3$), 32.1 ($\text{CH}_2\text{CH}_2\text{CH}_2\text{CH}_3$), 68.6 (C-6), 70.7 (C-5), 73.2 (C-2), 74.7 (CH_2Ph), 81.1 (C-3), 81.5 (C-4), 86.9 (C-1), 100.6 (CHArBr), 123.1, 127.8, 127.9, 128.0, 128.5, 131.4, 136.2, 138.3 (aromatics).

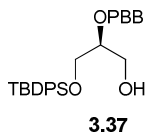
Butyl 4,6-*O*-(*p*-bromobenzylidene)-2-*O*-(*p*-methoxybenzyl)-3-*O*-benzyl-1-thio- β -D-glucopyranoside **3.3**



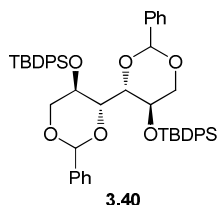
To a solution of butyl 4,6-*O*-(*p*-bromobenzylidene)-3-*O*-benzyl-1-thio- β -D-glucopyranoside **3.31** (1.84 g, 3.63 mmol) in DMF (20 mL) was slowly added NaH (60% suspension in mineral oil) (0.17 g, 7.26 mmol, 2 equiv) under an inert atmosphere at 0 °C. The reaction mixture was stirred for 30 min and BnBr (0.74 mL, 5.45 mmol, 1.5 equiv) was added to the suspension at 0 °C. The reaction mixture was stirred for 20 h at rt. To this suspension H_2O (2 mL) was added. The organic layer was washed with brine (100 mL) and extracted with EtOAc (100 mL x 2). The organic layers were combined, dried over MgSO_4 , filtered and concentrated under reduced pressure. Flash column chromatography (PetEt/ EtOAc 4:1) afforded the title compound **3.3** (2.01 g, 88%) as a white solid; $R_f = 0.71$ (PetEt/EtOAc 4:1); $[\alpha]_{\text{D}}^{22} = -26.35$ (c, 0.55 in CHCl_3); mp = 111-112 °C; ^1H NMR (500 MHz): δ 0.94 (t, $J = 7.4$ Hz, 3 H, CH_3), 1.43-1.48 (m, 2 H, CH_2CH_3), 1.62-1.66 (m, 2 H, $\text{CH}_2\text{CH}_2\text{CH}_3$), 2.69-2.80 (m, 2 H, $\text{CH}_2\text{CH}_2\text{CH}_2\text{CH}_3$), 3.40-3.47 (m, 2 H, H-2, H-5), 3.69 (pt, $J = 9.3$ Hz, 1 H, H-3), 3.75-3.79 (m, 2 H, H-6', H-4), 3.81 (s, 3 H, OCH_3), 4.35 (dd, $J = 5.0$ Hz, 10.5 Hz, 1 H, H-6), 4.53 (d, $J = 9.8$ Hz, 1 H, H-1), 4.76 (d, $J = 9.8$ Hz, 1 H, CHHPh), 4.81-4.84 (d x 2, $J = 9.8$ Hz, $J = 11.4$ Hz, 2 H, CHHPh , CHHArOMe), 4.92 (d, $J = 11.4$ Hz, 1 H, CHHArOMe), 5.52 (s, 1 H, CHArBr), 6.87-6.88, 7.30-7.38, 7.50-7.53 (m, 13 H, aromatics); ^{13}C NMR (125 MHz): δ_{C} 13.6 (CH_3), 21.9 (CH_2CH_3), 30.7 ($\text{CH}_2\text{CH}_2\text{CH}_3$), 31.9 ($\text{CH}_2\text{CH}_2\text{CH}_2\text{CH}_3$), 55.3 (ArOCH_3), 68.7 (C-6), 70.1 (C-5), 75.2 (OCH_2Ph), 76.8 (OCH_2ArOMe), 81.1 (C-2), 81.5

(C-3), 82.8 (C-4), 86.2 (C-1), 100.4 (CHArBr), 113.8, 123.0, 127.7, 127.8, 127.9, 128.4, 130.0, 130.1, 136.3, 138.4, 159.4 (aromatics); HRMS m/z (ESI+) 651.1401, ($C_{32}H_{37}BrO_6SNa$ $[M+Na]^+$ requires 651.1386).

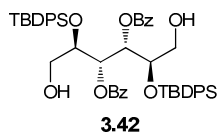
1-*O*-(*t*-butyldiphenylsilyl)-2-*O*-(*p*-bromobenzyl)-*sn*-glycerol **3.37**



$NaIO_4$ (1.99 g, 9.32 mmol, 5.5 equiv) was added to a stirred solution of 1,6-di-*O*-(*t*-butyldiphenylsilyl)-2,5-Di-*O*-(*p*-bromobenzyl)-*D*-mannitol **3.49** (1.69 g, 1.70 mmol) in THF: H_2O (25 mL, 4:1) at rt under N_2 . The reaction mixture was stirred for 3 h. It was diluted with EtOAc (50 mL); the organic layer was separated, washed with H_2O (25 × 2 mL), brine (25 × 2 mL), dried over $MgSO_4$, filtered and concentrated under reduced pressure. $NaBH_4$ (771 mg, 20.40 mmol, 12 equiv) was slowly added to a solution of the resulting aldehyde in EtOH: H_2O (24.5 mL, 9:1) and the reaction mixture was stirred for 2 h. AcOH was added drop-wise until the solution had a pH of approx. 8. The organic layer was extracted with EtOAc (20 mL × 3) and the combined organic layers were washed with satd. aq. $NaHCO_3$ (30 mL) solution, H_2O (30 mL). The reaction mixture was dried over $MgSO_4$, filtered and concentrated under reduced pressure. Flash column chromatography (PetEt/EtOAc 5:1 to 4:1) afforded the title compound **3.37** (1.05 g, 62% over two steps) as a pale yellow oil; R_f = 0.38 (PetEt/EtOAc 9:1); $[\alpha]_D^{25} = -14.5$ (c, 1.0 in $CHCl_3$); 1H NMR (500 MHz): δ 1.09 (s, 3 H, $C(CH_3)(CH_3)_2$), 1.09 (s, 3 H, $C(CH_3)(CH_3)_2$), 1.10 (s, 3 H, $C(CH_3)(CH_3)_2$), 2.23 (bs, 1 H, OH), 3.57-3.64 (m, 1 H, H-2), 3.72-3.76 (m, 1 H, H-3a), 3.78-3.84 (m, 3 H, H-3b, H-1a, H-1b), 4.51 (d, $J = 12.1$ Hz, 1 H, CHHArBr), 4.59 (d, $J = 12.1$ Hz, 1 H, CHHArBr), 7.17-7.19, 7.40-7.46, 7.69-7.71 (m, 14 H, aromatics); ^{13}C NMR (125 MHz): δ_c 19.1 ($C(CH_3)_3$), 26.8 ($C(CH_3)_3$), 62.7 (C-3), 63.5 (C-1), 71.2 (CH_2ArBr), 79.8 (C-2), 121.5, 127.7, 127.9, 129.2, 129.8, 131.4, 133.1, 135.5, 135.5, 137.3 (aromatics); HRMS m/z (ESI+) 521.1119 ($C_{26}H_{31}BrO_3SiNa$ $[M+Na]^+$ requires 521.1118).

1,3:4,6-Di-*O*-benzylidene-2,5-di-*O*-(*t*-butyldiphenylsilyl)-D-mannitol **3.40**

Imidazole (0.40 g, 5.86 mmol, 2.1 equiv) was added to a solution of dibenzylidene D-mannitol **3.39** (1.00 g, 2.79 mmol) in DMF (5 mL) followed by *t*-butyldiphenylchlorosilane (1.52 mL, 5.86 mmol, 2.1 equiv) under an inert atmosphere at 0 °C. The reaction mixture was stirred for 30 min, then stirred at 50 °C for 24 h. The suspension was diluted with EtOAc (100 mL) and washed with brine (50 mL × 2) followed by H₂O (50 mL). It was dried over MgSO₄, filtered and concentrated under reduced pressure. Recrystallisation in EtOAc/ PetEt afforded the title compound **3.40** (1.35 g, 82%) as a white solid; $R_f = 0.61$ (PetEt/EtOAc 5:1); $[\alpha]_D^{22} = +36.52$ (c, 0.55 in CHCl₃); mp = 171-173 °C; ¹H NMR (500 MHz): δ 1.12 (s, 18 H, 2 × C(CH₃)₃), 3.51-3.55 (m, 2 H, H-2, H-2'), 3.88-3.91 (m, 2H, H-3, H-3'), 4.20-4.24 (m, 4 H, H-1a, H-1b, H-1a', H-1b'), 5.14 (s, 2 H, 2 × CHPh), 7.19- 7.64 (m, 30 H, 6 × Ph); ¹³C NMR (125 MHz): δ_c 19.4 (C(CH₃)₃), 26.9 (C(CH₃)₃), 61.8 (C-1), 71.7, 78.4 (C-2, C-3), 100.9 (CHPh), 126.4, 127.7, 127.7, 128.0, 128.7, 129.9, 133.1, 133.5, 134.8, 135.8, 135.8, 137.7 (aromatics).

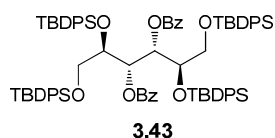
2,5-Di-*O*-(*tert*-butyldiphenylsilyl)-3,4-di-*O*-benzoyl-D-mannitol **3.42** ^[130, 263]

Aq. KBrO₃ solution (240 mg, 3.5 mL, 1.43 mmol, 6 equiv) was added to a solution of 1,3:4,6-di-*O*-benzylidene-2,5-di-*O*-(*t*-butyldiphenylsilyl)-D-mannitol **3.40** (200 mg, 0.24 mmol) in EtOAc (6 mL) followed by aq. Na₂S₂O₄ solution (250 mg, 3.5 mL 1.43 mmol, 6 equiv) and the biphasic mixture was vigorously stirred for 45 min. The organic layer was separated and washed with satd. Na₂SO₃ solution (10 mL). The aqueous layer was extracted with EtOAc (10 mL). The organic layers were

combined, dried over MgSO_4 , filtered and concentrated *in vacuo*. Flash column chromatography (EtOAc/Tol/PetEt 1:6:3) afforded the title compound **3.42** (73 mg, 40%) as a white foamy solid; $R_f=0.38$ (PetEt/EtOAc/toluene 3:1:6); $[\alpha]_{\text{D}}^{22} = +68.59$ (c, 0.4 in CHCl_3) (lit $[\alpha]_{\text{D}}^{26} = +74.5$ (c, 1.0 in CHCl_3))^[130, 263]; mp 179-183 °C (lit 180-184 °C)^[130, 263]; ^1H NMR (500 MHz): δ 1.04 (s, 18 H, $2 \times \text{C}(\text{CH}_3)_3$), 3.52-3.60 (m, 2 H, H-1, H-6), 3.75-3.78 (m, 2H, H-2, 5), 5.74 (d, $J = 5.3$ Hz, H-3, H-4), 7.13- 7.92 (m, 30 H, aromatics); ^{13}C NMR (125 MHz): δ_{C} 19.2 ($\text{C}(\text{CH}_3)_3$), 26.9 ($\text{C}(\text{CH}_3)_3$), 62.6 (C-1, C-6), 72.3 (C-3), 72.6 (C-2), 127.6, 127.6, 127.7, 127.7, 128.2, 128.2, 128.3, 129.5, 129.7, 129.8, 129.8, 132.3, 133.1, 133.8, 135.8, 135.9, 166.1 (aromatics).

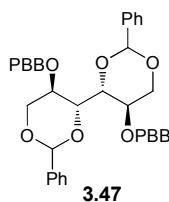
The NMR spectra are in agreement with literature.^[130]

1,6:2,5-Di-*O*-(*t*-butyldiphenylsilyl)-3,4-di-*O*-benzoyl-D-mannitol **3.43**



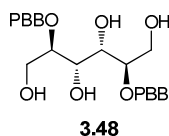
Imidazole (16 mg, 0.24 mmol, 2.05 equiv) was added to a solution of 2,5-di-*O*-(*t*-butyldiphenylsilyl)-3,4-di-*O*-benzoyl-D-mannitol **3.42** (101 mg, 0.12 mmol) in DMF (5 mL) followed by *t*-butyldiphenylchlorosilane (62 μL , 0.24 mmol, 2.05 equiv) under an inert atmosphere at 0 °C. The reaction mixture was stirred for 30 min, heated to rt and left stirring overnight. The suspension was diluted with EtOAc (10 mL) and washed with brine (10 mL \times 2) followed by H_2O (10 mL). It was dried over MgSO_4 , filtered and concentrated under reduced pressure. Flash column chromatography (EtOAc/Tol/Pet 1:6:3) afforded the title compound **3.43** (80 mg, 51%) as a pale yellow oil; $R_f=0.70$ (PetEt/EtOAc/toluene 3:1:6); ^1H NMR (500 MHz): δ 1.03 (s, 18 H, $\text{C}(\text{CH}_3)_3 \times 2$), 1.10 (s, 18 H, $\text{C}(\text{CH}_3)_3 \times 2$), 3.75-3.82 (m, 4 H, H-1a, H-1b, H-6a, H-6b), 3.86-3.87 (m, 2 H, H-2, H-5), 5.85 (d, $J = 8.9$ Hz, 2 H, H-3, H-4), 7.12-8.01 (m, 50 H, aromatics); ^{13}C NMR (125 MHz): δ_{C} 19.0 ($\text{C}(\text{CH}_3)_3$), 19.2 ($\text{C}(\text{CH}_3)_3$), 26.6 ($\text{C}(\text{CH}_3)_3$), 26.7 ($\text{C}(\text{CH}_3)_3$), 64.3 (C-1, C-6), 69.7 (C-2, C-5), 71.5 (C-3, C-4), 127.5, 127.7, 127.7, 128.5, 129.5, 129.6, 130.0, 132.9, 133.4, 134.8, 135.5, 135.6 (aromatics).

1,3:4,6-Di-*O*-benzylidene-2,5-di-*O*-(*p*-bromobenzyl)-D-mannitol **3.47**



NaH (60% suspension in mineral oil) (2.24 g, 0.09 mol, 4 equiv) was slowly added to a solution of dibenzylidene D-mannitol **3.39** (5.00 g, 0.01 mol) in DMF (45 mL) under an inert atmosphere at 0 °C. The reaction mixture was stirred for 30 min and *p*-bromobenzyl bromide (8.40 g, 0.03 mol, 2.4 equiv) was added to the suspension at 0 °C. The reaction mixture was stirred overnight at rt. To this suspension H₂O (2 mL) was added; the solution was diluted with EtOAc (100 mL) and washed with brine (100 mL × 2). The organic layers were combined, dried over MgSO₄, filtered and concentrated under reduced pressure. Flash column chromatography (PetEt/ EtOAc 9:1) afforded the title compound **3.47** (8.57 g, 88%) as a colourless oil; *R*_f = 0.66 (Pet/EtOAc 9:1); [α]²²_D = -44.7 (c, 1.0 in CHCl₃); ¹H NMR (500 MHz): δ 3.69 (t, *J* = 10.1 Hz, 2 H, H-1a, H-6a), 3.97- 4.02 (m, 2 H, H-2, H-5), 4.04 (d, *J* = 9.3 Hz, 2 H, H-3, H-4), 4.37 (dd, *J* = 5.0 Hz, 10.7 Hz, 2 H, H-1b, H-6b), 4.51-4.58 (d × 2, *J* = 12.0 Hz, 4 H, CHHArBr × 2, CHHArBr × 2), 5.41 (s, 2 H, CHPh × 2), 7.14-7.47 (m, 18 H, aromatic); ¹³C NMR (125 MHz): δ_C 66.7 (C-2, C-5), 69.4 (C-1, C-6), 71.6 (CH₂ArBr × 2), 77.2 (C-3, C-4), 101.0 (CHPh × 2), 121.9, 126.1, 128.1, 128.9, 129.5, 131.5, 136.8, 137.4 (aromatics); HRMS *m/z* (ESI+) 712.0904 (C₃₄H₃₂Br₂O₆NH₄ [M+NH₄]⁺ requires 712.0904).

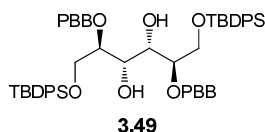
2,5-Di-*O*-(*p*-bromobenzyl)-D-mannitol **3.48**



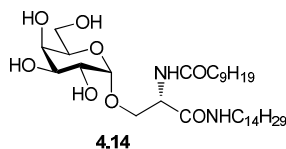
4 N aq. HCl (16 mL) solution was added to a solution of 1,3:4,6-di-*O*-benzylidene-2,5-di-*O*-(*p*-bromobenzyl)-D-mannitol **3.47** (8.57 g, 0.01 mol) in EtOH (200 mL) and the reaction mixture was refluxed for 18 h under N₂. After cooling, satd. aq. NaHCO₃ (200 mL) was added to the reaction mixture and was stirred for 30 min. The aqueous layer was extracted with EtOAc (100 mL × 3). The combined organic layers

were subsequently washed with satd. aq. NaHCO₃ (100 mL), brine (100 mL), H₂O (100 mL), dried over MgSO₄, filtered and concentrated under reduced pressure. Recrystallisation in PetEt/EtOAc afforded the title compound **3.48** (5.05 g, 79%) as colourless crystals; R_f = 0.36 (MeOH/CHCl₃ 1:9); [α]²⁵_D = + 9.9 (c, 1.0 in MeOH); mp = 128-129 °C; ¹H NMR (500 MHz, CD₃OD): δ 3.59-3.63 (m, 2 H, H-2, H-3), 3.78 (dd, *J* = 4.6, 11.9 Hz, 2 H, H-1a, H-6a), 3.94-3.97 (m, 4 H, H-3, H-4, H-1b, H-6b), 4.58, 4.73 (d × 2, *J* = 11.6 Hz, 4 H, CH₂Ph × 2), 7.32-7.48 (m, 8 H, aromatics); ¹³C NMR (125 MHz): δ_C 62.2 (C-1, C-6), 70.1 (C-3, C-4), 72.6 (CH₂ArBr), 81.5 (C-2, C-5), 122.2, 130.8, 132.4, 139.5 (aromatics); HRMS *m/z* (ESI+) 536.0213 (C₂₀H₂₄Br₂O₆NH₄ [M+NH₄]⁺ requires 536.0283).

1,6-Di-*O*-(*t*-butyldiphenylsilyl)-2,5-Di-*O*-(*p*-bromobenzyl)-D-mannitol **3.49**



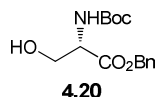
TBDPSCI (1.02 mL, 3.94 mmol, 2.05 equiv) was added to a stirred solution of 2,5-di-*O*-(*p*-bromobenzyl)-D-mannitol **3.48** (1.00 g, 1.9 mmol) and imidazole (323 mg, 4.75 mmol, 2.5 equiv) in DMF (3 mL) was added under N₂ at 0 °C. The reaction mixture was allowed to warm to rt and was stirred for 18 h. The reaction mixture was diluted with EtOAc (70 mL) and washed with brine (50 mL), H₂O (50 mL), dried over MgSO₄, filtered and concentrated under reduced pressure. Flash column chromatography (PetEt/EtOAc 9:1) afforded the title compound **3.49** (1.75 g, 93%) as a pale yellow oil; R_f = 0.56 (PetEt/EtOAc 9:1); [α]²²_D = -5.85 (c, 1.0 in CHCl₃); ¹H NMR (500 MHz): δ 1.06 (s, 18 H, C(CH₃)₃ × 2), 3.10-3.12 (m, 2 H, OH × 2), 3.70 (dd, *J* = 5.3 Hz, 11.2 Hz, 2H, H-2, H-5), 3.85-3.88 (dd, *J* = 4.9 Hz, 11.2 Hz, 2 H, H-1a, H-6a), 3.94 (dd, *J* = 4.9 Hz, 11.2 Hz, 2 H, H-1b, H-6b), 4.05 (d, *J* = 5.3 Hz, 2 H, H-3, H-4), 4.49 (d, *J* = 11.8 Hz, 2 H, CHHArBr × 2), 4.62 (d, *J* = 11.8 Hz, 2 H, CHHArBr × 2), 7.13-7.70 (m, 28 H, aromatics); ¹³C NMR (125 MHz): δ_C 19.2 (C(CH₃)₃ × 2), 26.8 (C(CH₃)₃ × 2), 64.0 (C-1, C-6), 69.9 (C-3, C-4), 72.3 (CH₂ArBr × 2), 80.5 (C-2, C-5), 121.5, 127.8, 127.8, 129.3, 129.8, 131.4, 132.9, 133.0, 135.6, 135.6, 137.3 (aromatics). HRMS *m/z* (ESI+) 995.2360 (C₅₂H₆₀Br₂O₆Si₂H [M+H]⁺ requires 995.2368).

7.2.3. Experimental procedures for Chapter 4***O*-(α -D-Galactopyranosyl)-*N*-(decanosyl)-L-serine tetradecyl amide **4.14****

AcOH (2 drops) were added to a solution of *O*-(2,3,4,6-tetra-*O*-benzyl- α -D-galactopyranosyl)-*N*-(decanosyl)-L-serine tetradecyl amide **4.87** (52 mg, 0.05 mmol) in EtOH/EtOAc (3:1, 4 mL). The resulting solution was added to Pd(C) (26 mg, 50% w/w) and was then de-oxygenated. Hydrogenolysis was performed on the suspension at 4 Barr pressure on a hydrogenator apparatus and was shaken for 18 h. It was filtered through Celite, washing with EtOH and concentrated *in vacuo*. The crude oily solid was re-subjected to hydrogenolysis for 4 h under the same conditions as described above. The reaction mixture was filtered through Celite, washing with EtOH and was concentrated *in vacuo* to yield the title compound **4.14** (29 mg, 88%, crude yield) as a white solid; $[\alpha]_D^{25} = +26.92$ (c, 0.52 in CH₂Cl₂); IR ν_{\max} (NaCl plate, CH₂Cl₂): 3409.9, 2922.4, 2851.9, 1718.8, 1634.7, 1466.5 cm⁻¹; ¹H NMR (300 MHz, d₄-MeOD): δ 0.90-0.92 (m, 6 H, CH₃ × 2), 1.30-1.31 (m, 34 H, CO(CH₂)₂(CH₂)₆CH₃, NH(CH₂)₂(CH₂)₁₁CH₃), 1.51-1.55 (m, 2 H, NHCH₂CH₂), 1.61-1.66 (m, 2 H, COCH₂CH₂), 2.29 (t, *J* = 7.2 Hz, 2 H, COCH₂), 3.18-3.22 (m, 2 H, NHCH₂), 3.69-3.89 (m, 9 H, H-1, H-2, H-3, H-4, H-5, H-6, H-6', H- β , H- β'), 4.54 (t, *J* = 6.8 Hz, 1 H, H- α); ¹³C-NMR (75 MHz): δ_c 13.0 (CH₃)^{xxiii}, 22.3, 25.4, 26.6, 28.9, 29.1, 29.1, 29.2, 29.4, 29.4, 31.7 (NHCH₂(CH₂)₁₂CH₃, COCH₂(CH₂)₇CH₃), 35.5 (COCH₂), 39.2 (NHCH₂), 53.3 (C- α), 67.7 (C-6), 68.1 (C- β), 68.7, 69.1, 69.6, 70.0, 71.4 (C-2, C-3, C-4, C-5), 99.8 (C-1), 170.8 (C=O), 175.3 (C=O); HRMS *m/z* (ESI⁺) 641.4635 (C₃₃H₆₄N₂O₈Na: [M+Na]⁺ requires 641.4616).

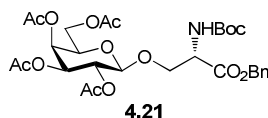
This compound is mentioned in the literature but NMR data is not reported.^[169a]

^{xxiii} Two overlapping signals.

***N*-tert-Butoxycarbonyl-L-serine benzyl ester 4.20**

NEt₃ (9.51 mL, 68.2 mmol, 2 equiv) was added to a solution of *N*-(*tert*-butoxycarbonyl)-L-serine **4.19** (7 g, 34.1 mmol) in DMF (30 mL) and the reaction mixture was stirred for 40 mins at rt. BnBr (11.59 mL, 97.5 mmol, 2 equiv) was added to this solution and the reaction mixture was stirred for 18 h. It was concentrated *in vacuo*. Brine (100 mL) was added and the suspension was extracted with EtOAc (100 mL × 2). The combined organic layers were dried over MgSO₄, filtered, concentrated *in vacuo*. Flash column chromatography (hexane/EtOAc 2:1) afforded the title compound **4.20** (7.53 g, 75%) as a white solid; R_f = 0.45 (hexane/EtOAc 1:1); [α]_D²⁰ = + 7.58 (c, 0.04 in CH₂Cl₂); mp = 55 – 60 °C (lit. 58-60 °C)^[264]; IR ν_{max} (NaCl plate, CH₂Cl₂): 3964.0, 3414.2, 3114.9, 3091.7, 3066.2, 3034.7, 2977.9, 2935.3, 2889.1, 2725.3, 2636.2, 2400.1, 2343.9, 2290.6, 2125.2, 1957.4, 1875.0, 1743.8, 1715.8, 1609.1, 1587.0, 1500.4 cm⁻¹; ¹H NMR (300 MHz, major product): δ 1.43 (s, 9 H, C=OOC(CH₃)₃), 3.27-3.30 (m, 1 H, CH₂OH), 3.92 (dd, *J* = 9.0 Hz, 33.3 Hz, CH₂OH), 4.39 (s, 1 H, H-α), 5.17 (s, 2 H, CH₂Ph), 5.68 (d, *J* = 9.0 Hz, 1 H NH), 7.34 (s, 5 H, Ph); ¹³C NMR (75 Hz): δ 28.3 (C=OOC(CH₃)₃), 55.9 (C-α), 63.2 (CH₂OH), 67.3 (CH₂Ph), 80.2 (C=OOC(CH₃)₃), 128.1, 128.4, 128.6, 135.3 (aromatics), 155.9 (C=O), 170.9 (C=O); HRMS *m/z* (ESI+) 318.1316, (C₁₅H₂₁NO₅Na [M+Na]⁺ requires 318.1312).

The NMR data are in agreement with the reported values.^[265]

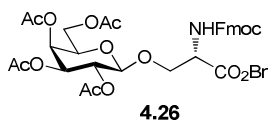
***N*-tert-Butoxycarbonylamino-*O*-(2,3,4,6-tetra-*O*-acetyl-β-D-galactopyranosyl)-L-serine benzyl ester 4.21**

A mixture of boc-L-serine benzyl ester **4.20** (82 mg, 0.28 mmol) and 2,3,4,6-tetra-*O*-acetyl-α-D-galactopyranosyl-1-trichloroacetimidate **4.33** (164 mg, 0.33 mmol, 1.2

equiv) in anhydrous CH_2Cl_2 (5 mL) containing 3 Å MS (50 mg) was stirred at rt in an inert atmosphere for 30 min. A solution of 0.04 N TMSOTf (0.83 mL, 0.03 mmol) in anhydrous CH_2Cl_2 (3 mL) was added to the solution. The reaction mixture was stirred for 2 h. The 3 Å MS were filtered off and the solvent was evaporated under reduced pressure and the residue purified by flash column chromatography (hexane /diethyl ether 1:2) to give the β -anomer **4.21** as white crystals (0.17 mg, 82%); $R_f = 0.43$ (hexane/EtOAc 2:1); $[\alpha]_D^{20} = +65.22$ (c 0.01, CH_2Cl_2); mp = 42- 50 °C; IR ν_{max} (NaCl plate, CH_2Cl_2): 3628.1, 3358.0, 3302.7, 3198.8, 3091.9, 3066.0, 3034.0, 2977.7, 2749.2, 2415.4, 2288.5, 2127.2, 1996.8, 1958.6, 1875.4, 1751.3, 1636.0, 1605.0, 1501.0 cm^{-1} ; ^1H NMR (300 MHz): δ 2.04 (s, 3 H, $\text{OC}(\text{O})\text{CH}_3$), 2.05 (s, 3 H, $\text{OC}(\text{O})\text{CH}_3$), 2.07 (s, 3 H, $\text{OC}(\text{O})\text{CH}_3$), 2.12 (s, 3 H, $\text{OC}(\text{O})\text{CH}_3$), 4.10-4.14 (m, 3 H, H-5, H-6, H-6'), 4.23-4.29 (m, 2 H, H-2, $\text{CHNHC}=\text{OOC}(\text{CH}_3)_3$), 5.01 (dd, $J = 3.3$ Hz, 6.6 Hz, 1 H, H-3), 5.20 (s, 2 H, CH_2Ph), 5.40-5.42 (m, 2 H, H-4, $\text{NHC}=\text{OOC}(\text{CH}_3)_3$), 5.68 (d, $J = 6.1$ Hz, 1 H, H-1), 7.35 (s, 5 H, aromatic); ^{13}C NMR (75 Hz): δ_c 20.6 ($\text{OC}(\text{O})\text{CH}_3$), 20.7 ($\text{OC}(\text{O})\text{CH}_3$), 20.7 ($\text{OC}(\text{O})\text{CH}_3$), 23.5 ($\text{OC}(\text{O})\text{CH}_3$), 28.3 ($\text{C}=\text{OOC}(\text{CH}_3)_3$), 53.7 (C- α), 61.2 (C-6), 63.2 (C- β), 65.9 (C-4), 67.5 (CH_2Ph), 69.2 (C-2), 71.4 (C-3), 73.8 (C-5), 80.2 ($\text{COC}(\text{CH}_3)_3$), 97.4 (C-1), 128.6-128.1, 135.3 (aromatics), 155.4 (C=O), 163.6 (C=O), 169.8 (C=O), 170.1 (C=O), 170.2 (C=O), 170.5 (C=O); HRMS m/z (ESI+) 647.2204, ($\text{C}_{29}\text{H}_{39}\text{NO}_{14}\text{Na}$ [$\text{M}+\text{Na}$] $^+$ requires 647.2210).

The NMR data are in agreement with the reported values.^[266]

***N*-(9-Fluoroenylmethoxycarbonyl)-*O*-(2,3,4,6-tetra-*O*-acetyl- β -D-galactopyranosyl)-*L*-serine benzyl ester **4.26**^[267]**

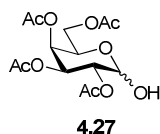


$\text{BF}_3 \cdot \text{OEt}_2$ (96 μL , 0.77 mmol, 3 equiv) was added to a solution of 1,2,3,4,6-penta-*O*-acetyl- β -D-galactopyranose **2.32** (100 mg, 0.26 mmol), and *N*-9-Fluorenylmethoxycarbonyl-Ser-OH **4.23** (101 mg, 0.31 mmol, 1.2 equiv) in MeCN (3 mL) under N_2 at rt. The reaction mixture was stirred for 1.5 h. It was diluted with CH_2Cl_2 (20 mL) and washed with 1 N aq. HCl solution (5 mL) followed by H_2O (5 mL).

The organic layer was dried over MgSO_4 , filtered and concentrated. NEt_3 (71 μL , 0.51 mmol, 2 equiv) was added to a stirring solution of the crude acid dissolved in DMF (3 mL) under N_2 at rt. It was stirred for 10 min and BnBr (61 μL , 0.51 mmol, 2 equiv) was added drop-wise to the solution. It was stirred for 18 h, concentrated *in vacuo*, re-dissolved in EtOAc (20 mL), washed with brine (20 mL). The organic layer was dried over MgSO_4 , filtered and rotary evaporated. Flash column chromatography (hexane/EtOAc 3:1 to 1:1, loaded in toluene) afforded the β -anomer **4.26** (59 mg, 31%) as a white solid; $R_f = 0.38$ (hexane/EtOAc 1:1); $^1\text{H NMR}$ (300 MHz): δ 1.99 (s, 3 H, OC(O)CH_3), 2.01 (s, 3 H, OC(O)CH_3), 2.10 (s, 3 H, OC(O)CH_3), 2.19 (s, 3 H, OC(O)CH_3), 3.78-3.91 (m, 2 H, H-5, H- β'), 4.09-4.12 (m, 2 H, H-6, H-6'), 4.18-4.24 (m, 1 H, H- β), 4.28-4.37 (m, 1 H, H- α), 4.41-4.43 (m, 1 H, *CH*-Fmoc), 4.48 (d, $J = 6.7$ Hz, 1 H, H-1), 4.98 (dd, $J = 3.4$ Hz, 10.5 Hz, 1 H, H-3), 5.13-5.17 (m, 1 H, H-2), 5.19-5.22 (m, 2 H, CH_2Ph), 5.36 (dd, $J = 0.9$ Hz, 3.4 Hz, 1 H, H-4), 5.62 (d, $J = 8.0$ Hz, 1 H, NH), 7.29-7.78 (m, 13 H, Ar-Fmoc, CH_2Ph); HRMS m/z (ESI+) 748.2576, ($\text{C}_{39}\text{H}_{41}\text{NO}_{14}\text{H}$ [$\text{M}+\text{H}$] $^+$ requires 748.2600).

The NMR data is in agreement with the reported values.^[177]

2,3,4,6- Tetra-*O*-acetyl- α/β -D-galactopyranose **4.27**

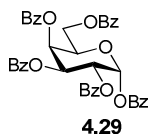


Dimethylamine (3.83 mL, 7.66 mmol, 2 equiv) was added to a stirring solution of 1,2,3,4,6-penta-*O*-acetyl- β -D-galactopyranose **2.32** (2 g, 3.83 mmol) in MeCN (20 mL) and the solution was refluxed for 24 h. The reaction mixture was concentrated *in vacuo*. Brine (50 mL) was added and the suspension was extracted with CH_2Cl_2 (50 mL \times 3). The combined organic layers were dried over MgSO_4 , filtered, concentrated *in vacuo* and the crude product was purified by flash column chromatography (hexane/EtOAc 1:1) to yield the title compound **4.27** as a brown oil (1.24 g, 93%, 1:100 α/β); Data recorded for mixture of anomers: $R_f = 0.28$ (hexane/EtOAc 1:1); $[\alpha]_D^{20} = +42.93$ (c, 0.03 in CH_2Cl_2); IR ν_{max} (NaCl plate, CH_2Cl_2): 3619.6, 3463.1, 3063.3, 2971.8, 2942.7, 2916.7, 2849.2, 2726.0, 2442.3, 2124.9,

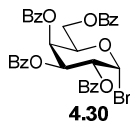
1961.9, 1747.7, 1648.1 cm^{-1} ; Data recorded for α -anomer: ^1H NMR (300 MHz): δ 1.99 (s, 3 H, $\text{OC}(\text{O})\text{CH}_3$), 2.06 (m, 6 H, $\text{OC}(\text{O})\text{CH}_3 \times 2$), 2.10 (s, 3 H, $\text{OC}(\text{O})\text{CH}_3$), 4.08-4.16 (m, 2 H, H-6, H-6'), 4.48 (pt, $J = 6.0$ Hz, 1 H, H-5), 5.15 (dd, $J = 3.4$ Hz, 12.0 Hz, 1 H, H-2), 5.43 (dd, $J = 6.2$ Hz, 12.0 Hz, 1 H, H-3), 5.47-5.48 (m, 1 H, H-4), 5.71-5.72 (m, 1 H, H-1); ^{13}C NMR (75 Hz): δ_{c} 20.7 ($\text{OC}(\text{O})\text{CH}_3$), 20.7 ($\text{OC}(\text{O})\text{CH}_3$), 20.8 ($\text{OC}(\text{O})\text{CH}_3$), 20.9 ($\text{OC}(\text{O})\text{CH}_3$), 60.5 (C-6), 65.9 (C-5), 68.2 (C-4), 68.4 (C-3), 68.7 (C-2), 90.7 (C-1), 170.3 (C=O), 170.5 (C=O), 170.6 (C=O), 170.6 (C=O).

The NMR data are in agreement with the reported values.^[268]

1,2,3,4,6-Penta-O-benzoyl- α -D-galactopyranose **4.29**^[269]

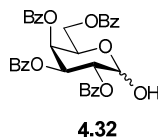


Over a period of 30 min, benzoyl chloride (48.33 mL, 0.42 mol, 5.5 equiv) was added drop-wise to a solution of D-galactose **4.28** (13.64 g, 75.7 mmol) in Pyr (120 mL) at 0 °C under N_2 . The reaction mixture was allowed warm to rt and stirred for 18 h. Ice water (200 mL) was added to the reaction mixture and stirred for 1 h. It was concentrated *in vacuo*. Flash column chromatography (hexane/EtOAc 2:1) yielded the α -anomer **4.29** (33.9 g, 64%) as a white solid; $R_f = 0.52$ (hexane/EtOAc 2:1); ^1H NMR (300 MHz): δ 4.49 (dd, $J = 6.3$ Hz, 11.2 Hz, 1 H, H-6'), 4.69 (dd, $J = 6.3$ Hz, 11.2 Hz, 1 H, H-6), 4.94 (pt, $J = 6.3$ Hz, 1 H, H-5), 6.13 (dd, $J = 3.3$ Hz, 11.8 Hz, 1 H, H-2), 6.24 (dd, $J = 3.0$ Hz, 11.8 Hz, 1 H, H-3), 6.26-6.30 (m, 1 H, H-4), 7.07 (d, $J = 3.3$ Hz, 1 H, H-1), 7.19-8.17 (m, 25 H, aromatics); ^{13}C NMR (75 Hz): δ 47.2 (C-6), 60.8 (C-3), 61.9 (C-2), 66.4 (C-3), 66.7 (C-4), 67.5 (C-5), 89.6 (C-1), 127.2, 127.28, 127.3, 127.6, 127.6, 127.6, 127.7, 127.9, 128.1, 128.2, 128.3, 128.4, 128.6, 128.8, 128.8, 129.1, 132.1, 132.3, 132.4, 132.6, 132.8, 163.4, 163.5, 164.4, 164.5, 164.6, 164.8, 164.9, 165.2 (aromatics); HRMS m/z (ESI+) 723.1811, ($\text{C}_{41}\text{H}_{32}\text{O}_{11}\text{Na}$ [$\text{M}+\text{Na}$] $^+$ requires 723.1837).

2,3,4,6-Tetra-*O*-benzoyl-1-bromo- α -D-galactopyranose 4.30 ^[184a]

HBr/AcOH (33%) (20 mL, 335 mmol, 27 equiv) was added to 1,2,3,4,6-penta-*O*-benzoyl- α -galactopyranose **4.29** (8.72 g, 12.4 mmol) in CH₂Cl₂ at 0 °C under N₂. Ac₂O (0.48 mL) was added and the reaction mixture was stirred for 2 h. The reaction mixture was diluted with CH₂Cl₂ (50 mL), washed with ice-water (40 mL), aqueous sodium bicarbonate (40 mL). The organic layer was dried over MgSO₄, filtered and rotary evaporated to yield the α -anomer **4.30** as a white solid (7.82 g, 96%, crude yield); R_f = 0.19 (hexane/EtOAc 4:1); For the α anomer: ¹H NMR (300 MHz): δ 4.48 (dd, *J* = 6.0 Hz, 11.5 Hz, 1 H, H-6'), 4.66 (dd, *J* = 6.8 Hz, 11.5 Hz, 1 H, H-6), 4.94 (pt, *J* = 6.3 Hz, 1 H, H-5), 5.70 (dd, *J* = 3.9 Hz, 10.4 Hz, 1 H, H-2), 6.09 (dd, *J* = 3.3 Hz, 10.4 Hz, 1 H, H-3), 6.16 (dd, *J* = 1.0 Hz, 3.3 Hz, 1 H, H-4), 7.01 (d, *J* = 3.9 Hz, 1 H, H-1), 7.22-8.09 (m, 20 H, aromatics); ¹³C NMR (75 Hz): δ_c 61.7 (C-6), 68.2 (C-4), 68.7 (C-2), 68.9 (C-3), 71.9 (C-5), 88.4 (C-1), 128.4, 128.5, 128.6, 128.6, 128.8, 128.9, 129.5, 129.8, 129.9, 129.9, 130.0, 130.1, 133.2, 133.4, 133.4, 133.7, 133.8, 165.4, 165.4, 165.6, 165.9 (aromatics).

The ¹H NMR data is in agreement with the literature. ^[184a]

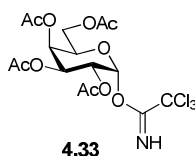
2,3,4,6-Tetra-*O*-benzoyl- α/β -D-galactopyranose 4.32

Ag₂CO₃ (0.48 mL, 1.73 mmol, 3 equiv) was added to a stirring solution of 2,3,4,6-tetra-*O*-benzoyl-1-bromo- α -D-galactopyranose **4.30** (0.38 g, 0.58 mmol) in acetone:H₂O (10 mL, 4:1) in the dark and the suspension was stirred for 2.5 h. It was washed through Celite with CH₂Cl₂. The solution was dried over MgSO₄, filtered and concentrated *in vacuo* to yield the title compound **4.32** as a brown oil (0.31 g, 90%, crude yield, α : β 3:1); Data recorded for mixture of anomer: R_f = 0.33

(toluene/EtOAc 9:1): ^1H NMR (300 MHz): δ 4.37-4.43 (m, 2 H, H-6' (α,β)), 4.58-4.64 (m, 2 H, H-6 (α,β)), 4.90 (pt, $J = 6.5$ Hz, 1 H, H-5 (α,β)), 5.15 (d, $J = 7.4$ Hz, 1 H, H-1 β), 5.73-5.78 (m, 3 H, H-2 (α,β), H-3 β), 5.89 (d, $J = 3.4$ Hz, 1 H, H-1 α), 6.03-6.05 (m, 1 H, H-4 β), 6.10-6.15 (m, 2 H, H-3 α , H-4 α), 7.18-8.11 (m, 20 H, aromatics).

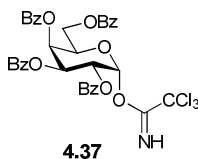
The NMR data is in agreement with the reported values.^[270]

2,3,4,6-Tetra-*O*-acetyl- α -D-galactopyranosyl-1-trichloroacetimidate **4.33** ^[271]



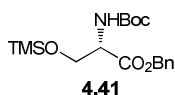
To a solution of 2,3,4,6-tetra-*O*-acetyl- α/β -D-galactopyranose **4.27** (918 mg, 2.64 mmol) in anhydrous CH_2Cl_2 (5 mL) was added trichloroacetonitrile (1.52 mL, 15.18 mmol), 1,8-diaza bicyclo[5.4.0]undec-7-ene (0.12 mL, 0.79 mmol) and 3 Å molecular sieves (500 mg) in an inert atmosphere. The reaction mixture was stirred for 3.5 h. The solvent was evaporated under reduced pressure and the residue purified by column chromatography (hexane/EtOAc 4:3) to give the α -anomer **4.33** as white crystal (1.08 g, 83%); $R_f = 0.57$ (hexane/EtOAc 1:1); ^1H NMR (300 MHz): δ 2.01 (s, 3 H, $\text{OC}(\text{O})\text{CH}_3$), 2.02 (s, 3 H, $\text{OC}(\text{O})\text{CH}_3$), 2.03 (s, 3 H, $\text{OC}(\text{O})\text{CH}_3$), 2.04 (s, 3 H, $\text{OC}(\text{O})\text{CH}_3$), 4.06-4.21 (m, 2 H, H-6, H-6'), 4.41 (td, $J = 1.1$ Hz, 12.6 Hz, 1 H, H-5), 5.34-5.46 (m, 2 H, H-2, H-3), 5.57 (dd, $J = 1.1$ Hz, 3.2 Hz, 1 H, H-4), 6.61-6.62 (d, $J = 3.0$ Hz, 1 H, H-1), 8.69 (s, 1 H, NH); ^{13}C NMR (75 Hz): δ_c 20.5 ($\text{OC}(\text{O})\text{CH}_3$), 20.5 ($\text{OC}(\text{O})\text{CH}_3$), 20.6 ($\text{OC}(\text{O})\text{CH}_3$), 20.6 ($\text{OC}(\text{O})\text{CH}_3$), 61.2 (C-6), 66.9 (C-3), 67.4 (C-4), 67.5 (C-2), 68.9 (C-5), 93.5 (C-1), 160.9 (C=NH), 169.9 (C=O), 170.0 (C=O), 170.0 (C=O), 170.2 (C=O).

The NMR data are in agreement with the reported values.^[272]

2,3,4,6-Tetra-*O*-benzoyl- α -D-galactopyranosyl-1-trichloroacetimidate 4.37

To a solution of 2,3,4,6-tetra-*O*-benzoyl- α/β -D-galactopyranose **4.32** (99 mg, 0.17 mmol) in anhydrous CH₂Cl₂ (1 mL) was added trichloroacetonitrile (0.08 mL, 0.83 mmol, 5 equiv), 1,8-diaza bicyclo[5.4.0]undec-7-ene (3 μ L, 0.02 mmol, 0.1 equiv) and 3Å molecular sieves (50 mg) in an inert atmosphere at 0 °C. The reaction mixture was stirred for 2 h at 0 °C. The solvent was evaporated under reduced pressure to yield the title compound **4.37** as white crystal (110 mg, 89%, crude yield); R_f = 0.82 (toluene/EtOAc 9:1); [α]_D²² = +100 (c, 4 in CH₂Cl₂); ¹H NMR (300 MHz): δ 4.41-4.48 (m, 1 H, H-6'), 4.58-4.65 (m, 1 H, H-6), 4.85-4.89 (m, 1 H, H-5), 5.98-5.99 (m, 1 H, H-2), 6.06-6.10 (m, 1 H, H-3), 6.16-6.16 (m, 1 H, H-4), 6.91(d, *J* = 3.6 Hz, 1 H, H-1), 7.16-8.13 (m, 20 H, aromatics), 8.64 (s, 1 H, NH).

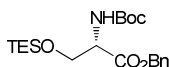
The NMR data is in agreement with reported values.^[270]

***N*-tert-Butoxycarbonyl-*O*-trimethylsilyl-L-serine benzyl ester 4.41**

TMSCl (0.24 mL, 1.87 mmol, 1.1 equiv) was added to a solution of *N*-(*tert*-butoxycarbonyl)-L-serine benzyl ester **4.20** (0.5 g, 1.70 mmol) in CH₂Cl₂ (4 mL) under N₂ at rt. It was stirred for 10 min and NEt₃ (0.24 mL, 1.87 mmol, 1 equiv) was added to this solution drop-wise producing a smoke in the round bottom. The reaction mixture was stirred for 2 h. It was concentrated *in vacuo*. Brine (10 mL) was added and the suspension was extracted with CH₂Cl₂ (10 mL \times 2). The combined organic layers were dried over MgSO₄, filtered, concentrated *in vacuo* to afford the title compound **4.41** (0.43 g, 69%, crude yield) as a white solid; R_f = 0.86 (toluene/EtOAc 9:2); [α]_D²⁶ = - 2.18 (c, 2.75 in CH₂Cl₂); IR ν_{\max} (NaCl plate, CH₂Cl₂): 3447.10, 2091.3, 1642.9, 1499.8 cm⁻¹; ¹H NMR (300 MHz): δ 0.00 (s, 9 H, Si(CH₃)₃), 1.40 (s, 9 H,

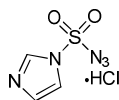
NHCO₂C(CH₃)₃, 3.75 (dd, *J* = 3.1 Hz, 10.1 Hz, 1 H, H-β'), 3.98 (dd, *J* = 2.4 Hz, 10.1 Hz, 1 H, H-β), 4.33-4.36 (m, 1 H, H-α), 5.11 (dd, *J* = 12.4 Hz, 22.0 Hz, 2 H, CH₂Ph), 5.40 (d, *J* = 3.7 Hz, 1 H, NH), 7.26-7.29 (m, 5 H, Ph); ¹³C NMR (75 Hz): δ_c 0.0 (Si(CH₃)₃), 29.1 (C(CH₃)₃), 56.3 (C-α), 63.8 (C-β), 67.8 (CH₂Ph), 80.6 (C(CH₃)₃), 126.0, 127.7, 128.9, 129.0, 129.0, 129.3, 129.4, 129.7, 129.8, 136.3 (aromatics), 156.2 (C=O), 171.5 (C=O); HRMS *m/z* (ESI-) 366.1736, (C₁₈H₂₈NO₅Si [M-H]⁻ requires 366.1742).

N*-tert-Butoxycarbonyl-*O*-triethylsilyl-L-serine benzyl ester **4.42*



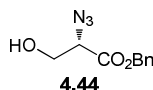
4.42

TESCl (0.24 mL, 1.41 mmol, 0.85 equiv) was added to a solution of *N*-(tert-butoxycarbonyl)-L-serine benzyl ester **4.20** (0.5 g, 1.70 mmol) in CH₂Cl₂ (4 mL) under N₂ at rt. It was stirred for 10 min and NEt₃ (0.24 mL, 1.87 mmol, 1 equiv) was added to this solution drop-wise producing a smoke in the round bottom. The reaction mixture was stirred for 2 h. It was concentrated *in vacuo*. Brine (10 mL) was added and the suspension was extracted with CH₂Cl₂ (10 mL × 2). The combined organic layers were dried over MgSO₄, filtered, concentrated *in vacuo* to afford the title compound **4.42** (0.47 g, 67%, crude yield) as a white solid; R_f = 0.78 (toluene/EtOAc 9:2); [α]_D²⁶ = +1.9 (c, 1.05 in CH₂Cl₂); IR ν_{max} (KBr): 3452.9, 2956.2, 2806.1, 1717.3 cm⁻¹; ¹H NMR (300 MHz) δ 0.53-0.58 (m, 6 H, Si(CH₂CH₃)₃), 0.90 (t, *J* = 7.8 Hz, 9 H, Si(CH₂CH₃)₃), 1.42-1.44 (m, 9 H, OC(CH₃)₃), 3.83 (dd, *J* = 2.9 Hz, 9.9 Hz, 1 H, H-β'), 4.07 (dd, *J* = 2.1 Hz, 9.9 Hz, 1 H, H-β), 4.37-4.40 (m, 1 H, H-α), 5.17 (dd, *J* = 12.4 Hz, 23.5 Hz, 2 H, CH₂Ph), 5.42 (d, *J* = 8.5 Hz, 1 H, NH), 7.30-7.33 (m, 5 H, Ph); ¹³C NMR (75 Hz): δ_c 3.2 (Si(CH₂CH₃)₃), 5.6 (Si(CH₂CH₃)₃), 27.3 (OC(CH₃)₃), 54.7 (C-α), 62.4 (C-β), 66.0 (CH₂Ph), 78.8 (OC(CH₃)₃), 126.0, 127.2, 127.3, 127.5, 127.6, 127.9, 128.0, 128.7, 134.5 (aromatics), 154.5 (C=O), 169.7 (C=O); HRMS *m/z* (ESI-) 408.2202, (C₂₁H₃₄NO₅Si [M-H]⁻ requires 408.2212).

Imidazole-1-sulfonyl azide hydrochloride 4.43 ^[195]**4.43**

Absolute EtOH (10 mL) was added to magnesium turnings (1 g) and I₂ (0.1 g) under N₂. The reaction mixture was heated until the solution underwent a colour change from dark red to colourless. Absolute EtOH (150 mL) was added and the solution was refluxed for 1 h to yield anhydrous EtOH. Sulfuryl chloride (5 mL, 61.7 mmol) was added drop-wise to an ice-cooled suspension of NaN₃ (4.01g, 61.7 mmol, 1 equiv) in MeCN (63 mL) and the mixture stirred for 17 h at rt under N₂. Imidazole (8.40 g, 123.4 mmol) was added portion-wise to the ice-cooled mixture and the resulting slurry stirred for 3 h at rt. The mixture was diluted with EtOAc (133 mL), washed with H₂O (133 mL × 2) then saturated aqueous NaHCO₃ (133 mL × 2), dried over MgSO₄ and filtered. (A solution of HCl in EtOH [obtained by the drop-wise addition of AcCl (6.58 mL, 92.5 mmol) to ice-cooled dry EtOH (25 mL)] was added drop-wise to the filtrate with stirring, the mixture chilled in an ice-bath, filtered and the filter cake washed with EtOAc (33 mL × 3) to give the title compound **4.43** (5.01 g, 39%, crude yield) as colourless needles; IR ν_{max} (KBr): 2172.9, 1322.4, 1162.7 cm⁻¹; ¹H NMR (300 MHz, D₂O) δ 7.67-7.68 (m, 1 H, H-4), 8.07-8.10 (m, 1 H, H-5), 9.53 (s, 1 H, H-2).

This data is in agreement with the reported values. ^[195]

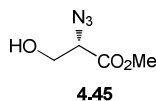
N-Azido-L-serine benzyl ester 4.44 ^[195]**4.44**

1 M aq. HCl solution (1 M, 0.5 mL) was added to *N*-*boc*-L-serine-benzyl ester **4.20** (0.10 g, 0.34 mmol) in CH₂Cl₂ (0.5 mL) at rt. The biphasic mixture was vigorously stirred for 18 h and concentrated *in vacuo*. Imidazole-1-sulfonyl azide hydrochloride **4.43** (109 mg, 0.52 mmol, 1 equiv) was then added to the resulting L-serine benzyl

ester hydrochloride salt (100 mg, 0.43 mmol) with K_2CO_3 (161 mg, 1.16 mmol, 2.7 equiv) and $CuSO_4 \cdot 5H_2O$ (1 mg, 4.31 mmol, 0.01 equiv) in *t*-BuOH (5 mL) and the mixture stirred at 28 °C for 6 h. The mixture was concentrated, diluted with H_2O (15 mL), acidified with conc. HCl and extracted with EtOAc (10 mL \times 3). The combined organic layers were dried over $MgSO_4$, filtered and concentrated. Flash column chromatography (hexane/EtOAc 2:1) afforded the title compound **4.44** (58 mg, 61% over two steps) as a white solid; R_f = 0.44 (hexane/EtOAc 2:1); IR ν_{max} (NaCl plate, CH_2Cl_2): 3443.5, 2110.5, 1740.3, cm^{-1} ; 1H NMR (300 MHz): δ 1.96 (s, 1 H, OH), 3.93 (d, J = 4.8 Hz, 1 H, H- β), 4.12 (t, J = 4.8 Hz, 1 H, H- α), 5.27 (s, 2 H, CH_2Ph), 7.37-7.39 (m, 5 H, Ph); ^{13}C NMR (75 Hz): δ_c 62.8 (CH_2OH), 63.4 (C- α), 128.4, 128.7, 128.7, 134.8 (aromatics), 168.6 (C=O).

This data is in agreement with the reported values.^[273]

N-Azido-L-serine methyl ester 4.45 ^[194a]

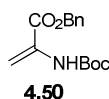


Tf_2O (2 mL, 11.8 mmol, 3 equiv) was added drop-wise to a pre-cooled (0 °C) vigorously stirring mixture of NaN_3 (1.53 g, 23.55 mmol, 6 equiv) in H_2O (5 mL) and CH_2Cl_2 (5 mL) in an inert atmosphere. It was stirred for 2 h at 0 °C. Satd. aq. $NaHCO_3$ (10 mL) was added to the reaction mixture slowly and transferred to a separating funnel upon evolution of gases. The aqueous layer was washed twice with CH_2Cl_2 (30 mL \times 2). The combined organic layers were washed with satd. aq. $NaHCO_3$ (10 mL) and the approx. 0.6 N TfN_3 (65 mL) solution was used without further purification (based on 50% conversion). (ratio of H_2O : CH_2Cl_2 = 1: 2.6) NOTE: highly explosive compound when dried so avoid concentration. In another round bottom, NEt_3 (1.64 mL, 11.8 mmol, 3 equiv) was added to a mixture of L-serine methyl ester hydrochloride **4.60** (611 mg, 3.93 mmol) and $CuSO_4 \cdot 5H_2O$ (10 mg, 0.039 mmol, 0.01 equiv) in H_2O (65 mL) (ratio of H_2O : CH_2Cl_2 : MeOH 3:3:10). The prepared TfN_3 solution in CH_2Cl_2 (65 mL) was added slowly in the presence of N_2 . MeOH (210 mL) was added to the reaction mixture very slowly and it was stirred for 18 h. It was

concentrated *in vacuo*. Flash column chromatography (hexane/ EtOAc 2:1) afforded the title compound **4.45** (326 mg, 57%) as a colourless oil; $R_f = 0.42$ (hexane/EtOAc 1:1); $^1\text{H NMR}$ (300 MHz): δ 3.80 (s, 3 H, OCH_3), 3.89-3.91 (m, 2 H, H- β , H- β'), 4.07 (t, $J = 4.7$ Hz, 1 H, H- α); $^{13}\text{C NMR}$ (75 Hz): δ_c 53.0 (OCH_3), 62.7 (C- β), 63.5 (C- α), 169.7 (CO); HRMS m/z (ESI+) 313.0881, ($\text{C}_8\text{H}_{14}\text{N}_6\text{O}_6\text{Na}$: $[2\text{M}+\text{Na}]^+$ requires 313.0867).

The NMR data are in agreement with the reported values.^[274]

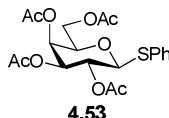
***N*-tert-Butoxycarbonyl-alanine benzyl ester 4.50**



To a solution of PPh_3 (127 mg, 0.48 mmol, 1.6 equiv) and 4 Å MS (50 mg) in anhydrous CH_2Cl_2 (2 mL) in an inert atmosphere was added a solution of 2,3,4,6-tetra-*O*-acetyl- α/β -D-galactopyranose **4.27** (105 mg, 0.30 mmol) and *N*-Boc-L-serine-benzyl ester **4.20** (89 mg, 0.54 mmol, 1.8 equiv) at rt and stirred for 15 min. DIAD (95 mg, 0.482 mmol, 1.6 equiv) in anhydrous CH_2Cl_2 (2 mL) was added to the reaction mixture drop-wise and the reaction mixture was stirred for 5 h. The 4 Å MS were filtered off and the solvent was evaporated under reduced pressure and the residue purified by flash column chromatography (toluene /EtOAc 1:1) to give dehydroalanine derivative **4.50** as a colourless oil (41 mg, 49%); $R_f = 0.87$ (toluene/EtOAc 1:1); $^1\text{H NMR}$ (300 MHz): δ 1.46-1.48 (m, 9 H, $\text{O}(\text{CH}_3)_3$), 5.25 (s, 2 H, CH_2Ph), 5.79 (s, 1 H, C= CHH), 6.18 (s, 1 H, C= CHH), 7.01-7.03 (m, 1 H, NH), 7.36-7.37 (m, 5 H, Ph).

The NMR data is in agreement with the reported values.^[197]

Phenyl-2,3,4,6-tetra-*O*-acetyl-1-thio- β -D-galactopyranoside 4.53

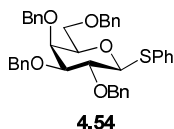


Thiophenol (2.26 mL, 22.1 mmol, 1 equiv) was added to a solution of 1,2,3,4,6-penta-*O*-acetyl- β -D-galactopyranose **2.32** (8.64 g, 22.1 mmol) in CH_2Cl_2 (100 mL) followed by $\text{BF}_3 \cdot \text{OEt}_2$ (8.33 mL, 66.3 mmol, 3 equiv) and the solution was stirred for

18 h. The reaction mixture was diluted with CH_2Cl_2 (100 mL) and washed with 1 M aq. NaOH (100 mL), brine solution (100 mL) and H_2O (100 mL). The organic layer was dried over MgSO_4 , filtered and concentrated *in vacuo*. Flash column chromatography (hexane/ EtOAc 3:1) afforded the β anomer **4.53** (7.67 g, 79%) as a white foamy solid; $R_f = 0.56$ (hexane/EtOAc 2:1); ^1H NMR (300 MHz): δ 1.96 (s, 3 H, OC(O)CH_3), 2.03 (s, 3 H, OC(O)CH_3), 2.09 (s, 3 H, OC(O)CH_3), 2.11 (s, 3 H, OC(O)CH_3), 3.92 (pt, $J = 6.2$ Hz, 1 H, H-5), 4.07-4.21 (m, 2 H, H-6, H-6'), 4.71 (d, $J = 12.0$ Hz, 1 H, H-1), 5.04 (dd, $J = 3.1$ Hz, 9.0 Hz, 1 H, H-3), 5.24 (dd, $J = 9.0$ Hz, 12.0 Hz, 1 H, H-2), 5.41 (dd, $J = 3.1$ Hz, 6.2 Hz, 1 H, H-4), 7.29-7.52 (m, 5 H, Ph); HRMS m/z (ESI+) 458.1501, ($\text{C}_{20}\text{H}_{24}\text{O}_9\text{SNH}_4$ [$\text{M}+\text{NH}_4$] $^+$ requires 458.1479).

The NMR data is in agreement with the reported values.^[275]

Phenyl-2,3,4,6-tetra-*O*-benzyl-1-thio- β -D-galactopyranoside **4.54**

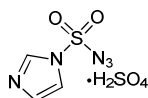


Na metal (13 mg approx., 0.58 mmol approx., 0.1 equiv approx.) was added to a solution of phenyl-2,3,4,6-tetra-*O*-acetyl-1-thio- β -D-galactopyranoside **4.53** (7.67 g, 5.83 mmol) in MeOH (70 mL) at 0 °C. It was stirred at rt for 1.5 h; quenched with Amberlite ion-exchange resin (H^+ form), filtered and concentrated *in vacuo*. The resulting white solid was then dissolved in DMF (10 mL) and NaH (60% suspension in mineral oil) (4.87 g, 0.12 mol, 8 equiv) was slowly added to it under an inert atmosphere at 0 °C. The suspension was stirred for 30 min and BnBr (10.83 mL, 0.09 mol, 6 equiv) was added at 0 °C. The reaction mixture was stirred overnight at rt. To this suspension MeOH (20 mL) was added followed by concentration *in vacuo*. It was dissolved in Et_2O (100 mL) and washed with water (100 mL \times 2). The aqueous layers were combined and washed with Et_2O (100 mL \times 2). The organic layers were combined, dried over MgSO_4 , filtered and concentrated under reduced pressure. Recrystallisation in EtOH afforded the β -anomer **4.54** (6.75 g, 79% over two steps) as white crystals; $R_f = 0.75$ (hexane/EtOAc 2:1); ^1H NMR (300 MHz): δ 3.59-3.68 (m, 4 H, H-3, H-5, H-6, H-6'), 3.93 (d, $J = 9.0$ Hz, H-2), 3.98 (t, $J = 3.3$ Hz, 1 H, H-4), 4.45-

4.50 (d × 2, $J = 9.0$ Hz, 2 H, *CHPh* × 2), 4.59-4.66 (d × 2, $J = 9.0$ Hz, 2 H, *CHPh* × 2), 4.73-4.81 (m, 4 H, *CH₂Ph*, *CHPh*, H-1), 4.97 (d, $J = 12.0$ Hz, *CHPh*), 7.18-7.20 (m, 3 H, *SPh*), 7.29-7.40 (m, 20 H, aromatics), 7.55-7.59 (m, 2 H, *SPh*); HRMS m/z (ESI+) 633.2658, (C₂₀H₂₇NO₉S₂H): [M+H]⁺ requires 633.2669).

The NMR data is in agreement with the reported values.^[202]

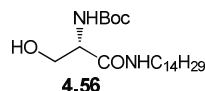
Imidazole-1-sulfonyl azide hydrogen sulfate 4.55^[203]



4.55

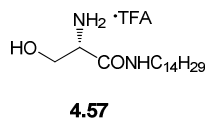
Absolute EtOH (10 mL) was added to magnesium turnings (1 g) and I₂ (0.1 g) under N₂. The reaction mixture was heated until the solution underwent a colour change from dark red to colourless. Absolute EtOH (150 mL) was added and the solution was refluxed for 1 h to yield anhydrous EtOH. Sulfuryl chloride (5 mL, 61.7 mmol) was added drop-wise to an ice-cooled suspension of NaN₃ (4.01g, 61.7 mmol, 1 equiv) in MeCN (63 mL) and the mixture stirred for 17 h at rt under N₂. Imidazole (8.40 g, 123.4 mmol) was added portion-wise to the ice-cooled mixture and the resulting slurry stirred for 3 h at rt. The mixture was diluted with EtOAc (133 mL), washed with H₂O (133 mL × 2) then satd. aq. NaHCO₃ (133 mL × 2), dried over MgSO₄ and filtered. Sulfuric acid (6.05 g, 61.7 mmol, 1 equiv) was added drop-wise to the solution (100 mL solution). It was stirred for 1 h. PetEt (100 mL) was added and the precipitate was filtered to give the title compound **4.55** (7.42 g, 20%) as white crystals; IR ν_{\max} (NaCl plate, CH₂Cl₂): 3107.2, 2173.3, 1579.7, 1508.9, 1449.7 cm⁻¹; ¹H NMR (300 MHz): δ 7.51 (s, 1 H, H-2), 8.10 (s, 1 H, H-5), 8.96 (s, 1 H, H-4).

The NMR data is in agreement with the reported values.^[203]

N*-tert-Butoxycarbonyl-L-serine tetradecyl amide **4.56* ^[276]

DMF (5 mL) was added to a mixture of *N*-boc-L-Serine **4.18** (250 mg, 1.22 mmol), TBTU (430 mg, 1.34 mmol) and HOBt (181 mg, 1.34 mmol) under N₂ and was left to stir for 10 min. Tetradecylamine (286 mg, 1.34 mmol) and NEt₃ (0.2 mL, 1.46 mmol) were then added under N₂ to the reaction mixture and were stirred for 18 h. The reaction mixture was rotary evaporated, diluted in CH₂Cl₂ (25 mL); washed with brine (30 mL) and 0.2 N aq. HCl (30 mL). The aqueous layer was extracted with CH₂Cl₂ (3 x 25 mL), and the combined organic layers were washed with satd. aq. NaHCO₃ (30 mL). The organic layer was dried over MgSO₄ and filtered. The solvent was then evaporated under reduced pressure, vacuum dried to give an oil that was purified by column chromatography (hexane/EtOAc 1:1) to give the title compound **4.56** as a white solid (337 mg, 59%); R_f = 0.42 (hexane/EtOAc 1:1); [α]²⁰_D = -8.58 (c, 0.013 in CH₂Cl₂); IR ν_{max} (NaCl plate, CH₂Cl₂): 3319.60, 3107.63, 2924.92, 2853.95, 1706.41, 1650.17, 1174.77 cm⁻¹; ¹H-NMR (300 MHz): δ = 0.88 (t, *J* = 6.4 Hz, 3 H, CH₂CH₃), 1.25 (s, 24 H, NHCH₂(CH₂)₁₂CH₃), 1.45 (s, 12 H; OC(CH₃)₃), 3.23-3.25 (m, 2 H; NHCH₂), 3.59-3.65 (m, 2 H, H-β', NHC=O), 4.04-4.14 (m, 2 H; H-α, H-β), 5.68 (d, *J* = 7.5 Hz, 1 H, OH), 6.79 (s, 1 H, NH); ¹³C-NMR (75 MHz): δ_c 14.1 (CH₂CH₃), 22.7 (CH₂CH₃), 28.3 (OC(CH₃)₃), 31.9-26.9 (NHCH₂CH₂(CH₂)₁₀), 39.5 (C=ONHCH₂CH₂), 54.8 (NHCHCH₂OH), 62.9 (NHCH₂), 77.5-76.6 (m, CDCl₃, CH₂OH), 80.5 (C(CH₃)₃), 156.3 (C=O), 171.3 (C=O).

The ¹H NMR data is in agreement with the literature. ^[276]

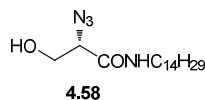
L-Serine tetradecyl amide trifluoroacetic acid **4.57** ^[276]

At 0°C to a solution of *N*-boc-L-serine tetradecyl amide **4.56** (1.09 g, 2.71 mmol) in CH₂Cl₂ (20 mL) was added TFA (3.03 mL, 40.70 mmol, 15 equiv). The reaction

mixture was stirred for 4 h at rt and then concentrated *in vacuo*. PetEt and diethyl ether was added to the waxy solid and the precipitate was filtered to give the title compound **4.57** (860 mg, 77%, crude yield) as a flaky white solid; $^1\text{H-NMR}$ (300 MHz, $\text{d}_6\text{-DMSO}$): δ 0.85 (t, $J = 6.9$ Hz, 3 H, CH_3), 1.22-1.24 (m, 22 H, $\text{NHCH}_2\text{CH}_2(\text{CH}_2)_{11}\text{CH}_3$), 1.41 (s, 2 H, NHCH_2CH_2), 3.07-3.11 (m, 2 H, NHCH_2CH_2), 3.63-3.74 (m, 3 H, H- α , H- β , H- β'), 5.49 (bs, 1 H, OH), 8.08 (bs, 3 H, NH_3), 8.33 (t, $J = 5.7$ Hz, 1 H, NH); HRMS m/z (ESI+) 301.285, ($\text{C}_{17}\text{H}_{36}\text{N}_2\text{O}_2\text{H}$: $[\text{M}+\text{H}]^+$ requires 301.2838).

The NMR data is in agreement with the reported values.^[276]

***N*-Azido-L-serine tetradecyl amide 4.58**

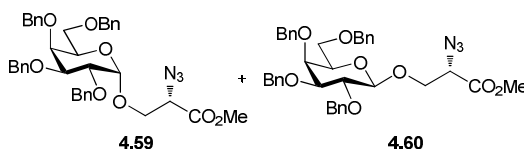


Imidazole-1-sulfonyl azide hydrogen sulfate **4.55** (113 mg, 0.31 mmol, 1.2 equiv) was added to a reaction mixture containing L-serine tetradecyl amide trifluoroacetic acid **4.57** (77 mg, 0.26 mmol), K_2CO_3 (78 mg, 0.57 mmol, 2.2 equiv) and $\text{CuSO}_4 \cdot 5\text{H}_2\text{O}$ (1 mg, 0.03 mmol, 0.1 equiv) in MeOH (3 mL) and the mixture stirred at rt for 18 h. The mixture was concentrated, diluted with H_2O (15 mL), acidified with conc. HCl and extracted with EtOAc (10 mL \times 3). The combined organic layers were dried over MgSO_4 , filtered and concentrated. Flash column chromatography (hexane/EtOAc 3:1) afforded a mixture of the desired product **4.58** (characteristic data described below) and an undesired product **4.58a**. A small amount of the undesired sulfonylamide product **4.58a** was isolated; $R_f = 0.10$ (PetEt/EtOAc 2:1); $^1\text{H-NMR}$ (300 MHz): δ 0.88 (t, $J = 6.9$ Hz, 3 H, CH_3), 1.24-1.25 (m, 22 H, $\text{NHCH}_2\text{CH}_2(\text{CH}_2)_{11}\text{CH}_3$), 1.49-1.54 (m, 2 H, NHCH_2CH_2), 2.97-3.02 (m, 1 H, OH), 3.25-3.31 (m, 2 H, NHCH_2), 3.62-3.71 (m, 1 H, H- β), 4.14-4.20 (m, 1 H, H- β'), 4.34-4.39 (m, 1 H, H- α), 6.42-6.44 (m, 1 H, NHCH_2), 7.52-7.54 (m, 1 H, $\text{NH}\text{SO}_2\text{N}_3$).

Tf_2O (1.02 mL, 6.09 mmol, 3 equiv) was added drop-wise to a pre-cooled (0 $^\circ\text{C}$) vigorously stirring mixture of NaN_3 (792 mg, 12.18 mmol, 6 equiv) in H_2O (2.5 mL) and CH_2Cl_2 (2.5 mL) in an inert atmosphere. It was stirred for 2 h at 0 $^\circ\text{C}$. Satd. aq. NaHCO_3 solution (5 mL) was added to the reaction mixture slowly and transferred

to a separating funnel upon evolution of gases. The aqueous layer was washed twice with CH_2Cl_2 (15 mL \times 2). The combined organic layers were washed with satd. aq. NaHCO_3 solution (5 mL) and the approx. 0.6 N TfN_3 (35 mL) solution was used without further purification (based on 50% conversion). (ratio of H_2O : CH_2Cl_2 1:2.6) NOTE: highly explosive compound when dried so avoid concentration of solution. In a separate round bottom, NEt_3 (848 μL , 6.09 mmol, 3 equiv) was added to a mixture of L-serine tetradecyl amide trifluoroacetic acid **4.57** (840 mg, 2.03 mmol) and $\text{CuSO}_4 \cdot 5\text{H}_2\text{O}$ (5 mg, 0.02 mmol, 0.01 equiv) in H_2O (35 mL) (ratio of H_2O : CH_2Cl_2 : MeOH 3:3:10). The prepared TfN_3 solution in CH_2Cl_2 (35 mL) was added slowly in the presence of N_2 by an addition funnel. MeOH (117 mL) was added to the reaction mixture very slowly and it was stirred for 2.5 h. Solid Na_2CO_3 (511 mg, 6.09 mmol, 3 equiv) was added and the reaction mixture was concentrated *in vacuo*. Flash column chromatography (PetEt to 3:1 PetEt: EtOAc) afforded the title compound **4.58** (663 mg, 100%) as a white solid; $R_f = 0.50$ (PetEt/EtOAc 1:1); $[\alpha]_D^{25} = +16.67$ (c, 0.6 in CH_2Cl_2); IR ν_{max} (NaCl plate, CH_2Cl_2): 3903.2, 3840.1, 3435.5, 2925.2, 2853.0, 2100.2, 1642.6 cm^{-1} ; $^1\text{H-NMR}$ (300 MHz): $\delta = 0.87$ (t, $J = 6.4$ Hz, 3 H, CH_2CH_3), 1.25 (s, 24 H, $\text{NHCH}_2(\text{CH}_2)_{12}\text{CH}_3$), 3.23-3.25 (m, 2 H, NHCH_2), 3.98-4.02 (m, 2 H, H- β , H- β'), 4.08-4.11 (m, 1 H, H- α), 6.43-6.49 (m, 1 H, NHCH_2); $^{13}\text{C-NMR}$ (75 MHz): δ_c 14.1 (CH_3), 22.7, 26.8, 29.2, 29.4, 29.5, 29.6, 29.7, 31.9 ($\text{NHCH}_2(\text{CH}_2)_{11}\text{CH}_3$) 39.6 ($\text{NHCH}_2(\text{CH}_2)_{11}\text{CH}_3$), 63.3 (C- β), 64.3 (C- α), 168.0 (C=O); HRMS m/z (ESI+) 327.2771, ($\text{C}_{17}\text{H}_{33}\text{N}_4\text{O}_2\text{H}$: $[\text{M}+\text{H}]^+$ requires 327.2755).

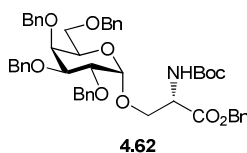
***N*-Azido-*O*-(2,3,4,6-tetra-*O*-benzyl- α,β -galactopyranosyl)-L-serine methyl ester
4.59 and 4.60**



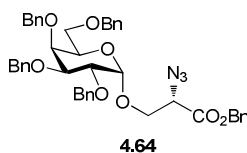
NIS (256 mg, 1.58 mmol, 2 equiv) was added to a solution of phenyl-2,3,4,6-tetra-*O*-benzyl-1-thio- β -D-galactopyranoside **4.54** (500 mg, 0.79 mmol), and *N*-azido-L-serine methyl ester **4.45** (229 mg, 1.58 mmol, 2 equiv) in CH_2Cl_2 (10 mL) in the dark under N_2 . TfOH (1 μL , 0.008 mmol, 0.01 equiv) was added and the reaction mixture

was stirred for 18 h. The reaction mixture was diluted with CH_2Cl_2 (10 mL) and washed with satd. aq. $\text{Na}_2\text{S}_2\text{O}_4$ (10 mL) followed by brine (10 mL). The organic layer was dried over MgSO_4 , filtered and concentrated to give a colourless oil (α/β ratio of 2.2:1). Flash column chromatography (hexane/EtOAc 3:1) afforded the α -anomer **4.59** (169 mg, 32%) as a white solid, the β -anomer **4.60** (127 mg, 25%) as a colourless oil and an undesired succinimide by-product **4.61** (103 mg, 21%). Data recorded for α -anomer **4.59**: $R_f = 0.40$ (PetEt/EtOAc 3:1); $[\alpha]_D^{22} = +21.33$ (c, 1.5 in CH_2Cl_2); IR ν_{max} (NaCl plate, CH_2Cl_2): 3435.1, 2103.0, 1642.5 cm^{-1} ; ^1H NMR (300 MHz): δ 3.48-3.59 (m, 2 H, H-6, H-6'), 3.70 (s, 3 H, CH_3), 3.85 (dd, $J = 6.1$ Hz, 10.6 Hz, 1 H, H- β'), 3.93-4.13 (m, 6 H, H-2, H-3, H-4, H-5, H- α , H- β), 4.41-4.87 (m, 7 H, CHPh , $\text{CH}_2\text{Ph} \times 3$), 4.90 (d, $J = 3.5$ Hz, 1 H, H-1), 4.96 (d, $J = 11.5$ Hz, 1 H, CHPh), 7.29-7.39 (m, 20 H, aromatic); ^{13}C NMR (75 Hz): δ_c 52.7 (OCH_3), 61.7 (C- α), 68.7 (C- β), 69.1 (C-6), 70.0 (C-5), 73.0 (CH_2Ph), 73.2 (CH_2Ph), 73.4 (CH_2Ph), 74.7 (CH_2Ph), 75.1 (C-4), 76.3 (C-2), 78.6 (C-3), 98.9 (C-1), 127.5, 127.6, 127.7, 128.2, 128.2, 128.2, 128.3, 128.3, 137.9, 138.5, 138.7, 138.7 (aromatics), 168.7 (C=O); HRMS m/z (ESI+) 690.2792, ($\text{C}_{38}\text{H}_{41}\text{N}_3\text{O}_8\text{Na}$: $[\text{M}+\text{Na}]^+$ requires 690.2786). Data recorded for β -anomer **4.60**: $R_f = 0.29$ (PetEt/EtOAc 3:1); $[\alpha]_D^{28} = +2.67$ (c, 0.75 in CH_2Cl_2); IR ν_{max} (NaCl plate, CH_2Cl_2): 3428.0, 2105.6, 1641.9, 1260.6 cm^{-1} ; ^1H NMR (300 MHz): δ 3.49-3.58 (m, 4 H, H-3, H-4 or H-5, H-6, H-6'), 3.74 (s, 3 H, CH_3), 3.77-3.83 (m, 1 H, H-2), 3.85-3.90 (m, 2 H, H- β' , H-4 or H-5), 4.07 (t, $J = 5.9$ Hz, 1 H, H- α), 4.19 (dd, $J = 5.9$ Hz, 10.3 Hz, 1 H, H- β), 4.39 (d, $J = 7.6$ Hz, 1 H, H-1), 4.42-4.95 (m, 8 H, $\text{CH}_2\text{Ph} \times 4$), 7.25-7.39 (m, 20 H, $\text{Ph} \times 4$); ^{13}C NMR (75 Hz): δ_c 52.8 (CH_3), 61.6 (C- α), 68.6 (C- β), 68.7 (C-6), 73.1 (CH_2Ph), 73.6, 73.5 (C-4, C-5), 73.7 (CH_2Ph), 74.6 (CH_2Ph), 75.1 (CH_2Ph), 79.1, 82.1 (C-2, C-3), 103.9 (C-1), 127.5, 127.6, 127.8, 127.9, 128.2, 128.2, 128.3, 128.3, 128.4, 128.5, 137.9, 138.4, 138.5, 138.7 (aromatics), 168.7 (C=O); HRMS m/z (ESI+) 690.2798, ($\text{C}_{38}\text{H}_{41}\text{N}_3\text{O}_8\text{Na}$: $[\text{M}+\text{Na}]^+$ requires 690.2786).

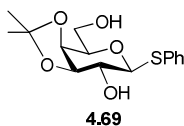
The data recorded for the succinimide byproduct **4.61** is in agreement with the reported values.^[200]

N*-tert-Butoxycarbonyl-*O*-(2,3,4,6-tetra-*O*-benzyl- α -galactopyranosyl)-L-serine 1-benzyl ester **4.62*

NIS (256 mg, 1.58 mmol, 2 equiv) was added to a solution of phenyl-2,3,4,6-tetra-*O*-benzyl-1-thio- β -D-galactopyranoside **4.54** (500 mg, 0.79 mmol) and *N*-Boc-L-serine-benzyl ester **4.20** (467 mg, 1.58 mmol, 2 equiv) in CH₂Cl₂ (5 mL) in the dark under N₂. TfOH (1 μ L, 0.008 mmol, 0.01 equiv) was added and the reaction mixture was stirred for 18 h. It was diluted with CH₂Cl₂ (10 mL) and washed with satd. aq. Na₂S₂O₄ solution (10 mL) followed by brine (10 mL). The organic layer was dried over MgSO₄, filtered and concentrated. Flash column chromatography (hexane/EtOAc 4:1) afforded the α -anomer **4.62** (199 mg, 44%) as a yellow oil; R_f = 0.37 (PetEt/EtOAc 3:1); $[\alpha]_D^{24} = +41.05$ (c, 0.95 in CH₂Cl₂); IR ν_{\max} (NaCl plate, CH₂Cl₂): 3427.6, 2097.9, 1642.1 cm⁻¹; ¹H NMR (300 MHz): δ 1.41 (s, 9 H, C=OOC(CH₃)₃), 3.49- 3.54 (m, 2 H, H-6, H-6'), 3.78-3.82 (m, 2 H, H-3, H- β'), 3.85-3.91 (m, 2 H, H-4, H-5), 4.00 (dd, *J* = 3.7 Hz, 10.1 Hz, 1 H, H-2), 4.16 (dd, *J* = 3.0 Hz, 10.6 Hz, 1 H, H- β), 4.39 (d, *J* = 11.9 Hz, 1 H, CHHPh), 4.49-4.56 (m, 3 H, CHHPh \times 2, H- α), 4.60 (d, *J* = 11.4 Hz, 1 H, CHHPh), 4.67-4.80 (m, 4 H, CH₂Ph, CHHPh, H-1), 4.91 (d, *J* = 11.4 Hz, 1 H, CHHPh), 5.10 (s, 2 H, CO₂CH₂Ph), 5.79 (d, *J* = 8.9 Hz, 1 H, NH), 7.16-7.35 (m, 25 H, aromatic); ¹³C NMR (75 Hz): δ_c 28.3 (C=OOC(CH₃)₃), 54.4 (C- α), 67.1 (CO₂CH₂Ph), 68.7 (C-6), 69.8 (C-4), 70.4 (C- β), 73.0 (CH₂Ph), 73.2 (CH₂Ph), 73.5 (CH₂Ph), 74.8 (C-5), 76.4 (CH₂Ph), 77.2 (C=OOC(CH₃)₃), 78.7 (C-2), 79.9 (C-3), 99.3 (C-1), 127.4, 127.5, 127.6, 127.7, 127.7, 127.8, 127.9, 128.2, 128.2, 128.3, 128.4, 128.5, 135.4, 137.9, 138.6, 138.7, (aromatics), 155.6 (C=O), 170.4 (C=O); HRMS *m/z* (ESI+) 1657.7469, (C₉₈H₁₁₀N₂O₂₀Na: [2M+Na]⁺ requires 1657.7544).

N*-Azido-*O*-(2,3,4,6-tetra-*O*-benzyl- α -galactopyranosyl)-*L*-serine 1-benzyl ester*4.64**

NIS (78 mg, 0.35 mmol, 1 equiv) was added to a solution of phenyl-2,3,4,6-tetra-*O*-benzyl-1-thio- β -D-galactopyranoside **4.54** (220 mg, 0.35 mmol), and *N*-azido-*L*-serine benzyl ester **4.44** (77 mg, 0.35 mmol, 1 equiv) in CH₂Cl₂ (5 mL) in the dark under N₂. TfOH (1 μ L, 0.003 mmol, 0.01 equiv) was added and the reaction mixture was stirred for 3 h. The solution was diluted with CH₂Cl₂ (5 mL) and washed with satd. aq. Na₂S₂O₄ (5 mL) followed by brine (5 mL). The organic layer was dried over MgSO₄, filtered and concentrated. Flash column chromatography (hexane/EtOAc 3:1) afforded the α -anomer **4.64** (47 mg, 26%) as a white solid; R_f = 0.43 (PetEt/EtOAc 3:1); IR ν_{\max} (NaCl plate, CH₂Cl₂): 3420.7, 2743.9, 2107.5, 1726.2 cm⁻¹; ¹H NMR (300 MHz): δ 3.44-3.56 (m, 2 H, H-6, H-6'), 3.81-4.13 (m, 6 H, H- α , H- β , H- β' , H-2, H-3, H-5), 4.37-4.94 (m, 9 H, CH₂Ph \times 4, H-4), 4.86 (d, J = 3.5 Hz, 1 H, H-1), 5.10 (dd, J = 12.3 Hz, 25.0 Hz, 2 H, CO₂CH₂Ph), 7.24-7.34 (m, 25 H, aromatics); ¹³C NMR (75 Hz): δ_c 60.7 (C- α), 66.7 (CO₂CH₂Ph), 67.7 (C-6), 68.1 (C- β), 69.0 (C-4), 72.1 (CH₂Ph), 72.4 (CH₂Ph), 73.7 (CH₂Ph), 73.8 (CH₂Ph), 73.7 (C-2), 75.3 (C-5), 77.6 (C-3), 97.9 (C-1), 126.5, 126.5, 126.6, 126.7, 126.7, 126.7, 127.2, 127.2, 127.3, 127.3, 127.3, 127.4, 127.5, 127.6, 128.9, 133.9, 136.9, 137.5, 137.7, 137.7 (aromatics), 167.3 (C=O); HRMS m/z (ESI+) 744.3279 (C₄₄H₄₅N₃O₈H: [M+H]⁺ requires 744.3281).

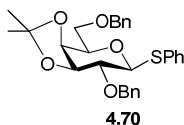
Phenyl 3,4-*O*-(isopropylidene)-1-thio- β -D-galactopyranoside 4.69

Na metal (2 mg approx., 0.10 mmol approx., 0.1 equiv approx.) was added to phenyl-2,3,4,6-tetra-*O*-acetyl-1-thio- β -D-galactopyranoside **4.53** (420 mg, 0.99 mmol) in THF/H₂O/MeOH (2:1:2, 5 mL) at 0 °C. It was stirred for 1 h and quenched with Amberlite ion exchange resin. The solution was filtered and concentrated *in*

vacuo. H₂SO₄ (100 μL) was added drop-wise to the crude glycoside (240 mg, 0.88 mmol) in acetone (6 mL) at rt and the reaction mixture was stirred for 36 h at rt. NEt₃ was added drop-wise to give a pH of 7. The reaction mixture was concentrated *in vacuo*. Flash column chromatography (PetEt/ EtOAc 1:1) yielded the β-anomer **4.69** (122 mg, 44%) as a white foam; IR ν_{\max} (NaCl plate, CH₂Cl₂): 3406.2, 2101.7, 1632.1, 1480.8 cm⁻¹; ¹H NMR (300 MHz): δ 1.33 (s, 3 H, CH₃), 1.41 (s, 3 H, CH₃), 3.57 (dd, *J* = 7.0 Hz, 10.1 Hz, 1 H, H-2), 3.79-3.89 (m, 2 H, H-5, H-6'), 3.98 (dd, *J* = 7.2 Hz, 11.1 Hz, 1 H, H-6), 4.11 (pt, *J* = 5.8 Hz, 1 H, H-3), 4.17 (dd, *J* = 1.6 Hz, 5.3 Hz, 1 H, H-4), 4.48 (d, *J* = 10.1 Hz, 1 H, H-1), 7.29-7.52 (m, 5 H, aromatics). HRMS *m/z* (ESI-) 348.0742, (C₁₅H₂₀O₅SCl: [M+Cl]⁻ requires 348.0758).

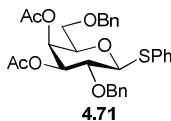
The NMR data is in agreement with the reported values.^[277]

Phenyl 2,5-di-*O*-benzyl-3,4-*O*-(isopropylidene)-1-thio-β-D-galactopyranoside **4.70**

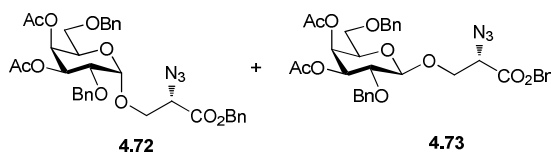


To a solution of phenyl 3,4-*O*-(isopropylidene)-1-thio-β-D-galactopyranoside **4.69** (303 mg, 0.97 mmol) in DMF (10 mL) was slowly added NaH (60% suspension in mineral oil) (155 mg, 3.88 mmol, 4 equiv) under an inert atmosphere at 0 °C. The reaction mixture was stirred for 30 min and BnBr (346 μL, 2.91 mmol, 3 equiv) was added to the suspension at 0 °C. The reaction mixture was stirred for 18 h at rt. To this suspension MeOH (2 mL) was added and was concentrated *in vacuo*. Flash column chromatography (PetEt/ EtOAc 9:1) afforded the title compound **4.70** (442 mg, 92%) as a white solid; R_f = 0.30 (PetEt/EtOAc 9:1); IR ν_{\max} (NaCl plate, CH₂Cl₂): 3421.8, 2921.9, 1638.1, 1081.8 cm⁻¹; ¹H NMR (300 MHz): δ 1.34 (s, 3 H, CH₃), 1.40 (s, 3 H, CH₃), 3.53 (dd, *J* = 6.0 Hz, 9.5 Hz, 1 H, H-2), 3.79 (dd, *J* = 1.9 Hz, 6.2 Hz, 2 H, H-6, H-6'), 3.94 (td, *J* = 1.9 Hz, 5.9 Hz, 1 H, H-5), 4.19-4.27 (m, 2 H, H-3, H-4), 4.49-4.84 (m, 5 H, CH₂Ph × 2, H-1), 7.20-7.56 (m, 15 H, aromatics).

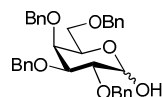
The NMR data is in agreement with the reported values.^[277]

Phenyl 2,5-di-O-benzyl-3,4-di-O-acetyl-1-thio-β-D-galactopyranoside 4.71 ^[212]

To phenyl 2,5-di-O-benzyl-3,4-O-(isopropylidene)-1-thio-β-D-galactopyranoside **4.70** (53 mg, 0.11 mmol) was added 80% AcOH (200 mL). The reaction was heated to 80 °C and was heated for 4 h. It was cooled and concentrated *in vacuo*. The waxy solid was diluted with CH₂Cl₂ and washed with H₂O, dried over MgSO₄, filtered and concentrated to yield the crude tetraol. Ac₂O (1 mL) was added to the compound dissolved in Pyr (2 mL) at rt at 0 °C. DMAP (2 mg, 0.007 mmol, 0.1 equiv) was added and the reaction mixture was stirred for 1.5 h at rt. The reaction mixture was concentrated *in vacuo* and the reaction mixture was re-dissolved in CH₂Cl₂ (10 mL). It was washed with satd. aq. NaCO₃ (10 mL × 3) followed by brine (10 mL). The organic layers were combined, dried over MgSO₄, filtered and rotary evaporated. Flash column chromatography (PetEt/ EtOAc 1:1) afforded the title compound **4.71** (35 mg, 93%) as a white solid; R_f = 0.23 (PetEt/EtOAc 3:1); [α]²⁴_D = -4.3 (c, 0.93 in CH₂Cl₂); IR ν_{max} (NaCl plate, CH₂Cl₂): 3423.2, 2095.5, 1642.1 cm⁻¹; ¹H NMR (300 MHz): δ 1.90 (s, 3 H, OCH₃), 2.03 (s, 3 H, CH₃), 3.46-3.52 (m, 1 H, H-6'), 3.56-3.62 (m, 1 H, H-6), 3.73 (t, *J* = 9.6 Hz, 1 H, H-2), 3.85 (t, *J* = 6.1 Hz, 1 H, H-5), 4.29-4.86 (m, 5 H, CH₂Ph × 2, H-1), 5.03 (dd, *J* = 3.3 Hz, 9.6 Hz, 1 H, H-3), 5.47-5.48 (m, 1 H, H-4), 7.25-7.60 (m, 15 H, aromatics); ¹³C NMR (75 Hz): δ_c 19.7 (CH₃ × 2), 66.9 (C-6), 67.2 (C-4), 72.5 (CH₂Ph), 73.3 (C-3), 74.4 (C-2, CH₂Ph), 74.7 (C-5), 86.9 (C-1), 126.6, 126.8, 126.8, 126.9, 127.3, 127.4, 127.9, 130.9, 132.5, 136.6, 136.9 (aromatics), 168.8 (C=O), 169.1 (C=O); HRMS *m/z* (ESI+) 577.1562 (C₃₀H₃₂O₇SK: [M+K]⁺ requires 577.1506).

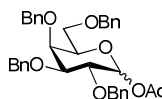
***N*-Azido-*O*-(2,5-di-*O*-benzyl-3,4-di-*O*-acetyl- α,β -galactopyranosyl)-*L*-serine 1-methyl ester **4.72** and **4.73**^[212]**

NIS (196 mg, 0.87 mmol, 1.1 equiv) was added to a cooled solution of *N*-azido-*L*-serine benzyl ester **4.44** (115 mg, 0.79 mmol) and phenyl 2,5-di-*O*-benzyl-3,4-di-*O*-acetyl-1-thio- β -D-galactopyranoside **4.71** (468 mg, 0.87 mmol, 1.1 equiv) on ice in anhydrous CH₂Cl₂ (5 mL) containing pre-dried 4Å MS in the dark under N₂. TMSOTf (40 μ L) was added and the reaction mixture was stirred for 1 h. NEt₃ (160 μ L) was added and the reaction mixture was concentrated *in vacuo*. Flash column chromatography (PetEt/EtOAc 5:1, loaded with toluene) afforded an inseparable mixture of anomers **4.72** and **4.73** (287 mg, 63% as a mixture of diastereoisomers (2:1 α : β)). A re-column (PetEt/EtOAc 5:1) afforded a small amount of α -anomer **4.72** for characterisation; Data recorded for α -anomer **4.72**: R_f = 0.52 (PetEt/EtOAc 3:1); $[\alpha]_D^{25} = +11.43$ (c, 0.35 in CH₂Cl₂); IR ν_{\max} (NaCl plate, CH₂Cl₂): 3435.7, 2100.3, 1642.3 cm⁻¹; ¹H NMR (300 MHz): δ 1.98 (s, 3 H, COCH₃), 2.02 (s, 3 H, COCH₃), 3.44-3.48 (m, 2 H, H-6, H-6'), 3.74 (s, 3 H, CO₂CH₃), 3.76-3.86 (m, 2 H, H- β , H-2), 4.03 (dd, $J = 3.8$ Hz, 10.6 Hz, 1 H, H- β'), 4.15-4.23 (m, 2 H, H- α , H-5), 4.41-4.70 (m, 4 H, CH₂Ph \times 2), 4.90 (d, $J = 3.5$ Hz, 1 H, H-1), 5.28 (dd, $J = 3.1$ Hz, 10.3 Hz, 1 H, H-3), 5.48-5.49 (m, 1 H, H-4), 7.29-7.33 (m, 10 H, aromatics); ¹³C NMR (75 Hz): δ_c 20.7 (OCH₃), 20.8 (OCH₃), 52.9 (CO₂CH₃), 61.7 (C- α), 67.9, 68.2, 68.5, 69.0, 69.6, 72.8, 73.4, 73.6 (C-2, C-3, C-4, C-5, C-6, C- β , CH₂Ph \times 2), 98.5 (C-1), 127.6, 127.8, 128.4, 137.6, 138.1 (aromatics), 168.5 (C=O), 169.9 (C=O), 170.1 (C=O); HRMS m/z (ESI+) 1167.4288 (C₅₆H₆₆N₆O₂₀Na: [2M+Na]⁺ requires 1167.4284).

2,3,4,6- Tetra-*O*-benzyl- α/β -D-galactopyranose 4.78 ^[278]**4.78**

NBS (1.69 g, 9.48 mmol, 3 equiv) was added to a stirring solution of phenyl-2,3,4,6-tetra-*O*-benzyl-1-thio- β -D-galactopyranoside **4.54** (2 g, 3.16 mmol) in acetone/H₂O (24 mL, 5:1) and the solution was heated to 75 °C for 24 h. The reaction mixture was concentrated *in vacuo*. Satd. aq. NaHCO₃ (50 mL) was added and the suspension was extracted with EtOAc (50 mL). The organic layer was washed with brine (50 mL). The organic layer was dried over MgSO₄, filtered, concentrated *in vacuo* and the crude product was purified by flash column chromatography (PetEt/EtOAc, 9:1, loaded in toluene) to yield the title compound **4.78** as a colourless oil (931 mg, 61% based on recovered starting material) as a mixture of anomers (2:1 α/β); Data recorded for mixture of anomers: R_f = 0.55 (PetEt/EtOAc 3:1); Data recorded for α -anomer: ¹H NMR (300 MHz): δ 3.56-3.69 (m, 3 H, H-6, H-6', H-5), 4.04-4.06 (m, 1 H, H-3), 4.11-4.13 (m, 1 H, H-2), 4.28 (pt, J = 6.4 Hz, 1 H, H-4), 4.45-5.06 (m, 8 H, CH₂Ph \times 4), 5.39 (d, J = 2.3 Hz, 1 H, H-1 α), 7.39-7.48 (m, 20 H, aromatics); HRMS m/z (ESI+) 540.2510 (C₃₄H₃₆O₆: [M⁺]⁺ requires 540.2506).

The NMR data is in agreement with the reported values.^[278]

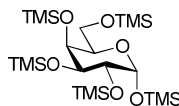
1-*O*-Acetyl-2,3,4,6- tetra-*O*-benzyl- α/β -D-galactopyranose 4.79**4.79**

Ac₂O (2 mL) was added to 2,3,4,6-tetra-*O*-benzyl- α/β -D-galactopyranose **4.78** (872 mg, 1.61 mmol) in Pyr (3 mL) at 0 °C. The reaction mixture was stirred for 18 h at rt and was rotary evaporated. Ice-water (200 mL) was added and the organic layer was extracted with EtOAc (100 mL \times 2). The organic layers were combined, dried over MgSO₄, filtered and concentrated. Flash column chromatography (PetEt/EtOAc 5:1) afforded the title compound **4.79** (367 mg, 41%) as a colourless oil (1:1

α/β); Data recorded for mixture of anomer: $R_f = 0.86$ (PetEt/EtOAc 3:1); ^1H NMR (300 MHz): δ 2.02 (s, 3 H, OC(O)CH₃), 2.11 (s, 3 H, OC(O)CH₃), 3.49-3.63 (m, 5 H, H-6 (α), H-5 (α), H-6 (β), H-6' (β), H-5 (β)), 3.67-3.72 (m, 1 H, H-6 (α)), 3.86-4.04 (m, 5 H, H-3 (α), H-4 (α), H-2 (β), H-3 (β), H-4 (β)), 4.17 (dd, $J = 3.7$ Hz, 10.1 Hz, 1 H, H-2 (α)), 4.36-4.97 (m, 8 H, CH₂Ph \times 4), 5.57 (d, $J = 8.1$ Hz, 1 H, H-1(β)), 6.37 (d, $J = 3.7$ Hz, 1 H, H-1(α)), 7.27-7.32 (m, 40 H, aromatics); HRMS m/z (ESI+) 605.2510 (C₃₆H₃₈O₇Na: [M+Na]⁺ requires 605.2536).

The NMR data is in agreement with the reported values.^[279]

1,2,3,4,6-Penta-O-trimethylsilyl- α -D-galactopyranose **4.82**

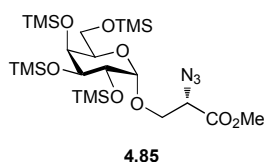


4.82

NEt₃ (766 μL , 5.5 mmol, 5.5 equiv) was added to D-galactose **4.28** in anhydrous DMF (2 mL) under N₂. TMSCl (698 μL , 5.5 mmol, 5.5 equiv) was added to the solution and additional DMF (2 mL) was added to solubilise the resulting precipitate. The reaction mixture was stirred at rt for 4 h. Pentane (50 mL) and crushed ice (50 mL) was added to the suspension. The aqueous layer was extracted with pentane (50 mL \times 2). The combined organic layers were washed with H₂O (50 mL \times 2), brine (50 mL \times 2), dried over MgSO₄, filtered and concentrated *in vacuo* to afford the α -anomer **4.82** (0.46 g, 89%, crude yield) as a colourless oil; $R_f = 0.88$ (PetEt/EtOAc 20:1); ^1H NMR (300 MHz): δ 0.11-0.27 (m, 15 H, Si(CH₃)₃ \times 5), 3.60 (dd, $J = 5.7$ Hz, 9.6 Hz, 1 H, H-6'), 3.70 (pt, $J = 9.6$ Hz, 1 H, H-6), 3.86-3.88 (m, 2 H, H-4, H-2), 3.95-3.97 (m, 2 H, H-3, H-5), 5.11 (d, $J = 3.2$ Hz, 1 H, H-1); ^{13}C NMR (75 Hz): δ_c - 0.5 (OCH₃), 0.2 (OCH₃), 0.3 (OCH₃), 0.5 (OCH₃), 0.6 (OCH₃), 61.2, 70.0, 70.5, 71.1, 72.3 (C-2, C-3, C-4, C-5, C-6), 94.6 (C-1).

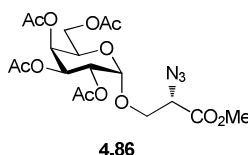
The NMR data is in agreement with the reported values.^[280]

2-Azido-3-(2,3,4,6-tetra-*O*-trimethylsilyl- α -D-galactopyranosyl)-L-serine 1-methyl ester **4.85**



TMSI (46 μ L, 0.034 mmol, 1 equiv) was added to a solution of 1,2,3,4,6-penta-*O*-trimethylsilyl- α -D-galactopyranose **4.82** (184 mg, 0.34 mmol) in CH_2Cl_2 (2 mL) at 0 $^\circ\text{C}$ under argon. The reaction mixture was stirred under argon for 15 min at rt. Benzene (2 mL) was added and the reaction mixture was concentrated *in vacuo*. 2,3,4,6-Tetra-*O*-trimethylsilyl- α -D-galactopyranose iodide **4.83** was re-dissolved in CH_2Cl_2 (2 mL) and kept under argon. In another round bottom, *N*-azido-L-serine methyl ester **4.45** (16 mg, 0.112 mmol, 0.33 equiv), TBAI (251 mg, 0.68 mmol, 2 equiv), DIPEA (89 μ L, 0.51 mmol, 1.5 equiv) and 4Å MS in CH_2Cl_2 (2 mL) were stirred for 15 min. 2,3,4,6-Tetra-*O*-trimethylsilyl- α -D-galactopyranose iodide **4.83** was added over a period of 15 min and the reaction mixture was stirred for 18 h. The reaction mixture was concentrated *in vacuo*, re-dissolved in Et_2O (20 ml), washed with H_2O (20 mL), dried over MgSO_4 , filtered and concentrated *in vacuo*. Flash column chromatography (PetEt/ EtOAc 20:1 to 9:1) afforded the α -anomer **4.85** (67 mg, 15%) as a colourless oil; Data recorded for α -anomer **4.85**: $R_f = 0.32$ (PetEt/EtOAc 9:1); $[\alpha]_D^{20} = +120.00$ (c, 0.20 in CH_2Cl_2); IR ν_{max} (NaCl plate, CH_2Cl_2): 3601.2, 3343.2, 2920.9, 1250.8 cm^{-1} ; ^1H NMR (300 MHz): δ 0.11-0.16 (m, 12 H, $\text{Si}(\text{CH}_3)_3 \times 5$), 3.40-3.50 (m, 1 H, H- β'), 3.60-3.66 (m, 7 H, H- β , H-5, H-6, H-6', CH_3), 3.76 (dd, $J = 2.7$ Hz, 9.2 Hz, 1 H, H-3), 3.85-3.93 (m, 2 H, H-2, H-4), 3.97 (t, $J = 6.9$ Hz, 1 H, H- α), 5.14 (d, $J = 3.5$ Hz, 1 H, H-1); ^{13}C NMR (75 Hz): δ_c -0.9 ($\text{Si}(\text{CH}_3)_3$), -0.2 ($\text{Si}(\text{CH}_3)_3$), 0.0 ($\text{Si}(\text{CH}_3)_3$), 0.2 ($\text{Si}(\text{CH}_3)_3$), 60.5 (CO_2CH_3), 69.6, 70.4, 71.2, 71.4, 76.8 (C- β , C-2, C-3, C-4, C-5, C-6), 93.4 (C-1).

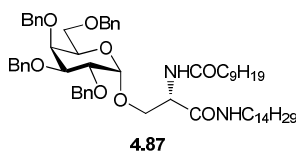
2-Azido-3-(2,3,4,6-tetra-*O*-acetyl- α -D-galactopyranosyl)-L-serine 1-methyl ester
4.86^[193]



TMSI (1.11 mL, 8.12 mmol, 1.1 equiv) was added to a pre-cooled solution of 1,2,3,4,6-penta-*O*-trimethylsilyl- α -D-galactopyranose **4.82** (3.99 mg, 7.38 mmol) in CH₂Cl₂ (6 mL) at 0 °C under argon. The reaction mixture was stirred under argon for 20 min at 0 °C. Benzene (20 mL) was added and the reaction mixture was rotary evaporated to give a viscous yellow oil. 2,3,4,6-Tetra-*O*-trimethylsilyl- α -D-galactopyranose iodide **4.83** was re-dissolved in CH₂Cl₂ (6 mL) and kept under argon. In a separate round bottom, *N*-azido-L-serine methyl ester **4.45** (719 mg, 2.43 mmol, 0.33 equiv), TBAI (4.09 g, 11.07 mmol, 1.5 equiv), DIPEA (1.93 mL, 11.07 mmol, 1.5 equiv) and 4Å MS in CH₂Cl₂ (10 mL) were stirred for 15 min. 2,3,4,6-Tetra-*O*-trimethylsilyl- α -D-galactopyranose iodide **4.83** was added over a period of 15 min and the reaction mixture was stirred for 48 h. The reaction mixture was concentrated *in vacuo*. 2-Azido-3-(2,3,4,6-tetra-*O*-trimethylsilyl- α -D-galactopyranosyl)-L-serine 1-methyl ester **4.85** was suspended in MeOH (30 mL) and Dowex (H⁺ form) (2g) was added. The reaction mixture was stirred for 5 h, filtered and rotary evaporated to yield a deacetylated brown oil. Ac₂O (1.84 mL, 19.44 mmol, 8 equiv) was added to the tetraol (747 mg, 2.43 mmol) in Pyr (2 mL) and the reaction mixture was stirred for 18 h. It was rotary evaporated. Flash column chromatography (3:1 PetEt/ EtOAc) afforded the title compound **4.86** (430 mg) as a white foam containing impurities. Repeated chromatography (EtOAc/Tol/PetEt 10:60:30) afforded the α -anomer **4.86** (32 mg, 3% , crude yield) as a yellow oil; Data recorded for α -anomer **4.86**: R_f = 0.25 (PetEt/EtOAc 2:1); [α]_D²⁰ = + 66.67 (c, 0.93 in CH₂Cl₂); IR ν_{\max} (NaCl plate, CH₂Cl₂): 3421.6, 2108.9, 1743.3, 1639.1 cm⁻¹; ¹H NMR (300 MHz): δ 1.99 (s, 3 H, OC(O)CH₃), 2.06 (s, 3 H, OC(O)CH₃), 2.09 (s, 3 H, OC(O)CH₃), 2.14 (s, 3 H, OC(O)CH₃), 3.82 (bs, 3 H, CH₃), 3.81-3.87 (m, 1 H, H- β'), 4.05-4.12 (m, 4 H, H- α , H- β , H-6, H-6'), 4.25 (pt, *J* = 6.8 Hz, 1 H, H-5), 5.10 (dd, *J* = 3.7 Hz, 10.8 Hz, 1 H, H-2), 5.16 (d, *J* = 3.7 Hz, 1 H, H-1), 5.33 (dd, *J* = 3.3 Hz,

10.8 Hz, 1 H, H-3), 5.47-5.48 (m, 1 H, H-4); ^{13}C NMR (75 Hz): δ_{c} 20.6 (OCH₃), 20.6 (OCH₃), 20.7 (OCH₃), 52.9 (CH₃), 61.4 (C- α), 61.7 (C-6), 66.9 (C-5), 67.3 (C-3), 67.9, 67.9 (C-2, C-4), 68.5 (C- β), 96.9 (C-1), 168.3 (C=O), 169.9 (C=O), 170.1 (C=O), 170.4 (C=O), 170.6 (C=O); HRMS m/z (ESI+) 476.1533 (C₁₈H₂₅N₃O₁₂H: [M+H]⁺ requires 476.1511).

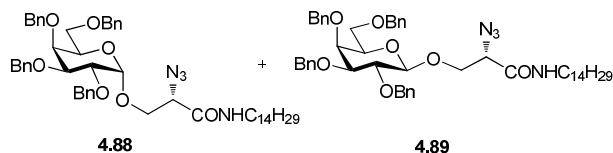
O-(2,3,4,6-Tetra-O-benzyl- α -D-galactopyranosyl)-N-(decanosyl)-L-serine tetradecyl amide **4.87**



10% Piperadine in CH₂Cl₂ (50 μL in 500 μL) was added to *N*-(9-fluorenylmethoxycarbonyl)-O-(2,3,4,6-tetra-O-benzyl- α -D-galactopyranosyl)-L-serine tetradecyl amide **2.67** (50 mg, 0.05 mmol) and the reaction mixture was stirred for 1 h at rt. The solution was diluted with CH₂Cl₂ (10 mL) and washed with 1 M aq. HCl solution (10 mL \times 3), brine (10 mL), dried over MgSO₄, filtered and concentrated to afford a crude amine (45 mg, 100%, crude yield) as a yellow oil; ^1H NMR (300 MHz): δ 0.87 (t, J = 6.9 Hz, 3 H, CH₃), 1.23-1.25 (m, 22 H, NHCH₂CH₂(CH₂)₁₁CH₃), 1.25-1.63 (m, 2 H, NHCH₂CH₂), 3.37-3.43 (m, 2 H, NHCH₂), 3.51-4.16 (m, 9 H, H-2, H-3, H-4, H-5, H-6, H-6', H- β , H- β' , H- α), 4.93-4.99 (m, 9 H, CH₂Ph \times 4, H-1), 7.26-7.35 (m, 20 H, aromatic), 7.75 (d, J = 7.3 Hz, 1 H, NHCH₂); HRMS m/z (ESI+) 823.5255 (C₅₁H₇₀N₂O₇H: [M+H]⁺ requires 823.5256). DMF (5 mL) was added to a round bottom containing decanoic acid (15 mg, 0.087 mmol), TBTU (31 mg, 0.0957 mmol, 1.2 equiv), HOBT (13 mg, 0.0957 mmol, 1.2 equiv) and DIPEA (45 μL , 0.261 mmol, 3 equiv) under N₂ and was stirred for 10 min. The crude amine (72 mg, 0.087 mmol, 1 equiv) was then added to the reaction mixture and was stirred for 18 h. The reaction mixture was concentrated, re-dissolved in CH₂Cl₂ (10 mL); washed with brine (10 mL). The organic layer was dried over MgSO₄, filtered and evaporated under reduced pressure. Flash column chromatography (chloroform/ether 95:5) and repeated flash column chromatography (PetEt/EtOAc 5:1) afforded α -anomer **4.87** (40 mg, 47%) as a white solid; R_f = 0.37 (PetEt/EtOAc

4:1); $[\alpha]_{\text{D}}^{27} = +34.67$ (c, 0.75 in CH_2Cl_2); IR ν_{max} (NaCl plate, CH_2Cl_2): 3821.8, 3301.9, 2922.2, 2852.5, 1635.2, 1542.9 cm^{-1} ; ^1H NMR (300 MHz): δ 0.87 (t, $J = 6.9$ Hz, 3 H, CH_3), 1.24-1.26 (m, 36 H, $\text{CO}(\text{CH}_2)_2(\text{CH}_2)_6\text{CH}_3$, $\text{NH}(\text{CH}_2)(\text{CH}_2)_{12}\text{CH}_3$), 1.57-1.62 (m, 2 H, COCH_2CH_2), 2.16 (t, $J = 8.0$ Hz, 2 H, COCH_2), 2.56-2.65, 3.02-3.13 (m \times 2, 2 H, NHCH_2), 3.38-3.45 (m, 1 H, H- β), 3.51-3.59 (m, 2 H, H-6', H-6), 3.85 (dd, $J = 2.5$ Hz, 10.1 Hz, 1 H, H-3), 3.93-4.00 (m, 3 H, H-4, H-5, H- β'), 4.11 (dd, $J = 3.7$ Hz, 10.1 Hz, 1 H, H-2), 4.33-4.95 (m, 8 H, $\text{CH}_2\text{Ph} \times 4$), 5.13 (d, $J = 3.7$ Hz, 1 H, H-1), 6.61 (d, $J = 6.3$ Hz, 1 H, NHCOCH_2), 7.03 (t, $J = 5.2$ Hz, 1 H, NHCH_2), 7.26-7.38 (m, 20 H, aromatics); ^{13}C NMR (75 Hz): δ_{C} 13.1 (CH_3)^{xxiv}, 21.7, 21.7, 24.5, 25.5, 25.8, 28.3, 28.3, 28.4, 28.4, 28.6, 28.7, 28.7, 30.9, 30.9 ($\text{NHCH}_2(\text{CH}_2)_{12}\text{CH}_3$, $\text{COCH}_2(\text{CH}_2)_7\text{CH}_3$), 35.5 (COCH_2), 38.4 (NHCH_2), 50.2 (C- α), 66.9 (C- β), 67.8 (C-6), 68.9 (C-5), 71.6, 72.5, 73.8 ($\text{CH}_2\text{Ph} \times 4$), 73.5 (C-4), 76.2 (C-2), 78.4 (C-3), 97.3 (C-1), 126.3, 126.6, 126.7, 126.8, 126.9, 127.1, 127.2, 127.3, 127.4, 127.4, 127.5, 127.7, 136.4, 136.8, 137.3, 137.5 (aromatics), 168.3 (C=O), 171.9 (C=O); HRMS m/z (ESI+) 977.6628 ($\text{C}_{61}\text{H}_{88}\text{N}_2\text{O}_8\text{H}$: $[\text{M}+\text{H}]^+$ requires 977.6613).

N*-Azido-*O*-(2,3,4,6-tetra-*O*-benzyl- α/β -*D*-galactopyranosyl)-*L*-serine tetradecyl amide **4.88** and **4.89*

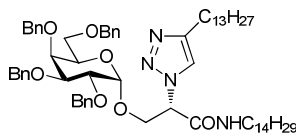


NIS (276 mg, 1.23 mmol, 2 equiv) was added to a solution of phenyl-2,3,4,6-tetra-*O*-benzyl-1-thio- β -*D*-galactopyranoside **4.54** (388 mg, 0.61 mmol), and *N*-azido-*L*-serine tetradecyl amide **4.58** (200 mg, 0.61 mmol, 1 equiv) in THF (6 mL) in the dark under N_2 . TfOH (1 μL , 0.006 mmol, 0.01 equiv) was added and the reaction mixture was stirred for 20 h. MeOH was added and the solution was concentrated *in vacuo*. The reaction mixture was diluted with CH_2Cl_2 (20 mL) and washed with satd. aq. $\text{Na}_2\text{S}_2\text{O}_4$ (20 mL) followed by brine (20 mL). The organic layer was dried over Na_2SO_4 , filtered and concentrated. Flash column chromatography (PetEt/EtOAc 5:1) afforded the mixture of diastereoisomers **4.88** and **4.89** (328 mg, 63%) as a

^{xxiv} Two overlapping signals.

colourless oil (α/β ratio 2.7:1). Additional flash column chromatography (PetEt to PetEt/EtOAc 9:1 to 5:1) afforded α -anomer **4.88** (81 mg, 35%); $R_f = 0.13$ (PetEt/EtOAc/toluene 3:1:6); Data recorded for α -anomer **4.88**: $[\alpha]_D^{25} = +34.29$ (c, 0.35 in CH_2Cl_2); IR ν_{max} (NaCl plate, CH_2Cl_2): 3350.5, 2924.3, 2858.2, 2108.2, 1726.4, 1452.2 cm^{-1} ; ^1H NMR (300 MHz): δ 0.87 (t, $J = 7.3$ Hz, 3 H, CH_3), 1.24-1.25 (m, 20 H, $(\text{CH}_2)_{10}\text{CH}_3$), 1.37-1.44 (m, 2 H, $\text{NHCH}_2\text{CH}_2(\text{CH}_2)_{10}\text{CH}_3$), 2.95-3.07 (m, 1 H, NHCH), 3.16-3.23 (m, 1 H, NHCH), 3.52-3.54 (m, 2 H, H-6, H-6'), 3.68-3.76 (m, 1 H, H- β'), 3.90-3.96 (m, 3 H, H-3, H-4, H-5), 4.04-4.13 (m, 3 H, H- α , H- β , H-2), 4.38-4.95 (m, 8 H, $\text{CH}_2\text{Ph} \times 4$), 4.87 (d, $J = 3.1$ Hz, 1 H, H-1), 6.59 (t, $J = 5.0$ Hz, 1 H, NH), 7.26-7.36 (m, 20 H, aromatics); ^{13}C -NMR (75 MHz): δ_c 14.2 (CH_3), 26.9, 29.3, 29.4, 29.5, 29.6, 29.6, 29.7, 29.7, 31.9 ($\text{NHCH}_2(\text{CH}_2)_{12}\text{CH}_3$), 39.6 ($\text{NHCH}_2(\text{CH}_2)_{12}\text{CH}_3$), 63.0 (C- α), 68.9 (C-6), 69.1 (C- β), 70.0 (C-5), 73.1, 73.6, 74.8 ($\text{CH}_2\text{Ph} \times 4$), 74.9, 78.8 (C-3, C-4), 98.9 (C-1), 127.4, 127.5, 127.6, 127.6, 127.7, 127.8, 127.9, 127.9, 128.1, 128.2, 128.3, 128.3, 128.4, 128.4, 137.9, 138.5, 138.6, 138.7 (aromatics), 166.9 (C=O); HRMS m/z (ESI+) 849.5190, ($\text{C}_{51}\text{H}_{68}\text{N}_4\text{O}_7\text{H}$: $[\text{M}+\text{H}]^+$ requires 849.5161).

1-(O-(2,3,4,6-Tetra-O-benzyl- α -D-galactopyranosyl)-L-serine tetradecyl amide)-4-(tridecyl)-1,2,3-triazole **4.90**



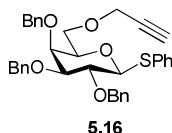
4.90

$\text{CuSO}_4 \cdot 5\text{H}_2\text{O}$ (2 mg, 9.54 μmol , 0.1 equiv) was added to a solution of *N*-azido-*O*-(2,3,4,6-tetra-*O*-benzyl- α -D-galactopyranosyl)-L-serine tetradecyl amide **4.88** (81 mg, 0.09 mmol) and pentadecyne (20 mg, 0.09 mmol, 1 equiv) in THF/ H_2O /MeOH (5 mL, 2:1:2) at rt. Sodium ascorbate (4 mg, 0.02 mmol, 0.2 equiv) was added and the reaction mixture was stirred for 18 h. The white precipitate was filtered, dissolved in CH_2Cl_2 (10 mL) and washed with brine (10 mL). The filtrate was reacted again under the exact conditions, concentrated, diluted with CH_2Cl_2 (10 mL) and washed with brine (10 mL). The organic layers were combined, dried over Na_2SO_4 , filtered and concentrated *in vacuo*. Flash column chromatography (PetEt/EtOAc 5:1) afforded the title compound **4.90** (72 mg, 75%) as a white solid; $R_f = 0.38$

(PetEt/EtOAc 3:1); $[\alpha]_D^{25} = +40.00$ (c, 0.65 in CH_2Cl_2); IR ν_{max} (NaCl plate, CH_2Cl_2): 3746.3, 3738.6, 3434.3, 2924.7, 2853.7, 2795.1, 2091.3, 1642.4, 1453.5, 1261.6, 1096.1, 696.7, 427.6, 411.1 cm^{-1} ; $^1\text{H NMR}$ (300 MHz, α anomer): δ 0.87 (t, $J = 6.9$ Hz, 3 H, CH_3), 1.24-1.25 (m, 44 H, $\text{NHCH}_2(\text{CH}_2)_{12}\text{CH}_3$, $\text{C}=\text{CCH}_2\text{CH}_2(\text{CH}_2)_{10}\text{CH}_3$), 1.59-1.64 (m, 2 H, $\text{C}=\text{CCH}_2\text{CH}_2$), 2.65 (t, $J = 8.3$ Hz, 2 H, $\text{C}=\text{CCH}_2\text{CH}_2$), 2.80-2.93 (m, 1 H, NHCHH), 3.01-3.13 (m, 1 H, NHCHH), 3.44-3.58 (m, 2 H, H-6, H-6'), 3.81 (dd, $J = 2.6$ Hz, 10.1 Hz, 1 H, H-3), 3.90-3.94 (m, 2 H, H-4, H-5), 4.05 (dd, $J = 2.6$ Hz, 6.3 Hz, 1 H, H-2), 4.11-4.15 (m, 2 H, H- β H- β'), 4.39-4.93 (m, 8 H, $\text{CH}_2\text{Ph} \times 4$), 4.90 (d, $J = 6.3$ Hz, 1 H, H-1), 5.36 (t, $J = 6.1$ Hz, 1 H, H- α), 6.45 (t, $J = 5.8$ Hz, 1 H, NHCH_2), 7.26-7.37 (m, 20 H, aromatic), 7.57 (s, 1 H, $\text{C}=\text{CH}$); $^{13}\text{C-NMR}$ (75 MHz): δ_{C} 13.1 (CH_3)^{xxv}, 16.5, 21.7, 24.7, 25.8, 28.2, 28.2, 28.3, 28.4, 28.4, 28.5, 28.60, 28.6, 28.7, 30.9 ($\text{NHCH}_2(\text{CH}_2)_{12}\text{CH}_3$, $\text{C}=\text{C}(\text{CH}_2)_{12}\text{CH}_3$), 38.74 (NHCH_2), 62.3 (C- α), 67.6 (C- β), 68.2 (C-6), 69.1 (C-5), 71.9 (CH_2Ph), 72.5 (CH_2Ph), 72.8 (CH_2Ph), 73.6 (C-4), 73.8 (CH_2Ph), 75.2 (C-2), 77.9 (C-3), 98.2 (C-1), 120.3 (C= CH), 126.4, 126.6, 126.7, 126.8, 126.8, 126.9, 127.1, 127.2, 127.3, 127.4, 127.5, 136.8, 137.0, 137.3, 137.4 (aromatics), 165.1 (C=O); HRMS m/z (ESI+) 1057.7359, ($\text{C}_{66}\text{H}_{96}\text{N}_4\text{O}_7\text{H}$: $[\text{M}+\text{H}]^+$ requires 1057.7352).

7.2.4. Experimental procedures for Chapter 5

Phenyl-2,3,4-tris-*O*-benzyl-6-*O*-propargyl-1-thio- β -D-galactopyranoside **5.16**



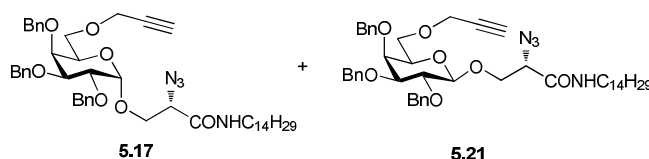
NaH (60% suspension in mineral oil) (10 mg, 0.240 mmol, 2 equiv) was slowly added to phenyl-2,3,4-tris-*O*-benzyl-1-thio- β -D-galactopyranoside **5.20** (65 mg, 0.12 mmol) dissolved in THF (5 mL) under an inert atmosphere at 0 °C. The reaction mixture was stirred for 30 min and then TBAI (2 mg, 0.006 mmol, 0.05 equiv) and propargyl bromide (80% in toluene) (32 μL , 0.3 mmol, 2.5 equiv) were added in succession. The reaction mixture was stirred for 18 h at rt. Ice-water (5 mL) was added and extracted with diethyl ether (10 mL). The aqueous layer was washed with diethyl ether (5 mL \times 3). The organic layers were combined and concentrated *in vacuo*.

^{xxv} Two overlapping signals.

Flash column chromatography (hexane/ EtOAc 3:1) followed by recrystallization in EtOH afforded the title compound **5.16** (33 mg, 47%) as a white solid; $R_f = 0.75$ (PetEt/EtOAc 3:1); $[\alpha]_D^{25} = +5.71$ (c 0.35, CH_2Cl_2 ; IR ν_{max} (NaCl plate, CH_2Cl_2): 3287.6, 3030.3, 2922.6, 1724.0, 1583.8, 1496.7, 1454.7 cm^{-1} ; ^1H NMR (300 MHz): δ 2.38 (t, $J = 2.4$ Hz, 1 H, $\text{CH}_2\text{C}\equiv\text{CH}$), 3.57-3.63 (m, 2 H, H-3, H-5), 3.66-3.69 (m, 2 H, H-6, H-6'), 3.91-4.06 (m, 4 H, $\text{CH}_2\text{C}\equiv\text{CH}$, H-2, H-4), 4.62-5.01 (m, 7 H, $\text{CH}_2\text{Ph} \times 3$, H-1), 7.20-7.59 (m, 20 H, aromatics); ^{13}C NMR (75 Hz): δ_c 58.6 ($\text{CH}_2\text{C}\equiv\text{CH}$), 68.4 (C-6), 72.7 (CH_2Ph), 73.4 (C-4), 74.4 ($\text{CH}_2\text{C}\equiv\text{CH}$), 74.8 (CH_2Ph), 75.7 (CH_2Ph), 77.1, 77.3 (C-2, C-3), 79.4 ($\text{CH}_2\text{C}\equiv\text{CH}$), 84.1 (C-5), 87.7 (C-1), 127.1, 127.5, 127.6, 127.7, 127.9, 128.2, 128.3, 128.5, 128.8, 131.7, 134.0, 138.2, 138.3, 138.8 (aromatics); HRMS m/z (ESI+) 620.1933, ($\text{C}_{36}\text{H}_{35}\text{KO}_5\text{SH}$: $[\text{M}+\text{H}]^+$ requires 620.1948).

This compound is mentioned in the literature but NMR data is not reported.^[239]

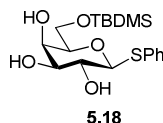
N*-Azido-*O*-(2,3,4-tris-*O*-benzyl-6-*O*-propargyl- α/β -D-galactopyranosyl)-L-serine tetradecyl amide **5.17** and **5.21*



NIS (68 mg, 0.61 mmol, 2 equiv) was added to a solution of phenyl-2,3,4-tris-*O*-benzyl-6-*O*-propargyl-1-thio- β -D-galactopyranoside **5.16** (176 mg, 0.30 mmol) and *N*-azido-L-serine tetradecyl amide **4.58** (99 mg, 0.30 mmol, 1 equiv) in THF (4 mL) containing 4Å MS in the dark under N_2 . TfOH (1 μL , 0.0006 mmol, 0.01 equiv) was added and the reaction mixture was stirred for 18 h. MeOH was added and the reaction mixture was concentrated *in vacuo*. The resulting solid was diluted with CH_2Cl_2 (20 mL) and washed with satd. aq. $\text{Na}_2\text{S}_2\text{O}_4$ (20 mL) followed by brine (20 mL). The organic layer was dried over Na_2SO_4 , filtered and concentrated to yield a mixture of diastereoisomers (α/β ratio 2.3:1). Flash column chromatography (PetEt/EtOAc 5:1) afforded the α -anomer **5.17** (39 mg, 16%) as a white solid; Data recorded for α -anomer **5.17**: $R_f = 0.27$ (PetEt/EtOAc 3:1); $[\alpha]_D^{25} = +37.04$ (c, 0.27 in CH_2Cl_2); IR ν_{max} (NaCl plate, CH_2Cl_2): 3776.6, 3370.1, 2103.4, 1642.7 cm^{-1} ; ^1H NMR (300 MHz): δ 0.88 (t, $J = 6.9$ Hz, 1 H, CH_3), 1.23-1.25 (m, 22 H, $(\text{CH}_2)_{11}\text{CH}_3$), 1.42 (pt,

$J = 6.7$ Hz, 2 H NHCH_2CH_2), 2.40 (t, $J = 2.4$ Hz, 1 H, $\text{CH}_2\text{C}\equiv\text{CH}$), 2.96-3.08 (m, 1 H, NHCHH), 3.15-3.27 (m, 1 H, NHCHH), 3.54-3.57 (m, 2 H, H-6, H-6'), 3.68-3.73 (m, 1 H, H- β'), 3.89-3.96 (m, 3 H, H-3, H-4, H-5), 4.05-4.14 (m, 5 H, H- α , H- β , H-2, $\text{CH}_2\text{C}\equiv\text{CH}$), 4.62-4.98 (m, 7 H, $\text{CH}_2\text{Ph} \times 3$, H-1), 6.63 (t, $J = 6.0$ Hz, 1 H, NH), 7.25-7.39 (m, 15 H, aromatics); ^{13}C -NMR (75 MHz): δ_{C} 22.7 (CH_3), 26.9, 29.3, 29.4, 29.5, 29.6, 29.6, 29.7, 29.7, 31.9 ($\text{NHCH}_2(\text{CH}_2)_{12}\text{CH}_3$), 39.6 ($\text{NHCH}_2(\text{CH}_2)_{12}\text{CH}_3$), 58.5 ($\text{CH}_2\text{C}\equiv\text{CH}$), 63.0 (C- α), 68.5 (C-6), 69.1 (C- β), 69.8 (C-5), 73.1 (CH_2Ph), 73.5 (CH_2Ph), 74.7 (CH_2Ph), 74.8, 74.9, 78.7 (C-3, C-4, $\text{CH}_2\text{C}\equiv\text{CH}$), 76.6 ($\text{CH}_2\text{C}\equiv\text{CH}$), 79.4 (C-2), 98.8 (C-1), 127.5, 127.6, 127.7, 127.8, 127.9, 128.3, 128.3, 128.4, 138.2, 138.4, 138.5, 138.6 (aromatics), 166.9 (C=O); HRMS m/z (ESI+) 797.4848, ($\text{C}_{47}\text{H}_{64}\text{N}_4\text{O}_7\text{H}$: $[\text{M}+\text{H}]^+$ requires 797.4823). A small amount of the β diastereoisomer **5.21** was isolated for characterisation; Data recorded for β -anomer **5.21**: $R_f = 0.26$ (PetEt/EtOAc 3:1); $[\alpha]_{\text{D}}^{23} = +48.88$ (c, 0.45 in CH_2Cl_2); IR ν_{max} (NaCl plate, CH_2Cl_2): 3430.2, 2105.8, 1642.5, 1261.4 cm^{-1} ; ^1H NMR (300 MHz): δ 0.88 (t, $J = 6.9$ Hz, 1 H, CH_3), 1.23-1.24 (m, 22 H, $(\text{CH}_2)_{11}\text{CH}_3$), 1.44 (pt, $J = 6.9$ Hz, 2 H, NHCH_2CH_2), 2.40 (t, $J = 2.4$ Hz, 1 H, $\text{CH}_2\text{C}\equiv\text{CH}$), 3.12-3.28 (m, 2 H, NHCH_2), 3.51-3.56 (m, 2 H, H-6, H-6'), 3.55-3.63 (m, 2 H, H-3, H-5), 3.80-3.90 (m, 2 H, H-4, H-2), 4.04-4.15 (m, 5 H, H- α , H- β , H- β' , $\text{CH}_2\text{C}\equiv\text{CH}$), 4.43 (d, $J = 7.8$ Hz, 1 H, H-1), 4.65-4.98 (m, 6 H, $\text{CH}_2\text{Ph} \times 3$), 6.43 (t, $J = 5.7$ Hz, 1 H, NH), 7.29-7.34 (m, 15 H, aromatics); ^{13}C -NMR (75 MHz): δ_{C} 14.1 (CH_3), 22.7, 26.8, 29.2, 29.4, 29.5, 29.6, 29.7, 29.7, 31.9 ($\text{NHCH}_2(\text{CH}_2)_{12}\text{CH}_3$), 39.6 (NHCH_2), 58.5 ($\text{CH}_2\text{C}\equiv\text{CH}$), 63.3 (C- α), 68.3 (C-6), 70.2 (C- β), 73.1 (CH_2Ph), 73.2 (C-4), 73.4 (C-5), 74.6 (CH_2Ph), 74.8 ($\text{CH}_2\text{C}\equiv\text{CH}$), 75.3 (CH_2Ph), 79.4 (C-2), 79.3 ($\text{CH}_2\text{C}\equiv\text{CH}$), 82.0 (C-3), 104.1 (C-1), 127.5, 127.6, 127.7, 127.9, 128.2, 128.3, 128.4, 138.3, 138.5, 138.6 (aromatics), 166.7 (C=O); HRMS m/z (ESI+) 797.4842, ($\text{C}_{47}\text{H}_{64}\text{N}_4\text{O}_7\text{H}$: $[\text{M}+\text{H}]^+$ requires 797.4823).

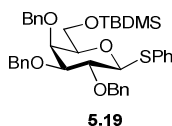
Phenyl-6-*O*-*tert*-butyldimethylsilyl-1-thio- β -D-galactopyranoside **5.18** ^[281]



Na metal (4 mg approx., 0.17 mmol approx., 0.1 equiv approx.) was added to a solution of phenyl-2,3,4,6-tetra-*O*-acetyl-1-thio- β -D-galactopyranoside **4.53** (737 mg, 1.67 mmol) in MeOH (2 mL) at 0 °C. The reaction mixture was stirred at rt for

1.5 h; quenched with Amberlite ion-exchange resin (H⁺ form), filtered and concentrated *in vacuo*. The resulting white solid (368 mg, 81%) was then dissolved in Pyr (10 mL) and TBDMSCl (407 mg, 2.70 mmol, 2 equiv) was slowly added under an inert atmosphere at -10 °C. NEt₃ (2 drops) was added and the reaction mixture was stirred for 1 h at -10 °C. The reaction mixture was allowed to warm to rt and stirred for 21 h at rt. The solution was diluted with CH₂Cl₂ (40 mL) and poured into ice-water (40 mL). The separated aqueous layer was extracted with CH₂Cl₂ (40 mL × 3). The combined organic layers were washed with satd. aq. NaHCO₃ (40 mL), brine (40 mL), dried over MgSO₄, filtered and concentration *in vacuo*. Flash column chromatography (hexane/ EtOAc 1:1) afforded the title compound **5.18** (410 mg, 79%) as a colourless oil; R_f = 0.40 (PetEt/EtOAc 1:1); ¹H NMR (300 MHz): δ 0.07 (s, 3H, SiCH₃), 0.09 (s, 3H, SiCH₃), 0.89 (s, 9 H, SiC(CH₃)₃), 3.51 (pt, *J* = 5.3 Hz, 1 H, H-5), 3.59 (dd, *J* = 3.1 Hz, 9.1 Hz, 1 H, H-3), 3.75 (pt, *J* = 9.1 Hz, 1 H, H-2), 3.87-3.90 (m, 2 H, H-6, H-6'), 4.05-4.07 (m, 1 H, H-4), 4.54 (d, *J* = 9.6 Hz, 1 H, H-1), 7.25-7.28, 7.52-7.56 (m, 5 H, aromatics); ¹³C NMR (75 Hz): δ_c -5.5 (Si(CH₃)₂), -5.4 (Si(CH₃)₂), 18.2 (SiC(CH₃)₃), 25.8 (SiC(CH₃)₃), 63.1 (C-6), 69.4 (C-4), 69.8 (C-2), 75.0 (C-3), 78.3 (C-5), 88.7 (C-1), 127.6, 128.9, 132.0, 133.0 (aromatics); HRMS *m/z* (ESI⁺) 387.1656, (C₁₈H₃₀O₅SSiH: [M+H]⁺ requires 387.1660).

Phenyl-2,3,4-tris-*O*-benzyl-6-*O*-*tert*-butyldimethylsilyl-1-thio-β-D-galactopyranoside 5.19^[240]

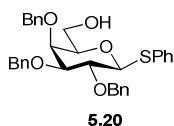


NaH (60% suspension in mineral oil) (55 mg, 1.37 mmol, 6 equiv) was slowly added to phenyl-6-*O*-*tert*-butyldimethylsilyl-1-thio-β-D-galactopyranoside **5.18** (88 mg, 0.23 mmol) dissolved in DMF (2 mL) under an inert atmosphere at 0 °C. The reaction mixture was stirred for 30 min and BnBr (162 μL, 1.37 mmol, 6 equiv) was added to the suspension at 0 °C. The reaction mixture was stirred for 2 h at 0 °C. To this suspension MeOH (2 mL) was added and poured into ice-water (1 mL); extracted with CH₂Cl₂ (2 mL × 2). The combined organic layers were washed with water, dried over MgSO₄, filtered and concentration *in vacuo*. Flash column

chromatography (hexane/ EtOAc 20:1) afforded the title compound **5.19** (46 mg, 31%) as a colourless oil; $R_f = 0.18$ (PetEt/EtOAc 20:1); $^1\text{H NMR}$ (300 MHz): δ 0.03 (bs, 6 H, $\text{Si}(\text{CH}_3)_2$), 3.45 (pt, $J = 6.6$ Hz, 1 H, H-5), 3.60 (dd, $J = 2.7$ Hz, 9.2 Hz, 1 H, H-3), 3.66-3.79 (m, 2 H, H-6, H-6'), 3.91-3.97 (m, 2 H, H-2, H-4), 4.61-5.00 (m, 7 H, $\text{CH}_2\text{Ph} \times 3$, H-1), 7.16-7.58 (m, 5 H, aromatics); $^{13}\text{C NMR}$ (75 Hz): δ_c -5.5 ($\text{Si}(\text{CH}_3)_2$), -5.3 ($\text{Si}(\text{CH}_3)_2$), 18.2 ($\text{Si}(\text{CH}_3)_3$), 26.1 ($\text{Si}(\text{CH}_3)_3$), 61.6 (C-6), 72.8 (CH_2Ph), 73.5 (C-2), 74.5 (CH_2Ph), 75.6 (CH_2Ph), 76.6 (C-4), 78.9 (C-5), 84.3 (C-3), 87.7 (C-1), 127.0, 127.4, 127.6, 127.7, 127.7, 128.0, 128.2, 128.3, 128.4, 128.4, 128.8, 131.4, 138.4, 138.4, 138.9 (aromatics).

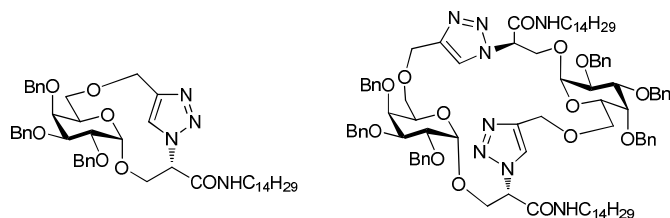
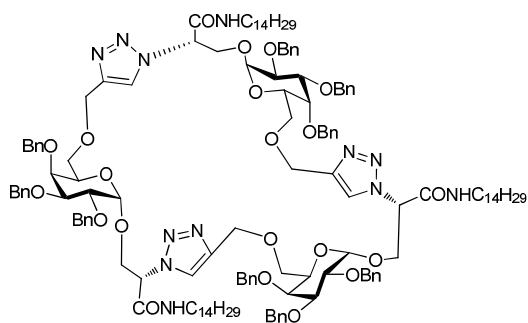
$^1\text{H NMR}$ data is in agreement with the literature.^[240]

Phenyl-2,3,4-tris-*O*-benzyl-1-thio- β -D-galactopyranoside **5.20**



A solution of TBAF (1 M in THF) (50 μL) was added drop-wise to phenyl-2,3,4-tris-*O*-benzyl-6-*O*-*tert*-butyldimethylsilyl-1-thio- β -D-galactopyranoside **5.19** (42 mg, 0.06 mmol) and crushed 4 \AA MS suspended in THF (3 mL) under an inert atmosphere at 0 $^\circ\text{C}$ and was allowed to warm to rt for 1 h. The reaction mixture was then stirred for 6 h at rt and concentrated *in vacuo*. It was re-dissolved in EtOAc and filtered through Celite, rinsing with EtOAc. The filtrate was washed with satd. aq. NaHCO_3 , water, dried over MgSO_4 , filtered and concentrated *in vacuo*. Flash column chromatography (hexane/ EtOAc 1:1) afforded the title compound **5.20** (33 mg, 94%) as a colourless oil; $R_f = 0.63$ (PetEt/EtOAc 1:1); $^1\text{H NMR}$ (300 MHz): δ 3.42-3.46 (m, 1 H, H-6), 3.49-3.54 (m, 1 H, H-6'), 3.61 (dd, $J = 2.8$ Hz, 9.3 Hz, 1 H, H-3), 3.81-3.86 (m, 2 H, H-4, H-5), 3.95 (pt, $J = 9.3$ Hz, 1 H, H-2), 4.62-5.00 (m, 7 H, $\text{CH}_2\text{Ph} \times 3$, H-1), 7.21-7.55 (m, 20 H, aromatics); HRMS m/z (ESI+) 543.2191, ($\text{C}_{33}\text{H}_{34}\text{O}_5\text{SH}$: $[\text{M}+\text{H}]^+$ requires 543.2200).

This NMR data is in agreement with the literature.^[282]

Macrocyclic Compounds **5.24**, **5.25** and **5.26**^{xxvi}**5.24****5.25****5.26**

$\text{CuSO}_4 \cdot 5\text{H}_2\text{O}$ (1 mg, 4.33 μmol , 0.1 equiv) was added to a solution of *N*-azido-*O*-(2,3,4-tris-*O*-benzyl-6-*O*-propargyl- α -D-galactopyranosyl)-L-serine tetradecyl amide **5.17** (81 mg, 0.09 mmol) in THF/ H_2O /MeOH (5 mL, 2:1:2, 8.5 mM concentration) at rt. Sodium ascorbate (2 mg, 0.02 mmol, 0.2 equiv) was added and the reaction mixture was stirred for 18 h. $\text{CuSO}_4 \cdot 5\text{H}_2\text{O}$ (1 mg, 4.33 μmol , 0.1 equiv) was added to the reaction mixture, followed by the addition of sodium ascorbate (2 mg, 0.02 mmol, 0.2 equiv). The reaction mixture was stirred at 45 °C for 3 h. The reaction mixture was then diluted with CH_2Cl_2 (50 mL) and washed with brine (20 mL). The organic layer was dried over Na_2SO_4 , filtered and concentrated *in vacuo*. Flash column chromatography (PetEt/EtOAc 2:1 to EtOAc/PetEt 2:1 to MeOH) afforded the title compounds **5.24**, **5.25** and **5.26** (53% w/w) as a white solid and as a mixture of compounds; IR ν_{max} (NaCl plate, MeOH): 3429.8, 2925.2, 2853.9, 2099.0, 1642.9, 1496.9, 1454.4 cm^{-1} ; ^1H NMR (600 MHz): δ 0.85-0.88 (m, 10 H), 1.22-1.24 (m, 41 H), 2.88-2.96 (m, 2 H), 2.99-3.14 (m, 2 H), 2.22-1.24 (m, 3 H), 3.32-3.38 (m, 1 H), 3.49-3.63 (m, 4 H), 3.73-4.24 (m, 14 H), 5.36-5.45 (m, 1 H), 7.26-7.33 (m, 29 H),

^{xxvi} Experimental data presented most likely represents the macrocyclic structures. However conclusive evidence is not given for the formation of these products.

Chapter 7: Experimental details

7.90-7.91 (m, 2 H); ^{13}C -NMR (150 MHz): δ_{c} 14.1 (CH_3), 22.7, 26.7, 26.9, 29.3, 29.7, 31.9, 69.1, 127.4, 127.7, 128.4, 129.8; HRMS m/z (ESI+) for monomer **5.24**, 797.4871, ($\text{C}_{47}\text{H}_{64}\text{N}_4\text{O}_7\text{H}$: $[\text{M}+\text{H}]^+$ requires 797.4848); for dimer **5.25**, 1615.9497, ($\text{C}_{94}\text{H}_{128}\text{N}_8\text{O}_{14}\text{Na}$: $[\text{M}+\text{Na}]^+$ requires 1615.9442); for trimer **5.26**, 2412.4150, ($\text{C}_{141}\text{H}_{192}\text{N}_{12}\text{O}_{21}\text{Na}$: $[\text{M}+\text{Na}]^+$ requires 2412.4217).

Bibliography

Bibliography

Bibliography

- [1] S. Takeshita, K. Nakatani, H. Kawase, S. Seki, M. Yamamoto, I. Sekine, S. Yoshioka, *J. Infect. Dis.* **1999**, *179*, 508-512.
- [2] G. Hölzl, S. Witt, N. Gaude, M. Melzer, M. A. Schöttler, P. Dörmann, *Plant Physiol.* **2009**, *150*, 1147-1159.
- [3] R. L. Schnaar, *Arch. Biochem. Biophys.* **2004**, *426*, 163-172.
- [4] E. Kobayashi, K. Motoki, T. Uchida, H. Fukushima, Y. Koezuka, *Oncol. Res.* **1995**, *7*, 529-534.
- [5] V. M. Dembitsky, *Lipids* **2004**, *39*, 933-953.
- [6] T. Bauersachs, J. Compaore, E. C. Hopmans, L. J. Stal, S. Schouten, D. J. S. Sinninghe, *Phytochem.* **2009**, *70*, 2034-2039.
- [7] (a)N. Lourith, M. Kanlayavattanakul, *Int. J. Cosmet. Sci.* **2009**, *31*, 255-261; (b)L. Rodrigues, I. M. Banat, J. Teixeira, R. Oliveira, *J. Antimicrob. Chemother.* **2006**, *57*, 609-618.
- [8] (a)S.-F. Lu, Q. O'Yang, Z.-W. Guo, B. Yu, Y.-Z. Hui, *J. Org. Chem.* **1997**, *62*, 8400-8405; (b)A. Fuerstner, T. Mueller, *J. Org. Chem.* **1998**, *63*, 424-425.
- [9] R. Pereda-Miranda, R. Mata, A. L. Anaya, D. B. M. Wickramaratne, J. M. Pezzuto, A. D. Kinghorn, *J. Nat. Prod.* **1993**, *56*, 571-582.
- [10] A. Fuerstner, T. Mueller, *J. Am. Chem. Soc.* **1999**, *121*, 7814-7821.
- [11] G. Hoelzl, P. Doermann, *Prog. Lipid Res.* **2007**, *46*, 225-243.
- [12] R. V. V. Tatituri, P. A. Illarionov, L. G. Dover, J. Nigou, M. Gilleron, P. Hitchen, K. Krumbach, H. R. Morris, N. Spencer, A. Dell, L. Eggeling, G. S. Besra, *J. Biol. Chem.* **2007**, *282*, 4561-4572.
- [13] N. Maeda, K. Matsubara, H. Yoshida, Y. Mizushina, *Mini-Rev. Med. Chem.* **2011**, *11*, 32-38.
- [14] A. P. Uldrich, O. Patel, G. Cameron, D. G. Pellicci, E. B. Day, L. C. Sullivan, K. Kyparissoudis, L. Kjer-Nielsen, J. P. Vivian, B. Cao, A. G. Brooks, S. J. Williams, P. Illarionov, G. S. Besra, S. J. Turner, S. A. Porcelli, J. McCluskey, M. J. Smyth, J. Rossjohn, D. I. Godfrey, *Nat. Immunol.* **2011**, *12*, 616-623.
- [15] C. R. H. Raetz, C. Whitfield, *Annu. Rev. Biochem.* **2002**, *71*, 635-700.
- [16] (a)T. K. Lindhorst, *Essentials of Carbohydrate Chemistry and Biochemistry (3rd ed.)* Elsevier Ltd., **2009**; (b)S. Mukherjee, L.-Y. Chen, T. J. Papadimos, S. Huang, B. L. Zuraw, Z. K. Pan, *J. Biol. Chem.* **2009**, *284*, 29391-29398.
- [17] H.-J. Gabius, Editor, *The Sugar Code: Fundamentals Of Glycosciences*, Wiley-VCH Verlag GmbH & Co. KGaA, **2009**.
- [18] H. Akiyama, N. Sasaki, S. Hanazawa, M. Gotoh, S. Kobayashi, Y. Hirabayashi, K. Murakami-Murofushi, *Biochim. Biophys. Acta, Mol. Cell Biol. Lipids* **2011**, *1811*, 314-322.
- [19] W. M. Holleran, Y. Takagi, G. K. Menon, G. Legler, K. R. Feingold, P. M. Elias, *J. Clin. Invest.* **1993**, *91*, 1656-1664.
- [20] J. Hildebrand, G. Hauser, *J. Biol. Chem.* **1969**, *244*, 5170-5180.
- [21] T. Natori, M. Morita, K. Akimoto, Y. Koezuka, *Tetrahedron* **1994**, *50*, 2771-2784.
- [22] A. Banchet-Cadeddu, E. Henon, M. Dauchez, J.-H. Renault, F. Monneaux, A. Haudrechy, *Org. Biomol. Chem.* **2011**, *9*, 3080-3104.
- [23] (a)G. Sodano, A. Soriente, A. Gambacorta, A. Trincone, *Korean J. Med. Chem.* **1996**, *6*, 290-293; (b)S. Kusumoto, M. Oikawa, *Synthesis of glycolipids*, Springer-Verlag, **2001**; (c)T. Ikami, H. Ishida, M. Kiso, *Methods Enzymol.* **2000**, *311*, 547-568; (d)N. Hada, T. Takeda, Kogyo Chosakai, **2009**, pp. 162-170; (e)R. Gigg, *Chem. Phys. Lipids* **1980**, *26*, 287-404; (f)J. Gigg, R. Gigg, *Top. Curr. Chem.* **1990**, *154*, 77-139.
- [24] (a)G. A. D. Goethals, V. Y. O. J. Lequart, P. E. M. Martin, J. C. Maziere, C. Maziere, P. R. M. Puillart, P. J. Villa, **2005**, 58 pp., WO2005077963A1; (b)V. N. Nigam, C. A. Brailovsky, C. Chopra, *Cancer Res.* **1978**, *38*, 3315-3321.

Bibliography

- [25] S. Matsumura, K. Imai, S. Yoshikawa, K. Kawada, T. Uchibori, *J. Am. Oil Chem. Soc.* **1990**, *67*, 996-1001.
- [26] (a)K. Miyamoto, S. Miyake, T. Yamamura, *Nature* **2001**, *413*, 531-534; (b)S. Ladisch, A. Hasegawa, R. Li, M. Kiso, *Biochemistry* **1995**, *34*, 1197-1202.
- [27] T. Nagano, J. Pospisil, G. Chollet, S. Schulthoff, V. Hickmann, E. Moulin, J. Herrmann, R. Mueller, A. Fuerstner, *Chem. Eur. J.* **2009**, *15*, 9697-9706, S9697/9691-S9697/9648.
- [28] (a)S. Boonyarattanakalin, X. Liu, M. Michieletti, B. Lepenies, P. H. Seeberger, *J. Am. Chem. Soc.* **2008**, *130*, 16791-16799; (b)K. Naresh, B. K. Bharati, P. G. Avaji, D. Chatterji, N. Jayaraman, *Glycobiology* **2011**, *21*, 1237-1254.
- [29] S. Toujima, K. Kuwano, Y. Zhang, N. Fujimoto, M. Hirama, T. Oishi, S. Fukuda, Y. Nagumo, H. Imai, T. Kikuchi, S. Arai, *Microbiol.* **2000**, *146*, 2317-2323.
- [30] Y. Kinjo, B. Pei, S. Bufali, R. Raju, S. K. Richardson, M. Imamura, M. Fujio, D. Wu, A. Khurana, K. Kawahara, C.-H. Wong, A. R. Howell, P. H. Seeberger, M. Kronenberg, *Chem. Biol.* **2008**, *15*, 654-664.
- [31] (a)K. Yoza, N. Amanokura, Y. Ono, T. Akao, H. Shinmori, M. Takeuchi, S. Shinkai, D. N. Reinhoudt, *Chem. Eur. J.* **1999**, *5*, 2722-2729; (b)R. J. H. Hafkamp, M. C. Feiters, R. J. M. Nolte, *J. Org. Chem.* **1999**, *64*, 412-426; (c)S. Kiyonaka, S. Shinkai, I. Hamachi, *Chem. Eur. J.* **2003**, *9*, 976-983.
- [32] (a)E. Soderlind, M. Wollbratt, C. C. von, *Int. J. Pharm.* **2003**, *252*, 61-71; (b)E. Soderlind, L. Karlsson, *Eur. J. Pharm. Biopharm.* **2006**, *62*, 254-259.
- [33] J. F. Spencer, P. A. Gorin, A. P. Tulloch, *Antonie van Leeuwenhoek* **1970**, *36*, 129-133.
- [34] S. Lang, *Curr. Opin. Colloid Interface Sci.* **2002**, *7*, 12-20.
- [35] (a)T. Yamane, *J. Am. Oil Chem. Soc.* **1987**, *64*, 1657-1662; (b)H. Mager, R. Roethlisberger, F. Wagner, **1987**, 7 pp., DE3526417A1; (c)M. Benincasa, A. Abalos, I. Oliveira, A. Manresa, *Antonie van Leeuwenhoek* **2004**, *85*, 1-8; (d)A. Abalos, A. Pinazo, M. R. Infante, M. Casals, F. Garcia, M. A. Manresa, *Langmuir* **2001**, *17*, 1367-1371.
- [36] S. B. Levy, *Adv. Drug Delivery Rev.* **2005**, *57*, 1446-1450.
- [37] C. Kunz, S. Rudloff, W. Baier, N. Klein, S. Strobel, *Annu. Rev. Nutr.* **2000**, *20*, 699-722.
- [38] R. J. Pieters, *Med. Res. Rev.* **2007**, *27*, 796-816.
- [39] (a)T. Mullen, M. Callaghan, S. McClean, *Microb. Pathog.* **2010**, *49*, 381-387; (b)D. W. Martin, C. D. Mohr, *Infect. Immun.* **2000**, *68*, 24-29; (c)E. Caraher, C. Duff, T. Mullen, K. S. Mc, P. Murphy, M. Callaghan, S. McClean, *J. Cystic Fibrosis* **2007**, *6*, 49-56.
- [40] J. J. Lipuma, *Curr. Opin. Pulm. Med.* **2005**, *11*, 528-533.
- [41] (a)F. A. Sylvester, U. S. Sajjan, J. F. Forstner, *Infect. Immun.* **1996**, *64*, 1420-1425; (b)H. C. Krivan, D. D. Roberts, V. Ginsburg, *Proc. Natl. Acad. Sci. U. S. A.* **1988**, *85*, 6157-6156.
- [42] C. Wright, R. Leyden, P. V. Murphy, M. Callaghan, T. Velasco-Torrijos, S. McClean, *Molecules* **2012**, *17*, 10065-10071.
- [43] S. Xiang, J. Ma, B. K. Gorityala, X.-W. Liu, *Carbohydr. Res.* **2011**, *346*, 2957-2959.
- [44] (a)B. G. Davis, *Chem. Rev.* **2002**, *102*, 579-601; (b)P. Norris, *Curr. Top. Med. Chem.* **2008**, *8*, 101-113.
- [45] M. C. Galan, D. Benito-Alifonso, G. M. Watt, *Org. Biomol. Chem.* **2011**, *9*, 3598-3610.
- [46] X. Chen, Y. Zheng, Y. Shen, *Curr. Med. Chem.* **2006**, *13*, 109-116.
- [47] I. M. von, W. Y. Wu, G. B. Kok, M. S. Pegg, J. C. Dyason, B. Jin, T. V. Phan, M. L. Smythe, H. F. White, *Nature* **1993**, *363*, 418-423.

Bibliography

- [48] M. Petitou, P. Duchaussoy, J.-M. Herbert, G. Duc, H. M. El, J.-F. Branellec, F. Donat, J. Necciari, R. Cariou, J. Bouthier, E. Garrigou, *Semin. Thromb. Hemostasis* **2002**, *28*, 393-402.
- [49] A. Imberty, Y. M. Chabre, R. Roy, *Chem. Eur. J.* **2008**, *14*, 7490-7499.
- [50] K. Marotte, C. Sabin, C. Preville, M. Moume-Pymbock, M. Wimmerova, E. P. Mitchell, A. Imberty, R. Roy, *Chem. Med. Chem* **2007**, *2*, 1328-1338.
- [51] N. Gilboa-Garber, *Methods Enzymol.* **1982**, *83*, 378-385.
- [52] S. Perret, C. Sabin, C. Dumon, M. Pokorna, C. Gautier, O. Galanina, S. Ilia, N. Bovin, M. Nicaise, M. Desmadril, N. Gilboa-Garber, M. Wimmerov, E. P. Mitchell, A. Imberty, *Biochem. J.* **2005**, *389*, 325-332.
- [53] K. Marotte, C. Preville, C. Sabin, M. Moume-Pymbock, A. Imberty, R. Roy, *Org. Biomol. Chem.* **2007**, *5*, 2953-2961.
- [54] S. Sahoo, N. Kumar, C. Bhattacharya, S. S. Sagiri, K. Jain, K. Pal, S. S. Ray, B. Nayak, *Des. Monomers Polym.* **2011**, *14*, 95-108.
- [55] N. M. Sangeetha, U. Maitra, *Chem. Soc. Rev.* **2005**, *34*, 821-836.
- [56] J. F. Toro-Vazquez, J. A. Morales-Rueda, E. Dibildox-Alvarado, M. Charo-Alonso, M. Alonzo-Macias, M. M. Gonzalez-Chavez, *J. Am. Oil Chem. Soc.* **2007**, *84*, 989-1000.
- [57] W. Jaunky, M. W. Hosseini, J. M. Planeix, C. A. De, N. Kyritsakas, J. Fischer, *Chem. Commun.* **1999**, 2313-2314.
- [58] D. J. Abdallah, R. G. Weiss, *J. Braz. Chem. Soc.* **2000**, *11*, 209-218.
- [59] D. J. Abdallah, R. G. Weiss, *Langmuir* **2000**, *16*, 352-355.
- [60] K. Leivo, Thesis, **2011**.
- [61] T. Brotin, R. Utermohlen, F. Fages, H. Bouas-Laurent, J. P. Desvergne, *J. Chem. Soc., Chem. Commun.* **1991**, 416-418.
- [62] T. Tachibana, T. Mori, K. Hori, *Bull. Chem. Soc. Jpn.* **1980**, *53*, 1714-1719.
- [63] N. Brosse, D. Barth, B. Jamart-Gregoire, *Tetrahedron Lett.* **2004**, *45*, 9521-9524.
- [64] G. Ghini, L. Lascialfari, C. Vinattieri, S. Cicchi, A. Brandi, D. Berti, F. Betti, P. Baglioni, M. Mannini, *Soft Matter* **2009**, *5*, 1863-1869.
- [65] G. Palui, F.-X. Simon, M. Schmutz, P. J. Mesini, A. Banerjee, *Tetrahedron* **2007**, *64*, 175-185.
- [66] E. J. H. Van, B. L. Feringa, *Angew. Chem., Int. Ed.* **2000**, *39*, 2263-2266.
- [67] S. Sahoo, N. Kumar, C. Bhattacharya, S. S. Sagiri, K. Jain, K. Pal, S. S. Ray, B. Nayak, *Des. Monomers Polym.* **2011**, *14*, 95-108.
- [68] F. Plourde, A. Motulsky, A.-C. Couffin-Hoarau, D. Hoarau, H. Ong, J.-C. Leroux, *J. Controlled Release* **2005**, *108*, 433-441.
- [69] B. Davis, A. Fairbanks, *Carbohydrate Chemistry*, Oxford University Press Inc., New York, **2002**.
- [70] M. Nitz, D. R. Bundle, *Glycoscience* **2001**, *2*, 1497-1542.
- [71] M. A. Maier, C. G. Yannopoulos, N. Mohamed, A. Roland, H. Fritz, V. Mohan, G. Just, M. Manoharan, *Bioconjugate Chem.* **2003**, *14*, 18-29.
- [72] X. Li, J. Turanek, P. Knoetigova, H. Kudlackova, J. Masek, S. Parkin, S. E. Rankin, B. L. Knutson, H.-J. Lehmler, *Colloids Surf., B* **2009**, *73*, 65-74.
- [73] D. B. Moody, V. Briken, T. Y. Cheng, C. Roura-Mir, M. R. Guy, D. H. Geho, M. L. Tykocinski, G. S. Besra, S. A. Porcelli, *Nat. Immunol.* **2002**, *3*, 435-442.
- [74] I. Toth, R. Falconer, C. S. E. De, R. P. McGeary, B. P. Ross, **2007**, 28pp., Cont-in-part of Appl. No. PCT/AU02/25, US7312194B2
- [75] M. M. Joullie, K. M. Lassen, *ARKIVOC* **2010**, 189-250.
- [76] I. Abdelmoty, F. Albericio, L. A. Carpino, B. M. Foxman, S. A. Kates, *Lett. Pept. Sci.* **1994**, *1*, 57-67.
- [77] B. Gutte, Editor, *Peptides: Synthesis, Structures, and Applications*, Academic, **1995**.
- [78] W. Konig, R. Geiger, *Chem. Ber.* **1970**, *103*, 788-798.

Bibliography

- [79] R. Subiros-Funosas, R. Prohens, R. Barbas, A. El-Faham, F. Albericio, *Chem. Eur. J.* **2009**, *15*, 9394-9403, S9394/9391-S9394/9334.
- [80] A. El-Faham, R. S. Funosas, R. Prohens, F. Albericio, *Chem. Eur. J.* **2009**, *15*, 9404-9416, S9404/9401-S9404/9434.
- [81] H. Hori, Y. Nishida, H. Ohru, H. Meguro, *J. Org. Chem.* **1989**, *54*, 1346-1353.
- [82] S. Peng, M. Zhao, S. Li, **2012**, 18pp., CN102477076A
- [83] T. Velasco-Torrijos, L. Abbey, R. O'Flaherty, *Molecules* **2012**, *17*, 11346-11362.
- [84] S.-X. Song, M.-L. Wu, X.-P. He, Y.-B. Zhou, L. Sheng, J. Li, G.-R. Chen, *Bioorg. Med. Chem. Lett.* **2012**, *22*, 2030-2032.
- [85] A. W. Harrison, J. F. Fisher, D. M. Guido, S. J. Couch, J. A. Lawson, D. M. Sutter, M. V. Williams, G. L. DeGraaf, J. E. Rogers, a. et, *Bioorg. Med. Chem.* **1994**, *2*, 1339-1361.
- [86] C. Elizabeth, P. Maljaars, K. M. Halkes, O. W. L. de, d. P. S. van, N. J. M. Pijnenburg, J. P. Kamerling, *J. Carbohydr. Chem.* **2005**, *24*, 353-367.
- [87] (a)P. Johannesson, Thesis, **2002**; (b)S. Capasso, L. Mazzarella, F. Sica, A. Zagari, S. Salvadori, *J. Chem. Soc., Chem. Commun.* **1992**, 919-921; (c)S. Capasso, L. Mazzarella, F. Sica, A. Zagari, S. Salvadori, *J. Chem. Soc., Chem. Comm.* **1992**, 919-921.
- [88] M. Tanaka, T. Ikeda, J. Mack, N. Kobayashi, T. Haino, *J. Org. Chem.* **2011**, *76*, 5082-5091.
- [89] J. B. Lin, D. Dasgupta, S. Cantekin, A. P. H. J. Schenning, *Beilstein J. Org. Chem.* **2010**, *6*, 960-965, No. 107.
- [90] B. Gao, H. Li, D. Xia, S. Sun, X. Ba, *Beilstein J. Org. Chem.* **2011**, *7*, 198-203, No. 126.
- [91] G. S. Lim, B. M. Jung, S. J. Lee, H. H. Song, C. Kim, J. Y. Chang, *Chem. Mater.* **2007**, *19*, 460-467.
- [92] S.-J. Yoon, J. H. Kim, J. W. Chung, S. Y. Park, *J. Mater. Chem.* **2011**, *21*, 18971-18973.
- [93] (a)G. Roy, J. F. Miravet, B. Escuder, C. Sanchez, M. Llusar, *J. Mater. Chem.* **2006**, *16*, 1817-1824; (b)D.-C. Lee, B. Cao, K. Jang, P. M. Forster, *J. Mater. Chem.* **2010**, *20*, 867-873.
- [94] C. Wright, G. Herbert, R. Pilkington, M. Callaghan, S. McClean, *Lett. Appl. Microbiol.* **2010**, *50*, 500-506.
- [95] J. Letourneau, C. Levesque, F. Berthiaume, M. Jacques, M. Mourez, *J. Visualized Exp.* **2011**, No pp. given.
- [96] World Health Organisation, <http://www.who.int/en/>, **March 2012**.
- [97] C. Dye, (Ed.: S. Gillespie), Henry Stewart Talks Ltd, London, **2009**.
- [98] C. D. Mitnick, S. S. Shin, K. J. Seung, M. L. Rich, S. S. Atwood, J. J. Furing, G. M. Fitzmaurice, V. F. A. Alcantara, S. C. Appleton, J. N. Bayona, C. A. Bonilla, K. Chalco, S. Choi, M. F. Franke, H. S. F. Fraser, D. Guerra, R. M. Hurtado, D. Jazayeri, K. Joseph, K. Llaro, L. Mestanza, J. S. Mukherjee, M. Munoz, E. Palacios, E. Sanchez, A. Sloutsky, M. C. Becerra, *N. Engl. J. Med.* **2008**, *359*, 563-574.
- [99] A. A. Velayati, M. R. Masjedi, P. Farnia, P. Tabarsi, J. Ghanavi, A. H. Ziazarifi, S. E. Hoffner, *Chest* **2009**, *136*, 420-425.
- [100] M. Protopopova, C. Hanrahan, B. Nikonenko, R. Samala, P. Chen, J. Gearhart, L. Einck, C. A. Nancy, *J. Antimicrob. Chemother.* **2005**, *56*, 968-974.
- [101] M. Matsumoto, H. Hashizume, T. Tomishige, M. Kawasaki, H. Tsubouchi, H. Sasaki, Y. Shimokawa, M. Komatsu, *PLoS Med.* **2006**, *3*, 2131-2144.
- [102] R. Singh, U. Manjunatha, H. I. M. Boshoff, Y. H. Ha, P. Niyomrattanakit, R. Ledwidge, C. S. Dowd, I. Y. Lee, P. Kim, L. Zhang, S. Kang, T. H. Keller, J. Jiricek, C. E. Barry, III, *Science* **2008**, *322*, 1392-1395.
- [103] A. H. Diacon, A. Pym, M. Grobusch, R. Patientia, R. Rustomjee, L. Page-Shipp, C. Pistorius, R. Krause, M. Bogoshi, G. Churchyard, A. Venter, J. Allen, J. C. Palomino,

Bibliography

- M. T. De, H. R. P. G. van, N. Lounis, P. Meyvisch, J. Verbeeck, W. Parys, B. K. de, K. Andries, D. F. McNeeley, *N. Engl. J. Med.* **2009**, *360*, 2397-2405.
- [104] (a)A. K. Mishra, N. N. Driessen, B. J. Appelmek, G. S. Besra, *FEMS Microbiol. Rev.* **2011**, *35*, 1126-1157; (b)D. Chatterjee, K.-H. Khoo, *Glycobiology* **1998**, *8*, 113-120.
- [105] A. K. Mishra, S. Batt, K. Krumbach, L. Eggeling, G. S. Besra, *J. Bacteriol.* **2009**, *191*, 4465-4472.
- [106] (a)C. E. Ballou, Y. C. Lee, *Biochemistry* **1964**, *3*, 682-685; (b)M. Gilleron, V. R. F. J. Quesniaux, G. Puzo, *J. Biol. Chem.* **2003**, *278*, 29880-29889.
- [107] D. Kaur, A. Obregon-Henao, H. Pham, D. Chatterjee, P. J. Brennan, M. Jackson, *Proc. Natl. Acad. Sci. U. S. A.* **2008**, *105*, 17973-17977.
- [108] Y. S. Morita, T. Fukuda, C. B. C. Sena, Y. Yamaryo-Botte, M. J. McConville, T. Kinoshita, *Biochim. Biophys. Acta - General Subjects* **2011**, *1810*, 630-641.
- [109] D. J. Lea-Smith, K. L. Martin, J. S. Pyke, D. Tull, M. J. McConville, R. L. Coppel, P. K. Crellin, *J. Biol. Chem.* **2008**, *283*, 6773-6782.
- [110] A. K. Mishra, C. Klein, S. S. Gurcha, L. J. Alderwick, P. Babu, P. G. Hitchen, H. R. Morris, A. Dell, G. S. Besra, L. Eggeling, *Antonie van Leeuwenhoek* **2008**, *94*, 277-287.
- [111] B. A. Wolucka, M. R. McNeil, L. Kalbe, C. Cocito, P. J. Brennan, *Biochim. Biophysica Acta - Lipids and Lipid Metabol.* **1993**, *1170*, 131-136.
- [112] A. K. Mishra, C. Klein, S. S. Gurcha, L. J. Alderwick, P. Babu, P. G. Hitchen, H. R. Morris, A. Dell, G. S. Besra, L. Eggeling, *Antonie van Leeuwenhoek* **2008**, *94*, 277-287.
- [113] O. J. Plante, S. L. Buchwald, P. H. Seeberger, *J. Am. Chem. Soc.* **2000**, *122*, 7148-7149.
- [114] R. R. Schmidt, J. Michel, *Angew. Chem.* **1980**, *92*, 763-764.
- [115] F. Yamazaki, S. Sato, T. Nukada, Y. Ito, T. Ogawa, *Carbohydr. Res.* **1990**, *201*, 31-50.
- [116] J. A. Watt, S. J. Williams, *Org. Biomol. Chem.* **2005**, *3*, 1982-1992.
- [117] (a)I. Cumpstey, *Carbohydr. Res.* **2008**, *343*, 1553-1573; (b)A. Ishiwata, Y. J. Lee, Y. Ito, *Org. Biomol. Chem.* **2010**, *8*, 3596-3608; (c)A. J. Fairbanks, *Synlett* **2003**, 1945-1958; (d)P. J. Garegg, *Chemtracts: Org. Chem.* **1992**, *5*, 389-393.
- [118] F. Barresi, O. Hindsgaul, *J. Am. Chem. Soc.* **1991**, *113*, 9376-9377.
- [119] (a)G. Stork, G. Kim, *J. Am. Chem. Soc.* **1992**, *114*, 1087-1088; (b)G. Stork, C. J. J. La, *J. Am. Chem. Soc.* **1996**, *118*, 247-248.
- [120] D. Kahne, S. Walker, Y. Cheng, E. D. Van, *J. Am. Chem. Soc.* **1989**, *111*, 6881-6882.
- [121] (a)Y. Ito, T. Ogawa, *Angew. Chem.* **1994**, *106*, 1843-1845; (b) *Angew. Chem., Int. Ed. Engl.* **1994**, 1833-1847.
- [122] Y. Ito, H. Ando, M. Wada, T. Kawai, Y. Ohnishi, Y. Nakahara, *Tetrahedron* **2001**, *57*, 4123-4132.
- [123] (a)A. Dan, Y. Ito, T. Ogawa, *J. Org. Chem.* **1995**, *60*, 4680-4681; (b)A. Dan, M. Lergenmuller, M. Amano, Y. Nakahara, T. Ogawa, Y. Ito, *Chem. Eur. J.* **1998**, *4*, 2182-2190; (c)Y. Ito, Y. Ohnishi, T. Ogawa, Y. Nakahara, *Synlett* **1998**, 1102-1104.
- [124] P. J. Garegg, H. Hultberg, *Carbohydr. Res.* **1981**, *93*, C10-C11.
- [125] M. Ek, P. J. Garegg, H. Hultberg, S. Oscarson, *J. Carbohydr. Chem.* **1983**, *2*, 305-311.
- [126] R. Johnsson, M. Ohlin, U. Ellervik, *J. Org. Chem.* **2010**, *75*, 8003-8011.
- [127] C. D. Leigh, C. R. Bertozzi, *J. Org. Chem.* **2008**, *73*, 1008-1017.
- [128] C.-T. Ren, Y.-H. Tsai, Y.-L. Yang, W. Zou, S.-H. Wu, *J. Org. Chem.* **2007**, *72*, 5427-5430.
- [129] M. Miyashita, A. Yoshikoshi, P. A. Grieco, *J. Org. Chem.* **1977**, *42*, 3772-3774.
- [130] P. M. Senthilkumar, A. Aravind, S. Baskaran, *Tetrahedron Lett.* **2007**, *48*, 1175-1178.
- [131] S. David, S. Hanessian, *Tetrahedron* **1985**, *41*, 643-663.

Bibliography

- [132] B. Cao, X. Chen, Y. Botte, M. Richardson, K. Martin, G. Khairallah, T. Rupasinghe, R. O'Flaherty, R. O'Hair, J. Ralton, P. Crellin, R. Coppel, M. McConville, S. J. Williams, *Chemical Science* **2012**, *Submitted*.
- [133] (a)M. Kronenberg, *Annu. Rev. Immunol.* **2005**, *23*, 877-900; (b)Y. Kinjo, B. Pei, S. Bufali, R. Raju, S. K. Richardson, M. Imamura, M. Fujio, D. Wu, A. Khurana, K. Kawahara, C.-H. Wong, A. R. Howell, P. H. Seeberger, M. Kronenberg, *Chem. Biol.* **2008**, *15*, 654-664.
- [134] W. C. Florence, R. K. Bhat, S. Joyce, *Expert Rev. Mol. Med.* **2008**, *10*, e20.
- [135] M. Tsuji, *Cell. Mol. Life Sci.* **2006**, *63*, 1889-1898.
- [136] M. Skoeld, S. M. Behar, *Infect. Immun.* **2003**, *71*, 5447-5455.
- [137] D. R. Lucey, M. Clerici, G. M. Shearer, *Clin. Microbiol. Rev.* **1996**, *9*, 532-562.
- [138] T. Natori, Y. Koezuka, T. Higa, *Tetrahedron Lett.* **1993**, *34*, 5591-5592.
- [139] F. L. Schneiders, R. J. Scheper, B. B. M. E. von, A. M. Woltman, H. L. A. Janssen, d. E. A. J. M. van, H. M. W. Verheul, G. T. D. de, d. V. H. J. van, *Clin. Immunol.* **2011**, *140*, 130-141.
- [140] T. Kawano, J. Cui, Y. Koezuka, I. Toura, Y. Kaneko, H. Sato, E. Kondo, M. Harada, H. Koseki, T. Nakayama, Y. Tanaka, M. Taniguchi, *Proc. Natl. Acad. Sci. U. S. A.* **1998**, *95*, 5690-5693.
- [141] (a)M. Nieda, M. Okai, A. Tazbirkova, H. Lin, A. Yamaura, K. Ide, R. Abraham, T. Juji, D. J. Macfarlane, A. J. Nicol, *Blood* **2004**, *103*, 383-389; (b)D. H. Chang, K. Osman, J. Connolly, A. Kukreja, J. Krasovsky, M. Pack, A. Hutchinson, M. Geller, N. Liu, R. Annable, J. Shay, K. Kirchoff, N. Nishi, Y. Ando, K. Hayashi, H. Hassoun, R. M. Steinman, M. V. Dhodapkar, *J. Exp. Med.* **2005**, *201*, 1503-1517.
- [142] M. Koch, V. S. Stronge, D. Shepherd, S. D. Gadola, B. Mathew, G. Ritter, A. R. Fersht, G. S. Besra, R. R. Schmidt, E. Y. Jones, V. Cerundolo, *Nat. Immunol.* **2005**, *6*, 819-826.
- [143] M. Schombs, F. E. Park, W. Du, S. S. Kulkarni, J. Gervay-Hague, *J. Org. Chem.* **2010**, *75*, 4891-4898.
- [144] H. Nambu, S. Nakamura, N. Suzuki, S. Hashimoto, *Trends Glycosci. Glycotechnol.* **2010**, *22*, 26-40.
- [145] T. Kawano, J. Cui, Y. Koezuka, I. Toura, Y. Kaneko, K. Motoki, H. Ueno, R. Nakagawa, H. Sato, E. Kondo, H. Koseki, M. Taniguchi, *Science* **1997**, *278*, 1626-1629.
- [146] S. Sidobre, O. V. Naidenko, B.-C. Sim, N. R. J. Gascoigne, K. C. Garcia, M. Kronenberg, *J. Immunol.* **2002**, *169*, 1340-1348.
- [147] J. J. O'Konek, P. Illarionov, D. S. Khursigara, E. Ambrosino, L. Izhak, B. F. Castillo, II, R. Raju, M. Khalili, H.-Y. Kim, A. R. Howell, G. S. Besra, S. A. Porcelli, J. A. Berzofsky, M. Terabe, *J. Clin. Invest.* **2011**, *121*, 683-694.
- [148] (a)L. Barbieri, V. Costantino, E. Fattorusso, A. Mangoni, E. Aru, S. Parapini, D. Taramelli, *Eur. J. Org. Chem.* **2004**, 468-473; (b)L. Barbieri, V. Costantino, E. Fattorusso, A. Mangoni, N. Basilico, M. Mondani, D. Taramelli, *Eur. J. Org. Chem.* **2005**, 3279-3285.
- [149] M. Trappeniers, B. K. Van, T. Decruy, U. Hillaert, B. Linclau, D. Elewaut, C. S. Van, *J. Am. Chem. Soc.* **2008**, *130*, 16468-16469.
- [150] Y.-J. Chang, J.-R. Huang, Y.-C. Tsai, J.-T. Hung, D. Wu, M. Fujio, C.-H. Wong, A. L. Yu, *Proc. Natl. Acad. Sci. U. S. A.* **2007**, *104*, 10299-10304.
- [151] T. Tashiro, R. Nakagawa, S. Inoue, M. Shiozaki, H. Watarai, M. Taniguchi, K. Mori, *Tetrahedron Lett.* **2008**, *49*, 6827-6830.
- [152] T. Ebensen, C. Link, P. Riese, K. Schulze, M. Morr, C. A. Guzman, *J. Immunol.* **2007**, *179*, 2065-2073.

Bibliography

- [153] S. Sidobre, K. J. L. Hammond, L. Benazet-Sidobre, S. D. Maltsev, S. K. Richardson, R. M. Ndonge, A. R. Howell, T. Sakai, G. S. Besra, S. A. Porcelli, M. Kronenberg, *Proc. Natl. Acad. Sci. U. S. A.* **2004**, *101*, 12254-12259.
- [154] J.-J. Park, J. H. Lee, S. C. Ghosh, G. Bricard, M. M. Venkataswamy, S. A. Porcelli, S.-K. Chung, *Bioorg. Med. Chem. Lett.* **2008**, *18*, 3906-3909.
- [155] M. Trappeniers, R. Chofor, S. Aspeslagh, Y. Li, B. Linclau, D. M. Zajonc, D. Elewaut, C. S. Van, *Org. Lett.* **2010**, *12*, 2928-2931.
- [156] R. D. Goff, Y. Gao, J. Mattner, D. Zhou, N. Yin, C. Cantu, III, L. Teyton, A. Bendelac, P. B. Savage, *J. Am. Chem. Soc.* **2004**, *126*, 13602-13603.
- [157] S. Oki, A. Chiba, T. Yamamura, S. Miyake, *J. Clin. Invest.* **2004**, *113*, 1631-1640.
- [158] D. Wu, D. M. Zajonc, M. Fujio, B. A. Sullivan, Y. Kinjo, M. Kronenberg, I. A. Wilson, C.-H. Wong, *Proc. Natl. Acad. Sci. U. S. A.* **2006**, *103*, 3972-3977.
- [159] G. Velmourougane, R. Raju, G. Bricard, J. S. Im, G. S. Besra, S. A. Porcelli, A. R. Howell, *Bioorg. Med. Chem. Lett.* **2009**, *19*, 3386-3388.
- [160] T. Lee, M. Cho, S.-Y. Ko, H.-J. Youn, D. J. Baek, W.-J. Cho, C.-Y. Kang, S. Kim, *J. Med. Chem.* **2007**, *50*, 585-589.
- [161] D. E. Levy, C. Tang, Editors, *The Chemistry of C-Glycosides*, Pergamon, **1995**.
- [162] (a)H. Tomiyama, T. Yanagisawa, M. Nimura, A. Noda, T. Tomiyama, **2001**, 22 pp., DE10128250A1; (b)R. T. Dere, X. Zhu, *Org. Lett.* **2008**, *10*, 4641-4644; (c)Y. Harrak, C. M. Barra, C. Bedia, A. Delgado, A. R. Castano, A. Llebaria, *Chem. Med. Chem.* **2009**, *4*, 1608-1613; (d)T. Tashiro, R. Nakagawa, T. Hirokawa, S. Inoue, H. Watarai, M. Taniguchi, K. Mori, *Tetrahedron Lett.* **2007**, *48*, 3343-3347; (e)T. Tashiro, R. Nakagawa, T. Hirokawa, S. Inoue, H. Watarai, M. Taniguchi, K. Mori, *Bioorg. Med. Chem.* **2009**, *17*, 6360-6373.
- [163] M. L. Blauvelt, M. Khalili, W. Jaung, J. Paulsen, A. C. Anderson, S. B. Wilson, A. R. Howell, *Bioorg. Med. Chem. Lett.* **2008**, *18*, 6374-6376.
- [164] P. J. Brennan, R. V. V. Tatituri, M. Brigl, E. Y. Kim, A. Tuli, J. P. Sanderson, S. D. Gadola, F.-F. Hsu, G. S. Besra, M. B. Brenner, *Nat. Immunol.*, *12*, 1202-1211.
- [165] K. Motoki, E. Kobayashi, T. Uchida, H. Fukushima, Y. Koezuka, *Bioorg. Med. Chem. Lett.* **1995**, *5*, 705-710.
- [166] (a)T. Sakai, O. V. Naidenko, H. Iijima, M. Kronenberg, Y. Koezuka, *J. Med. Chem.* **1999**, *42*, 1836-1841; (b)G.-W. Xing, D. Wu, M. A. Poles, A. Horowitz, M. Tsuji, D. D. Ho, C.-H. Wong, *Bioorg. Med. Chem.* **2005**, *13*, 2907-2916; (c)T. Sakai, H. Ueno, T. Natori, A. Uchimura, K. Motoki, Y. Koezuka, *J. Med. Chem.* **1998**, *41*, 650-652.
- [167] M. R. Chaulagain, M. H. D. Postema, F. Valeriote, H. Pietraszkwicz, *Tetrahedron Lett.* **2004**, *45*, 7791-7794.
- [168] G.-T. Fan, Y.-s. Pan, K.-C. Lu, Y.-P. Cheng, W.-C. Lin, S. Lin, C.-H. Lin, C.-H. Wong, J.-M. Fang, C.-C. Lin, *Tetrahedron* **2005**, *61*, 1855-1862.
- [169] (a)L.-D. Huang, H.-J. Lin, P.-H. Huang, W.-C. Hsiao, L. V. Raghava Reddy, S.-L. Fu, C.-C. Lin, *Org. Biomol. Chem.* **2011**, *9*, 2492-2504; (b)Y.-S. Lin, L.-D. Huang, C.-H. Lin, P.-H. Huang, Y.-J. Chen, F.-H. Wong, C.-C. Lin, S.-L. Fu, *J. Biol. Chem.* **2011**, *286*, 43782-43792.
- [170] B. Helferich, E. Schmitz-Hillebrecht, *Ber. Dtsch. Chem. Ges. B* **1933**, *66B*, 378-383.
- [171] (a)S. Kusumi, S. Wang, T. Watanabe, K. Sasaki, D. Takahashi, K. Toshima, *Org. Biomol. Chem.* **2010**, *8*, 988-990; (b)A. Stevenin, F.-D. Boyer, J.-M. Beau, *Eur. J. Org. Chem.* **2012**, *2012*, 1699-1702, S1699/1691-S1699/1621.
- [172] L. A. Salvador, M. Elofsson, J. Kihlberg, *Tetrahedron* **1995**, *51*, 5643-5656.
- [173] J. Brask, K. J. Jensen, *Bioorg. Med. Chem. Lett.* **2001**, *11*, 697-700.
- [174] A. Rashid, W. Mackie, I. J. Colquhoun, D. Lamba, *Can. J. Chem.* **1990**, *68*, 1122-1127.
- [175] H. B. Boren, P. J. Garegg, L. Kenne, A. Pilotti, S. Svensson, C. G. Swahn, *Acta Chem. Scand.* **1973**, *27*, 2740-2748.

Bibliography

- [176] P. H. Fairclough, L. Hough, A. C. Richardson, *Carbohydr. Res.* **1975**, *40*, 285-298.
- [177] A. Rajca, M. Wiessler, *Carbohydr. Res.* **1995**, *274*, 123-136.
- [178] K. Yoshiizumi, F. Nakajima, R. Dobashi, N. Nishimura, S. Ikeda, *Bioorg. Med. Chem.* **2002**, *10*, 2445-2460.
- [179] P. J. Garegg, T. Norberg, *Acta Chem. Scand., Ser. B* **1979**, *B33*, 116-118.
- [180] J. Guo, X.-S. Ye, *Molecules* **2010**, *15*, 7235-7265.
- [181] R. R. Schmidt, *Angew. Chem.* **1986**, *25*, 212-235.
- [182] (a)M. H. D. Postema, K. TenDyke, J. Cutter, G. Kuznetsov, Q. Xu, *Org. Lett.* **2009**, *11*, 1417-1420; (b)G. Zhang, M. Fu, J. Ning, *Carbohydr. Res.* **2005**, *340*, 155-159.
- [183] R. R. Schmidt, M. Stumpp, *Liebigs Annalen der Chemie* **1983**, *1983*, 1249-1256.
- [184] (a)Garegg, Norberg, *Acta Chem. Scand., Ser. B: Org. Chem. Biochem.* **1979**, *33*, 116; (b)Garegg, Kvarnstrom, *Acta Chem. Scand., Series B: Org. Chem. Biochem.* **1976**, *30*, 655,656, 658; (c)D. Crich, Z. Dai, S. Gastaldi, *J. Org. Chem.* **1999**, *64*, 5224-5229.
- [185] A. F. Bochkov, V. I. Betaneli, N. K. Kochetkov, *Russ. Chem. Bull.* **1974**, *23*, 1299-1304.
- [186] I. A. Ivanova, A. J. Ross, A. J. Ferguson, A. V. Nikolaev, *J. Chem. Soc., Perk. Trans. 1: Org. Bioorg. Chem.* **1999**, *12*, 1743-1754.
- [187] U. Chiacchio, V. Pistara, G. Romeo, A. Corsaro, *Curr. Org. Chem.* **2004**, *8*, 511-538.
- [188] (a)V. Neto, R. Granet, P. Krausz, *Tetrahedron*, *66*, 4633-4646; (b)J. Seo, N. Michaelian, S. C. Owens, S. T. Dashner, A. J. Wong, A. E. Barron, M. R. Carrasco, *Org. Lett.* **2009**, *11*, 5210-5213.
- [189] M. Polakova, N. Pitt, M. Tosin, P. V. Murphy, *Angew. Chem., Int. Ed.* **2004**, *43*, 2518-2521.
- [190] N. Nakamura, *J. Am. Chem. Soc.* **1983**, *105*, 7172-7173.
- [191] D. E. Kahne, **1994**, 137 pp, WO9419360A1.
- [192] R. Polt, L. Szabo, J. Treiberg, Y. Li, V. J. Hruby, *J. Am. Chem. Soc.* **1992**, *114*, 10249-10258.
- [193] W. Du, J. Gervay-Hague, *Org. Lett.* **2005**, *7*, 2063-2065.
- [194] (a)P. T. Nyffeler, C.-H. Liang, K. M. Koeller, C.-H. Wong, *J. Am. Chem. Soc.* **2002**, *124*, 10773-10778; (b)S. K. Ramanathan, J. Keeler, H.-L. Lee, D. S. Reddy, G. Lushington, J. Aub, *Org. Lett.* **2005**, *7*, 1059-1062.
- [195] E. D. Goddard-Borger, R. V. Stick, *Org. Lett.* **2007**, *9*, 3797-3800.
- [196] (a)S. Hosokawa, T. Ogura, H. Togashi, K. Tatsuta, *Tetrahedron Lett.* **2005**, *46*, 333-337; (b)H. Sugimura, A. Koizumi, W. Kiyohara, *Nucleos. Nucleot. Nucleic Acids* **2003**, *22*, 727-729.
- [197] R. Ramesh, K. De, S. Chandrasekaran, *Tetrahedron* **2007**, *63*, 10534-10542.
- [198] J. M. Lacombe, A. A. Pavia, *J. Org. Chem.* **1983**, *48*, 2557-2563.
- [199] D. R. Mootoo, P. Konradsson, U. Udodong, B. Fraser-Reid, *J. Am. Chem. Soc.* **1988**, *110*, 5583-5584.
- [200] Z. Zhang, I. R. Ollmann, X.-S. Ye, R. Wischnat, T. Baasov, C.-H. Wong, *J. Am. Chem. Soc.* **1999**, *121*, 734-753.
- [201] X. Zhu, R. R. Schmidt, *Angew. Chem., Inter.Ed.* **2009**, *48*, 1900-1934.
- [202] J. Dinkelaar, J. A. R. de, M. R. van, M. Somers, G. Lodder, H. S. Overkleeft, J. D. C. Codee, d. M. G. A. van, *J. Org. Chem.* **2009**, *74*, 4982-4991.
- [203] N. Fischer, E. D. Goddard-Borger, R. Greiner, T. M. Klapotke, B. W. Skelton, J. Stierstorfer, *J. Org. Chem.* **2012**, *77*, 1760-1764.
- [204] I. G. Dmitrieva, L. V. Dyadyuchenko, V. D. Strelkov, E. A. Kaigorodova, *Chem. Heterocycl. Compd.* **2008**, *44*, 1267-1274.
- [205] G. H. Veeneman, S. H. van Leeuwen, J. H. van Boom, *Tetrahedron Lett.* **1990**, *31*, 1331-1334.

Bibliography

- [206] M. Nishizawa, W. Shimomoto, F. Momii, H. Yamada, *Tetrahedron Lett.* **1992**, *33*, 1907-1908.
- [207] B. Wegmann, R. R. Schmidt, *J. Carbohydr. Chem.* **1987**, *6*, 357-375.
- [208] H. K. Chenault, A. Castro, L. F. Chafin, J. Yang, *J. Org. Chem.* **1996**, *61*, 5024-5031.
- [209] A. V. Demchenko, Wiley-VCH Verlag GmbH & Co. KGaA, **2008**, pp. 1-27.
- [210] K. Fukase, I. Kinoshita, T. Kanoh, Y. Nakai, A. Hasuoka, S. Kusumoto, *Tetrahedron* **1996**, *52*, 3897-3904.
- [211] (a)M. Adinolfi, G. Barone, L. Guariniello, A. Iadonisi, *Tetrahedron Lett.* **2000**, *41*, 9005-9008; (b)A. V. Demchenko, E. Rousson, G.-J. Boons, *Tetrahedron Lett.* **1999**, *40*, 6523-6526.
- [212] Z. Li, L. Zhu, J. Kalikanda, *Tetrahedron Lett.* **2011**, *52*, 5629-5632.
- [213] P. J. Meloncelli, A. D. Martin, T. L. Lowary, *Carbohydr. Res.* **2009**, *344*, 1110-1122.
- [214] R. U. Lemieux, K. B. Hendriks, R. V. Stick, K. James, *J. Am. Chem. Soc.* **1975**, *97*, 4056-4062.
- [215] M. J. Hadd, J. Gervay, *Carbohydr. Res.* **1999**, *320*, 61-69.
- [216] P. J. Jervis, L. R. Cox, G. S. Besra, *J. Org. Chem.* **2011**, *76*, 320-323.
- [217] Y. Angell, D. Chen, F. Brahim, H. U. Saragovi, K. Burgess, *J. Am. Chem. Soc.* **2008**, *130*, 556-565.
- [218] M. A. Dasari, P.-P. Kiatsimkul, W. R. Sutterlin, G. J. Suppes, *Appl. Catal., A* **2005**, *281*, 225-231.
- [219] (a)D. V. Jarikote, P. V. Murphy, *Eur. J. Org. Chem.* **2010**, 4959-4970; (b)S. Doerner, B. Westermann, *Chem. Commun.* **2005**, 2852-2854.
- [220] A. Fuerstner, *Eur. J. Org. Chem.* **2004**, 943-958.
- [221] D. Doyle, P. V. Murphy, *Carbohydr. Res.* **2008**, *343*, 2535-2544.
- [222] L. Achnine, R. Pereda-Miranda, R. Iglesias-Prieto, R. Moreno-Sanchez, B. Lotina-Hennsen, *Physiol. Plant.* **1999**, *106*, 246-252.
- [223] H. C. Kolb, K. B. Sharpless, *Drug Discovery Today* **2003**, *8*, 1128-1137.
- [224] V. Ladmiral, E. Melia, D. M. Haddleton, *Eur. Polym. J.* **2004**, *40*, 431-449.
- [225] T. Loftsson, M. Masson, *Int. J. Pharm.* **2001**, *225*, 15-30.
- [226] K. D. Bodine, D. Y. Gin, M. S. Gin, *J. Am. Chem. Soc.* **2004**, *126*, 1638-1639.
- [227] R. P. McGeary, D. P. Fairlie, *Curr. Opin. Drug Discovery Dev.* **1998**, *1*, 208-217.
- [228] J. F. Billing, U. J. Nilsson, *J. Org. Chem.* **2005**, *70*, 4847-4850.
- [229] R. Huisgen, *Angew. Chem., Int. Ed.* **1963**, *2*, 565-598.
- [230] C. W. Tornoe, C. Christensen, M. Meldal, *J. Org. Chem.* **2002**, *67*, 3057-3064.
- [231] V. V. Rostovtsev, L. G. Green, V. V. Fokin, K. B. Sharpless, *Angew. Chem., Int. Ed.* **2002**, *41*, 2596-2599.
- [232] H. C. Kolb, M. G. Finn, K. B. Sharpless, *Angew. Chem., Int. Ed.* **2001**, *40*, 2004-2021.
- [233] J. E. Hein, V. V. Fokin, *Chem. Soc. Rev.* **2010**, *39*, 1302-1315.
- [234] F. Himo, T. Lovell, R. Hilgraf, V. V. Rostovtsev, L. Noodleman, K. B. Sharpless, V. V. Fokin, *J. Am. Chem. Soc.* **2005**, *127*, 210-216.
- [235] V. D. Bock, H. Hiemstra, M. J. H. van, *Eur. J. Org. Chem.* **2005**, 51-68.
- [236] V. O. Rodionov, V. V. Fokin, M. G. Finn, *Angew. Chem., Int. Ed.* **2005**, *44*, 2210-2215.
- [237] M. Meldal, C. W. Tornoe, *Chem. Rev.* **2008**, *108*, 2952-3015.
- [238] T. Velasco-Torrijos, P. V. Murphy, *Org. Lett.* **2004**, *6*, 3961-3964.
- [239] S. Manabe, A. Ueki, Y. Ito, *Tetrahedron Lett.* **2008**, *49*, 5159-5161.
- [240] Y. Jin, N. Hada, J. Oka, O. Kanie, S. Daikoku, Y. Kanie, H. Yamada, T. Takeda, *Chem. Pharm. Bull.* **2006**, *54*, 485-492.
- [241] E. J. Corey, A. Venkateswarlu, *J. Amer. Chem. Soc.* **1972**, *94*, 6190-6191.
- [242] H. Finkelstein, *Ber. Dtsch. Chem. Ges.* **1910**, *43*, 1528-1532.
- [243] J. W. Steed, J. L. Atwood, Editors, *Supramolecular Chemistry, Second Edition*, John Wiley & Sons, Ltd., **2009**.

Bibliography

- [244] J. W. Moore, C. L. Stanitski, P. C. Jurs, *Principles of Chemistry: The Molecular Science*, **2009**.
- [245] G. L. Bertrand, <http://web.mst.edu/~gbert/basic/thermo.html>, **2012**.
- [246] (a)J. A. Opsteen, H. J. C. M. van, *Chem. Commun.* **2005**, 57-59; (b)D. Quemener, T. P. Davis, C. Barner-Kowollik, M. H. Stenzel, *Chem. Commun.* **2006**, 5051-5053.
- [247] (a)H. Mirzaei, M.-Y. Brusniak, L. N. Mueller, S. Letarte, J. D. Watts, R. Aebersold, *Mol. Cell. Proteomics* **2009**, *8*, 1934-1946; (b)M. P. Balogh, *LCGC North Am.* **2007**, *25*, 554-570; (c)K. Strupat, *Methods Enzymol.* **2005**, *405*, 1-36; (d)C. E. Bobst, I. A. Kaltashov, *Curr. Pharm. Biotechnol.* **2011**, *12*, 1517-1529.
- [248] K. Varga, L. Aslimovska, I. Parrot, M. T. Dauvergne, M. Haertlein, V. T. Forsyth, A. Watts, *Biochim. Biophys. Acta, Biomembr.* **2007**, *1768*, 3029-3035.
- [249] P. Angibeaud, J. Defaye, A. Gabelle, J. P. Utille, *Synthesis* **1985**, 1123-1125.
- [250] W. C. Still, M. Kahn, A. Mitra, *J. Org. Chem.* **1978**, *43*, 2923-2925.
- [251] R. Hori, Y. Ikegami, *Yakugaku Zasshi* **1959**, *79*, 80-83.
- [252] D. S. Johnston, E. Coppard, D. Chapman, *Biochim. Biophys. Acta, Biomembr.* **1985**, *815*, 325-333.
- [253] M. L. Wolfrom, A. Thompson, *Methods Carbohydr. Chem.* **1963**, 211-215.
- [254] Z. Wang, M. Raifu, M. Howard, L. Smith, D. Hansen, R. Goldsby, D. Ratner, *J. Immunol. Methods* **2000**, *233*, 167-177.
- [255] R. Kumar, P. Tiwari, P. R. Maulik, A. K. Misra, *Carbohydr. Res.* **2005**, *340*, 2335-2339.
- [256] A. W. Harrison, J. F. Fisher, D. M. Guido, S. J. Couch, J. A. Lawson, D. M. Sutter, M. V. Williams, G. L. DeGraaf, J. E. Rogers, a. et, *Bioorg. Med. Chem.* **1994**, *2*, 1339-1361.
- [257] B. Faroux-Corlay, L. Clary, C. Gadras, D. Hammache, J. Greiner, C. Santaella, A. M. Aubertin, P. Vierling, J. Fantini, *Carbohydr. Res.* **2000**, *327*, 223-260.
- [258] S. C. Timmons, D. L. Jakeman, *Org. Lett.* **2007**, *9*, 1227-1230.
- [259] (a)J.-R. Ella-Menye, X. Nie, G. Wang, *Carbohydr. Res.* **2008**, *343*, 1743-1753; (b)C. Nobrega, J. T. Vazquez, *Tetrahedron: Asymmetry* **2003**, *14*, 2793-2801.
- [260] (a)Z. J. Li, H. Li, M. S. Cai, *Carbohydr. Res.* **1999**, *320*, 1-7; (b)L. V. Bakinovskii, N. E. Bairamova, Y. E. Tsvetkov, V. I. Betaneli, *Carbohydr. Res.* **1981**, *98*, 181-193.
- [261] A. G. Roth, S. Redmer, C. Arenz, *Bioorg. Med. Chem.* **2010**, *18*, 939-944.
- [262] K. Takeo, S. Kitamura, Y. Murata, *Carbohydr. Res.* **1992**, *224*, 111-122.
- [263] M. Adinolfi, G. Barone, L. Guariniello, A. Iadonisi, *Tetrahedron Lett.* **1999**, *40*, 8439-8441.
- [264] P. T. Nyffeler, C.-H. Liang, K. M. Koeller, C.-H. Wong, *J. Am. Chem. Soc.* **2002**, *124*, 10773-10778.
- [265] J. A. Sowinski, P. L. Toogood, *J. Org. Chem.* **1996**, *61*, 7671-7676.
- [266] K. Yoshiizumi, F. Nakajima, R. Dobashi, N. Nishimura, S. Ikeda, *Bioorg. Med. Chem.* **2002**, *10*, 2445-2460.
- [267] L. A. Salvador, M. Eloffson, J. Kihlberg, *Tetrahedron* **1995**, *51*, 5643-5656.
- [268] J. M. Palomo, M. Filice, R. Fernandez-Lafuente, M. Terreni, J. M. Guisan, *Adv. Synth. Catal.* **2007**, *349*, 1969-1976.
- [269] V. Deulofeu, J. O. Deferrari, *J. Org. Chem.* **1952**, *17*, 1097-1101.
- [270] W. Pilgrim, P. V. Murphy, *J. Org. Chem.* **2010**, *75*, 6747-6755.
- [271] M. A. Brimble, R. Kowalczyk, P. W. R. Harris, P. R. Dunbar, V. J. Muir, *Org. Biomol. Chem.* **2008**, *6*, 112-121.
- [272] A. J. Ross, O. V. Sizova, A. V. Nikolaev, *Carbohydr. Res.* **2006**, *341*, 1954-1964.
- [273] S. K. Ramanathan, J. Keeler, H.-L. Lee, D. S. Reddy, G. Lushington, J. Aube, *Org. Lett.* **2005**, *7*, 1059-1062.
- [274] S. Manabe, K. Sakamoto, Y. Nakahara, M. Sisido, T. Hohsaka, Y. Ito, *Bioorg. Med. Chem.* **2002**, *10*, 573-581.

Bibliography

- [275] J. Xie, A. Molina, S. Czernecki, *J. Carbohydr. Chem.* **1999**, *18*, 481-498.
- [276] J. W. Antoon, J. Liu, M. M. Gestaut, M. E. Burow, B. S. Beckman, M. Foroozesh, *J. Med. Chem.* **2009**, *52*, 5748-5752.
- [277] A. J. Janczuk, W. Zhang, P. R. Andreana, J. Warrick, P. G. Wang, *Carbohydr. Res.* **2002**, *337*, 1247-1259.
- [278] X.-S. Ye, F. Sun, M. Liu, Q. Li, Y. Wang, G. Zhang, L.-H. Zhang, X.-L. Zhang, *J. Med. Chem.* **2005**, *48*, 3688-3691.
- [279] A. Dondoni, G. Mariotti, A. Marra, *J. Org. Chem.* **2002**, *67*, 4475-4486.
- [280] A. S. Bhat, J. Gervay-Hague, *Org. Lett.* **2001**, *3*, 2081-2084.
- [281] A. Keliris, T. Ziegler, R. Mishra, R. Pohmann, M. G. Sauer, K. Ugurbil, J. Engelmann, *Bioorg. Med. Chem.* **2011**, *19*, 2529-2540.
- [282] C.-T. Ren, Y.-H. Tsai, Y.-L. Yang, W. Zou, S.-H. Wu, *J. Org. Chem.* **2007**, *72*, 5427-5430.

Author Publications

Bibliography

Author Publications